STRUCTURAL MECHANICS

Tomasz Wierzbicki
Massachusetts Institute of Technology

LibreTexts™

Structural Mechanics

Tomasz Wierzbicki

Massachusetts Institute of Technology

The LibreTexts libraries are Powered by NICE CXone Expert and was supported by the Department of Education Open Textbook Pilot Project, the California Education Learning Lab, the UC Davis Office of the Provost, the UC Davis Library, the California State University Affordable Learning Solutions Program, and Merlot. This material is based upon work supported by the National Science Foundation under Grant No. 1246120, 1525057, and 1413739.

Any opinions, findings, and conclusions or recommendations expressed in this material are those of the author(s) and do not necessarily reflect the views of the National Science Foundation nor the US Department of Education.

TABLE OF CONTENTS

5: Moderately Large Deflection Theory of Beams

- 5.1: General Formulation
- 5.2: Solution for a Beam on Roller Support
- 5.3: Solution for a Beam with Fixed Axial Displacements
- 5.4: Galerkin Method of Solving Non-linear Differential Equation
- 5.5: Generalization to Arbitrary Non-linear Problems in Plates and Shells

6: Bending Response of Plates and Optimum Design

- 6.1: Beam Deflection Equation
- 6.2: Deflections of Circular Plates
- 6.3: Equivalence of Square and Circular Plates
- 6.4: Design Concept for Plates
- 6.5: Sandwich Plates
- 6.6: Stiffened Plates
- 6.7: Plates versus Grillages
- 6.8: The Concept of Equivalent Thickness
- 6.9: Shear Lag

7: Energy Methods in Elasticity

- 7.1: The Concept of Potential Energy
- 7.2: Equivalence of the Minimum Potential Energy and Principle of Virtual Work
- 7.3: Two Formulations for Beams
- 7.4: Fourier Series Expansion and the Ritz Method
- 7.5: Solution by Taylor expansion
- 7.6: Castigliano Theorem

8: Stability of Elastic Structures

- 8.1: Prelude to Stability of Elastic Structures
- 8.2: Trefftz Condition for Stability
- 8.3: Stability of Elastic Column Using the Energy Method
- 8.4: Effect of Structural Imperfections
- 8.5: Stability in Tension
- 8.6: Plastic Buckling of Columns
- 8.7: Mode Transition (Advanced)

9: Advanced Topic in Column Buckling

- 9.1: The Tallest Column
- 9.2: Deflection Behavior for Beam with Compressive Axial Loads and Transverse Loads
- 9.3: Snap-through of a Two Bar System
- 9.4: Dynamic Snap-Through

10: Buckling of Plates and Sections

- 10.1: Governing Equations and Boundary Conditions
- 10.2: Buckling of a Simply Supported Plate
- 10.3: Effect of Boundary Conditions
- 10.4: Buckling of Sections
- 10.5: Post-buckling Response of Plates (Advanced)

Licensing

*A detailed breakdown of this resource's licensing can be found in **Back Matter/Detailed Licensing**.*

CHAPTER OVERVIEW

1: The Concept of Strain

Strain is a fundamental concept in continuum and structural mechanics. Displacement fields and strains can be directly measured using gauge clips or the Digital Image Correlation (DIC) method. Deformation patterns for solids and deflection shapes of structures can be easily visualized and are also predictable with some experience. By contrast, the stresses can only be determined indirectly from the measured forces or by the inverse engineering method through a detailed numerical simulation. Furthermore, a precise determination of strain serves to define a corresponding stress through the work conjugacy principle. Finally the equilibrium equation can be derived by considering compatible fields of strain and displacement increments, as explained in Chapter 2. The present author sees the engineering world through the magnitude and shape of the deforming bodies. This point of view will dominate the formulation and derivation throughout the present lecture note. Chapter 1 starts with the definition of one dimensional strain. Then the concept of the threedimensional (3-D) strain tensor is introduced and several limiting cases are discussed. This is followed by the analysis of strains-displacement relations in beams (1-D) and plates (2- D). The case of the so-called moderately large deflection calls for considering the geometric non-linearities arising from rotation of structural elements. Finally, the components of the strain tensor will be re-defined in the polar and cylindrical coordinate system.

1.1: One-dimensional Strain

Consider a prismatic, uniform thickness rod or beam of the initial length l_o. The rod is fixed at one end and subjected a tensile force (Figure (1.1.1)) at the other end. The current, deformed length is denoted by l. The question is whether the resulting strain field is homogeneous or not. The concept of homogeneity in mechanics means independence of the solution on the spatial coordinates system, the rod axis in the present case. It can be shown that if the stress-strain curve of the material is convex or linear, the rod deforms uniformly and a homogeneous state of strains and stresses are developed inside the rod. This means that local and average strains are the same and the strain can be defined by considering the total lengths. The displacement at the fixed end $x = 0$ of the rod is zero, $u(x = 0)$ and the end displacement is

$$u(x = l) = l - l_o \tag{1.1.1}$$

The strain is defined as a relative displacement. Relative to what? Initial, current length or something else? The definition of strain is simple but at the same time is non-unique.

$$\epsilon \overset{\text{def}}{=} \frac{l - l_o}{l_o} \text{ Engineering Strain} \tag{1.1.2}$$

$$\epsilon \overset{\text{def}}{=} \frac{1}{2}\frac{l^2 - l_o^2}{l^2} \text{ Cauchy Strain} \tag{1.1.3}$$

$$\epsilon \overset{\text{def}}{=} \ln\frac{l}{l_o} \text{ Logarithmic Strain} \tag{1.1.4}$$

Each of the above three definitions satisfy the basic requirement that strain vanishes when $l = l_o$ or $u = 0$ and that strain in an increasing function of the displacement u.

Consider a limiting case of Equation 1.1.1 for small displacements $\frac{u}{l_o} \ll 1$, for which $l_o + l \approx 2l_o$ in Equation 1.1.3. Then, the Cauchy strain becomes

$$\epsilon = \frac{l - l_o}{l_o}\frac{l + l_o}{2l_o} \cong \frac{l - l_o}{l_o}\frac{2l}{2l_o} \cong \frac{l - l_o}{l_o} \tag{1.1.5}$$

Thus, for small strain, the Cauchy strain reduces to the engineering strain. Likewise, expanding the expression for the logarithmic strain, Equation 1.1.4 in Taylor series around $l - l_o \cong 0$,

$$\ln\frac{l}{l_o}\Big|_{l/l_o=1} \cong \frac{l - l_o}{l_o} - \frac{1}{2}\left(\frac{l+l_o}{l_o}\right)^2 + \ldots \approx \frac{l - l_o}{l_o} \tag{1.1.6}$$

one can see that the logarithmic strain reduces to the engineering strain.

The plots of ϵ versus $\frac{l}{l_o}$ according to Equations 1.1.2-1.1.4 are shown in Figure (1.1.1).

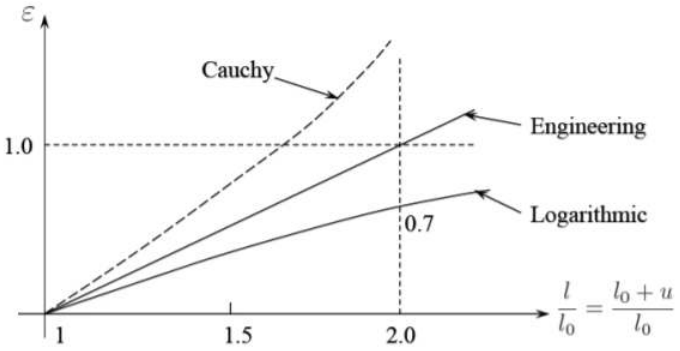

Figure 1.1.1: Comparison of three definitions of the uniaxial strain.

Inhomogeneous Strain Field

The strain must be defined locally and not for the entire structure. Consider an infinitesimal element dx in the undeformed configuration, Figure 1.1.2. After deformation the length of the original material element becomes $dx + du$. The engineering strain is then

$$\epsilon_{\text{eng}} = \frac{(dx + du) - dx}{dx} = \frac{du}{dx} \tag{1.1.7}$$

The spatial derivative of the displacement field is called the **displacement gradient** $F = \frac{du}{dx}$. For uniaxial state the strain is simply the displacement gradient. This is not true for general 3-D case.

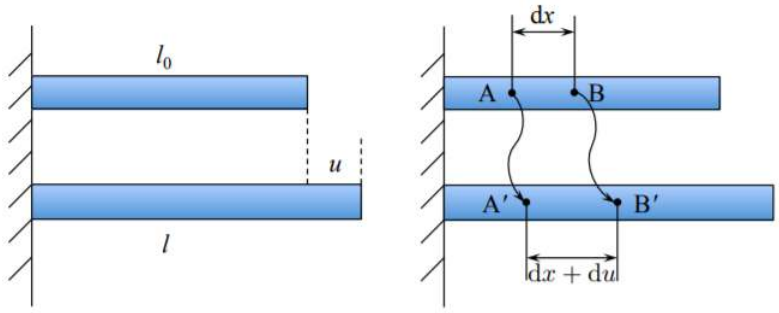

Figure 1.1.2: Undeformed and deformed element in the homogenous and inhomogeneous strain field in the bar.

The local Cauchy strain is obtained by taking relative values of the difference of the square of the lengths. As shown in Equation 1.1.5, in order for the Cauchy strain to reduce to the engineering strain, the factor 2 must be introduced in the definition. Thus

$$\epsilon_c = \frac{1}{2}\frac{(dx + du)^2 - dx^2}{dx^2} = \frac{du}{dx} + \frac{1}{2}\left(\frac{du}{dx}\right)^2 \tag{1.1.8}$$

or $\epsilon_c = F + \frac{1}{2}F^2$. For small displacement gradients,

$$\epsilon_c = \epsilon_{\text{eng}} \tag{1.1.9}$$

1.2: Extension to the 3-D case

Equation (1.1.7) can be re-written in an alternative form

$$du = \epsilon dx \tag{1.2.1}$$

Consider an Euclidian space and denote by $\boldsymbol{x} = \{x_1, x_2, x_3\}$ or x_i the vector representing a position of a generic point of a body. In the general three-dimensional case, the displacement of the material point is also a vector with components $\boldsymbol{u} = \{u_1, u_2, u_3\}$ or u_i where $i = 1, 2, 3$. Recall that the increment of a function of three variables is a sum of three components

$$du_1(x_1, x_2, x_3) = \frac{\partial u_1}{\partial x_1} dx_1 + \frac{\partial u_1}{\partial x_2} dx_2 + \frac{\partial u_1}{\partial x_3} dx_3 \tag{1.2.2}$$

In general, components of the displacement increment vector are

$$du_i(x_i) = \frac{\partial u_i}{\partial x_1} dx_1 + \frac{\partial u_i}{\partial x_2} dx_2 + \frac{\partial u_i}{\partial x_3} dx_3 = \sum_{j=1}^{3} \frac{\partial u_i}{\partial x_j} dx_j \tag{1.2.3}$$

where the repeated j is the so called “dummy” index. The displacement gradient

$$\boldsymbol{F} = \frac{\partial u_i}{\partial x_j} \tag{1.2.4}$$

is not a symmetric tensor. It also contains terms of rigid body rotation. This can be shown by re-writing the expression for $\boldsymbol{F}$ in an equivalent form

$$\frac{\partial u_i}{\partial x_j} = \frac{1}{2}\left(\frac{\partial u_i}{\partial x_j} + \frac{\partial u_j}{\partial x_i}\right) + \left(\frac{1}{2}\frac{\partial u_i}{\partial x_j} - \frac{\partial u_j}{\partial x_i}\right) \tag{1.2.5}$$

Strain tensor ϵ_{ij} is defined as a “symmetric” part of the displacement gradient, which is the first term in Equation 1.2.5.

$$\epsilon_{ij} = \frac{1}{2}\left(\frac{\partial u_i}{\partial x_j} + \frac{\partial u_j}{\partial x_i}\right) \tag{1.2.6}$$

Now, interchange (transpose) the indices i and j in Equation 1.2.6:

$$\epsilon_{ji} = \frac{1}{2}\left(\frac{\partial u_j}{\partial x_i} - \frac{\partial u_i}{\partial x_j}\right) \tag{1.2.7}$$

The first term in Equation 1.2.7 is the same as the second term in Equation 1.2.6. And the second term in Equation 1.2.7 is identical to the first term in Equation 1.2.6. Therefore the strain tensor is symmetric

$$\epsilon_{ij} = \epsilon_{ji} \tag{1.2.8}$$

The reason for introducing the symmetry properties of the strain tensor will be explained later in this section. The second terms in Equation 1.2.5 is called the **spin tensor** ω_{ij}

$$\omega_{ij} = \frac{1}{2}\left(\frac{\partial u_i}{\partial x_j} + \frac{\partial u_j}{\partial x_i}\right) \tag{1.2.9}$$

Using similar arguments as before it is easy to see that the spin tensor is antisymmetric

$$w_{ij} = -w_{ji} \tag{1.2.10}$$

From the definition it follows that the diagonal terms of the spin tensor are zero, for example $w_{11} = -w_{11} = 0$. The components, of the strain tensor are:

- $i = 1, j = 1$

$$\epsilon_{11} = \frac{1}{2}\left(\frac{\partial u_1}{\partial x_1} + \frac{\partial u_1}{\partial x_1}\right) = \frac{\partial u_1}{\partial x_1} \tag{1.2.11}$$

- $i = 2, j = 2$

$$\epsilon_{22} = \frac{\partial u_2}{\partial x_2} \tag{1.2.12}$$

- $i = 3, j = 3$

$$\epsilon_{33} = \frac{\partial u_3}{\partial x_3} \tag{1.2.13}$$

- $i = 1, j = 2$

$$\epsilon_{12} = \epsilon_{21} = \frac{1}{2}\left(\frac{\partial u_1}{\partial x_2} + \frac{\partial u_2}{\partial x_1}\right) \tag{1.2.14}$$

- $i = 2, j = 3$

$$\epsilon_{23} = \epsilon_{32} = -\frac{1}{2}\left(\frac{\partial u_2}{\partial x_3} + \frac{\partial u_3}{\partial x_2}\right) \tag{1.2.15}$$

- $i = 3, j = 1$

$$\epsilon_{31} = \epsilon_{13} = -\frac{1}{2}\left(\frac{\partial u_3}{\partial x_1} + \frac{\partial u_1}{\partial x_3}\right) \tag{1.2.16}$$

For the geometrical interpretation of the strain and spin tensor consider an infinitesimal square element (dx_1, dx_2) subjected to several simple cases of deformation. The partial derivatives are replaced by finite differences, for example

$$\frac{\partial u_1}{\partial x_1} = \frac{\Delta u_1}{\Delta x_1} = \frac{u_1(x_1) - u_1(x_1 + h)}{h} \tag{1.2.17}$$

Rigid body translation

Along x_1 axis:

$$u_1(x_1) = u_1(x_1 + h) \tag{1.2.18}$$

$$u_2 = u_3 = 0 \tag{1.2.19}$$

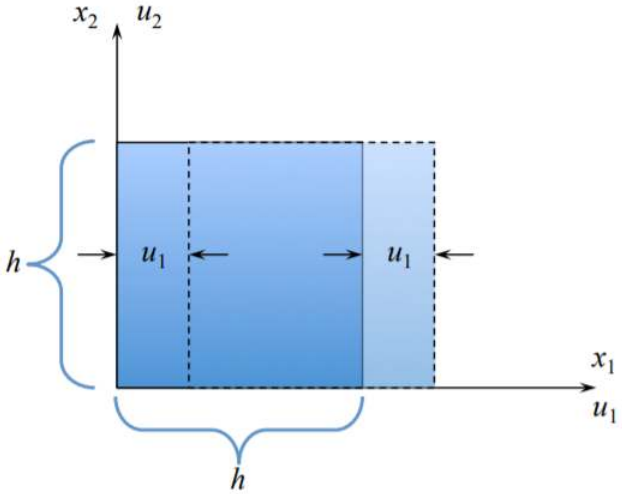

Figure 1.2.1: Rigid body translation of the infinitesimal square element.

It follows from 1.2.11 that the corresponding strain component vanishes, $\epsilon_{11} = 0$. The first component of the spin tensor is zero from the definition, $\omega_{11} = 0$.

Extension along x_1 axis

At x_1: $u_1 = 0$.

At $x_1 + h$: $u_1 = u_o$.

The corresponding strain is $\epsilon_{11} = \frac{u_o}{h}$.

Pure shear on the x_1x_2 plane

At $x_1 = 0$ and $x_2 = 0$: $u_1 = u_2 = 0$

At $x_1 = h$ and $x_2 = 0$: $u_1 = 0$ and $u_2 = u_o$

At $x_1 = 0$ and $x_2 = h$: $u_1 = u_o$ and $u_2 = 0$

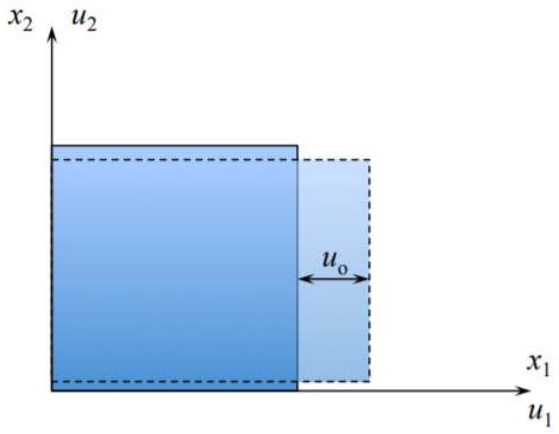

Figure **1.2.2**: The square element is stretched in one direction.

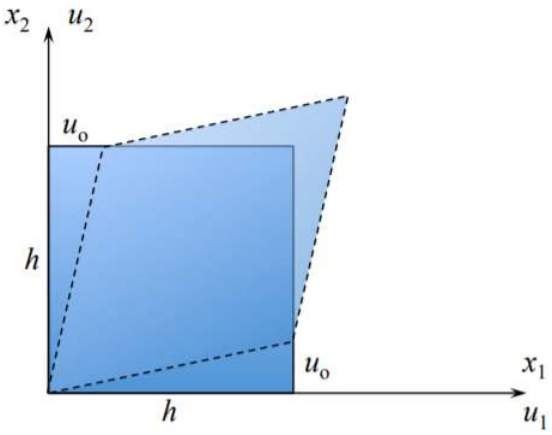

Figure **1.2.3**: Imposing constant deformative gradients.

It follows from Equation 1.2.10 and Equation 1.2.6 that:

$$\epsilon_{12} = \frac{1}{2}\left(\frac{u_o}{h} + \frac{u_o}{h}\right) = \frac{u_o}{h} \tag{1.2.20}$$

$$\omega_{12} = \frac{1}{2}\left(\frac{u_o}{h} - \frac{u_o}{h}\right) = 0 \tag{1.2.21}$$

The resulting strain is representing change of angles of the initial rectilinear element.

Rigid body rotation

At $x_1 = 0$ and $x_2 = 0$: $u_1 = u_2 = 0$

At $x_1 = h$ and $x_2 = 0$: $u_1 = 0$ and $u_2 = u_o$

At $x_1 = 0$ and $x_2 = h$: $u_1 = -u_o$ and $u_2 = 0$

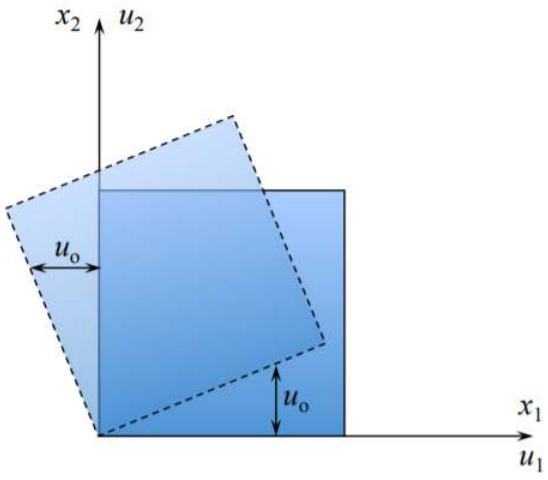

Figure **1.2.4**: An infinitesimal square element subjected to rigid body rotation.

Changing the sign of u_1 at $x_1 = 0$ and $x_2 = h$ from u_o to $-u_o$ results in non-zero spin but zero strain

$$\epsilon_{12} = \frac{1}{2}\left(\frac{u_o}{h} + \left(-\frac{u_o}{h}\right)\right) = 0 \tag{1.2.22}$$

$$\omega_{12} = \frac{1}{2}\left(\frac{u_o}{h} + \left(-\frac{u_o}{h}\right)\right) = \frac{u_o}{h} \tag{1.2.23}$$

The last example provides an explanation why the strain tensor was defined as a symmetric part of the displacement gradient. The physics dictates that rigid body translation and rotation should not induce any strains into the material element. In rigid body rotation displacement gradients are not zero. The strain tensor, defined as a symmetric part of the displacement gradient removes the effect of rotation in the state of strain in a body. In other words, strain described the change of length and angles while the spin, element rotation.

1.3: Description of Strain in the Cylindrical Coordinate System

In this section the strain-displacement relations will be derived in the cylindrical coordinate system (r, θ, z).

The polar coordinate system is a special case with $z = 0$. The components of the displacement vector are $\{u_r, u_\theta, u_z\}$. There are two ways of deriving the kinematic equations. Since strain is a tensor, one can apply the transformation rule from one coordinate to the other. This approach is followed for example on pages 125-128 of the book on "A First Course in Continuum Mechanics" by Y.C. Fung. Or, the expression for each component of the strain tensor can be derived from the geometry. The latter approach is adopted here. The diagonal (normal) components ϵ_{rr}, $\epsilon_{\theta\theta}$, and ϵ_{zz} represent the change of length of an infinitesimal element. The non-diagonal (shear) components describe the change of angles.

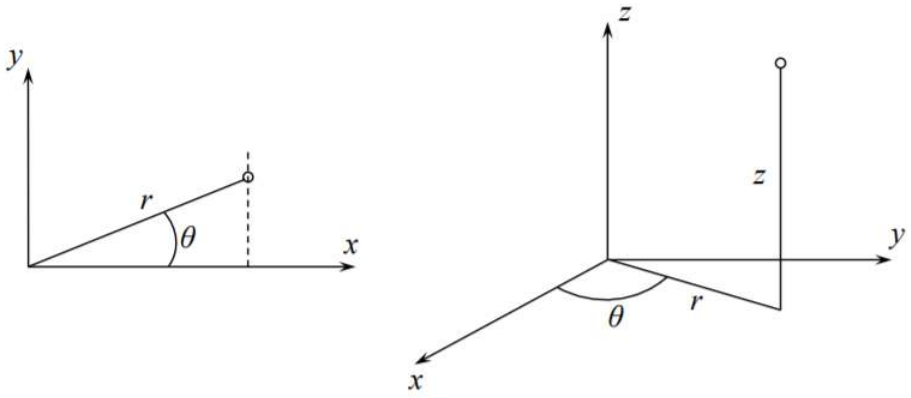

Figure 1.3.1: Rectangular and cylindrical coordinate system.

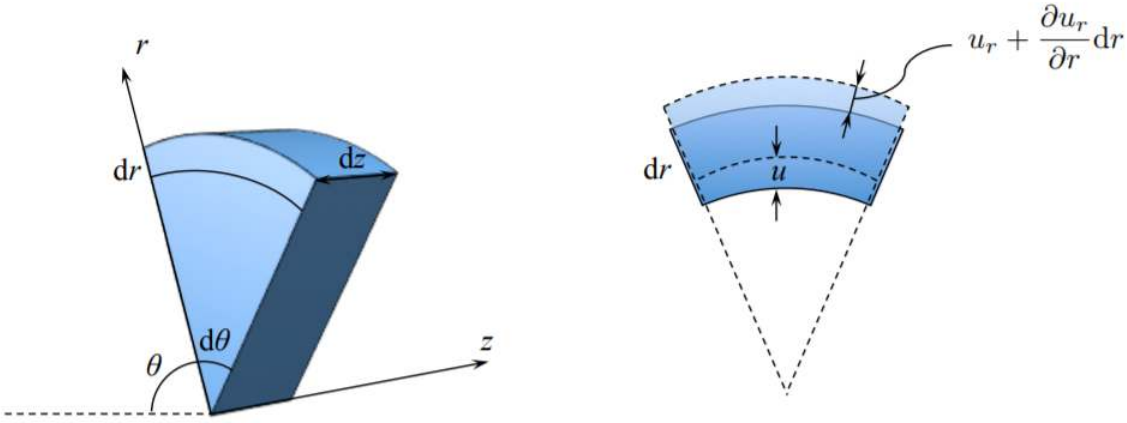

Figure 1.3.2: Change of length in the radial direction.

The radial strain is solely due to the presence of the displacement gradient in the r-direction

$$\epsilon_{rr} = \frac{\left\{u_r + \frac{\partial u_r}{\partial r} dr - u_r\right\}}{dr} = \frac{\partial u_r}{\partial r} \tag{1.3.1}$$

The circumferential strain has two components

$$\epsilon_{\theta\theta} = \epsilon_{\theta\theta}^{(1)} + \epsilon_{\theta\theta}^{(2)} \tag{1.3.2}$$

The first component is the change of length due to radial displacement, and the second component is the change of length due to circumferential displacement.

From Figure (1.3.3) the components $\epsilon_{\theta\theta}^{(1)}$ and $\epsilon_{\theta\theta}^{(2)}$ are calculated as

$$\epsilon_{\theta\theta}^{(1)} = \frac{(r + u_r)d\theta - rd\theta}{rd\theta} = \frac{u_r}{r} \tag{1.3.3}$$

$$\epsilon_{\theta\theta}^{(2)} = \frac{u_\theta + \frac{\partial u_\theta}{\partial \theta} d\theta - u_\theta}{r d\theta} = \frac{1}{r}\frac{\partial u_\theta}{\partial \theta} \tag{1.3.4}$$

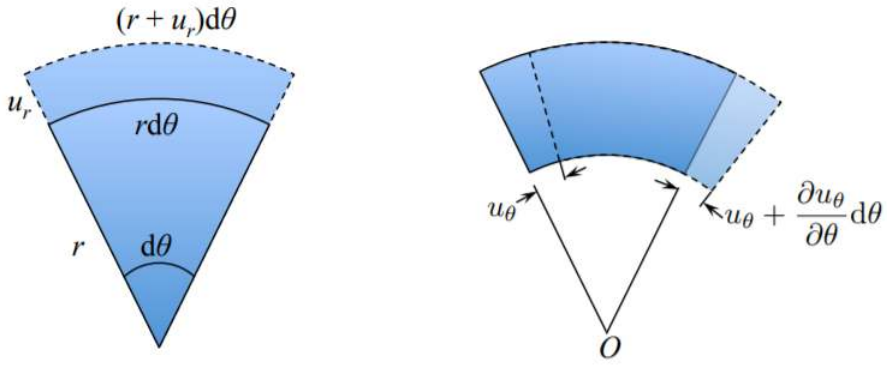

Figure **1.3.3**: Two deformation modes responsible for the circumferential (hoop) strain.

The total circumferential (hoop) component of the strain tensor is

$$\epsilon_{\theta\theta} = \frac{u_r}{r} + \frac{1}{r}\frac{\partial u_\theta}{\partial d\theta} \tag{1.3.5}$$

The strain components in the z-direction is the same as in the rectangular coordinate system

$$\epsilon_{zz} = \frac{\partial u_z}{\partial z} \tag{1.3.6}$$

The shear strain $\epsilon_{r\theta}$ describes a change in the right angle.

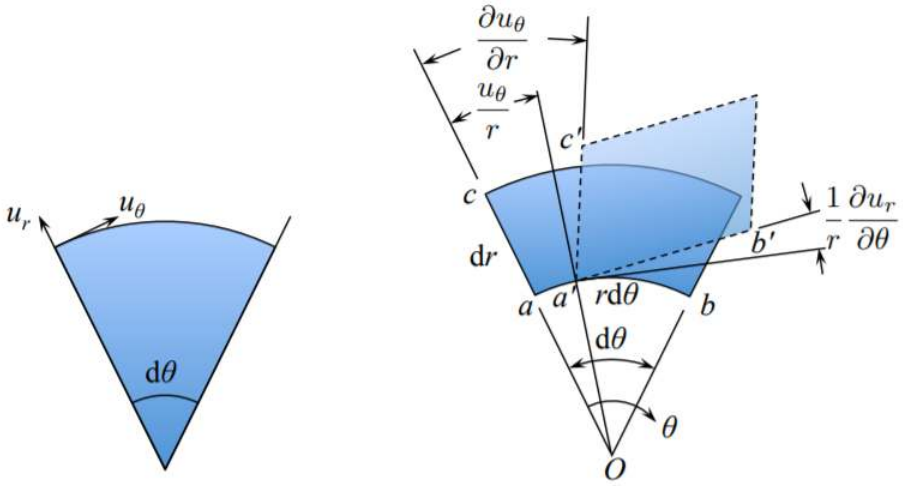

Figure **1.3.4**: Construction that explains change of angles due to radial and circumferential displacement.

From Figure (**1.3.4**) the shear strain over the $\{r, \theta\}$ plane is

$$\epsilon_{r\theta} = \frac{1}{2}\left[\frac{\partial u_\theta}{\partial r} - \frac{u_\theta}{r} + \frac{1}{r}\frac{\partial u_r}{\partial \theta}\right] \tag{1.3.7}$$

On the $\{r, z\}$ plane, the ϵ_{rz} shear develops from the respective gradients, see Figure (**1.3.5**).

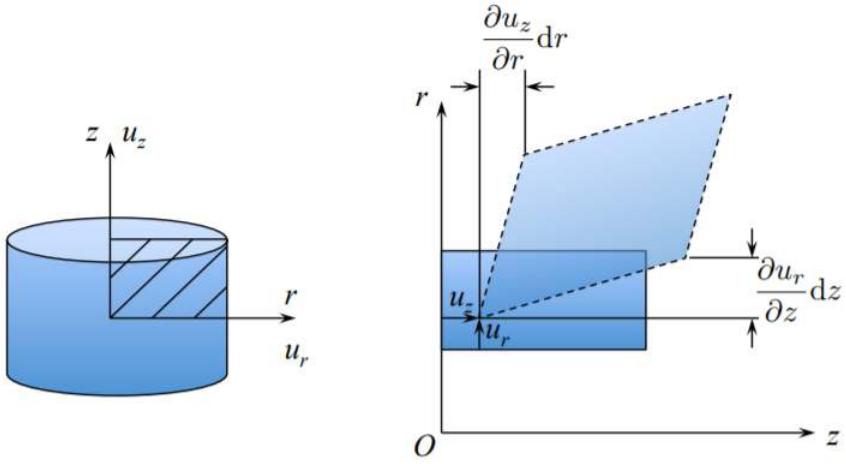

Figure 1.3.5: Change of angles are $\{r, z\}$ plane.

From the construction in Figure (1.3.4), the component ϵ_{rz} is

$$\epsilon_{rz} = \frac{1}{2}\left(\frac{\partial u_r}{\partial z} + \frac{\partial u_z}{\partial r}\right) \tag{1.3.8}$$

Finally, a similar picture is valid on the (tangent) $\{z, \theta\}$ plane

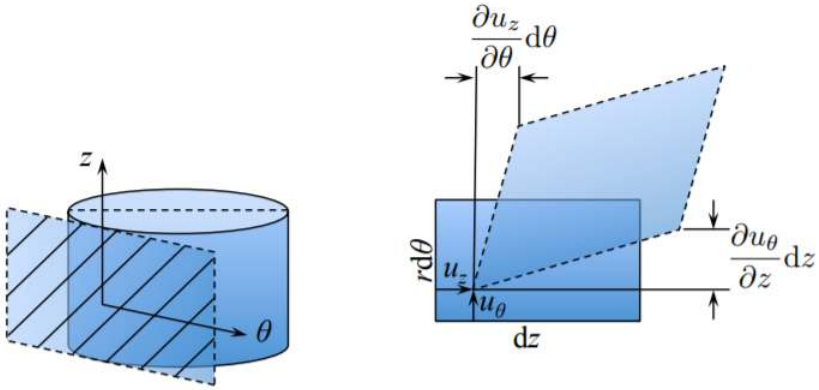

Figure 1.3.6: Visualization of the strain component $\epsilon_{\theta z}$.

The component $\epsilon_{\theta z}$ of the strain tensor is one half of the change of angles, i.e.

$$\epsilon_{\theta z} = \frac{1}{2}\left(\frac{\partial u_z}{r\partial \theta} + \frac{\partial u_\theta}{\partial z}\right) \tag{1.3.9}$$

To sum up the derivation, the six components of the infinitesimal strain tensor in the cylindrical coordinate system are

$$\epsilon_{rr} = \frac{\partial u_r}{\partial r} \tag{1.3.10}$$

$$\epsilon_{\theta\theta} = \frac{u_r}{r} + \frac{1}{r}\frac{\partial u_\theta}{\partial \theta} \tag{1.3.11}$$

$$\epsilon_{zz} = \frac{\partial u_z}{\partial z} \tag{1.3.12}$$

$$\epsilon_{r\theta} = \epsilon_{\theta r} = \frac{1}{2}\left(\frac{1}{r}\frac{\partial u_r}{\partial \theta} + \frac{\partial u_\theta}{\partial r} - \frac{u_\theta}{r}\right) \tag{1.3.13}$$

$$\epsilon_{\theta z} = \epsilon_{z\theta} = \frac{1}{2}\left(\frac{\partial u_z}{r\partial \theta} + \frac{\partial u_\theta}{\partial z}\right) \tag{1.3.14}$$

$$\epsilon_{zr} = \epsilon_{rz} = \frac{1}{2}\left(\frac{\partial u_r}{\partial z} + \frac{\partial u_z}{\partial r}\right) \tag{1.3.15}$$

Considerable simplifications are obtained in the case of axial (rotational symmetry for which $u_\theta = 0$ and $\frac{\partial}{\partial\theta}[\,] = 0$

$$\epsilon_{rr} = \frac{\partial u_r}{\partial r} \quad \epsilon_{r\theta} = 0 \tag{1.3.16}$$

$$\epsilon_{\theta\theta} = \frac{u_r}{r} \quad \epsilon_{\theta z} = 0 \tag{1.3.17}$$

$$\epsilon_{zz} = \frac{\partial u_z}{\partial z} \quad \epsilon_{zr} = \frac{1}{2}\left(\frac{\partial u_r}{\partial z} + \frac{\partial u_z}{\partial r}\right) \tag{1.3.18}$$

The application of the above geometrical relations for axi-symmetric loading of circular plates and cylindrical shells will be given in subsequent chapters.

1.4: Kinematics of the Elementary Beam Theory

The word “kinematics” is derived from the Greek word “kinema”, which means movements, motion. Any motion of a body involves displacements u_i, their increments du_i and velocities $\dot{u}_i$. If the rigid body translations and rotations are excluded, strains develop. We often say “Kinematic assumption” or “Kinematic boundary conditions” or “Kinematic quantities” etc. All it means that statements are made about the displacements and strains and/or their rates. By contrast, the word “static” is reserved for describing stresses and/or forces, even though a body could move. The point is that for statically determined structures, one could determine stresses and forces without invoking motion. Such expressions as “static formulation”, “static boundary conditions”, “static quantities” always refer to stresses and forces.

Elementary is another word in the title of this section that requires explanation. A beam is a slender structure that can be compressed, extended or bent. The beam must be subjected to a transverse load (perpendicular to its axis). Otherwise it becomes something else, as explained in Figure (1.4.1).

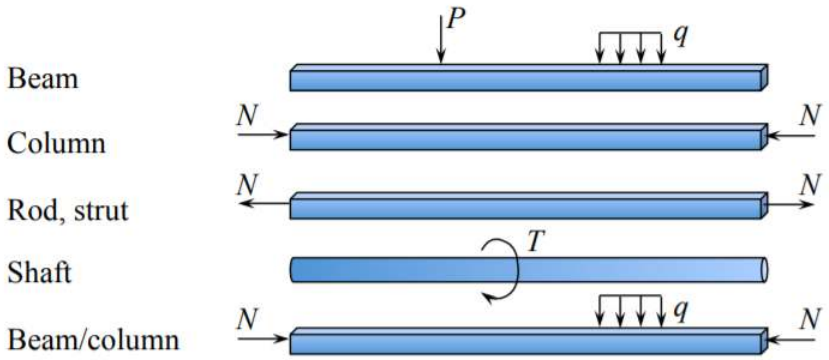

Figure 1.4.1: The type of loading distinguishes between five different types of structures.

All the above structures may have a similar slenderness. How slender the structure must be to become a beam. The slenderness is defined as a length to thickness ratio $\frac{l}{h}$. If $\frac{l}{h} > 20$, the beam obeys the simplified kinematic assumptions and it is called an “Euler beam”. Much shorter beams with $\frac{l}{h} < 10$ develop considerable shear stresses in addition to bending stresses and must be treated by a different set of assumptions. Such beams are referred to as Timoshenko beams. The intermediate range $10 < \frac{l}{h} < 20$ is a grey area where the simplifying assumptions of the elementary beam theory gradually lose validity.

This section deals with a solid section beams, as opposed to thin-walled sections. In the present lecture notes, the rectangular right handed coordinate system (x, y, z) is consistently used. The x-axis is directed along the length of the beam with an origin at a convenient location, usually the end of the center of the beam. The y-axis is in the width direction with its origin on the symmetry plane of the cross-section, Figure (1.4.2). Finally, the z-axis is pointing out down and it is measured from the centroidal axis of the cross-section (see Recitation 2 for the definition of a centroidal axis).

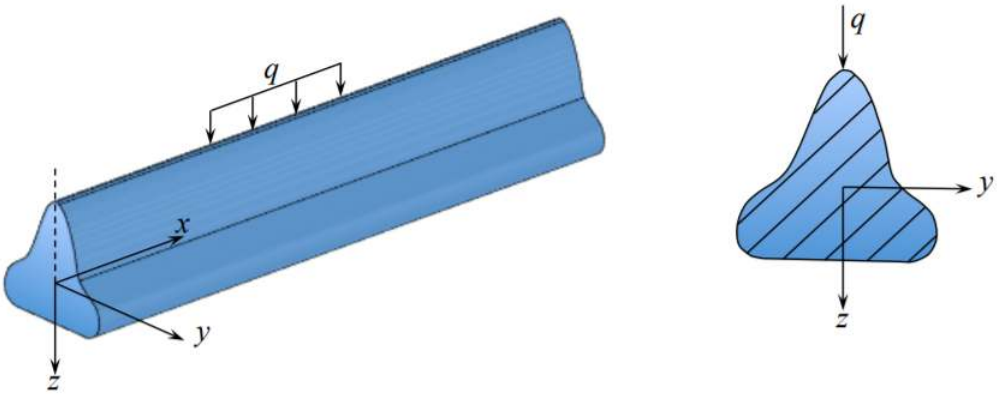

Figure 1.4.2: A prismatic slender beam with a symmetric cross-section.

In structural mechanics the components of the displacement vector in x, y, and z directions are denoted respectively by (u, v, w). The development of elementary beam theory is based on three kinematic assumptions. Additional assumptions on the stress state will be introduced later.

1.5: Euler-Bernoulli Hypothesis

In this section reference is often made to the beam axis. The meaning of the beam axis is intuitive for a prismatic beam with a rectangular cross-section. It is the middle axis. Other terms, such as: neutral axis, bending axis and centroidal axis are also frequently used. They all express the same property that no axial stresses σ_{xx} should develop on the axis under pure bending.

Hypothesis 1: Plan Remains Plane

This is illustrated in Figure (1.5.1) showing an arbitrary cross-section of the beam before and after deformation.

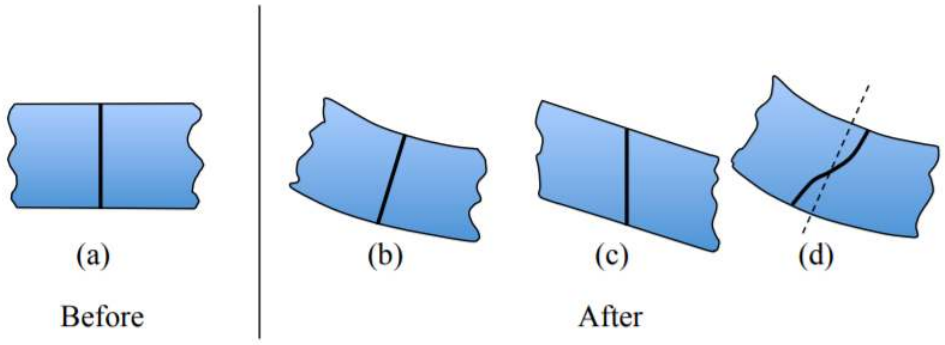

Figure 1.5.1: Flat (b) and (c) and warped (d) cross-sections after deformations.

Imagine a straight cut made through the undeformed beam. The plane-remains-plane hypothesis means that all material points on the original cut align also on a plane in the deformed beam. The cases (b) and (c) obey the hypothesis but the warped section (d) violates it.

Hypothesis 2: Normal Remains Normal

If the initial cut were made at right angle of the undeformed beam axis as in Figure (1.5.2(a)), it should remain normal to the deformed axis, see Figure (1.5.2(b)).

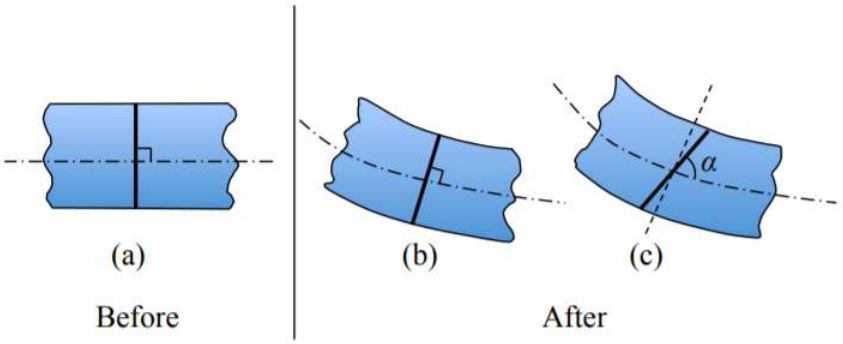

Figure 1.5.2: Testing the normal-remains-normal hypothesis.

In the sketch on Figure (1.5.2(c)) the hypothesis is violated when the angle $\alpha \neq 90°$.

The Euler-Bernoulli hypothesis gives rise to an elegant theory of infinitesimal strains in beams with arbitrary cross-sections and loading in two out-of-plane directions. The interested reader is referred to several monographs with a detailed treatment of the subject, of bi-axial loading of beams. The present set of notes on beams is developed under the assumption of planar deformation. This means that the beam axis motion is restricted only to one plane.

Mathematically, the Hypothesis 1 is satisfied when the u-component of the displacement vector is a linear function of z.

$$u(z) = u^{\circ} - \theta z \text{ at any } x \tag{1.5.1}$$

The constant first term, u° is the displacement of the beam axis (due to axial force). The second term is due to bending alone, Figure (1.5.3).

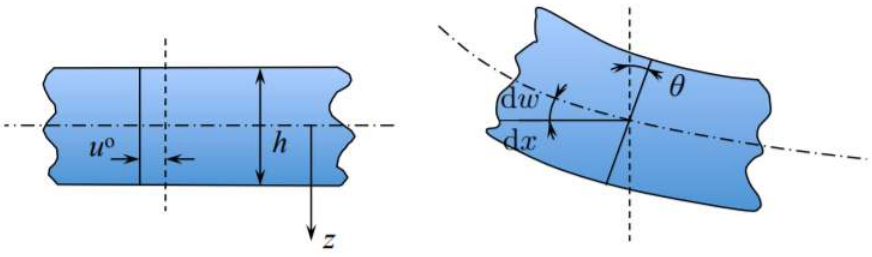

Figure 1.5.3: Linear displacement field through the thickness of the beams.

The second Euler-Bernoulli hypothesis is satisfied if the rotation of the deformed crosssection θ is equal to the local slope of the bent middle axis $\frac{dw}{dx}$

$$\theta = \frac{dw}{dx} \tag{1.5.2}$$

Eliminating the rotation angle θ between equations 1.5.1 and 1.5.2 yields

$$u(x,z) = u^\circ - \frac{dw}{dx} z \tag{1.5.3}$$

It can be seen from Figure (1.5.3) that the displacement at the bottom (tensile) side of the beam is negative, which explains the minus sign in the second term of Equations 1.5.2 and 1.5.3.

Hypothesis 3

The cross-sectional shape and size of the beam remain unchanged. This means that the vertical component of the displacement vector does not depend on the z-coordinate. All points of the cross-section move by the same amount.

$$w = w(x) \tag{1.5.4}$$

In the case of planar deformation, which covers most of the practical cases of the beam response, the y-component of the displacement vector vanishes

$$v = 0 \tag{1.5.5}$$

We are now in the position to calculate all components of the strain tensor from Equation (1.2.10)

$$\epsilon_{xx} = \frac{du_x}{dx} = \frac{du}{dx} \tag{1.5.6}$$

$$\epsilon_{zz} = \frac{du_y}{dy} = \frac{dv}{dy} = 0 \text{ on account of 1.5.13} \tag{1.5.7}$$

$$\epsilon_{zz} = \frac{du_{zz}}{dz} = \frac{dw(x)}{dz} = 0 \text{ from 1.5.4} \tag{1.5.8}$$

$$\epsilon_{xy} = \frac{1}{2}\left(\frac{du_x}{dy} + \frac{du_y}{dx}\right) = 0 \text{ from 1.5.3 and 1.5.13} \tag{1.5.9}$$

$$\epsilon_{yz} = \frac{1}{2}\left(\frac{du_y}{dz} + \frac{du_z}{dy}\right) = \frac{1}{2}\left(\frac{dv}{dz} + \frac{dw}{dy}\right) = 0 \tag{1.5.10}$$

$$\begin{aligned} \epsilon_{xx} &= \frac{1}{2}\left(\frac{du_z}{dx} + \frac{du_x}{dz}\right) = \frac{1}{2}\left(\frac{dw}{dx} + \frac{du}{dz}\right) \\ &= \frac{1}{2}\left(\frac{dw}{dx} - \frac{dw}{dx}\right) = 0 \end{aligned} \tag{1.5.11}$$

It is seen that all components of the strain tensor vanish except the one in the direction of beam axis.

Note that ϵ_{xx} is the only component of the strain tensor in the elementary beam theory. Therefore the subscript "xx" can be dropped and, unless specified otherwise $\epsilon_{xx} = \epsilon$. Introducing Equation 1.5.3 into Equation 1.5.4 one gets

$$\epsilon(x,z) = \frac{du^\circ(x)}{dx} - \frac{d^2w(x)}{dx^2}z \tag{1.5.12}$$

The first term represents the strain arising from a uniform extension of the entire cross-section

$$\epsilon^\circ(x) = \frac{du^\circ(x)}{dx} \tag{1.5.13}$$

The second term adds a contribution of bending. Introducing the definition of the curvature of the beam axis

$$\kappa \overset{\text{def}}{=} -\frac{d^2w(x)}{dx^2}, \tag{1.5.14}$$

the expression for strain can be put in the final form:

$$\epsilon(x,z) = \epsilon^\circ(x) + z\kappa \tag{1.5.15}$$

Mathematically, the curvature is defined as a gradient of the slope of a curve. The minus sign in Equation (1.3.4) follows from the rigorous description of the curvature of a line in the assumed coordinate system. Physically, it assumes that strains on the tensile side of the beam are positive. A quite different interpretation of the Euler-Bernoulli hypothesis is offered by considering a two-term expansion of the exact strain profile in the Taylor series around the point

$$\epsilon(x,z) = \epsilon(x,z) = |_{z=0} + \left.\frac{d\epsilon}{dz}\right|_{z=0} z + \frac{1}{2}\left.\frac{d^2\epsilon}{dz^2}\right|_{z=0} z^2 + \ldots \tag{1.5.16}$$

Taking only the first two terms is a good engineering approximation but leads to some internal inconsistencies of the elementary beam theory. These inconsistencies will be explained in the two subsequent chapters.

1.6: Strain-Displacement Relation of Thin Plates

The present course 2.080 is a prerequisite for a more advanced course 2.081 on Plates and Shells. A complete set of lecture notes for 2.081 is available on OpenCourseWare. The interested reader will find there a complete presentation of the theory of moderately large deflection of plates, derived from first principles. Here only a short summary is given.

Notation

In the lectures on plates and shells two notations will be used. The formulation and some of the derivation will be easier (and more elegant) by invoking the tensorial notation. Here students should flip briefly to Recitation 1 where the above mathematical manipulations are explained. For the purpose of the solving plate problems, the expanded notation will be used.

Points on the middle surface of the plate are described by the vector $\{x_1, x_2\}$ or x_α, $\alpha = 1, 2$ in tensor notation or $\{x, y\}$ in expanded notation.

Likewise, the in-plane components of the displacement vector are denoted by $\{u, v\}$. The vertical component of the displacement vector in the z-direction is denoted by w.

Plate versus Beam Theory

The plate theory requires fewer assumptions and is more self-consistent than the beam theory. For one, there are no complications arising from the concept of the centroidal axis for arbitrarily shaped prismatic beams. The z-coordinate is measured from the middle plane which is self explanatory. Finally, the flexural/torsional response of non-symmetric and/or thin-walled cross-section beams is not present in plates. The complexity of the plate formulation comes from the two-dimensionality of the problem. The ordinary differential equations in beams are now becoming partial differential equations.

1.7: Advanced Topic- Derivation of the Strain-Displacement Relation for Thin Plates

The Love-Kirchoff hypothesis extends the one-dimensional Euler-Bernoulli assumptions into plates. A plate can be bent in two directions, forming a double curvature surface. Therefore the plane-remains-plane and normal-remains-normal properties are now required in both directions. Thus, Equation (1.5.1) and Equation (1.5.2) take the form

$$u_\alpha = u_\alpha^\circ - \theta_\alpha z \tag{1.7.1}$$

$$\theta_\alpha = \frac{\partial w}{\partial x_\alpha} \overset{\text{def}}{=} w_{,\alpha} \tag{1.7.2}$$

where θ_α is the slope (rotation) in x_α-direction. Upon elimination of θ_α between the above equation, one gets the familiar linear dependence of the in-plane components of the displacement vector on the z-coordinate

$$u_\alpha(x_\alpha, z) = u_\alpha^\circ(x_\alpha) - z w_{,\alpha} \tag{1.7.3}$$

The constant thickness $(w = \dot{w}(x_\alpha))$ is the third kinematic assumption of the plate theory.

Now, watch carefully how the strain components in the plate are calculated. Considering all components of the strain tensor, one can distinguish three in-plane strain components $\epsilon_{\alpha\beta}$ (framed area on the matrix below) and three out-of-plane components.

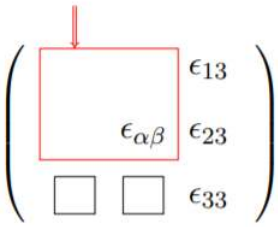

The through thickness strain component vanishes on the assumption of independence of the vertical displacement on the coordinate z

$$\epsilon_{33} = \epsilon_{zz} = \frac{\delta w}{\delta z} = 0 \tag{1.7.4}$$

The two out-of-plane shear components of the strain tensor $\epsilon_{\alpha 3}$ vanish due to the LoveKirchoff hypothesis, Equation 1.7.3,

$$\epsilon_{\alpha 3} = \frac{1}{2}\left(\frac{\delta u_\alpha}{\delta z} + \frac{\delta w}{\delta x_\alpha}\right) = \frac{1}{2}(u_{\alpha,z} + w_{,\alpha}) = \frac{1}{2}\left[\frac{d}{dz}(u_\alpha^\circ(x_\alpha) + w_{,\alpha}\right] = 0 \tag{1.7.5}$$

The non-vanishing components of the strain tensor are the in-plane strain components

$$\epsilon_{\alpha\beta} = \frac{1}{2}(u_{\alpha,\beta} + u_{\beta,\alpha})\alpha, \beta = 1, 2 \tag{1.7.6}$$

where u_α is defined by Equation (1.3.9). Performing the differentiation one gets

$$\epsilon_{\alpha\beta} = \frac{1}{2}[u_\alpha^\circ - z w_{,\alpha}]_{,\beta} + \frac{1}{2}[u_\beta^\circ - z w_{,\beta}]_{,\alpha} = \frac{1}{2}(u_{\alpha,\beta}^\circ + u_{\beta,\alpha}^\circ) - \frac{1}{2} z[w_{,\alpha\beta} + w_{,\beta\alpha}] \tag{1.7.7}$$

The first term in Equation 1.7.7 is the strain $\epsilon_{\alpha\beta}^\circ$ arising from the membrane action in the plate. It is a symmetric gradient of the middle plane displacement u_α°. Since the order of partial differentiation is not important, Equation 1.7.7 simplifies to

$$\epsilon_{\alpha\beta}(x_\alpha, z) = \epsilon_{\alpha\beta}^\circ(x_\alpha) - z w_{,\alpha\beta} \tag{1.7.8}$$

Defining the curvature tensor $\kappa_{\alpha\beta}$ by

$$\kappa_{\alpha\beta} = -w_{,\alpha\beta} = -\frac{\partial^2 w}{\partial x_\alpha \partial x_\beta} \tag{1.7.9}$$

The strain-displacement relation for thin plates takes the final form

$$\epsilon_{\alpha\beta} = \epsilon^{\circ}_{\alpha\beta} + z\kappa_{\alpha\beta} \tag{1.7.10}$$

where

$$\epsilon^{\circ}_{\alpha\beta} = \frac{1}{2}(u^{\circ}_{\alpha,\beta} + u^{\circ}_{\beta,\alpha}) \tag{1.7.11}$$

1.8: Expanded Form of Strain-Displacement Relation

Having derived the geometric relations in the tensorial notations, equations (1.7.10) and (1.7.11) will be re-written in the coordinate system (x, y) and physical interpretation will be given to each term. Consider first (1.7.11)

$$\alpha = 1, \beta = 1 \; x_1 = x, \; \epsilon^{\circ}_{xx} = \frac{1}{2}\left(\frac{\partial u^{\circ}_x}{\partial x} + \frac{\partial u^{\circ}_x}{\partial x}\right) = \frac{\partial u^{\circ}_x}{\partial x} \tag{1.8.1}$$

$$\alpha = 2, \beta = 2 \; x_2 = y, \; \epsilon^{\circ}_{xx} = \frac{1}{2}\left(\frac{\partial u^{\circ}_y}{\partial y} + \frac{\partial u^{\circ}_y}{\partial y}\right) = \frac{\partial u^{\circ}_y}{\partial y} \tag{1.8.2}$$

$$\alpha = 1, \beta = 2 \; x_1 = x, x_2 = y, \; \epsilon^{\circ}_{xy} = \frac{1}{2}\left(\frac{\partial u^{\circ}_x}{\partial y} + \frac{\partial u^{\circ}_y}{\partial x}\right) \tag{1.8.3}$$

The ϵ°_{xx} and ϵ°_{yy} components denote strains of the middle surface of the plate in the x and y directions, respectfully. The membrane strains are due to the imposed displacements or membrane forces applied to the edges. In the theory of small deflection of plates, lateral pressure loading will not produce membrane strains. By contrast, membrane strains do develop in the theory of moderately large deflection of plates due to transverse loading. This topic will be covered later in Chapter 6.

The third component of the strain tensor is the in-plane shear strain ϵ°_{xy}. It represents the change of angles in the plane of the plate due to the shear loading at the edges. The geometrical interpretation of the membrane strain tensor is similar to that given for the general strain tensor in Figures (1.2.2) and (1.2.3).

The curvature tensor $\kappa_{\alpha\beta}$ requires a careful explanation. Consider an infinitesimal segment ds of a curve and fit into it a circle of an instantaneous radius ρ, Figure (**1.8.1**). Then

$$ds = \rho d\theta \tag{1.8.4}$$

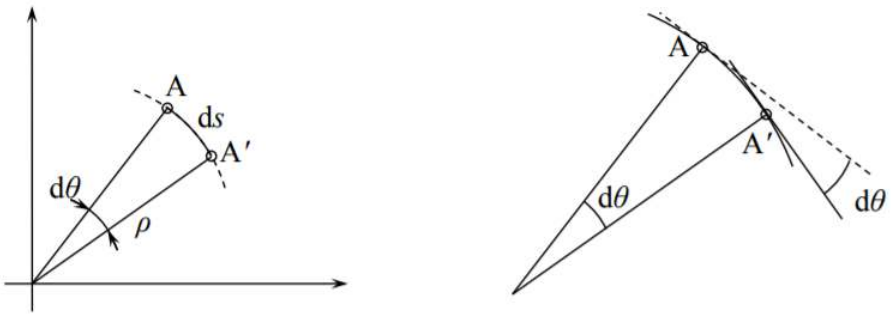

Figure **1.8.1**: Change of slope of a line between two points

Mathematically, the curvature of any line κ is the change of the slope as one moves along the curve

$$\kappa \overset{\text{def}}{=} \frac{d\theta}{ds} \tag{1.8.5}$$

By comparing Equation 1.8.5 with Equation (1.7.2), the curvature in $[\frac{1}{m}]$ is the reciprocity of the radius of curvature $\kappa = \frac{1}{\rho}$. The first component of the curvature tensor, defined by Equation (1.7.10) is

$$\alpha = 1, \beta = 1 \; x_1 = x \; \kappa_{xx} = -\frac{\partial^2 w}{\partial x^2} = -\frac{\partial}{\partial x}\left(\frac{\partial w}{\partial x}\right) = \frac{\partial}{\partial x}(-\theta_x) \tag{1.8.6}$$

This will be the only component of the curvature tensor if the plate is subject to the so-called cylindrical bending.

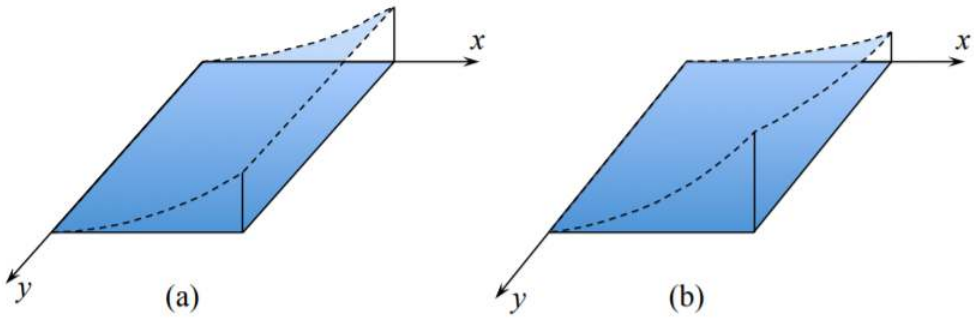

Figure 1.8.2: (a) cylindrical bending of a plate, and (b) bending with a twist.

The interpretation of the κ_{yy} components of the curvature tensor

$$\alpha = 2, \beta = 2 \; x_2 = y \; \kappa_{yy} = -\frac{\partial^2 w}{\partial y^2} = -\frac{\partial}{\partial y}(-\theta_y) \tag{1.8.7}$$

is similar as before. More interesting is the mixed component of the curvature tensor

$$\alpha = 1, \beta = 2 \; x_1 = x, x_2 = y \; \kappa_{xy} = -\frac{\partial^2 w}{\partial x \partial y} = -\frac{\partial}{\partial y}(-\theta_x) \tag{1.8.8}$$

To detect κ_{xy} one has to check if the slope in one direction, say θ_x changes along the second y-direction. It does not for a cylindrical bending, Figure (1.4.2(a)). But if it does, the plate is twisted, as shown in Figure (1.4.2(b)). Therefore, the component κ_{xy} is called a twist.

An important parameter that distinguishes between these classes of the deformed shape of a plate is the Gaussian curvature, κ_G. The Gaussian curvature is defined as a product of two principal curvatures

$$\kappa_G = \kappa_I \kappa_{II} \tag{1.8.9}$$

The curvature is a tensor, so its components change by rotating the coordinate system by an angle ψ to a new direction (x\prime , y\prime). There is one such an angle ψ_p for which the twisting components vanish. The remaining diagonal components are called principal curvature. The full coverage of the transformation formulae for vectors and tensors are presented in Recitation 2. Using these results, the Gaussian curvature can be expressed in terms of the components of the curvature tensor

$$\kappa_G = \kappa_{xx} \kappa_{yy} - \kappa_{xy}^2 \tag{1.8.10}$$

For cylindrical bending the twist κxy as well as one of the principal curvatures vanishes so that the Gaussian curvature is zero. The sign of the Gaussian curvature distinguishes between three types of the deformed plate, the bowl, the cylinder and the saddle, Figure (1.8.3).

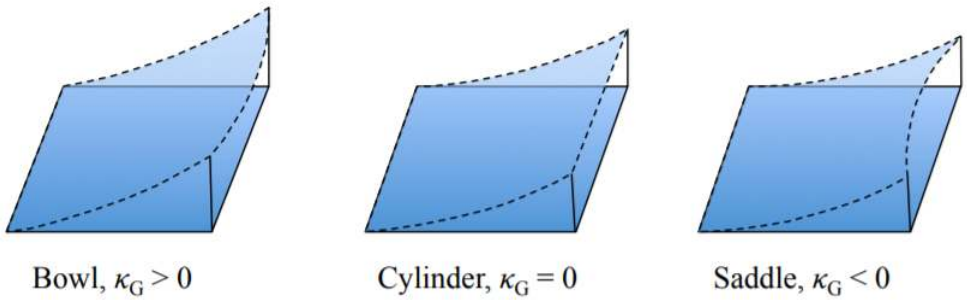

Figure 1.8.3: Deformed plate with three different classes of shapes.

The consideration of Gaussian curvature introduces important simplifications in formulation and applications of the energy method in structural mechanics. A separate lecture will be devoted to this topic.

1.9: Moderately Large Deflections of Beams and Plates

A complete presentation of the theory of moderately large deflections of plates, derived from first principles is presented in the course 2.081 Plates and Shells. The lecture notes for this course are available on OpenCourseWare. There the strain-displacement relation for the theory of moderately large deflection of beams are derived. Here the corresponding equations for plates are only stated with a physical interpretation. An interested reader is referred to the Plates and Shells notes for more details.

Defining moderately large deflections of beams

What are the "moderately large deflections" and how do they differ from the "small deflection". To see the difference, it is necessary to consider the initial and deformed configuration of the beam axis. The initial and current length element in the undeformed and deformed configuration respectively is denoted dx and ds, as in Figure (**1.9.1**)

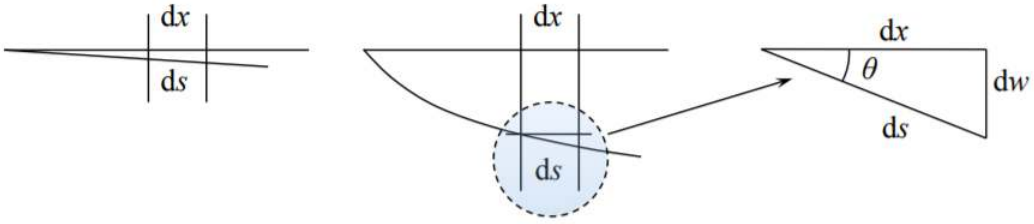

Figure **1.9.1**: Change of length of the beam axis produced by rotation.

From the geometry of the problem

$$dx = ds\cos\theta \approx ds\left[1-\frac{\theta^2}{2}\right] \tag{1.9.1}$$

One can distinguish between three theories:

(i) Small deflections, linear geometry $\theta^2 \ll 1,\ dx \approx ds$, Figure (**1.9.1**(a)).

(ii) Moderately large deflections. The two-term expansion of the cosine function gives a good approximation for $0 < \theta < 10°$. Relation between dx and ds is given by Equation 1.9.1, Figure (**1.9.1**(b)).

(iii) For larger rotation, a full nonlinearity of the problem must be considered.

The present derivation refers to case (ii) above. The Cauchy strain measure, defined in Equation (1.1.3) is adopted:

$$\epsilon = \frac{ds^2 - dx^2}{2dx^2} \tag{1.9.2}$$

The current length ds can be expressed in terms of dx and dw, see Figure (**1.9.1**)

$$ds^2 = dx^2 + dw^2 \tag{1.9.3}$$

From the above two equations, the strain of the beam axis due to element rotation, ϵ_{rot} is

$$\epsilon = \frac{1}{2}\left(\frac{dw}{dx}\right)^2 = \frac{1}{2}\theta^2 \tag{1.9.4}$$

The beam axis also extends due to the gradient of the axial component of the displacement vector, defined by Equation (1.5.13). Therefore the total strain of the beam axis due to the combined extension and rotation is

$$\epsilon^\circ = \frac{du}{dx} + \frac{1}{2}\left(\frac{dw}{dx}\right)^2 \tag{1.9.5}$$

It can be noticed that the second term in the above equation is always positive while the first term can be either positive or negative. In a special case the two terms can cancel one another even though a beam undergoes large deformation.

The question often asked by students is if the expression for the curvature, given by Equation (1.5.14) should also be modified due to larger rotation. From the mathematical point of view the answer is YES. But engineers have a way to get around it.

In the rectangular coordinate system the exact definition of the curvature of the line is:

$$\kappa = \frac{-\frac{d^2w}{dx^2}}{\left(1+\left(\frac{dw}{dx}\right)^2\right)^{3/2}} \tag{1.9.6}$$

In the limit $\frac{dw}{dx} \to 0$ the linear definition is recovered from the nonlinear equation Equation **1.9.6**. The difference between Equation (1.5.14) and Equation **1.9.6** is small in the case of moderately large deflection.

The total strain at an arbitrary point of a beam undergoing moderately large deflection is

$$\epsilon = \underbrace{\frac{du}{dx} + \frac{1}{2}\left(\frac{dw}{dx}\right)^2}_{\text{membrane strain } \epsilon^o} + \underbrace{z\kappa}_{\text{bending strain } z\kappa} \tag{1.9.7}$$

Extension to Moderately Large Deflection of Plates

In the compact tensorial notation, the nonlinear strain-displacement relation takes the form

$$\epsilon_{\alpha\beta} = \frac{1}{2}(u_{\alpha,\beta} + u_{\beta,\alpha}) + \frac{1}{2}w_{,\alpha}w_{,\beta} + z\kappa_{\alpha\beta} \tag{1.9.8}$$

By comparing with a similar expression for the small deflection theory, Equation (1.7.10) and Equation (1.7.11), the new nonlinear term is

$$\frac{1}{2}w_{,\alpha}w_{,\beta} = \frac{1}{2}\frac{\partial w}{\partial x_\alpha}\frac{\partial w}{\partial x_\beta} \tag{1.9.9}$$

This term forms a 2×2 matrix:

$$\begin{vmatrix} \frac{1}{2}\left(\frac{\partial w}{\partial x}\right)^2 & \frac{1}{2}\frac{\partial w}{\partial w}\frac{\partial x}{\partial y} \\ \frac{1}{2}\frac{\partial w}{\partial y}\frac{\partial w}{\partial x} & \frac{1}{2}\left(\frac{\partial w}{\partial y}\right)^2 \end{vmatrix} = \begin{vmatrix} \frac{\theta_x^2}{2}, \frac{1}{2}\theta_x\theta_y \\ \frac{1}{2}\theta_x\theta_y, \frac{\theta_y^2}{2} \end{vmatrix} \tag{1.9.10}$$

The diagonal terms represent square of the slope of the deflection shape in x and y directions. The non-diagonal terms are symmetric and are a product of slopes in the two directions. This term vanishes for cylindrical bending.

1.10: Strain-Displacement Relations for Circulate Plates

The theory of circular plates is formulated in the cylindrical coordinate system (r, θ, z). The corresponding components of the displacement vector are (u, v, w). In the remainder of the notes, the axi-symmetric deformation is assumed, which would require the loading to be axi-symmetric as well. This assumption brings four important implications

i. The circumferential component of the displacement is zero, $v \equiv 0$
ii. There are no in-plane shear strains, $\epsilon_{r\theta} = 0$
iii. The radial and circumferential strains are principal strains
iv. The partial differential equations for plates reduces to the ordinary differential equation where the radius is the only space variable.

Many simple closed-form solutions can be obtained for circular and annular plates under different boundary and loading conditions. Therefore such plates are often treated as prototype structures on which certain physical principles could be easily explained.

The membrane strains on the middle surface are stated without derivation

$$\epsilon^{\circ}_{rr} = \frac{du}{dr} + \frac{1}{2}\left(\frac{dw}{dr}\right)^2 \tag{1.10.1}$$

$$\epsilon^{\circ}_{\theta\theta} = \frac{u}{r} \tag{1.10.2}$$

The two principal curvatures are

$$\kappa_{rr} = -\frac{d^2w}{dr^2} \tag{1.10.3}$$

$$\kappa_{\theta\theta} = -\frac{1}{r}\frac{dw}{dr} \tag{1.10.4}$$

The sum of the bending and membrane strains is thus given by

$$\epsilon_{rr}(r, z) = \epsilon^{\circ}_{rr}(r) + z\kappa_{rr} \tag{1.10.5}$$

$$\epsilon_{\theta\theta}(r, z) = \epsilon^{\circ}_{\theta\theta}(r) + z\kappa_{\theta\theta} \tag{1.10.6}$$

It can be noticed that the expression for the radial strains and curvature are identical to those of the beam when r is replaced by x. The expressions in the circumferential direction are quite different.

CHAPTER OVERVIEW

2: The Concept of Stress, Generalized Stresses and Equilibrium

---

2.1: Stress Tensor

We start with the presentation of simple concepts in one and two dimensions before introducing a general concept of the stress tensor. Consider a prismatic bar of a square cross-section subjected to a tensile force F,

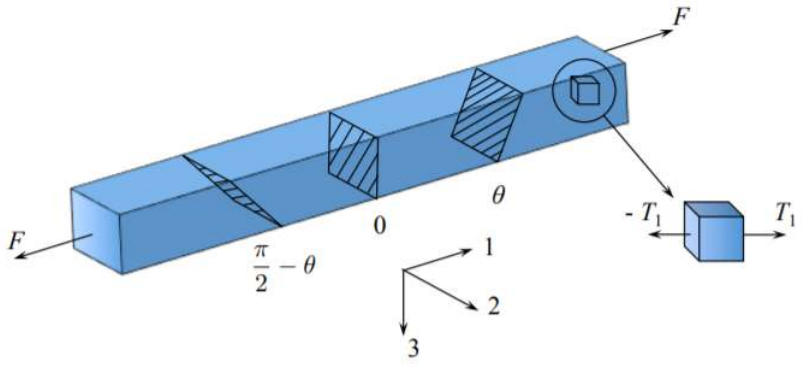

Figure 2.1.1: A long bar with three different cuts at $\theta, \theta = 0$ and $\pi/2 - \theta$.

The force per unit area is called the surface traction T:

$$T = \sigma = \frac{\text{force}}{\text{area}} = \frac{F}{A_o} \left[\frac{\text{N}}{\text{mm}^2}\right] \tag{2.1.1}$$

In the uniaxial case, the surface traction is the only component of the stress tensor in the global coordinate system, commonly referred to as σ.

How can one apply a force to the end section of a bar? This can be done in a number of different ways (see Figure (2.1.2)). A pin connection can be glued (or welded) to the end section, or a hole can be drilled through the bar to attach a pin.

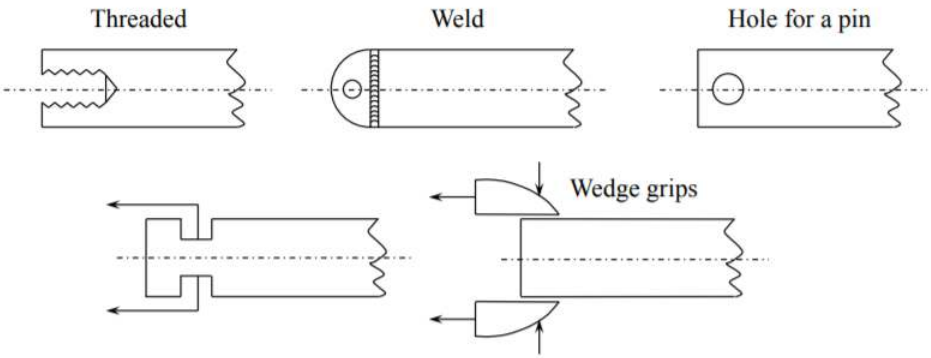

Figure 2.1.2: How to apply tension to the end of a bar.

Or an internal or external thread can be machined. Finally, axial force could be applied through frictional or mechanical grips. Except the welded or glued connector, a complex state of stress is created near the bar ends where the stress state is multi-axial. Such stress states is confined to a relatively short segment of the bar comparable with the height or diameter of the bar. Along this section a gradual transition takes place from the multi-axial state of stress to the uniaxial state, for which Equation 2.1.1 holds.

Note

The above example an serve as a practical application of the Saint-Venant's principle (1856). This principle named after the French elasticity theorist, Jean Claude Barre' de Saint-Venant can be stated as: "the difference between the effects of two different but statically equivalent loads become very small at sufficiently large distances from load."

Think what are the “two” equivalent loads that are applied to the bar ends? We usually think of a cross-section being cut perpendicular to the axis of the bar. Consider now two cuts at the angles θ and $(\frac{\pi}{2}-\theta)$ to the normal direction. The planes are defined by the unit normal vector $\boldsymbol{n}$.

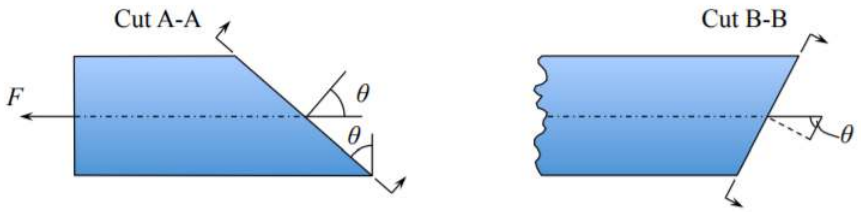

Figure **2.1.3**: Normal and tangential forces acting on the slant section of the bar.

From the free body diagram, the components of the normal and tangential forces:

$$F_{\mathrm{N}} = F\cos\theta \tag{2.1.2}$$

$$F_{\mathrm{n}} = F\cos(\frac{\pi}{2}-\theta) \tag{2.1.3}$$

$$F_{\mathrm{T}} = F\sin\theta \tag{2.1.4}$$

$$F_{\mathrm{t}} = F\sin(\frac{\pi}{2}-\theta) \tag{2.1.5}$$

The slant cross-section $\boldsymbol{A}$ is larger and is related to the reference cross-section by

$$A_o = A_{\mathrm{A}}\cos\theta,\ A_o = A\mathrm{B}\cos(\frac{\pi}{2}-\theta) \tag{2.1.6}$$

Consider now a unit volume cubic element located at the intersections of cuts A-A and B-B, Figure (**2.1.4**).

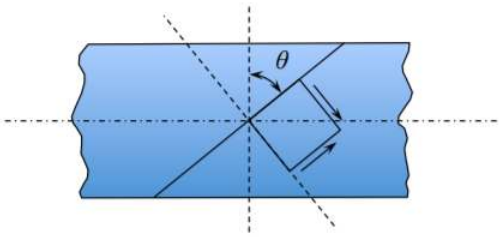

Figure **2.1.4**: The volume element with surface traction acting on two adjacent facets.

The surface traction (force per unit area) on the two perpendicular facets are

$$\textbf{Facet parallel to A-A:}\quad T_{\mathrm{n}} = T\cos^2\theta \tag{2.1.7}$$

$$T_{\mathrm{t}} = T\sin\theta\cos\theta \tag{2.1.8}$$

$$\textbf{Facet parallel to B-B:}\quad T_{\mathrm{n}} = T\cos^2(\frac{\pi}{2}-\theta) \tag{2.1.9}$$

$$T_{\mathrm{t}} = T\sin(\frac{\pi}{2}-\theta)\cos(\frac{\pi}{2}-\theta) \tag{2.1.10}$$

It can be observed that the tangential components of the surface traction vector on A-A and B-B cuts are identical. The normalized plots of the above quantities versus the orientation angle of the cross-section are shown in Figure (**2.1.5**).

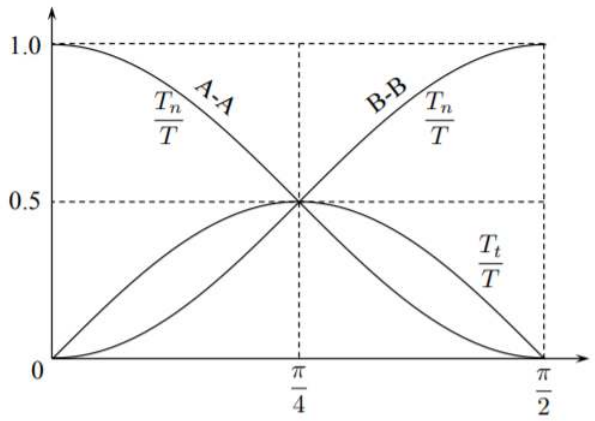

Figure **2.1.5**: Relative values of normal and shear components of the surface traction as a function of the orientation of the cut.

It can be noted that the tangential component attains maximum at **45°**. This means that if the material fails due to shear loading, the fracture surface will always be oriented at **45°**. The above example teaches us that there are infinite combinations of normal and tangential components of surface tractions which are in equilibrium with the applied load. For each orientation of the cross-section there is a different pair of $\{T_n, T_t\}$. The orientation of the surface element is uniquely defined by the unit normal vector $n\{n_1, n_2, n_3\}$. At the same time the components of the surface traction vector acting on the same element are $T\{T_1, T_2, T_3\}$.

The components of the surface traction vector acting on this surface element are $T\{T_1, T_2, T_3\}$. For example, the orientation of facets of the unit material cube is shown in Figure (**2.1.6**).

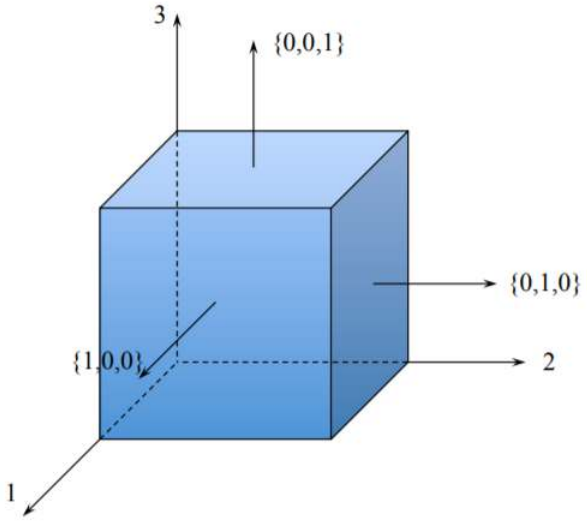

Figure **2.1.6**: Components of the unit normal vector on facets of a unit cube.

The relation between the vectors of surface tractions, unit normal vector defining the surface element and the stress tensor are given by the famous Cauchy formula

$$T_i = T_{ij} n_j \tag{2.1.11}$$

or in the expanded notation,

$$T_1 = \sigma_{1j} n_j = \sigma_{11} n_1 + \sigma_{12} n_2 + \sigma_{13} n_3 \tag{2.1.12}$$

$$T_2 = \sigma_{2j} n_j = \sigma_{21} n_1 + \sigma_{22} n_2 + \sigma_{23} n_3 \tag{2.1.13}$$

$$T_3 = \sigma_{3j} n_j = \sigma_{31} n_1 + \sigma_{32} n_2 + \sigma_{33} n_3 \tag{2.1.14}$$

To a large extent the Cauchy relation is analogous to the strain-displacement relation put in the form of Equations 2.1.2 - 2.1.5.

$$du_i = F_{ij} dx_j \tag{2.1.15}$$

The displacement gradient F_{ij} transforms the increment of the length element dx_j into the increment of displacement du_i. In the same way the stress tensor transforms the orientation of the surface element n into the surface traction acting on this element.

In order to get a physical interpretation of the concept of the stress tensor, let us see how the Cauchy formula works in the case of one and two-dimensional problems of the axially loaded bar. Consider first the normal cut of the bar with the longitudinal axis as 1-axis. The components of the surface tractions are given in Figure (2.1.7). The corresponding components of the unit normal vector were defined in Figure (2.1.6), where $T = \frac{F}{A_o}$.

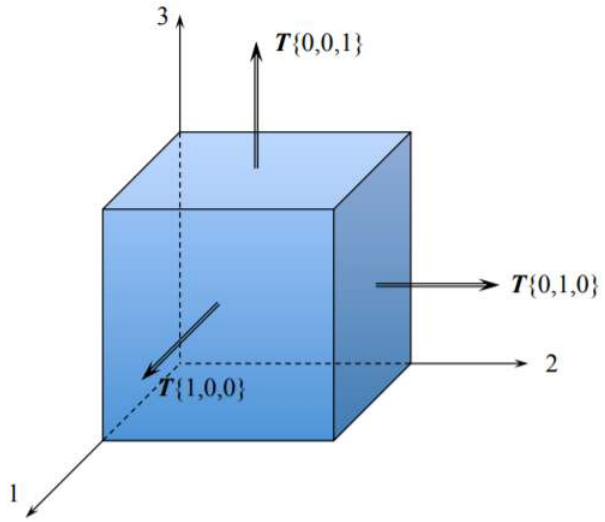

Figure 2.1.7: The unit volume element aligned with the axis of the bar.

Substituting the values of the components of the two vectors into Equation 2.1.13 one gets the following expressions:

Facet(1, 0, 0)	Facet(0, 1, 0)	Facet(0, 0, 1)
$T_1 = \sigma_{11}$	$0 = \sigma_{12}$	$0 = \sigma_{13}$
$0 = \sigma_{21}$	$0 = \sigma_{22}$	$0 = \sigma_{23}$
$0 = \sigma_{31}$	$0 = \sigma_{32}$	$0 = \sigma_{33}$

(2.1.16)

Therefore the components of the stress 3×3 matrix in the global coordinate system are

$$\sigma = \begin{vmatrix} T & 0 & 0 \\ 0 & 0 & 0 \\ 0 & 0 & 0 \end{vmatrix} \tag{2.1.17}$$

This is the uniaxial state of stress. The two-dimensional example of the slant cut is much more interesting. This time a local coordinate system, rotated with respect to the 3-axis will be used. In this system the components n are the same as in the global system. The components of the surface traction vector on three facets, calculated in Equation 2.1.8 are defined in Figure (2.1.8).

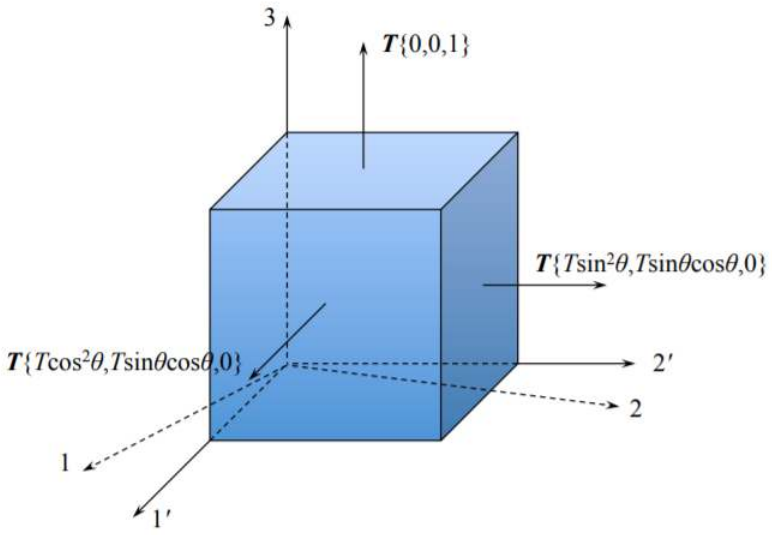

Figure 2.1.8: Components of the surface tractions on the rotated volume element.

Substituting the above values into the Cauchy formula we obtain

$$\begin{array}{c|c|c} \text{Facet}(1,0,0) & \text{Facet}(0,1,0) & \text{Facet}(0,0,1) \\ T\cos^2\theta = \sigma_{11} & T\sin\theta\cos\theta = \sigma_{12} & 0 = \sigma_{13} \\ T\sin\theta\cos\theta = \sigma_{21} & T\sin^2\theta = \sigma_{22} & 0 = \sigma_{23} \\ 0 = \sigma_{31} & 0 = \sigma_{32} & 0 = \sigma_{33} \end{array} \tag{2.1.18}$$

The plane stress components of the stress tensor are

$$\sigma = \begin{vmatrix} T\cos^\theta & T\sin\theta\cos\theta & 0 \\ T\sin\theta\cos\theta & T\sin^2\theta & 0 \\ 0 & 0 & 0 \end{vmatrix} \tag{2.1.19}$$

It is interesting that the matrices Equation 2.1.17 and Equation 2.1.19 represent the same state of stress seen in two coordinate systems rotated with respect to one another. The transformation of the stress tensor from one coordinate system to the other is the subject Recitation 1 where the relation between Equation 2.1.17 and Equation 2.1.19 will be derived in a different way.

Symmetry of the stress tensor

It should also be noted from Equation 2.1.19 that stress tensor is symmetric meaning that $\sigma_{12} = \sigma_{21}$. The symmetry of the stress tensor comes from the moment equilibrium equation of are infinitesimal volume element. In general

$$\sigma_{ij} = \sigma_{ji} \tag{2.1.20}$$

The symmetry of the stress tensor reduce the nine components of the 3×3 metric to only six independent components. The meaning of the two subscripts of the stress tensor is explained below

$$\sigma_{??}$$

The first subscript defines the plane on which the surface tractions are acting. For example “1” denotes the surface element perpendicular to the axis x_1. The second subscript indicates direction of a particular component of the surface tractions. This convention is explained in Figure (2.1.9).

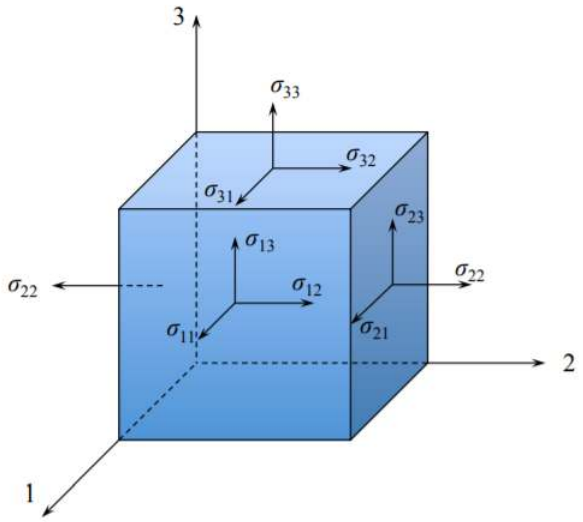

Figure **2.1.9**: Components of the stress tensor on three facets of the infinitesimal surface element.

Sign convention

The Cauchy formula can also be consistently used to determine the sign of the components of the stress tensor. The point is that the sign of the components of the vectors is known from the chosen coordinate system. For illustration, let us orient the volume element along the x_1 axis. With positive direction to the right.

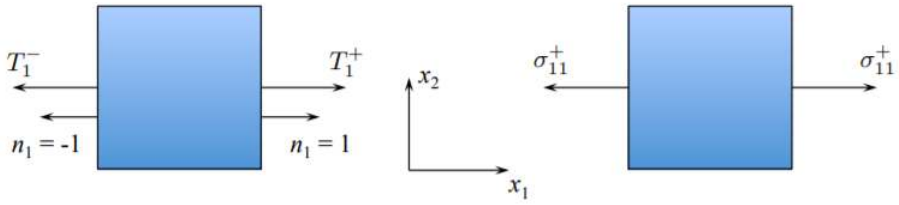

Figure **2.1.10**: Explanation of the sign convention of the stress tensor.

From the Cauchy formula

$$T_1 = \sigma_{11} n_1 \tag{2.1.21}$$

On the right facet both the surface traction and the unit normal vector is positive and so must be the normal component of the stress tensor σ_{11}. On the left facet both T_1 and to the x_1 axis. In order for Equation 2.1.21 to hold the component σ_{11} must be positive, even if its visualization points out in the negative direction. in the above example the stress state is uniform along the x_1 axis. This is the case of a bar under tension. In general there is a gradient of the components of the stress tensor so that stresses on both sides of the infinitesimal element differ by a small amount of $d\sigma_{11}$. The sign convention is opening the way for deriving the equations of equilibrium for the 3-D continuum. This topic is the subject of the next section.

Equilibrium

The equilibrium equation for an infinitesimal volume element are derived first using two methods. Referring to Figure (**2.1.9**), indicated on Figure (**2.1.11**) are only those components of the stress tensor that are directed along x_2 axis. These are σ_{12}, σ_{22} and σ_{32}.

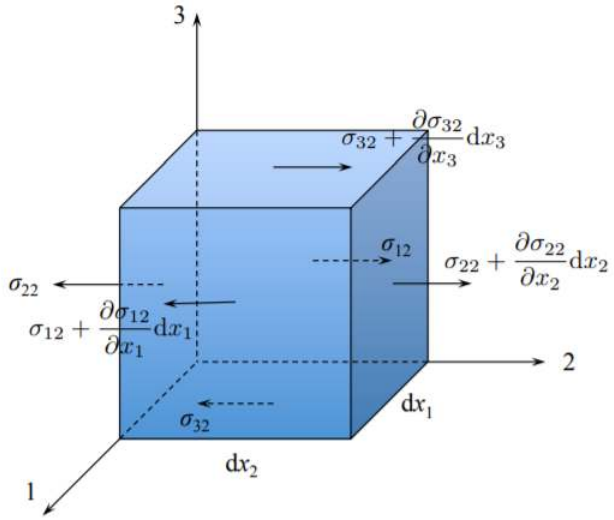

Figure 2.1.11: All components of the stress tensor contributing to the force equilibrium in x_2 direction must be in equilibrium.

According to Newton's law, the sum of all forces (stress times the surface area) acting along x_2 must be zero

$$\left(\sigma_{22} + \frac{\partial \sigma_{22}}{\partial x_2} dx_2\right) dx_1 dx_3 - \sigma_2 dx_1 dx_3 + \left(\sigma_{12} + \frac{\partial \sigma_{12}}{\partial x_1} dx_1\right) dx_2 dx_3 - \sigma_{12} dx_2 dx_3 + \left(\sigma_{32} + \frac{\partial \sigma_{32}}{\partial x_3} dx_3\right) dx_1 dx_2 - \sigma_{32} dx_1 dx_2 + B_2 dx_1 dx_2 dx_3 = 0 \tag{2.1.22}$$

For generality, the body force (force per unit volume) was included as well. The body force represent for example gravity force $B = \rho g$ or d'Alambert inertia force $B = \rho \ddot{u}$ so that the derivation is valid both for static and dynamic problems. Summing up the forces one gets the first equilibrium equation

$$\frac{\partial \sigma_{22}}{\partial x_2} + \frac{\partial \sigma_{12}}{\partial x_1} + \frac{\partial \sigma_{32}}{\partial x_3} + B_2 = 0 \tag{2.1.23}$$

Invoking the index notation

$$\frac{\partial \sigma_{j2}}{\partial x_j} + B_2 = 0 \rightarrow \sigma_{j2,j} + B_2 = 0 \tag{2.1.24}$$

with the summation and coma convention. A similar procedure of summing-up forces can be repeated in the x_1 and x_3 direction, yielding two additional equations of equilibrium. One can immediately notice that by replacing the life subscripts "2" in Equation 2.1.24 respectively by "1" and "3", the final compact form of the equation of equilibrium reads

$$\sigma_{ij,j} + B_i = 0 \text{ or } \frac{\partial \sigma_{ij}}{\partial x_j} + B_i = 0 \tag{2.1.25}$$

In the expanded notation and replacing x_i by (x, y, z), the familiar form of the equilibrium equation is

$$\frac{\partial \sigma_{xx}}{\partial x} + \frac{\partial \sigma_{xy}}{\partial y} + \frac{\partial \sigma_{xz}}{\partial z} + B_x = 0 \tag{2.1.26}$$

$$\frac{\partial \sigma_{yx}}{\partial x} + \frac{\partial \sigma_{yy}}{\partial y} + \frac{\partial \sigma_{yz}}{\partial z} + B_y = 0 \tag{2.1.27}$$

$$\frac{\partial \sigma_{zx}}{\partial x} + \frac{\partial \sigma_{zy}}{\partial y} + \frac{\partial \sigma_{zz}}{\partial z} + B_z = 0 \tag{2.1.28}$$

The plane stress case, prevailing in thin plate and shells is defined by

$$\sigma_{3j} = 0 \text{ or } \sigma_{31} = \sigma_{32} = \sigma_{33} = 0 \tag{2.1.29}$$

In other words all components of the stress tensor pointing out in the z-directions are zero, $\sigma_{zz} = \sigma_{xz} = \sigma_{zy} = 0$. The components of the plane stress tensor are highlighted by the framed area, thus $\boldsymbol{\sigma}$ is equal to

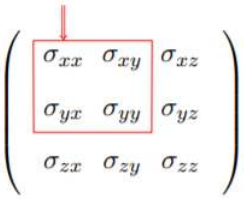

For plane stress, the subscripts run only over two dimensions and the Greek letters are commonly used, $\alpha, \beta = 1, 2$. In the compact notation, the plane stress equilibrium equation reads

$$\sigma_{\alpha\beta,\beta} + B_\alpha = 0 \tag{2.1.30}$$

In the uniaxial case only one component of the equilibrium survives, giving

$$\frac{d\sigma_{xx}}{dx} + B = 0 \tag{2.1.31}$$

With no body force, $B = 0$, Equation 2.1.31 predicts a constant stress along the length of the bar. The addition of the d'Alambert inertia force will lead to the one-dimensional wave equation.

2.2: Advanced Topic - Local Equilibrium from the Principle of Virtual Work

The derivation of the local equation of equilibrium from the global principle of virtual work is an elegant method in continuum and structural mechanics. This procedure also formulates static and kinematic boundary condition. There are two mathematical tools involved. One is the divergence theorem (Gauss-Green identity) and the other one is the concept of the calculus of variation.

The Gauss theorem transforms the volume integral into a surface integral

$$\int_V A_{i,i} dV = \int_S A_i n_i dS, \; A_{i,i} = \frac{\partial A_i}{\partial x_i} \tag{2.2.1}$$

where A_i is a vector and ni is the unit normal vector of the surface element dS. In the simplest one-dimensional case, Equation 2.2.1 is reduced to

$$\int_{x_1}^{x_2} \frac{dA}{dx} dx = A|_{x_1}^{x_2} = A(x_2) - A(x_1) \tag{2.2.2}$$

Starting from the definition of the infinitesimal strain given by Equation (2.1.22), the increments of the strain tensor and displacement vector are also linearly related

$$\delta\epsilon_{ij} = \frac{1}{2}(\delta u_{i,j} + \delta u_{j,i}) \tag{2.2.3}$$

There is a fine difference between the symbol δu and du, which is explained in Figure (2.2.1).

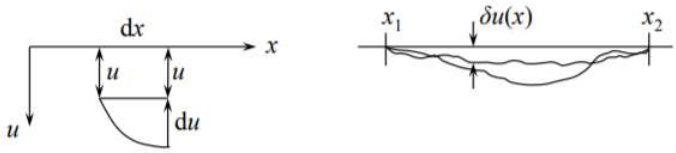

Figure 2.2.1: The local increment δu over the infinitesimal length dx and the global small (virtual) displacement from the equilibrium configuration satisfying kinematic boundary conditions.

Both are linear operators and the rule for differentiations are the same.

The principle of virtual work states that the incremental work of strains on the stresses over the volume of the body must be equal to the work of surface tractions in the incremental displacements over the surface of the body. Figure (2.2.2) helps to visualize the notation.

A part of the surface on which the displacement are zero $\delta u_i = 0$ is denoted by S_U. The remainder of the surface $S - S_U$ is denoted by S_T. Mathematically the principle of virtual work states

$$\int_V \sigma_{ij} \delta\epsilon_{ij} dV = \int_S T_i \delta u_i dS \tag{2.2.4}$$

where $\delta\epsilon_{ij}$ are calculated from δu_i using Equation 2.2.3. The one-dimensional graphical interpretation of the principle is shown in Figure (2.2.3).

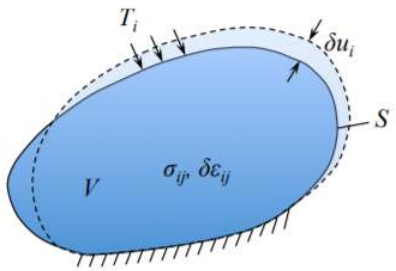

Figure 2.2.2: The 3-D potato (body) subjected to stress and displacement boundary condition develops internal stresses and incremental displacements.

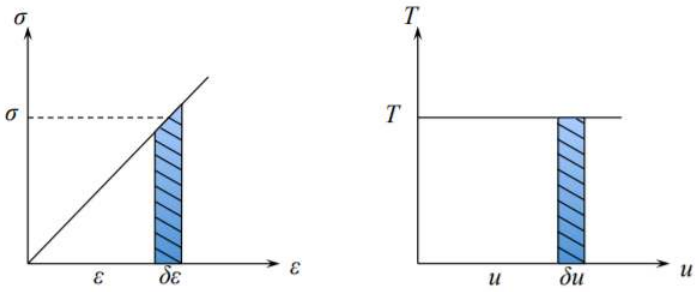

Figure 2.2.3: Incremental internal and external energies.

The integrand of the left hand side of Equation 2.2.4 can be transformed to a simpler form using the symmetry property of the stress tensor $\sigma_{ij} = \sigma_{ji}$

$$\frac{1}{2}\sigma_{ij}\delta u_{i,j} + \frac{1}{2}\sigma_{ji}\delta u_{j,i} = \sigma_{ij}\delta u_{i,j} \tag{2.2.5}$$

Recall an elementary rule of differentiation of the product of two functions

$$(ab)' = a'b + ab' \tag{2.2.6}$$

which in application to our problem reads

$$\sigma_{ij}(\delta u_i)_{,j} = (\sigma_{ij}\delta u_i)_{,j} - (\sigma_{ij})_{,j}\delta u_i \tag{2.2.7}$$

Now, the left hand side of Equation 2.2.4 is transformed to

$$\int_V \sigma_{ij}\delta\epsilon_{ij}dV = \int_V \underbrace{(\sigma_{ij}\delta u_i)}_{A_i}{}_{,j}\, dV - \int_V (\sigma_{ij})_{,j}\delta u_i dV \tag{2.2.8}$$

The first volume integral is now transformed to the surface integral according to Equation 2.2.1. Substituting this result into the statement of virtual work one gets

$$\int_S \sigma_{ij}\delta u_i n_j dS - \int_V \sigma_{ij,j}\delta u_i dV = \int_S T_i \delta u_i dS \tag{2.2.9}$$

Combining the two surface integrals into one integral we finally arrive at

$$\int_S (\sigma_{ij}n_i - T_i)\delta u_i dS - \int_V \sigma_{ij,j}\delta u_i dV = 0 \tag{2.2.10}$$

The first integral vanishes when either

$$\sigma_{ij}n_i - T_i = 0 \text{ on } S_T \tag{2.2.11}$$

$$\text{or } \delta u_i = 0 \text{ on } S_U \tag{2.2.12}$$

The above equations represent respectively the stress and displacement boundary condition. The meaning of second integral should be interpreted in the spirit of the first lemma of the calculus of variation. The increment of the displacement vector δu_i can not vanish over the whole volume of the body because this would mean rigid body motion. The point is that the second integral in Equation 2.2.7 must be zero not for one particular shape of δu_i but for all possible variation of the displacement field, as shown in Figure (2.2.1). Thus, the calculus of variation tell us that this is possible only when

$$\sigma_{ij,j} = 0 \text{ in } V \tag{2.2.13}$$

The principle of virtual work is often called the weak (global) statement of equilibrium while Equation 2.2.13 is the local equation of equilibrium but is not called strong. The weak statement of equilibrium is a starting point of developing most approximate methods in continuum and structural mechanics such as eigenvalue expansion, finite difference or finite element method. The critical assumption of the first lemma of the calculus of variation is that an infinity of different virtual velocities are considered.

This is achieved by considering a large but finite degrees of freedom through many terms in the eigenvalue expansion or many discrete elements. Through this assumption the equivalence of the global and local formulation is achieved.

An alternative form of the principle of virtual work, extensively in plasticity theory is the principle of virtual velocity. By observing that

$$\delta u = \frac{du}{dt}\delta t = \dot{u}\delta t \tag{2.2.14}$$

Equation 2.2.4 is transformed to

$$\int_V \sigma_{ij}\dot{\epsilon}_{ij}dV = \int_S T_i\dot{u}_i dS \tag{2.2.15}$$

where $\dot{\epsilon}_{ij}$ is the instantaneous velocity field obtained from the incremental velocities $\dot{u}_i$ through the linear geometric relation, Equation 2.2.4.

Generalized Stresses

This concept is introduced in order to reduce the two-dimensional problem in x and z in beams to one-dimensional problem in x, governed by an ordinary differential equation.

At an arbitrary cross-section in a beam one can distinguish a vector of bending moments $\{M_x, M_y, T\}$ where M_x is bending the beam in the (x, z) plane, M_y and T is the torque. (Do not confuse torque with surface traction vector). The meaning of the moment vector is explained in Figure (2.2.4).

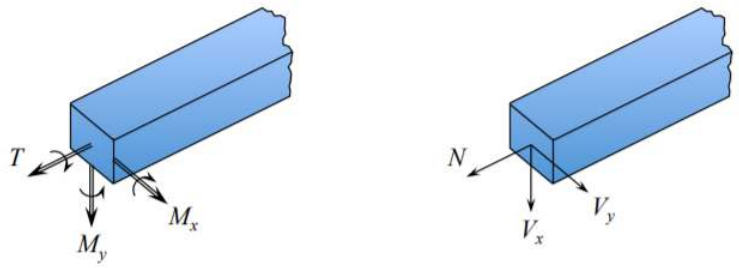

Figure 2.2.4: Imagine short shafts rotating a rigid slice of the beam.

These are components of the bending moment vector. The components of the force vector acting at an arbitrary cross-section are $\{V_x, V_y, N\}$ is the axial (membrane) force. In planar bending of a beam only three out of six components of the generalized stress resultants survival. They are defined by

$$M_x = M \stackrel{\text{def}}{=} \int_A \sigma_{xx} z\, dA \text{ [Nm]} \tag{2.2.16}$$

$$N \stackrel{\text{def}}{=} \int_A \sigma_{xx}\, dA \text{ [N]} \tag{2.2.17}$$

$$V_x = V \stackrel{\text{def}}{=} \int_A \sigma_{xz}\, dA \text{ [N]} \tag{2.2.18}$$

The product $\sigma_{xx}dA$ in Equation (3.36a) is the incremental force. Multiplying this force by the "arm" z from the beam bending axis gives the incremental bounding moment $dM = (\sigma_{xx}dA)z$. The total bending moment is an integral of dM over the beam cross-section. The sign of the generalized quantities is decided by the sign of the stress.

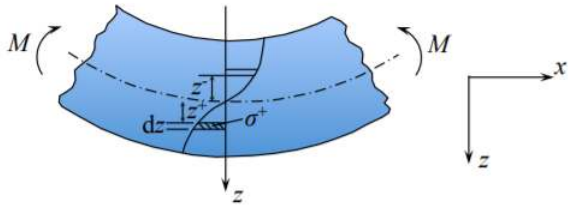

Figure **2.2.5**: The bending moment in a “smiling” beam is positive.

Imagine that the beam is bent in the way shown is Figure (**2.2.5**). On the tensile side of the beam the stress is positive, σ^{+} and so is the distance from the beam axis. On the compressive side both the stress and force arms are negative $\sigma^{-}z^{-}$, but the product is positive. Therefore the tensile and compressive side of the beam contribute to the positive bending moment. The beam (or its portion) where the bending moment is negative is called the “smiling beam”. Therefore looking at the deformed shape of the beam one can determine immediately the sign of the bending moment. The sign of the axial and shear force can be easily determined from Figure (**2.2.6**).

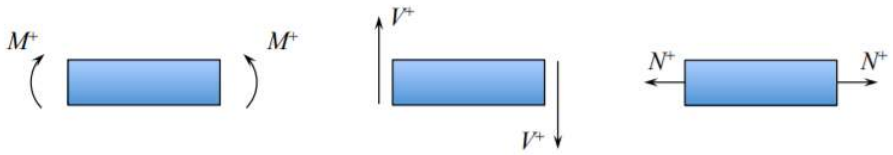

Figure **2.2.6**: Positive shear and normal stresses in a beam.

2.3: Generalized Forces and Bending Moments in Plates

In plates there are three in-plane components of the stress tensor $\sigma_{\alpha\beta}\{\sigma_{xx},\sigma_{yy},\sigma_{xy}\}$. Replacing σ_{xx} by $\sigma_{\alpha\beta}$ or $\sigma_{z\alpha}$ in Equations (2.2.16-2.2.18) the generalized forces and couples are defined

$$M_{\alpha\beta}=\int_{-\frac{h}{2}}^{\frac{h}{2}}\sigma_{\alpha\beta}z dz\ [\mathrm{Nm/m}]=[\mathrm{N}] \tag{2.3.1}$$

$$N_{\alpha\beta}=\int_{-\frac{h}{2}}^{\frac{h}{2}}\sigma_{\alpha\beta} dz\ [\mathrm{Nm/m}] \tag{2.3.2}$$

$$V_{\alpha}=\int_{-\frac{h}{2}}^{\frac{h}{2}}\sigma_{z\alpha} dz\ [N/m] \tag{2.3.3}$$

Note that in the plate theory the integration is performed over the thickness of the plate rather than the entire surface. Therefore the dimensions of the quantities defined by Equations 2.3.1-2.3.3 are “per unit length”.

2.4: Advanced Topic - Principle of Virtual Work for Beams

This principle can be derived directly from the general 3-D principle, Equation (2.2.3) assuming one-dimensional stress state and kinematic assumption of the elementary beam theory

Illegal pream-token (\\)

The left hand (LH) side of Equation (2.2.4) becomes

$$\mathrm{LH} = \int_V \sigma_{ij}\delta\epsilon_{ij}dV = \int_0^l \left\{ \int_A [\sigma_{xx}\delta\epsilon^\circ(x)dA + \sigma_{xx}z\delta\kappa dA] \right\} dx \tag{2.4.1}$$

Both $\delta\epsilon^\circ(x)$ and $\delta\kappa(x)$ are extension and curvature of the beam axis and are constant with respect to integration over the area. The above equation can be further simplified

$$\mathrm{LH} = \int_0^l \left[\delta\epsilon^\circ(x) \int_A \sigma_{xx}dA + \delta\kappa(x) \int_A \sigma_{xx}zdA \right] dx \tag{2.4.2}$$

Recalling the definition of the axial force, Equation (2.2.17) and the bending moment, Equation (2.2.16), the final expression for the virtual work inside the volume of the beam takes this simple form

$$\mathrm{LH} = \int_0^l (N\delta\epsilon^\circ + M\delta\kappa)dx \tag{2.4.3}$$

where l is the length of the beam. Evaluation of the right hand side (RH) of Equation (2.2.4) is more interesting.

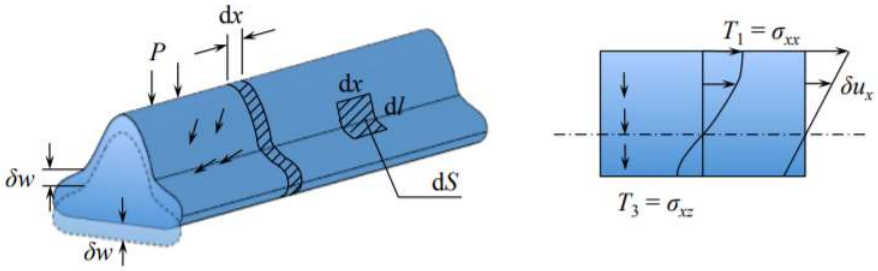

Figure 2.4.1: The outer surface of the beam consists of two parts: the lateral surface S_L on which the surface traction are acting and the end cuts A.

Note that all points on a slice of the beam move downward with the virtual displacement δw. The end cuts translate and rotate, according to Equation (1.5.1). Then the right hand side of Equation (2.2.4) becomes

$$\mathrm{RH} = \int_0^l q\delta w dx + \int_A \sigma_{xx}[\delta u^\circ - \delta\theta z]dA + \int_A \sigma_{xz}\delta w dA \tag{2.4.4}$$

where q is the integrated pressure over the circumference of a slice

$$q = \oint T_i V_i ds \tag{2.4.5}$$

and V_i are direction cosine of the surface traction vector with respect to the z-axis. In the case of the rectangular section $(h \times b)$, Equation 2.4.5 reduces to

$$q = pb \tag{2.4.6}$$

where p is the distributed pressure on the upper side of the beam and q is called the line load. The second term in Equation 2.4.4 can be simplified using the definitions Equations (2.2.16-2.2.18)

$$\bar{M} = \int_{A_{\mathrm{end}}} \sigma_{xx}zdA \tag{2.4.7}$$

$$\bar{N} = \int_{A_{\text{end}}} \sigma_{xx} dA \tag{2.4.8}$$

$$\bar{V} = \int_{A_{\text{end}}} \sigma_{xz} dz \tag{2.4.9}$$

where the bar over the symbol indicates that this is the value at the beam end. The final expression for the principle of virtual work for a beam takes the form

$$\int_0^l (N\delta\epsilon^\circ + M\delta\kappa)\, dx = \int_0^l q(x)\delta w dx + \bar{N}\delta u^\circ - \bar{M}\delta\theta + \bar{V}\delta w \tag{2.4.10}$$

The above principle will be used to derive approximate solutions of the beam problems and also to obtain the equations of equilibrium and boundary conditions.

2.5: Derivation of Equation of Equilibrium for Beams from the Principle of Virtual Work

The needed mathematical apparatus is the integration by parts. The starting point in Equation (2.2.6) which is put in an alternative form

$$\frac{da}{dx}b = \frac{d}{dx}(ab) - a\frac{db}{dx} \tag{2.5.1}$$

Integrating both sides of the above equation on gets

$$\int \frac{da}{dx}bdx = ab|_{\text{ends}} - \int a\frac{db}{dx}dx \tag{2.5.2}$$

To simplify the notation the “prime” convention will be used throughout

$$\frac{d[]}{dx} = []'; \ \frac{d^2[]}{dx^2} = []'' \tag{2.5.3}$$

We turn now the left hand side of the principle of virtual work, Equation (2.1.22) and recall the definition of beam curvature and axial strain

$$\kappa = -w'' \tag{2.5.4}$$

$$\epsilon^\circ = u' \tag{2.5.5}$$

The virtual increments are

$$\delta\kappa = -\delta w'' = (\delta w')' \tag{2.5.6}$$

$$\delta\epsilon^\circ = \delta u' \tag{2.5.7}$$

Substituting Equation 2.5.7 into the LH side of Equation (2.1.22) and integrating twice by parts we get

$$\text{LH} = -\int_0^l M(\delta w')'dx + \int_0^l N\delta u'dx \tag{2.5.8}$$

$$= -\left(M\delta w'|_0^l - \int_0^l M'\delta w'dx\right) + \left(N\delta u|_0^l - \int_0^l N\delta udx\right) \tag{2.5.9}$$

$$= -M\delta w'|_0^l + M'\delta w|_0^l - \int_0^l M''\delta wdx + N\delta u|_0^l - \int_0^l N'\delta udx \tag{2.5.10}$$

The second term represents the work increment at the beam end on downward virtual displacement. Therefore the corresponding generalized force must be the shear force V

$$V = M' \tag{2.5.11}$$

Introducing Equation 2.5.10 into Equation (2.4.11) and grouping the terms yields

$$\int_0^l (M'' + q)\delta wdx + \int_0^l N'\delta udx + (M - \bar{M})\delta w' \tag{2.5.12}$$
$$|_0^l - (N - \bar{N})\delta u|_0^l - (V - \bar{V})\delta w|_0^l = 0$$

The above equation should hold not for one specific incremental displacement but for arbitrary variations $(\delta w, \delta w', \delta u)$, independent inside $0 < x < l$ and on the boundaries. Therefore by the first lemma of the calculus of variation, the local (strong) form of the beam equilibrium follows

$$M'' + q = 0 \tag{2.5.13}$$

$$N' = 0 \tag{2.5.14}$$

along with the boundary conditions

$$(M - \bar{M})\delta w' = 0 \tag{2.5.15}$$

$$(V - \bar{V})\delta u = 0 \tag{2.5.16}$$

$$(N - \bar{N})\delta w = 0 \tag{2.5.17}$$

In order to satisfy the boundary condition

$$\text{either } M = \bar{M} \text{ or } \delta w' = 0 \tag{2.5.18}$$

$$\text{either } V = \bar{V} \text{ or } \delta w = 0 \tag{2.5.19}$$

$$\text{either } N = \bar{N} \text{ or } \delta u = 0 \tag{2.5.20}$$

The quantities with a bar denotes the quantities prescribed at the ends of a beam. In particular $\bar{M}$, $\bar{V}$, and $\bar{N}$ could be equal to zero. The first column in Equations 2.5.18-2.5.20 represents the static boundary conditions while the second column the kinematic boundary conditions. There are also mixed boundary conditions. The following combinations satisfy all boundary conditions, Figure (2.5.1).

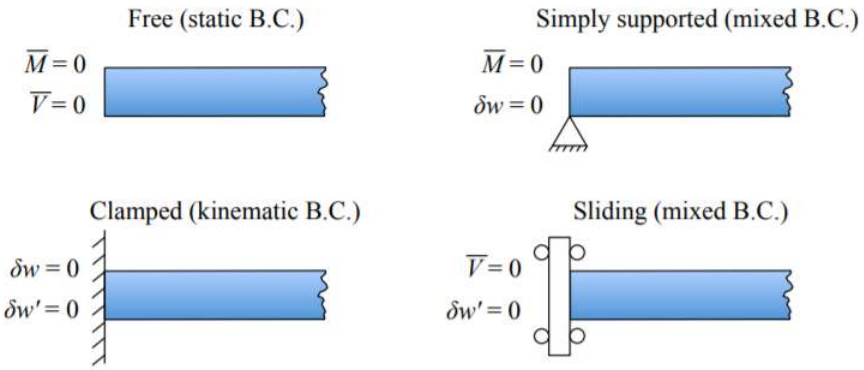

Figure 2.5.1: Boundary conditions in the axial direction.

In addition the beam could freely slide at the end along x-axis or can be restrained from sliding, Figure (2.5.2).

In the case of symmetric loading of the beam, it suffices to consider only one half of the beam with the symmetry boundary condition. The symmetry B.C. is identical to the sliding boundary conditions, as explained in Figure (2.5.3).

Figure 2.5.2: Shear force V and rotation angle $\delta w'$ vanishes at the symmetry plane.

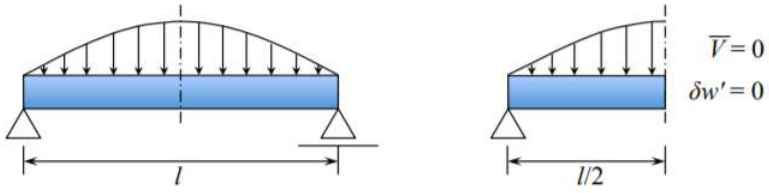

Figure 2.5.3: Shear force V and rotation angle $\delta w'$ vanishes at the symmetry plane.

2.6: Advanced Topic - Mathematical Theory of Beams

The equations of equilibrium of a beam with a rectangular cross-section can be derived in an elegant way from the 3-D equilibrium equation. With zero body forces, the equation of equilibrium in the compact index notation is

$$\sigma_{ij,j} = 0 \tag{2.6.1}$$

or the expanded notation

$$i = 1,\ \sigma_{1j,j} = 0 \rightarrow \sigma_{11,1} + \sigma_{12,2} + \sigma_{13,3} = 0 \tag{2.6.2}$$

$$i = 2,\ \sigma_{2j,j} = 0 \rightarrow \sigma_{21,1} + \sigma_{22,2} + \sigma_{23,3} = 0 \tag{2.6.3}$$

$$i = 3,\ \sigma_{3j,j} = 0 \rightarrow \sigma_{31,1} + \sigma_{32,2} + \sigma_{33,3} = 0 \tag{2.6.4}$$

In the engineering notation, the full set of equilibrium equation, already given by Equations (2.1.26-2.1.28), is

$$\begin{pmatrix} \frac{\partial \sigma_{xx}}{\partial x} & \frac{\partial \sigma_{xy}}{\partial y} & \frac{\partial \sigma_{xz}}{\partial z} \\ \frac{\partial \sigma_{yx}}{\partial x} & \frac{\partial \sigma_{yy}}{\partial y} & \frac{\partial \sigma_{yz}}{\partial z} \\ \frac{\partial \sigma_{zx}}{\partial x} & \frac{\partial \sigma_{zy}}{\partial y} & \frac{\partial \sigma_{zz}}{\partial z} \end{pmatrix} \tag{2.6.5}$$

which of the components of the stress tensor will survive beam assumption. Consider a rectangular cross-section beam $(h \times b)$ undergoing planar bending, Figure (2.6.1).

The beam is subjected to pressure loading p at the plane $z = -\frac{h}{2}$. In the case of planar bending there must be no gradient of stresses in the y-direction. Therefore the term $\frac{\partial \sigma_{xy}}{\partial y} = 0$. The surviving components lie outside the shaded box in Equation 2.6.5, and are:

$$\frac{\partial \sigma_{xx}}{\partial x} + \frac{\partial \sigma_{xz}}{\partial z} = 0 \tag{2.6.6}$$

Equation in the y-direction is satisfied identically (2.6.7)

$$\frac{\partial \sigma_{zx}}{\partial x} + \frac{\partial \sigma_{zz}}{\partial z} = 0 \tag{2.6.8}$$

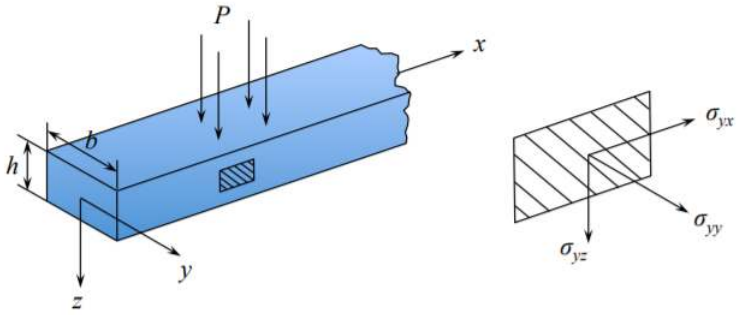

Figure 2.6.1: Vanishing components of the stress vector.

Boundary Conditions

Boundary conditions are specified by the Cauchy formula. The lateral surfaces $y = \pm\frac{b}{2}$ as well as the lower shelf $z = \frac{h}{2}$ are stress free. Consider only the upper shelf $z = -\frac{h}{2}$, defined by the unit normal vector $n[0, 0, -1]$. Assume that no shear loading is applied,

so that the distributed load is directed along z-axis.

The components of surface traction on the upper shelf are $\boldsymbol{T}[0,0,p]$. From the Cauchy formula, calculate the z-component of the surface traction $T_3 = \sigma_{3j}n_j = \sigma_{31}n_1 + \sigma_{32}n_2 + \sigma_{33}n_3$. Only the last term, for which $n_3 = -1$ remains and so

$$T_3 = p = -\sigma_{33} = -\sigma_{zz} \tag{2.6.9}$$

It was straightforward to see that the pressure p must be equilibrated by the σ_{zz} component. However, for a precise determination of the sign, the Cauchy formula happened to be useful. All other components of the stress tensor on the lateral surface of the beam are zero.

The derivation consists of three steps. First Equation 2.6.6 is integrated with respect to z and multiplied by the beam width b

$$\int_{-\frac{h}{2}}^{\frac{h}{2}} \frac{\partial \sigma_{xx}}{\partial x} dz + b\int_{-\frac{h}{2}}^{\frac{h}{2}} \frac{\partial \sigma_{xz}}{\partial z} dz = 0 \tag{2.6.10}$$

Next, for a definite integral, the differentiation of the integrant in the first is equivalent to the differentiation of the integral. The second term can be integrated to give

$$\int_{-\frac{h}{2}}^{\frac{h}{2}} \sigma_{xx} b dz + \sigma_{xz}|_{-\frac{h}{2}}^{\frac{h}{2}} = 0 \tag{2.6.11}$$

Noting that $bdz = dA$, the first integral represents the axial force N, according to the definition, Equation 2.6.7. The shear stress σ_{xz} is non-zero inside the beam height but vanishes at the lower and upper shelves, $\sigma_{xz} = 0$, at $z = \frac{h}{2}$ and $z = -\frac{h}{2}$. Only the first term survives, which is the force equilibrium in the x-direction

$$\frac{dN}{dx} = 0 \text{ or } N' = 0 \tag{2.6.12}$$

In the second step both sides of Equation 2.6.6 are multiplied by bz and integrated again with respect to z

$$\int_{-\frac{h}{2}}^{\frac{h}{2}} \frac{\partial \sigma_{xx}}{\partial x} z(bdz) + b\int_{-\frac{h}{2}}^{\frac{h}{2}} \frac{\partial \sigma_{xz}}{\partial z} z(bdz) = 0 \tag{2.6.13}$$

The second term is now integrated by parts

$$\frac{d}{dx}\int_{-\frac{h}{2}}^{\frac{h}{2}} \sigma_{xx} z dA + \{\sigma_{xz}|_{-\frac{h}{2}}^{\frac{h}{2}} - \int_{-\frac{h}{2}}^{\frac{h}{2}} \sigma_{xz} dA\} = 0 \tag{2.6.14}$$

The second term vanishes, as before. The first integral is the bending moment M while the second one-the shear force V (see the definitions, Equations 2.6.6-2.6.8. So, the above equation represent the moment equilibrium

$$\frac{dM}{dx} - V = 0 \tag{2.6.15}$$

In the third, final step, Equation 2.6.15 is integrated with respect to z after being multiplied by b.

$$\int_{-\frac{h}{2}}^{\frac{h}{2}} \frac{\partial \sigma_{xz}}{\partial x}(bdz) + \int_{-\frac{h}{2}}^{\frac{h}{2}} \frac{\partial \sigma_{zz}}{\partial z}(bdz) = 0 \tag{2.6.16}$$

After integration one gets

$$\frac{d}{dx}\int_{-\frac{h}{2}}^{\frac{h}{2}} \sigma_{xz} dA + b\left[\sigma_{zz}|_{\frac{h}{2}} - \sigma_{zz}\Big|_{-\frac{h}{2}}\right] = 0 \tag{2.6.17}$$

Recalling the boundary condition $\sigma_{zz}|_{\frac{h}{2}}$ and $\sigma_{zz}|_{\frac{h}{2}} = -p$, Equation 2.6.17 yields

$$\frac{dV}{dx} + b(-1)(-p) = 0 \tag{2.6.18}$$

or using $bp = q$

$$\frac{dV}{dx} + q = 0 \tag{2.6.19}$$

Eliminating the shear force between Equation 2.6.15 and Equation 2.6.19, the beam equilibrium equation is obtained.

$$\frac{d^2M}{dx^2} + q(x) = 0 \tag{2.6.20}$$

This equation is identical to the one derived from the principle of virtual work.

2.7: Equilibrium in the Theory of Moderately Large Deflections of Beams

In Chapter 1, it was shown that finite rotation of the beam element introduced the additional term $\frac{1}{2}\theta^2$ in the expression for the axial strain. Let's see if consideration of finite slope would require modification of the equation of the equilibrium.

In Figure (2.5.3) the beam element is shown in the theory of small deflections (infinitesimal rotation) and moderately large deflections (finite rotation).

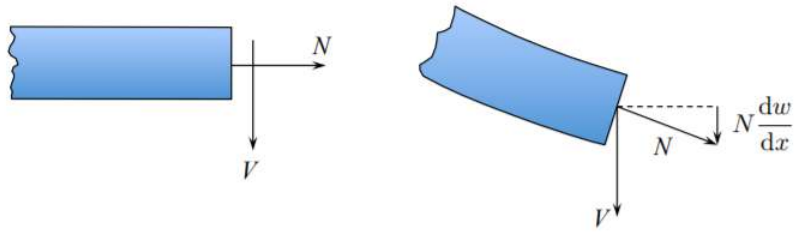

Figure **2.7.1**: In finite rotation the axial force contributes to the total shear force.

The so-called effective shear force V^* is a sum of the cross-sectional shear V and projection of the axial force into the vertical direction. Thus,

$$V^* = V + N\frac{dw}{dx} \tag{2.7.1}$$

Note that this result is valid as long as $\cos\theta \approx 1$ and $\sin\theta \approx \tan\theta \approx \theta$. Will the derivation of the force equilibrium change? The answer is no.

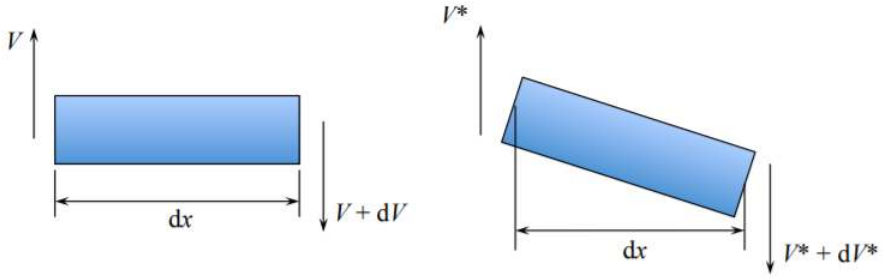

Figure **2.7.2**: Direction of forces to equilibrate the infinitesimal beam element.

To ensure vertical equilibrium

$$(V^* + dV^*) - V^* + qdx = 0 \tag{2.7.2}$$

or

$$\frac{dV^*}{dx} + q = 0 \tag{2.7.3}$$

where V^* is defined by Equation 2.7.1. Equilibrium of the horizontal (axial) forces stays the same as before since $\cos\theta \approx 1$.

$$\frac{dN}{dx} = 0 \tag{2.7.4}$$

Eliminating V^* between Equation 2.7.1 and Equation 2.7.3 gives

$$\frac{dV}{dx} + \frac{d}{dx}\left(N\frac{dw}{dx}\right) + q = \frac{dV}{dx} + \frac{dN}{dx}\frac{dw}{dx} + N\frac{d^2w}{dx^2} + q = 0 \tag{2.7.5}$$

The second term vanishes on account of Equation 2.7.4. The modified force equilibrium equation becomes

$$\frac{dV}{dx} + N\frac{d^2w}{dx^2} + q = 0 \tag{2.7.6}$$

The new nonlinear term vanishes if (i) the axial force is zero or (ii) for small deflections and rotation. The moment equilibrium equation, Equation (2.6.15) is not affected by moderately large rotations. Together with Equation 2.7.6 we arrive at the governing equation of the theory of moderately large deflection of beams

$$\frac{d^2M}{dx^2} + N\frac{d^2w}{dx^2} + q = 0 \tag{2.7.7}$$

On closing this section, two important remarks should be made. All equations of equilibrium for infinitesimal deformations of 3-D bodies and small deflections of beams involved only static quantities and their gradients (M, V, N). In the theory of moderately large deflections there is coupling between static and kinematic quantities through the second nonlinear terms.

Secondly, Equation 2.7.7 includes leading in the in-plane direction (through N) and out-of-plane direction through q. Therefore, it is after referred as the equation describing a beam/columns.

2.8: Equilibrium of Rectangular Plates

A step-by-step derivation of the equation of equilibrium and boundary conditions for rectangular plates is presented in the lecture notes of the course 2.081 Plates and Shells. This equation takes the following form in the tensor notation

$$M_{\alpha\beta,\alpha\beta} + p = 0 \tag{2.8.1}$$

and in the extended notation

$$\frac{\partial^2 M_{xx}}{\partial x^2} + 2\frac{\partial^2 M_{xy}}{\partial x \partial y} + \frac{\partial^2 M_{yy}}{\partial y^2} + p = 0 \tag{2.8.2}$$

Recall that the dimensions of the bending moments in plates are $[\mathrm{Nm/m}] = [N]$. In the case of cylindrical bending the twist M_{xy} and M_{yy} vanish. Multiplying Equation 2.8.2 by the width b, one gets

$$\frac{d^2}{dx^2}[bM_{xx}] + q = 0 \tag{2.8.3}$$

which is identical to the previously derived equation equilibrium of a beam, Equation (2.6.20). Therefore wide beams are a special class of rectangular plates.

The boundary conditions for plates are similar to those for beams in the local coordinate system at the edges, (n, t), Figure (2.8.1).

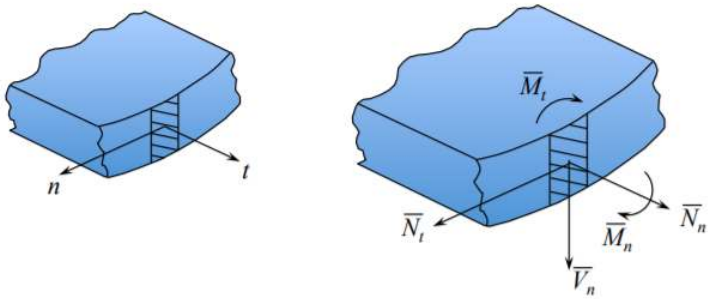

Figure 2.8.1: Local coordinate system at the plate edge with applied generalized forces.

Therefore Equations (2.5.13-2.5.15) for beams should now read

$$(M_n - \bar{M}_n)\delta w' = 0 \tag{2.8.4}$$

$$(V_n - \bar{V}_n)\delta w = 0 \tag{2.8.5}$$

$$(N_n - \bar{N}_n)\delta u_n = 0 \tag{2.8.6}$$

$$(N_t - \bar{N}_t)\delta u_t = 0 \tag{2.8.7}$$

2.9: Circular Plates

It is relatively easy to derive the equation of equilibrium of a circular plate from the principle of virtual work. Bending and in-plane responses is considered separately

$$\int_{R_1}^{R_2}(M_r\delta\kappa_r+M_\theta\delta\kappa_\theta)dr+\int_{R_1}^{R_2}p\delta wrdr+r\bar{M}_r\delta w'|_{R_1}^{R_2}+r\bar{V}_r\delta w|_{R_1}^{R_2} \tag{2.9.1}$$

where the radial and circumferential curvatures and their variations are defined (without proof) by

$$\kappa_r=\frac{\partial^2 w}{\partial r^2},\ \delta\kappa_r=\frac{\partial^2(\delta w)}{\partial r^2} \tag{2.9.2}$$

$$\kappa_\theta=\frac{1}{r}\frac{\partial w}{\partial r},\ \delta\kappa_\theta=\frac{1}{r}\frac{\partial(\delta w)}{\partial r} \tag{2.9.3}$$

Integrating the left hand side of Equation 2.9.1 by parts and using similar arguments as in the case of a beam, one gets equilibrium:

$$\frac{d}{dr}\left(r\frac{dM_r}{dr}\right)+\frac{dM_r}{dr}-\frac{dM_\theta}{dr}=pr \tag{2.9.4}$$

and boundary conditions

$$(M_r-\bar{M}_r)\delta w'=0 \tag{2.9.5}$$

$$(V_r-\bar{V}_r)\delta w=0 \tag{2.9.6}$$

where

$$V_r=\frac{d}{dr}(rM_r) \tag{2.9.7}$$

When $R_1=0$, we have a circular plate. Otherwise the plate is annular with the inner and outer radius R_1 and R_2, respectively.

When the circular plate is loaded in the in-plane direction only, it remains flat and the components of the mid-surface extensions and their variations are

$$\epsilon_r^\circ=\frac{du_r}{dr},\ \delta\epsilon_r^\circ=\frac{d}{dr}(\delta u_r) \tag{2.9.8}$$

$$\epsilon_\theta^\circ=\frac{u_r}{r},\ \delta\epsilon_\theta^\circ=\frac{\delta u_r}{r} \tag{2.9.9}$$

The principle of virtual work can be easily established in the form

$$\int_{R_1}^{R_2}(N_r\delta\epsilon_r^\circ+N_\theta\delta\epsilon_\theta^\circ)rdr=rN_r\delta u_r|_{R_1}^{R_2} \tag{2.9.10}$$

The equation of equilibrium in the in-plane direction are easily derived by integrating by parts

$$\frac{d}{dr}(rN_r)-N_\theta=0 \tag{2.9.11}$$

subject to the boundary condition

$$(N_r-\bar{N}_r)\delta u_r|_{R_1}^{R_2}=0 \tag{2.9.12}$$

Note that $\bar{N}_\theta$ is zero at the boundaries, ensuring that there will be no in-plane shearing force $N_{r\theta}$ and the radial and hoop membrane forces are principal forces.

CHAPTER OVERVIEW

3: Development of Constitutive Equations of Continuum, Beams and Plates

---

3.1: Prologue to Development of Constitutive Equations for Continuum, Beams and Plates

This chapter deals with the determination of relations between stresses and strains, called the constitutive equations. For an elastic material the term elasticity law or the Hooke's law are often used. In one dimension we would write

$$\sigma = E\epsilon \tag{3.1.1}$$

where E is the Young's (elasticity) modulus. All types of steels, independent on the yield stress have approximately the same Young modulus $E = 2$. GPa. The corresponding value for aluminum alloys is $E = 0.80$ GPa. What actually is σ and ϵ in the above equation? We are saying the "uni-axial" state but such a state does not exist simultaneously for stresses and strains. One dimensional stress state produces three-dimensional strain state and vice versa.

3.2: Elasticity Law in 3-D Continuum

The second question is how to extend Equation (3.1.1) to the general 3-D state. Both stress and strain are tensors so one should seek the relation between them as a linear transformation in the form

$$\sigma_{ij} = C_{ij,kl}\epsilon_{kl} \tag{3.2.1}$$

where $C_{ij,kl}$ is the matrix with $9 \times 9 = 81$ coefficients. Using symmetry properties of the stress and strain tensor and assumption of material isotropy, the number of independent constants are reduced from 81 to just two. These constants, called the Lame' constants, are denoted by \((\chi, \mu). The general stress strain relation for a linear elastic material is

$$\sigma_{ij} = 2\mu\epsilon_{ij} + \lambda\epsilon_{kk}\delta_{ij} \tag{3.2.2}$$

where δ_{ij} is the identity matrix, or Kronecker "δ", defined by

Illegal pream-token (\)

and ϵ_{kk} is, according to the summation convention,

$$\epsilon_{kk} = \epsilon_{11} + \epsilon_{22} + \epsilon_{33} = \frac{dV}{V} \tag{3.2.3}$$

In the expanded form, Equation 3.2.2 reads

$$\sigma_{11} = 2\mu\epsilon_{11} + \lambda(\epsilon_{11} + \epsilon_{22} + \epsilon_{33}), \qquad \delta_{11} = 1 \tag{3.2.4}$$

$$\sigma_{22} = 2\mu\epsilon_{22} + \lambda(\epsilon_{11} + \epsilon_{22} + \epsilon_{33}), \qquad \delta_{22} = 1 \tag{3.2.5}$$

$$\sigma_{33} = 2\mu\epsilon_{33} + \lambda(\epsilon_{11} + \epsilon_{22} + \epsilon_{33}), \qquad \delta_{33} = 1 \tag{3.2.6}$$

$$\sigma_{12} = 2\mu\epsilon_{12} \qquad \delta_{12} = 0 \tag{3.2.7}$$

$$\sigma_{23} = 2\mu\epsilon_{23} \qquad \delta_{23} = 0 \tag{3.2.8}$$

$$\sigma_{31} = 2\mu\epsilon_{31} \qquad \delta_{31} = 0 \tag{3.2.9}$$

Our task is to express the Lame' constants by a pair of engineering constants ($E(\nu)$, where ν is the Poisson ratio). For that purpose, we use the virtual experiment of tension of a rectangular bar

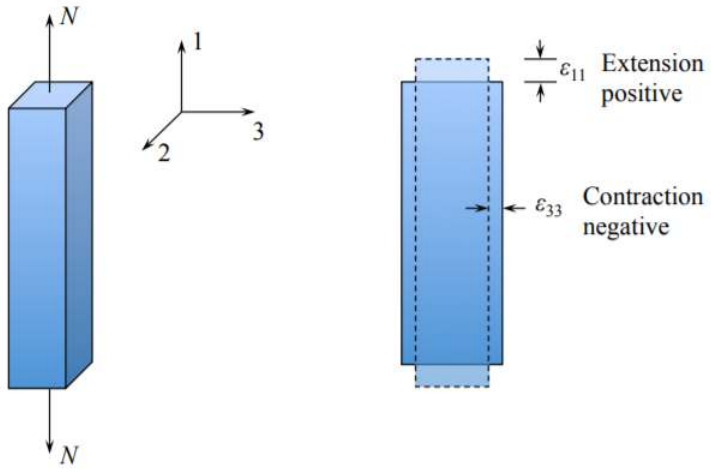

Figure 3.2.1: Uniaxial tension of a bar.

In the conceptual test, measured are the force, displacement and change in the crosssectional dimension. The experimental observations can be summarized as follows:

- σ_{11} is proportional to $\epsilon_{11}, \sigma_{11} = E\epsilon_{11}$
- ϵ_{22} is proportional to $\epsilon_{11}, \epsilon_{22} = -\nu\epsilon_{11}$

- ϵ_{33} is proportional to $\epsilon_{11}, \epsilon_{33} = -\nu\epsilon_{11}$

Thus the uniaxial tension is producing the one-dimensional state of stress but three-dimensional state of strain

$$\sigma_{ij} = \begin{vmatrix} \sigma_{11} & 0 & 0 \\ 0 & 0 & 0 \\ 0 & 0 & 0 \end{vmatrix} \quad \epsilon_{ij} = \begin{vmatrix} \epsilon_{11} & 0 & 0 \\ 0 & \epsilon_{22} & 0 \\ 0 & 0 & \epsilon_{33} \end{vmatrix} \tag{3.2.10}$$

We introduce now the above information into Equations 3.2.4-3.2.9.

$$\sigma_{11} = 2\mu\epsilon_{11} + \chi(\epsilon_{11} - \nu\epsilon_{11} - \nu\epsilon_{11}) = E\epsilon_{11} \tag{3.2.11}$$

$$\sigma_{22} = 2\mu(-\nu\epsilon_{11}) + \chi(\epsilon_{11} - \nu\epsilon_{11} - \nu\epsilon_{11}) = 0 \tag{3.2.12}$$

and obtain two linear equations relating (χ, μ) with (E, ν)

$$2\mu + \chi(1 - 2\nu) = E \tag{3.2.13}$$

$$-2\mu\nu + \chi(1 - 2\nu) = 0 \tag{3.2.14}$$

Solving Equations 3.2.13-3.2.14 for μ and χ gives

$$\mu = \frac{E}{2(1-\nu)} \tag{3.2.15}$$

$$\chi = \frac{E\nu}{(1+\nu)(1-2\nu)} \tag{3.2.16}$$

The general, 3-D elasticity law, expressed in terms of (E, ν) is

$$\sigma_{ij} = \frac{E}{1+\nu}\left[\epsilon_{ij} + \frac{\nu}{1-2\nu}\epsilon_{kk}\delta_{ij}\right] \tag{3.2.17}$$

The mean stress p where $-p = \frac{1}{3}\sigma_{kk} = \frac{1}{3}(\sigma_{11} + \sigma_{22} + \sigma_{33})$ is called the hydrostatic pressure. At the same time the sum of the diagonal components of the strain tensor denotes the change of volume. Let us make the so-called "contraction" of the stress tensor in Equation 3.2.17, meaning that $i = j = k$

$$\sigma_{kk} = \frac{E}{1+\nu}\left[\epsilon_{kk} + \frac{\nu}{1-2\nu}\epsilon_{kk} \cdot 3\right] \tag{3.2.18}$$

where $\delta_{kk} = (\delta_{11} + \delta_{22} + \delta_{33}) = 1 + 1 + 1 = 3$. From the above equations the following relation is obtained between the hydrostatic pressure and volume change

$$-p = \kappa\frac{dV}{V} \tag{3.2.19}$$

where κ is the bulk modulus

$$\kappa = \frac{E}{3(1-2\nu)} \tag{3.2.20}$$

The elastic material is clearly compressible. It is the crystalline lattice that is compressed but on removal the forces returns to the original volume.

The inverted form of the 3-D Hook's law is

$$\epsilon_{ij} = \frac{1+\nu}{E}\sigma_{ij} - \frac{\nu}{E}\sigma_{kk}\delta_{ij} \tag{3.2.21}$$

which in terms of the components yields

$$\epsilon_{11} = \frac{1}{E}[\sigma_{11} - \nu(\sigma_{22} + \sigma_{33})] \tag{3.2.22}$$

$$\epsilon_{22} = \frac{1}{E}[\sigma_{22} - \nu(\sigma_{11} + \sigma_{33})] \tag{3.2.23}$$

$$\epsilon_{33} = \frac{1}{E}[\sigma_{33} - \nu(\sigma_{11} + \sigma_{22})] \tag{3.2.24}$$

$$\epsilon_{12} = \frac{1}{2\epsilon}\sigma_{12} \tag{3.2.25}$$

$$\epsilon_{23} = \frac{1}{2\epsilon}\sigma_{23} \tag{3.2.26}$$

$$\epsilon_{31} = \frac{1}{2\epsilon}\sigma_{31} \tag{3.2.27}$$

where $G = \frac{E}{2(1+\nu)}$ is called the shear modulus. Equations 3.2.22 - 3.2.27 illustrates the coupling of individual direct strains with all direct (diagonal) components of the stress tensor. At the same time there is no coupling in shear response. The shear strain is proportional to the corresponding shear stress.

3.3: Specification to the 2-D Continuum

Plane Stress

This is the state of stress that develops in thin plates and shells so it requires a careful consideration. The stress state in which $\sigma_{3j} = 0$, where the $x_3 = z$ axis is in the through thickness direction. The non-zero components of the stress tensor are:

$$\sigma_{ij} = \begin{vmatrix} \sigma_{11} & \sigma_{12} & 0 \\ \sigma_{21} & \sigma_{22} & 0 \\ 0 & 0 & 0 \end{vmatrix} \quad \epsilon_{ij} = \begin{vmatrix} \epsilon_{11} & \epsilon_{12} & 0 \\ \epsilon_{21} & \epsilon_{22} & 0 \\ 0 & 0 & \epsilon_{33} \end{vmatrix} \tag{3.3.1}$$

where $i, j = 1, 2, 3$ and $\alpha, \beta = 1, 2$. Accordingly, $\sigma_{kk} = \sigma_{11} + \sigma_{22} + \sigma_{33} = \sigma_{\gamma\gamma} + 0$. The 2-D elasticity law takes the following form in the tensor notation

$$\epsilon_{\alpha\beta} = \frac{1+\nu}{E}\sigma_{\alpha\beta} - \frac{\nu}{E}\sigma_{\gamma\gamma}\delta_{\alpha\beta} \tag{3.3.2}$$

It can be easily checked from Equation 3.3.2 that in plane stress $\epsilon_{13} = \epsilon_{23} = 0$ but $\epsilon_{33} = -\frac{\nu}{E}(\sigma_{11} + \sigma_{22})$. The through-thickness component of the strain tensor is not zero. Because it does not enter the plane stress strain-displacement relation, its presence does not contribute to the solutions. It can only be determined afterwards from the known stresses σ_{11} and σ_{22}.

By making contraction $\epsilon_{kk} = \frac{1-\nu}{E}\sigma_{kk}$, one can easily invert Equation 3.3.2 in the form

$$\sigma_{\alpha\beta} = \frac{E}{1+\nu^2}[(1-\nu)\epsilon_{\alpha\beta} + \nu\epsilon_{\gamma\gamma}\delta_{\alpha\beta}] \tag{3.3.3}$$

The above equation is a starting point for deriving the elasticity law in generalized quantities for plates and shells. We shall return to that task later in this lecture. Before that, let's discuss three other important limiting cases

$$\sigma_{11} = \frac{E}{1-\nu^2}(\epsilon_{11} + \nu\epsilon_{22}) \tag{3.3.4}$$

$$\sigma_{22} = \frac{E}{1-\nu^2}(\epsilon_{22} + \nu\epsilon_{11}) \tag{3.3.5}$$

$$\sigma_{13} = \frac{E}{1+\nu}\epsilon_{12} \tag{3.3.6}$$

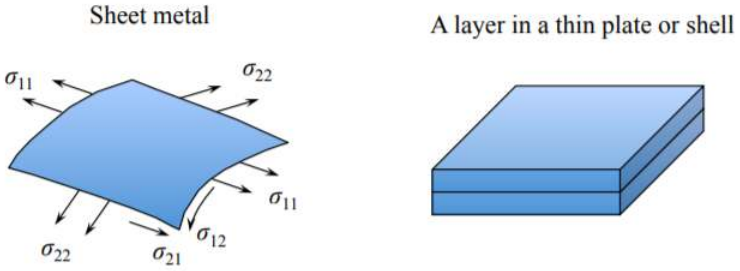

Figure 3.3.1: Examples of plane stress structures.

Plane strain holds whenever $\epsilon_{2j} = 0$. By imposing a constraint on $\epsilon_{22} = 0$, a reaction immediately develops in the direction as $\sigma_{22} \neq 0$.

The components of the strain and Equations (3.2.12-3.2.13) stress tensors are

$$\epsilon_{ij} = \begin{vmatrix} \epsilon_{11} & \epsilon_{12} & 0 \\ \epsilon_{21} & \epsilon_{22} & 0 \\ 0 & 0 & 0 \end{vmatrix} \quad \sigma_{ij} = \begin{vmatrix} \sigma_{11} & \sigma_{12} & 0 \\ \sigma_{21} & \sigma_{22} & 0 \\ 0 & 0 & \sigma_{33} \end{vmatrix} \tag{3.3.7}$$

Can you show that under the assumption of the plane strain, the reaction stress $\sigma_{33} = \nu(\sigma_{11} + \sigma_{22})$? The plane strain is encountered in many practical situations, such as cylindrical bending of a plate or wide beam.

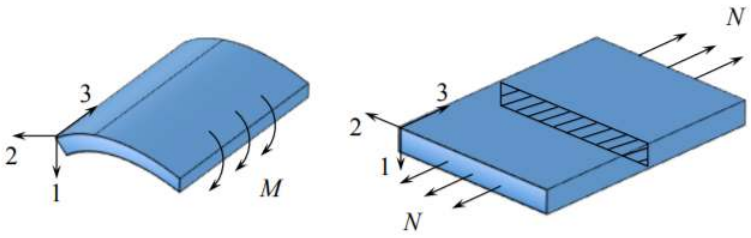

Figure **3.3.2**: Tension of bending of a wide sheet/plate gives rise to plane strain.

Uniaxial Strain

Uniaxial strain is achieved when the displacement in two directions are constrained. For example, soil or granular materials are tested in a cylinder (called confinement) with a piston, Figure (**3.3.3**). The uniaxial strain also develops in a compressed layer between two rigid plates. Also high velocity plate-to-plate impact products the one-dimensional strain. Here the only component of the strain tensor is the volumetric strain. The plate-to-plate experiments are conducted to establish the nonlinear compressibility of metals under very high hydrostatic loading $\sigma_{kk} = -3p$. Similarly, the plane wave in the 3-D space is generating a uniaxial strain.

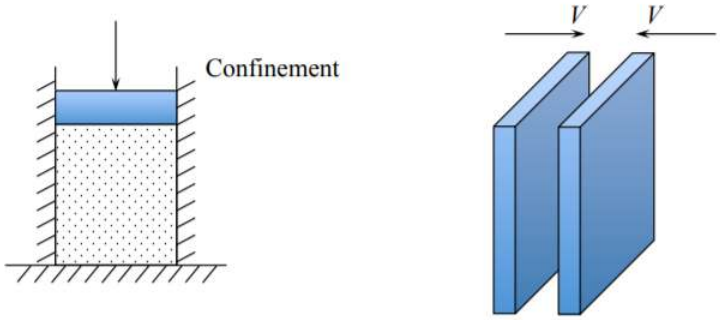

Figure **3.3.3**: Examples of problems in which the strain state is uniaxial.

The components of the stress and strain tensor in the uniaxial strain are:

$$\sigma_{ij} = \begin{vmatrix} \sigma_{11} & \sigma_{12} & 0 \\ \sigma_{21} & \sigma_{22} & 0 \\ 0 & 0 & \sigma_{33} \end{vmatrix}$$

and

$$\epsilon_{ij} = \begin{vmatrix} \epsilon_{11} & 0 & 0 \\ 0 & 0 & 0 \\ 0 & 0 & 0 \end{vmatrix}$$

where the reaction stresses are related to the active stress σ_{11} by $\sigma_{22} = \sigma_{33} = \frac{\nu(1+\nu)\sigma_{11}}{1-\nu^2}$. Can you prove that?

The uniaxial stress state was discussed earlier in this lecture when converting the Lame' constants into the engineering constants (E, ν).

3.4: Hook's Law in Generalized Quantities for Beams

There are three generalized forces in beams (M, N, ν) but only two generalized kinematic quantities (ϵ°, κ). There is no generalized displacement on which the shear force could exert work. So the shear force is treated as a reaction in the elementary beam theory. This gives rise to some internal inconsistency in the beam theory, which will be enumerated in a separate section.

The starting point in the derivation of the elasticity law for beams is the Euler-Bernoulli hypothesis,

$$\epsilon(z) = \epsilon^\circ + z\kappa \tag{3.4.1}$$

and the one-dimensional Hook law, Equation (3.1.1), and the definition of the bending moment and axial force in the beam, Equations (2.2.16-2.2.18). Let's calculate first the axial force N

$$\begin{aligned} N &= \int_A \sigma_{xx} dA = \int_A E\epsilon_{xx} dA = E\int_A (\epsilon^\circ + z\kappa) dA \\ &= E\int_A \epsilon^\circ dA + E\int_A \kappa z dA = E\epsilon^\circ \int_A dA + E\kappa \int_A z dA \end{aligned} \tag{3.4.2}$$

Note that the strain of the middle axis ϵ° and the curvature of the beam axis are independent of the z-coordinate and could be brought in front of the respective integrals. Also $Q = \int_A z dA$ is the static (first) moment of inertia of the cross-section. From the definition of the neutral axis, $Q = 0$. The expression for the axial force reduces then to

$$N = EA\epsilon^\circ \tag{3.4.3}$$

where EA is called the axial rigidity of the beam. We calculate next the bending moment in a similar way

$$\begin{aligned} N &= \int_A \sigma_{xx} z dA = \int_A E(\epsilon^\circ + z\kappa) z dA \\ &= E\epsilon^\circ \int_A z dA + E\kappa \int_A z^2 dA \end{aligned} \tag{3.4.4}$$

Because the first term involving the static moment of inertia vanishes, and the expression for the bending moment becomes

$$M = EI\kappa \tag{3.4.5}$$

where EI is called the bending rigidity and

$$I = \int_A z^2 dA \tag{3.4.6}$$

is the second moment of inertia. For the rectangular cross-section $(b \times h)$

$$I = \frac{bh^3}{12} \tag{3.4.7}$$

The significance of the above derivation is that the bending response is uncoupled from the axial response and vice versa. This property allows to derive the famous stress formula for beams. This is indeed one line derivation

$$\begin{aligned} \sigma = E\epsilon = E(\epsilon^\circ + z\kappa) = E\left(\frac{N}{EA} + \frac{Mz}{EI}\right) \\ \sigma(z) = \frac{N}{A} + \frac{Mz}{I} \end{aligned} \tag{3.4.8}$$

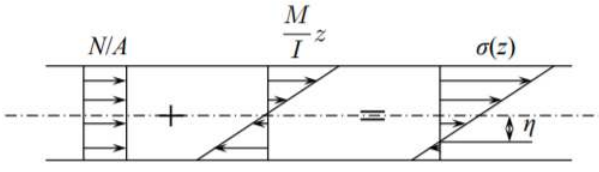

Figure 3.4.1: Linear distribution of stresses along the height of the beam.

Both axial force and bending moment contribute to the stress distribution along the along the height of the beam, as illustrated in Figure (3.4.1).

From Equation 3.4.8 one can calculate the point $z = \eta$ where the stresses become zero

$$\eta = -\frac{I}{A}\frac{N}{M} = -\rho^2\frac{N}{M} \tag{3.4.9}$$

where ρ is the moment of giration of the cross-section defined by $I = \rho^2 A$. The position of the zero stress axis depends on the ratio of axial force to bending moment. If $\eta < h$, where h is the thickness of a rectangular section beam, the zero stress point is inside the beam boundary, there is a bending dominated response. The tension dominated response is when η is several times larger than h.

3.5: Inconsistencies in the Elementary Beam Theory

The equations presented in Section 2.6 under the ADVANCED TOPIC were derived without any approximate assumption. In order for the beam to be in equilibrium, shear force V must be present, when the beam is under pure bending (uniform bending over the length of the beam). It is the shear stress σ_{xz} that give rise to the shear force, according to the definition, Equations (2.4.8-2.4.10). Therefore any inconsistencies must come from the strain-displacement relations as well as constitutive equations, where some approximations were introduced.

The presence of the shear stresses $\sigma_{xz} = \sigma_{13}$ means that shear strains $\epsilon_{13} = \epsilon_{xz}$ must develop according to Equation (4.16).

$$\epsilon_{xz}(z) = \frac{\sigma_{xz}(z)}{2G} \tag{3.5.1}$$

The shear strain is defined as

$$\epsilon_{xz} = \frac{1}{2}\left(\frac{\partial u_x}{\partial z} + \frac{\partial u_z}{\partial x}\right) \tag{3.5.2}$$

The Euler-Bernoulli assumption tells us that the shear strain vanishes. Then, Equation 3.5.1 is violated because the LH is zero while the RH is not. Suppose for a while that $\epsilon_{xz} = 0$. Then

$$\frac{\partial u_x}{\partial z} = -\frac{\partial w(x)}{\partial x} = -\theta(x) \tag{3.5.3}$$

where $u_z = w(x)$ is independent of the coordinate z. Integrating Equation 3.5.3 one gets

$$u_x(z) = u^\circ - z\theta \tag{3.5.4}$$

which is equivalent to the plane-remain-plane and normal-remain-normal hypothesis, introduced in Chapter 1. Assume now that the out-of-plane strain is a certain given function of z. Performing the integration of Equation 3.5.1 in a similar way as before, one gets

$$u_x(z) = u^\circ - z\theta + \int \epsilon_{xz}(z)dz \tag{3.5.5}$$

It transpires from the above results that deformed section are not flat but are warped instead. The amount of warping is given by the third term in Equation 3.5.5.

Can we estimate the amount of warping? Yes, but we have to go ahead of the presented material and quota the solution for the deflected slope θ of the beam. Le's settle on the simplest case of a clamped cantilever beam loaded at its tip by the point force P

$$\theta = \frac{Pl^2}{2EI} \tag{3.5.6}$$

This solution will be derived in Chapter 4.

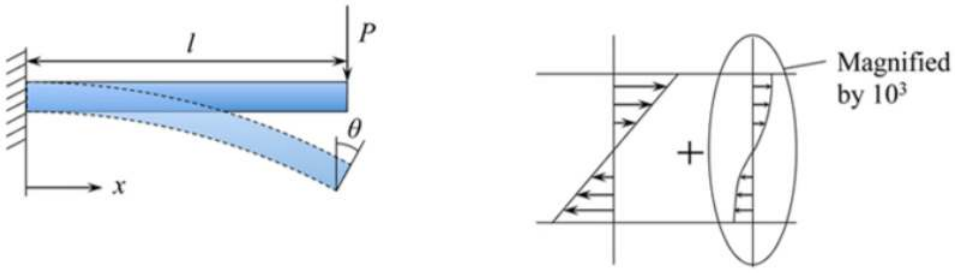

Figure 3.5.1: Warping of the end section of the cantilever beam.

Another result needed is the distribution of shear stresses across the height of the beam. For the rectangular section beam $(b \times h)$, the shear stress is a parabolic function of z

$$\sigma_{xz}(z) = \frac{3}{2}\frac{P}{A}\left[1 - \frac{z^2}{(h/2)^2}\right] \tag{3.5.7}$$

The corresponding strain is calculated from Equation 3.5.1. Assume that there is no axial force, $N = 0$, so from Equation (3.4.3) $\epsilon^\circ = 0$ and $u^\circ = 0$. After integration, the displacement profile defined by Equation 3.5.5 becomes

$$u_x(z) = -\frac{Pl^2}{2EI}z + \frac{1}{2\epsilon}\frac{3}{2}\frac{P}{A}\left[z - \frac{z^3}{3(h/2)^2}\right] \tag{3.5.8}$$

In order to quantify the correction of the displacement field due to warping, let's calculate the maximum values of the two terms at $z = -\frac{h}{2}$. The first term arising from the EulerBernoulli assumption gives

$$u_x^{\mathrm{I}}(z = -\frac{h}{2}) = \frac{\rho l^2}{2EI}\frac{h}{2} \tag{3.5.9}$$

The second correction term is

$$u_x^{\mathrm{II}}(z = -\frac{h}{2}) = \frac{1}{2G}\frac{P}{A}\frac{h}{2} \tag{3.5.10}$$

The ratio of the two terms is

$$\left|\frac{u_x^{\mathrm{II}}}{u_x^{\mathrm{I}}}\right| = \frac{E}{2G}\frac{I}{Al^2} = \frac{E}{2G}(\frac{\rho}{l})^2 \tag{3.5.11}$$

where ρ is the radius of giration of the cross-section. For a rectangular cross-section $(b \times h)$,

$$\rho^2 = \frac{I}{A} = \frac{bh^3}{12bh} = \frac{h^2}{12} \tag{3.5.12}$$

The ratio $E/2G$ is

$$\frac{E}{2G} = \frac{E}{2\frac{E}{2(1+\nu)}} = (1+\nu) \tag{3.5.13}$$

Then, the relative amplitude of warping from Equation 3.5.11 is

$$\left|\frac{u_x^{\mathrm{II}}}{u_x^{\mathrm{I}}}\right| = \frac{(1+\nu)}{12}\left(\frac{h}{l}\right)^2 \tag{3.5.14}$$

For a typical beam with $\frac{l}{h} = 20$, the above ratio becomes 0.25×10^{-3}!!! In order to compare the plane and wrapped cross-section, the amount of warping had to be magnified thousand times, see Figure (3.5.1). It can be concluded that the effect of warping is of an order of 0.1 and can be safely neglected in the engineering beam theory. In other words the "rein" of the Euler-Bernoulli assumption is unchallenged.

Another inconsistency of the elementary beam theory is that the uniaxial stress gives rise to the tri-axial strain state. In particular, from the 3-D constitutive equation, the strain components

$$\epsilon_{yy} = \epsilon_{zz} = -\frac{\nu}{E}\sigma_{xx} \tag{3.5.15}$$

Let's take as an example the same cantilever beam with a tip load. The bending moment at root of the beam is $M = Pl$, and from the stress formula,

$$\sigma_{xx} = \frac{Pl}{I}z \tag{3.5.16}$$

From the definition $\epsilon_{yy} = \frac{du_y}{dy}$, and after integrating with respect to y, one gets

$$u_y = -\frac{Pl\nu}{IE}zy \tag{3.5.17}$$

The maximum displacement occurs at $z = \frac{h}{2}$ and $y = \frac{b}{2}$. Making use of the beam deflection formula (see Chapter 4)

$$\delta = \frac{Pl^3}{3EI} \text{ or } \frac{Pl}{EI} = \frac{3\delta}{l^2} \tag{3.5.18}$$

the formula for the maximum displacement of a beam, normalized with respect to the beam thickness becomes

$$\frac{(u_y)_{max}}{h} = \frac{3}{4}\nu\left(\frac{\delta}{h}\right)\left(\frac{h}{l}\right)^2 \tag{3.5.19}$$

What is the range of the normalized beam deflections δ? The beam deflects elastically until the most stressed fibers reach yield of the materials, $\sigma_{xx}|_{z=\frac{h}{2}} = \sigma_y$.

Then, from the stress formula

$$\sigma_y = \frac{Pl}{I}\frac{h}{2} \tag{3.5.20}$$

Combining the above expression with the beam deflection formula, Equation 3.5.18, the estimate for the maximum elastic tip displacement

$$\frac{\delta}{h} = \frac{2}{3}\frac{\sigma_y}{E}\left(\frac{l}{h}\right)^2 \tag{3.5.21}$$

Combining Equations 3.5.19 and 3.5.21, the expression for the maximum normalized displacement of the corner of the cross-section becomes

$$\frac{(u_y)_{max}}{h} = \frac{\nu}{2}\frac{\delta_y}{E} \tag{3.5.22}$$

With realistic values $\nu = \frac{1}{3}$ and $\frac{\sigma_y}{E} = 10^{-3}$, the amount of maximum change of the width of the beam is 0.1 of the beam height. Such a tiny change in the cross-sectional dimension has no practical effect on the beam solution. A similar analysis can be performed to estimate the change in the height of the beam.

When the signs of z and y coordinates is properly taken into account, the present calculations predict the following change in the shape of the cross-section.

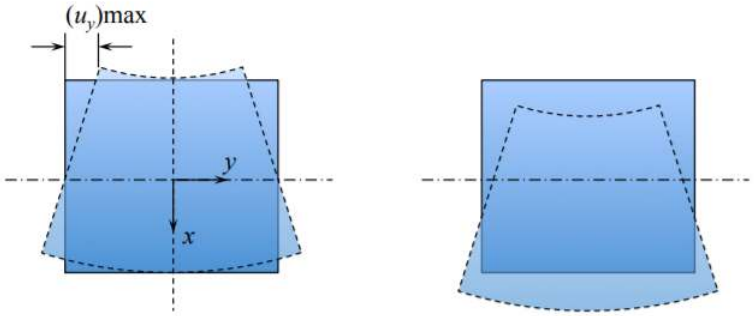

Figure 3.5.2: Predicted (left) and actual "anticlastic" deformed cross-section of the beam subjected to pure bending. Note that the deflections were magnified by a factor of 10^4 .

The anticlastic deformation can be easily seen by bending a rubber eraser, which is a very short beam. We can conclude the present section that the internal inconsistencies of the beam theory do not produce any significant errors in engineering applications. Therefore, one can safely assume that the cross-section of the beam does not deform and only moves as a rigid body with the increasing beam deflections.

3.6: Derivation of Constitutive Equations for Plates (Advanced)

For convenience, the set of equations necessary to derive the elasticity law for plates is summarized below.

Hook's law in plane stress reads:

$$\sigma_{\alpha\beta} = \frac{E}{1-\nu^2}[(1-\nu)\epsilon_{\alpha\beta} + \nu\epsilon_{\gamma\gamma}\delta_{\alpha\beta}] \tag{3.6.1}$$

In terms of components:

$$\sigma_{xx} = \frac{E}{1-\nu^2}(\epsilon_{xx} + \nu\epsilon_{yy}) \tag{3.6.2}$$

$$\sigma_{yy} = \frac{E}{1-\nu^2}(\epsilon_{yy} + \nu\epsilon_{xx}) \tag{3.6.3}$$

$$\sigma_{xy} = \frac{E}{1-\nu}\epsilon_{xy} \tag{3.6.4}$$

Here, strain tensor can be obtained from the strain-displacement relations:

$$\epsilon_{\alpha\beta} = \epsilon^{\circ}_{\alpha\beta} + z\kappa_{\alpha\beta} \tag{3.6.5}$$

Now, define the tensor of bending moment:

$$M_{\alpha\beta} \equiv \int_{-\frac{h}{2}}^{\frac{h}{2}} \sigma_{\alpha\beta} z dz \tag{3.6.6}$$

and the tensor of axial force (membrane force):

$$N_{\alpha\beta} \equiv \int_{-\frac{h}{2}}^{\frac{h}{2}} \sigma_{\alpha\beta} z dz \tag{3.6.7}$$

Bending Moments and Bending Energy

The bending moment $M_{\alpha\beta}$ is now calculated by substituting Equation 3.6.1 with Equation 3.6.6

$$\begin{aligned} M_{\alpha\beta} &= \frac{E}{1-\nu^2}\int_{-\frac{h}{2}}^{\frac{h}{2}}[(1-\nu)\epsilon_{\alpha\beta} + \nu\epsilon_{\gamma\gamma}\delta_{\alpha\beta}]z dz \\ &= \frac{E}{1-\nu^2}[(1-\nu)\epsilon^{\circ}_{\alpha\beta} + \nu\epsilon^{\circ}_{\gamma\gamma}\delta_{\alpha\beta}]\int_{-\frac{h}{2}}^{\frac{h}{2}} z dz \\ &+ \frac{E}{1-\nu^2}[(1-\nu)\kappa_{\alpha\beta} + \nu\kappa_{\gamma\gamma}\delta_{\alpha\beta}]\int_{-\frac{h}{2}}^{\frac{h}{2}} z^2 dz \\ &= \frac{Eh^3}{12(1-\nu^2)}[(1-\nu)\kappa_{\alpha\beta} + \nu\kappa_{\gamma\gamma}\delta_{\alpha\beta}] \end{aligned} \tag{3.6.8}$$

Note that the term $\int_{-\frac{h}{2}}^{\frac{h}{2}} z dz$ is zero, as shown in the case of beams. Therefore there are no mid-surface strains $\epsilon^{\circ}_{\alpha\beta}$ entering the moment-curvature relation.

Here we define the bending rigidity of a plate D as follows:

$$D = \frac{Eh^3}{12(1-\nu^2)} \tag{3.6.9}$$

Now, one gets the moment-curvature relations in the tensorial form

$$\boxed{M_{\alpha\beta} = D[(1-\nu)\kappa_{\alpha\beta} + \nu\kappa_{\gamma\gamma}\delta_{\alpha\beta}]} \tag{3.6.10}$$

$$M_{\alpha\beta} = \begin{vmatrix} M_{11} & M_{22} \\ M_{21} & M_{22} \end{vmatrix} \tag{3.6.11}$$

where $M_{12} = M_{21}$ due to symmetry. In the expanded notation,

$$M_{11} = D(\kappa_{11} + \nu\kappa_{22}) \tag{3.6.12}$$

$$M_{22} = D(\kappa_{22} + \nu\kappa_{11}) \tag{3.6.13}$$

$$M_{12} = D(1-\nu)\kappa_{12}) \tag{3.6.14}$$

One-dimensional Bending Energy Density

Here, we use the hat notation for a function of certain argument, such as:

$$\begin{aligned} M_{11} &= \hat{M}_{11}(\kappa_{11}) \\ &= D\kappa_{11} \end{aligned} \tag{3.6.15}$$

Then, the bending energy density $\bar{U}_b$ reads:

$$\begin{aligned} \bar{U}_b &= \int_0^{\bar{\kappa}} \hat{M}_{11}(\kappa_{11}) d\kappa_{11} \\ &= D\int^{\bar{\kappa}_{11}} \kappa_{11} d\kappa_{11} \\ &= \frac{1}{2} D(\bar{\kappa}_{11})^2 \end{aligned} \tag{3.6.16}$$

$$\bar{U}_b = \frac{1}{2} M_{11}\bar{\kappa}_{11} \tag{3.6.17}$$

General Case

General definition of the bending energy density reads:

$$\bar{U}_b = \oint M_{\alpha\beta} d\kappa_{\alpha\beta} \tag{3.6.18}$$

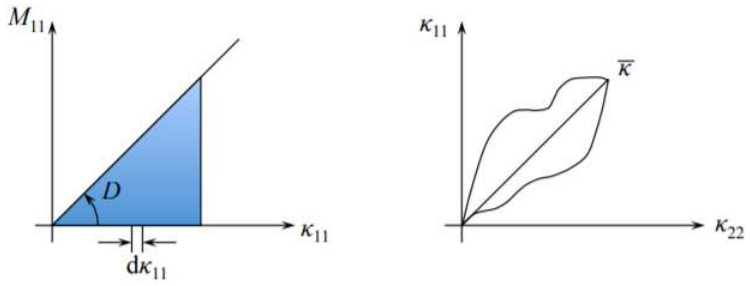

Figure **3.6.1**: In one dimension the energy density is the area under the linear moment-curvature plot. In the multi-axial case the final value can be reached along the straight or nonlinear path.

where the symbol $\oint$ denotes integration along a certain loading path.

Let's calculate the energy density stored when the curvature reaches a given value $\bar{\kappa}_{\alpha\beta}$ along a straight loading path:

$$\kappa_{\alpha\beta} = \eta\bar{\kappa}_{\alpha\beta} \tag{3.6.19}$$

$$d\kappa_{\alpha\beta} = \bar{\kappa}_{\alpha\beta} d\eta \tag{3.6.20}$$

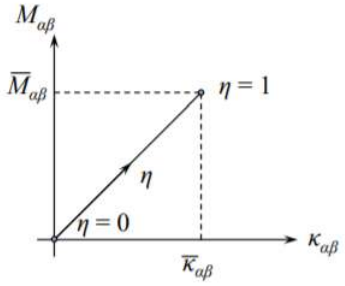

Figure **3.6.2**: The straight loading path in the 3-dimensional space of bending moments..

From the linearity of the moment-curvature relation, Equation **3.6.10**, it follows that

$$\begin{aligned} M_{\alpha\beta} &= \hat{M}_{\alpha\beta}(\kappa_{\alpha\beta}) \\ &= \hat{M}_{\alpha\beta}(\eta\bar{\kappa}_{\alpha\beta}) \\ &= \eta\hat{M}_{\alpha\beta}(\bar{\kappa}_{\alpha\beta}) \end{aligned} \tag{3.6.21}$$

where $\hat{M}_{\alpha\beta}(\kappa_{\alpha\beta})$ is a homogenous function of degree one.

$$\begin{aligned} \bar{U}_b &= \oint \hat{M}_{\alpha\beta}(\kappa_{\alpha\beta})d\kappa_{\alpha\beta} \\ &\int_0^1 \eta\hat{M}_{\alpha\beta}(\bar{\kappa}_{\alpha\beta})\bar{\kappa}_{\alpha\beta}d\eta \\ &= \hat{M}_{\alpha\beta}(\bar{\kappa}_{\alpha\beta})\bar{\kappa}_{\alpha\beta}\int_0^1 \eta d\eta \\ &\frac{1}{2}\hat{M}_{\alpha\beta}(\bar{\kappa}_{\alpha\beta})\bar{\kappa}_{\alpha\beta} \\ &= \frac{1}{2}M_{\alpha\beta}\bar{\kappa}_{\alpha\beta} \end{aligned} \tag{3.6.22}$$

Now, the bending energy density reads

$$\begin{aligned} \bar{U}_b &= \frac{D}{2}[(1-\nu)\bar{\kappa}_{\alpha\beta} + \nu\bar{\kappa}_{\gamma\gamma}\delta_{\alpha\beta}]\bar{\kappa}_{\alpha\beta} \\ &= \frac{D}{2}[(1-\nu)\bar{\kappa}_{\alpha\beta}\bar{\kappa}_{\alpha\beta} + \nu\bar{\kappa}_{\gamma\gamma}\bar{\kappa}_{\alpha\beta}\delta_{\alpha\beta}] \\ &= \frac{D}{2}[(1-\nu)\bar{\kappa}_{\alpha\beta}\bar{\kappa}_{\alpha\beta} - \nu(\bar{\kappa}_{\gamma\gamma})^2] \end{aligned} \tag{3.6.23}$$

The bending energy density expressed in terms of components are:

$$\begin{aligned} \bar{U}_b &= \frac{D}{2}\{(1-\nu)[(\bar{\kappa}_{11})^2 + 2(\bar{\kappa}_{12})^2 + (\bar{\kappa}_{22})^2] + \nu(\bar{\kappa}_{11} + \bar{\kappa}_{22})^2\} \\ &= \frac{D}{2}\{(1-\nu)[(\bar{\kappa}_{11} + \bar{\kappa}_{22})^2 - 2\bar{\kappa}_{11}\bar{\kappa}_{22} + 2(\bar{\kappa}_{12})^2] + \nu(\bar{\kappa}_{11} + \bar{\kappa}_{22})^2\} \\ &= \frac{D}{2}\{(\bar{\kappa}_{11} + \bar{\kappa}_{22})^2 - 2\bar{\kappa}_{11}\bar{\kappa}_{22} + 2(\bar{\kappa}_{12})^2 - \nu[-2\bar{\kappa}_{11}\bar{\kappa}_{22} + 2(\bar{\kappa}_{12})^2]\} \\ &= \frac{D}{2}\{(\bar{\kappa}_{11} + \bar{\kappa}_{22})^2 - 2\bar{\kappa}_{11}\bar{\kappa}_{22} + 2(\bar{\kappa}_{12})^2 - \nu[-2\bar{\kappa}_{11}\bar{\kappa}_{22} + 2(\bar{\kappa}_{12})^2]\} \\ &= \frac{D}{2}\{(\bar{\kappa}_{11} + \bar{\kappa}_{22})^2 + 2(1-\nu)[-\bar{\kappa}_{11}\bar{\kappa}_{22} + (\bar{\kappa}_{12})^2]\} \end{aligned} \tag{3.6.24}$$

$$\boxed{\bar{U}_b = \frac{D}{2}\{(\bar{\kappa}_{11} + \bar{\kappa}_{22})^2 - 2(1-\nu)[\bar{\kappa}_{11}\bar{\kappa}_{22} - (\bar{\kappa}_{12})^2]\}} \tag{3.6.25}$$

The term in the square brackets is the Gaussian curvature, κ_G, introduced in Chapter 1, Equation (1.8.9). Should the Gaussian curvature vanish, as it is often the case in plates, then the bending energy density assumes a very simple form $\bar{U}_b = \frac{1}{2}D(\bar{\kappa}_{11} + \bar{\kappa}_{22})^2$.

Total Bending Energy

The total bending energy is the integral of the bending energy density over the area of plate:

$$U_b = \int_S \bar{U}_b dA \tag{3.6.26}$$

Membrane Forces and Membrane Energy

The axial force can be calculated in a similar way as before

$$\begin{aligned} N_{\alpha\beta} &= \frac{E}{1-\nu^2}\int_{-\frac{h}{2}}^{\frac{h}{2}}[(1-\nu)\epsilon_{\alpha\beta}+\nu\epsilon_{\gamma\gamma}\delta_{\alpha\beta}]dz \\ &= \frac{E}{1-\nu^2}\int_{-\frac{h}{2}}^{\frac{h}{2}}[(1-\nu)\epsilon^{\circ}_{\alpha\beta}+\nu\epsilon^{\circ}_{\gamma\gamma}\delta_{\alpha\beta}]dz \\ &+ \frac{E}{1-\nu^2}\int_{-\frac{h}{2}}^{\frac{h}{2}}[(1-\nu)\kappa_{\alpha\beta}+\nu\kappa_{\gamma\gamma}\delta_{\alpha\beta}]zdz \\ &= \frac{E}{1-\nu^2}[(1-\nu)\epsilon^{\circ}_{\alpha\beta}+\nu\epsilon^{\circ}_{\gamma\gamma}\delta_{\alpha\beta}]\int_{-\frac{h}{2}}^{\frac{h}{2}}dz \\ &+ \frac{E}{1-\nu^2}[(1-\nu)\kappa_{\alpha\beta}+\nu\kappa_{\gamma\gamma}\delta_{\alpha\beta}]\int_{-\frac{h}{2}}^{\frac{h}{2}}dz \\ &= \frac{Eh}{1-\nu^2}[(1-\nu)\epsilon^{\circ}_{\alpha\beta}+\gamma\epsilon^{\circ}_{\gamma\gamma}\delta_{\alpha\beta}] \end{aligned} \tag{3.6.27}$$

The integral $\int_{-\frac{h}{2}}^{\frac{h}{2}} zdz$ is zero which means that there is no coupling between the membrane force and curvatures.

Here we define the axial rigidity of a plate C as follows:

$$C = \frac{Eh}{1-\nu^2} \tag{3.6.28}$$

Now, one gets the membrane force-extension relation in the tensor notation:

$$\boxed{N_{\alpha\beta} = C[(1-\nu)\epsilon^{\circ}_{\alpha\beta}+\nu\epsilon^{\circ}_{\gamma\gamma}\delta_{\alpha\beta}]} \tag{3.6.29}$$

$$N_{\alpha\beta} = \begin{vmatrix} N_{11} & N_{12} \\ N_{21} & N_{22} \end{vmatrix} \tag{3.6.30}$$

where $N_{12} = N_{21}$ due to symmetry. In components,

$$N_{11} = C(\epsilon^{\circ}_{11}+\nu\epsilon^{\circ}_{22}) \tag{3.6.31}$$

$$N_{22} = C(\epsilon^{\circ}_{22}+\nu\epsilon^{\circ}_{11}) \tag{3.6.32}$$

$$N_{12} = C(1-\nu)\epsilon^{\circ}_{11} \tag{3.6.33}$$

Membrane Energy Density

Using the similar definition used in the calculation of the bending energy density, the extension energy (membrane energy) reads:

$$\bar{U}_m = \oint N_{\alpha\beta}d\epsilon^{\circ}_{\alpha\beta} \tag{3.6.34}$$

Let's calculate the energy stored when the extension reaches a given value $\bar{\epsilon}^{\circ}_{\alpha\beta}$. Consider a straight path:

$$\epsilon^{\circ}_{\alpha\beta} = \eta\bar{\epsilon}^{\circ}_{\alpha\beta} \tag{3.6.35}$$

$$d\epsilon^{\circ}_{\alpha\beta} = \bar{\epsilon}^{\circ}_{\alpha\beta}d\eta \tag{3.6.36}$$

$$\begin{aligned} N_{\alpha\beta} &= \hat{N}_{\alpha\beta}(\epsilon^{\circ}_{\alpha\beta}) \\ &= \hat{N}_{\alpha\beta}(\eta\bar{\epsilon}^{\circ}_{\alpha\beta}) \\ &= \eta\hat{N}_{\alpha\beta}(\bar{\epsilon}^{\circ}_{\alpha\beta}) \end{aligned} \tag{3.6.37}$$

where $\hat{N}_{\alpha\beta}(\epsilon^{\circ}_{\alpha\beta})$ is a homogenous function of degree one.

$$\bar{U}_m = \int_0^{\mathring{\epsilon}_{\alpha\beta}} \hat{N}_{\alpha\beta}(\mathring{\epsilon}_{\alpha\beta}) d\mathring{\epsilon}_{\alpha\beta} \tag{3.6.38}$$
$$= \int_0^1 \eta \hat{N}_{\alpha\beta}(\mathring{\bar{\epsilon}}_{\alpha\beta}) \mathring{\bar{\epsilon}}_{\alpha\beta} d\eta$$
$$= \frac{1}{2} \hat{N}_{\alpha\beta}(\mathring{\bar{\epsilon}}_{\alpha\beta}) \mathring{\bar{\epsilon}}_{\alpha\beta}$$
$$= \frac{1}{2} N_{\alpha\beta} \mathring{\bar{\epsilon}}_{\alpha\beta}$$

Now, the extension energy reads:

$$\tilde{U}_m = \frac{C}{2}[(1-\nu)\mathring{\bar{\epsilon}}_{\alpha\beta} + \nu \mathring{\bar{\epsilon}}_{\gamma\gamma}\delta_{\alpha\beta}]\mathring{\bar{\epsilon}}_{\alpha\beta} \tag{3.6.39}$$
$$= \frac{C}{2}[(1-\nu)\mathring{\bar{\epsilon}}_{\alpha\beta}\mathring{\bar{\epsilon}}_{\alpha\beta} + \nu(\mathring{\bar{\epsilon}}_{\gamma\gamma})^2]$$

The extension energy density expressed in terms of components is:

$$\bar{U}_m = \frac{C}{2}\{(1-\nu)[(\mathring{\bar{\epsilon}}_{11})^2 + 2(\mathring{\bar{\epsilon}}_{12})^2 + (\mathring{\bar{\epsilon}}_{22})^2] + \nu(\mathring{\bar{\epsilon}}_{11} + \mathring{\bar{\epsilon}}_{22})^2\} \tag{3.6.40}$$
$$= \frac{C}{2}\{(1-\nu)[(\mathring{\bar{\epsilon}}_{11} + \mathring{\bar{\epsilon}}_{22})^2 - 2\mathring{\bar{\epsilon}}_{11}\mathring{\bar{\epsilon}}_{22} + 2(\mathring{\bar{\epsilon}}_{12})^2] + \nu(\mathring{\bar{\epsilon}}_{11} + \mathring{\bar{\epsilon}}_{22})^2\}$$
$$= \frac{C}{2}\{(\mathring{\bar{\epsilon}}_{11} + \mathring{\bar{\epsilon}}_{22})^2 - 2\mathring{\bar{\epsilon}}_{11}\mathring{\bar{\epsilon}}_{22} + 2(\mathring{\bar{\epsilon}}_{12})^2 - \nu[-2\mathring{\bar{\epsilon}}_{11}\mathring{\bar{\epsilon}}_{22} + 2(\mathring{\bar{\epsilon}}_{12})^2]\}$$
$$= \frac{C}{2}\{(\mathring{\bar{\epsilon}}_{11} + \mathring{\bar{\epsilon}}_{22})^2 + 2(1-\nu)[-\mathring{\bar{\epsilon}}_{11}\mathring{\bar{\epsilon}}_{22} + (\mathring{\bar{\epsilon}}_{12})^2]\}$$

$$\boxed{\bar{U}_m = \frac{C}{2}\{(\mathring{\bar{\epsilon}}_{11} + \mathring{\bar{\epsilon}}_{22})^2 - 2(1-\nu)[\mathring{\bar{\epsilon}}_{11}\mathring{\bar{\epsilon}}_{22} - (\mathring{\bar{\epsilon}}_{12})^2]\}} \tag{3.6.41}$$

The total membrane energy is the integral of the membrane energy density over the area of plate:

$$U_m = \int_S \bar{U}_m dS \tag{3.6.42}$$

3.7: Stress Formula for Plates

\)In the section on beams, it was shown that the profile of axial stress can be determined from the known bending moment M and axial force N, see Equation (3.4.8). A similar procedure can be developed for plates by comparing Equations (3.6.10-3.6.29) with Equation (3.6.1). The stress-strain curve for the plane stress can be expressed in terms of the middle surface strain tensor $\epsilon^{\circ}_{\alpha\beta}$ and curvature tensor $\kappa_{\alpha\beta}$ by combining Equations (3.6.1) and (3.6.5).

$$\sigma_{\alpha\beta} = \frac{E}{1-\nu^2}[(1-\nu)\epsilon^{\circ}_{\alpha\beta} + \nu\epsilon^{\circ}_{\gamma\gamma}\delta_{\alpha\beta}] + \frac{E}{1-\nu^2}[(1-\nu)\kappa_{\alpha\beta} + \nu\kappa_{\gamma\gamma}\delta_{\alpha\beta}]z \tag{3.7.1}$$

From the moment-curvature relation, Equation (3.6.10):

$$(1-\nu)\kappa_{\alpha\beta} + \nu\kappa_{\gamma\gamma}\delta_{\alpha\beta} = \frac{M_{\alpha\beta}}{D} \tag{3.7.2}$$

Similarly, from Equation (3.6.24)

$$(1-\nu)\epsilon^{\circ}_{\alpha\beta} + \nu\epsilon^{\circ}_{\gamma\gamma}\delta_{\alpha\beta} = \frac{N_{\alpha\beta}}{C} \tag{3.7.3}$$

where $D = \frac{Eh^3}{12(1-\nu^2)}$ is the bending rigidity, and $C = \frac{Eh}{1-\nu^2}$ is the axial rigidity of the plate.

From the above system, one gets

$$\sigma_{\alpha\beta} = \frac{Ez}{1-\nu^2}\frac{M_{\alpha\beta}}{D} + \frac{E}{1-\nu^2}\frac{N_{\alpha\beta}}{C} \tag{3.7.4}$$

or using the definitions of D and C

$$\sigma_{\alpha\beta} = \frac{N_{\alpha\beta}}{h} + \frac{zM_{\alpha\beta}}{h^3/12} \tag{3.7.5}$$

The above equation is dimensionally correct, because both $N_{\alpha\beta}$ and $M_{\alpha\beta}$ are respective quantities per unit length. In particular stress in the case of cylindrical bending is

$$\sigma_{xx} = \frac{N_{xx}}{h} + \frac{zM_{xx}}{h^3/12} \tag{3.7.6}$$

Multiplying both the numerators and denominators of the two terms above by b yields

$$\sigma_{xx} = \frac{N_{xx}b}{hb} + \frac{zM_{xx}b}{bh^3/12} \tag{3.7.7}$$

Now, observing that $N_{xx}b = N$ is the beam axial force, $bM_{xx} = M$ is the beam bending moment, $hb = A$ is the cross-section of the rectangular section beam, and $\frac{bh^3}{12}$ is the moment of inertia, the familiar beam stress formula is obtained

$$\sigma = \frac{N}{A} + \frac{Mz}{I} \tag{3.7.8}$$

CHAPTER OVERVIEW

4: Solution Method for Beam Deflections

4.1: Governing Equations

So far we have established three groups of equations fully characterizing the response of beams to different types of loading. In Chapter 1 relations were established to calculate strains from the displacement field.

$$\epsilon(x,z) = \epsilon^{\circ}(x) + z\kappa \tag{4.1.1}$$

where

$$\epsilon^{\circ}(x) = \frac{du}{dx} + \frac{1}{2}\left(\frac{dw}{dx}\right)^2 \ , \ \kappa = -\frac{d^2w}{dx^2} \tag{4.1.2}$$

The above geometrical relation are independent on equilibrium and apply to any kind of materials.

The second set of equations, derived in Chapter 2, is the equilibrium requirement

$$\frac{dV^*}{dx} + q(x) = 0 \quad - \quad \text{force equilibrium} \tag{4.1.3}$$

$$\frac{dM}{dx} - V = 0 \quad - \quad \text{moment equilibrium} \tag{4.1.4}$$

where $V^* = V + N\frac{dw}{dx}$ is the effective shear.

$$\frac{dN}{dx} = 0 \tag{4.1.5}$$

Eliminating V and V^* between the above equations, the beam equilibrium equation was obtained (See Equation (2.7.1))

$$\frac{d^2M}{dx^2} + N\frac{d^2w}{dx^2} + q = 0 \tag{4.1.6}$$

The derivation of the equilibrium is valid for all types of materials. In the theory of moderately large deflections, the equilibrium is coupled with the kinematics.

The third group of equation define the material behavior and relates the generalized strains to generalized forces

$$N = EA\epsilon^{\circ} \tag{4.1.7}$$

$$M = EI\kappa \tag{4.1.8}$$

Independence of geometry and equilibrium on constitutive equation allows to develop the general framework of a solver in the Finite Element codes. The constitutive equations can then be added as a user Defined Subroutines.

Let's consider first the infinitesimal deformations (small rotations for which the term $\frac{1}{2}\left(\frac{dw}{dx}\right)^2$ vanish in Equation 4.1.2 and the term $\frac{d^2w}{dx^2} = 0$ in Equation 4.1.6. Then from Equations 4.1.2, 4.1.4 and 4.1.7 one obtains

$$EA\frac{d^2u}{dx^2} = 0 \tag{4.1.9}$$

Eliminating the curvature and bending moments between Equations 4.1.2, 4.1.6 and 4.1.8, the beam deflection equation is obtained

$$EI\frac{d^4w}{dx^4} = q(x) \tag{4.1.10}$$

The concentrated load P can be treated as a special case of the distributed load $q(x) = P\delta(x - x_0)$, where δ is the Dirac delta function.

Let's consider first Equation 4.1.4 for the axial displacement. The boundary conditions in the x-direction are

$$(N - \bar{N})\delta u = 0 \tag{4.1.11}$$

The general solution for $u(x)$ is

$$\frac{du}{dx} = D_1 \ , \ u = D_1 x + D_0 \tag{4.1.12}$$

There are two integration constants, and two boundary conditions are needed. There are only four combinations of boundary conditions:

1. Beam restricted from axial motion, see Figure (4.1.1).

$$u(x=0)=u(x=l)=0 \tag{4.1.13}$$

This gives rise to the solution of two algebraic equation

$$0=D_0+D_1\cdot 0 \tag{4.1.14}$$

$$0=D_0+D_1 l \tag{4.1.15}$$

which gives $D_0=D_1=0$ and $u(x)=0$. This is a trivial case, for which the axial force $N=EA\frac{du}{dx}$ vanishes as well.

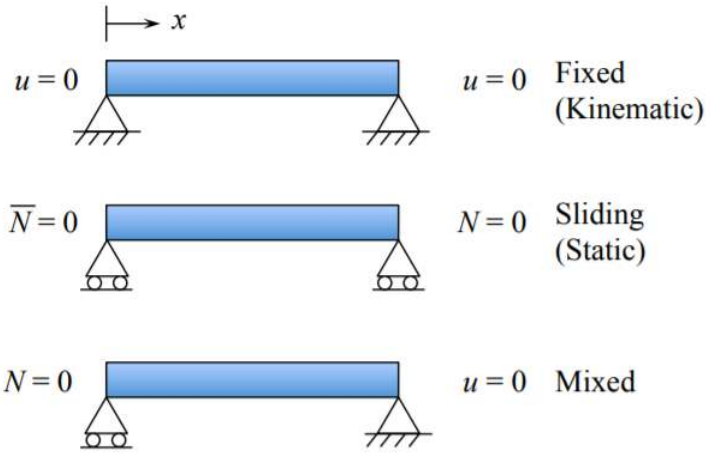

Figure 4.1.1: Three combinations of in-plane boundary conditions for $u(x)$.

2. Beam allowed to slide in the x-direction on both ends.

$$\bar{N}=N=0 \text{ at } x=0 \text{ and } x=l \tag{4.1.16}$$

The axial force is proportional to $\frac{du}{dx}$. From Equation 4.1.12 we can see that the gradient of u is zero along the entire beam. So, if $\bar{N}=0$ or $\frac{du}{dx}$ vanishes at one end, say $x=0$, $D_1=0$ and automatically $\bar{N}=0$ is satisfied at the other end, $x=l$. The integration constant D_0 is undetermined meaning that the rigid body translation of the entire beam is allowed.

3. In order to prevent the rigid body translation, one end of the beam, say $x=0$, must be fixed against motion in the x-direction. Thus

$$\bar{N}=0 \text{ or } \frac{du}{dx}=0 \quad \text{at} \quad x=0 \tag{4.1.17}$$

$$u=0 \quad \text{at} \quad x=l \tag{4.1.18}$$

which are precisely the boundary conditions for the third case. From Equation 4.1.12 we get

$$D_1=0 \tag{4.1.19}$$

$$D_1 l+D_2=0 \rightarrow D_2=0 \tag{4.1.20}$$

Now, the axial displacement vanishes, $u(x)=0$ but the rigid body translation is eliminated.

For all the above three cases of kinematic static and mixed boundary conditions, the axial force was zero.

4. If one end of the beam (bar) is loaded by a given force $\bar{N}$ and the other one is fixed, the boundary conditions (BC) are

$$\begin{aligned} N=-\bar{N}\,,\ EA\tfrac{du}{dx}=0 \quad & \text{at } x=0 \\ u=0 \quad & \text{at } x=l \end{aligned} \tag{4.1.21}$$

$$D_1 = -\frac{\bar{N}}{EA}\ ,\ D_2 = \frac{\bar{N}l}{EA} \tag{4.1.22}$$

and the solution is

$$u(x) = \frac{\bar{N}}{EA}(l - x) \tag{4.1.23}$$

The case in which the nonlinear term is retained in Equation 4.1.2 is much more interesting. This will be dealt with in the section on moderately large deflection of beams.

We now turn our attention to the solution of the beam deflection, Equation 4.1.10. This is the fourth-order linear inhomogeneous equation which requires four boundary conditions. There are four types of boundary conditions, defined by

$$(M - \bar{M})\delta w' = 0 \tag{4.1.24}$$

$$(V - \bar{V})\delta w = 0 \tag{4.1.25}$$

For the sake of illustration, we select a pin-pin BC for a beam loaded by the uniform like load q, Figure (4.1.2).

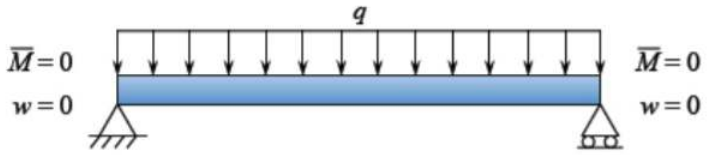

Figure 4.1.2: Pin support allows for rotation but not for vertical translation.

The bending moment is proportional to the curvature. Equation 4.1.10 is then subjected to the following boundary conditions:

$$w(x = 0) = w(x = l) = 0 \tag{4.1.26}$$

$$\left.\frac{d^2w}{dx^2}\right|_{x=0} = \left.\frac{d^2w}{dx^2}\right|_{x=l} = 0 \tag{4.1.27}$$

Let's integrate the differential equation four times with respect to x:

$$\frac{d^3w}{dx^3} = \frac{qx}{EA} + C_1 \tag{4.1.28}$$

$$\frac{d^2w}{dx^2} = \frac{qx^2}{EA2} + C_1x + C_2 \tag{4.1.29}$$

$$\frac{dw}{dx} = \frac{qx^3}{EA6} + \frac{C_1x^2}{2} + C_2x + C_3 \tag{4.1.30}$$

$$w = \frac{qx^4}{EA24} + \frac{C_1x^3}{6} + \frac{C_2x^2}{2} + C_3x + C_4 \tag{4.1.31}$$

Substituting the BC into the general solutions, one gets

$$0 = C_2 \tag{4.1.32}$$

$$0 = \frac{ql^3}{2EA} + C_1l + C_2 \tag{4.1.33}$$

$$0 = C_4 \tag{4.1.34}$$

$$0 = \frac{ql^4}{24EA} + \frac{C_1l^3}{6} + \frac{C_2l^2}{2} + C_3l + C_4 \tag{4.1.35}$$

The solution of the above system is

$$C_1 = -\frac{ql}{2} \tag{4.1.36}$$

$$C_2 = 0 \tag{4.1.37}$$

$$C_3 = \frac{ql^3}{12} \tag{4.1.38}$$

$$C_4 = 0 \tag{4.1.39}$$

The load-displacement relation becomes

$$w(x) = \frac{qx}{24EA}(l^3 - 2lx^2 + x^3) \tag{4.1.40}$$

Differentiating Equation 4.1.40 twice, the expression for the bending moment is

$$M(x) = \frac{qx}{2}(l - x) \tag{4.1.41}$$

and differentiating again, the shear force becomes

$$V(x) = \frac{dM}{dx} = \frac{q}{2}(l - 2x) \tag{4.1.42}$$

Plots of the normalized bending moments and shear forces are shown in Figure (4.1.3).

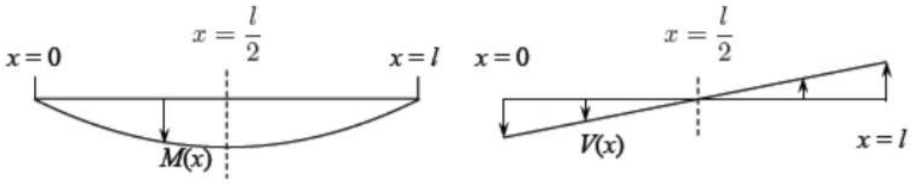

Figure 4.1.3: Parabolic distribution of the bending moment and linear variation of the shear force.

The shear force $V = EI\frac{d^3w}{dx^3}$ is seen to vanish at the mid-span of the beam. Also the slope $\frac{dw}{dx}$ is zero at this location. We have proved that at the symmetry plane

$$V(x = \frac{l}{2}) = 0 \tag{4.1.43}$$

$$\frac{dw}{dx}\Big|_{x=\frac{l}{2}} = 0 \tag{4.1.44}$$

Inversely, if the problem is symmetric, that Equations 4.1.43-4.1.44 must hold at the symmetry plane. As an alternative formulation, one can consider a half of the beam with the symmetry BC.

Can you solve the above problem and compare it with solution of the pin-pin beam, Equation 4.1.40?

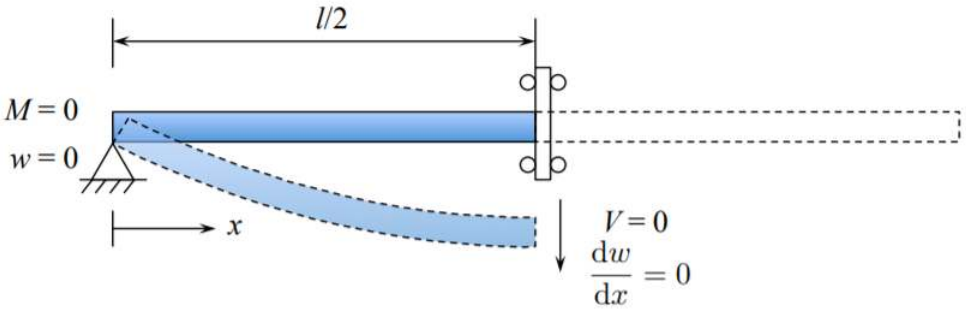

Figure 4.1.4: Simply-supported plate with symmetry boundary conditions.

It should be mentioned that the pin-pin supported beam is a statically determinate structure. Therefore the distribution of shear forces and bending moments can be determined from the equilibrium equation alone. Can you do it and get correctly the signs?

The purpose of Chapter 4 is to present properties of the governing equations and solutions. interested students are referred to end chapter of problem sets where many beams with different loading and BC are considered. Also the recommended reference book and monographs present solution to some common beam problems.

4.2: General Properties of the Beam Governing Equation- General and Particular Solutions

Recall from the Calculus that solution of the inhomogeneous, linear ordinary differential equation is a sum of the general solution of the homogeneous equation w_g and the particular solution of the inhomogeneous equation w_p. The property of homogeneity means that $f(Ax) = Af(x)$. The homogeneous counterpart of Equation (4.1.11) is

$$EI\frac{d^4w}{dx^4} = 0 \quad \text{or} \quad \frac{d^4w}{dx^4} = 0 \tag{4.2.1}$$

and its solution, obtained by four integrations is the third order polynomial

$$w_g(x) = \frac{C_1x^3}{6} + \frac{C_2x^2}{2} + C_3x + C_4 \tag{4.2.2}$$

The particular solution w_p of the beam deflection equation, Equation (4.1.11) depends on the loading, but not the boundary conditions. For the uniformly loaded beam the particular solution is the first term in Equation (4.1.27-4.1.28). As an illustration, consider the same pin-pin supported beam loaded by the triangular line load

$$q(x) = q_0\frac{2x}{l}\ ,\ 0 < x < \frac{l}{2} \tag{4.2.3}$$

where q_0 is the load intensity at mid-span $x = l/2$. The particular solution of this problem, satisfying the governing equation is

$$w_p = \frac{q_0x^5}{60EIl} \tag{4.2.4}$$

Then, the full solution is $w(x) = w_g + w_p$.

Beam loaded by concentrated forces (or moments) requires special consideration.

Continuity requirements

A sudden change in the beam cross-section or loading may produce a discontinuous solution. What quantities may suffer a jump and what must be continuous?

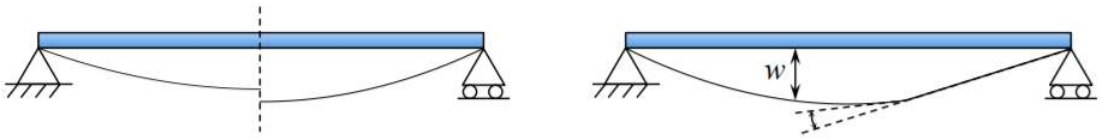

Figure 4.2.1: The displacement and slope discontinuities are not allowed in beams.

In mechanics the discontinuity of a given function is denoted by a square bracket

$$[f(\xi)] = f(\xi^+) - f(\xi^-) \tag{4.2.5}$$

where ξ^+ and ξ^- denote the values of the argument on the right and left hand of a discontinuity. In the quasi-static theory of beam

$$[w] = 0 \tag{4.2.6}$$

$$\left[\frac{dw}{dx}\right] = 0 \tag{4.2.7}$$

The discontinuity in the vertical displacement means separation so of course it may not occur. Why then slopes must be continuous for elastic beams? This is simple. A change of slope is called a curvature. A jump in the slope gives an infinite curvature, and thus an infinite bending moments. Such a situation is impossible, because the beam cross-section will go into plastic range, and the beam will no longer stay elastic. Quantities that can be discontinuous are

$$\text{Bending moments} \quad [M] = \bar{M} \tag{4.2.8}$$

$$\text{Shear force} \quad [V] = \bar{V} \tag{4.2.9}$$

As an illustration, consider a pin-pin supported beam loaded at mid-span by a point force P.

As mentioned earlier, the point load can be considered as a limiting case of a continuous line load with the help of the Dirac delta function

$$q(x) = P\delta(x - \frac{l}{2}), \quad \text{where } \int \delta(x - \frac{l}{2})dx = 1 \tag{4.2.10}$$

Even though techniques have been developed to deal with singularity functions for beams, they require to use the apparatus of the mathematical theory of distribution. This

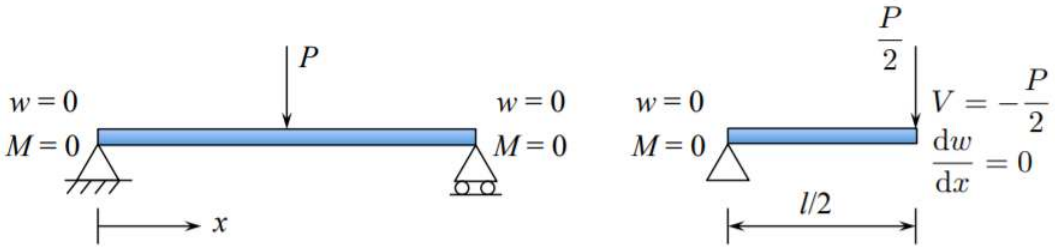

Figure 4.2.2: Symmetric loading of a beam by a concentrated force.

is not the avenue that we will take. instead, a symmetry boundary condition will be imposed. Now, the concentrated load is not applied inside the beam $0 < x < l$, governed by the inhomogeneous differential equation, but at the boundary. Each half of the beam is carrying half of the load. Therefore, the boundary conditions are

$$\text{at } x = 0 \; w = 0 \tag{4.2.11}$$

$$\frac{d^2w}{dx^2} = 0 \tag{4.2.12}$$

$$\text{at } x = \frac{l}{2} \; V = -\frac{P}{2} \tag{4.2.13}$$

$$\frac{dw}{dx} = 0 \tag{4.2.14}$$

Because the loading is applied on the boundary, the differential equation becomes homogeneous. The solution of Equation 4.2.1 is given by the third order polynomial, substituting the above BC into the solution given by Equation 4.2.2, a system of four linear algebraic equations is obtained, where the solution is

$$C_1 = -\frac{D}{2EI}, \; C_2 = 0, \; C_3 = \frac{Pl^2}{16EI}, \; C_4 = 0 \tag{4.2.15}$$

The deflection line is given by

$$w(x) = \frac{Px}{48EI}(3l^2 - 4x^2) \tag{4.2.16}$$

and the central deflection (something to remember) is

$$w_0 = w(x = \frac{l}{2}) = \frac{pl^3}{48EI} \tag{4.2.17}$$

The plot of the distribution of bending moment and shear forces along the length of the beam determined from the calculated deflection line is shown in Figure (4.2.3).

Note that the jump in the internal shear force is equal to the applied force

$$[V] = V_{\text{right}}(x = \frac{l}{2}) - V_{\text{left}}(x = \frac{l}{2}) = P \tag{4.2.18}$$

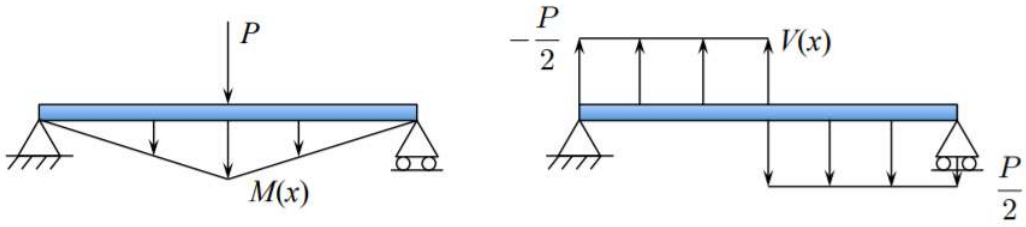

Figure **4.2.3**: Bending moment is continuous at the mid-span, but the shear force is not.

If the point load is not applied at the mid-span but at an arbitrary distance $x = a$, the beam must be divided into two parts $0 < x < a$, $a < x < l$, and each part must be solved independently.

$$\textbf{First segment } 0 < x < a \; w^{\mathrm{I}}(x) = \frac{C_1 x^3}{6} + \frac{C_2 x^2}{2} + C_3 x + C_4 \tag{4.2.19}$$

$$\textbf{Second segment } a < x < l \; w^{\mathrm{II}}(x) = \frac{C_5 x^3}{6} + \frac{C_6 x^2}{2} + C_7 x + C_8 \tag{4.2.20}$$

This gives rise to eight integration constants, four for each side. Would there be enough conditions to determine these constants? The answer is YES. There are two boundary conditions at $x = 0$, four continuity conditions at $x = a$, given by Equations 4.2.6-4.2.9 and, again, two boundary conditions at $x = l$. In summary

BC, $x = 0$	Continuity, $x = a$	BC, $x = l$
$w = 0$	$[w] = 0$	$w = 0$
$M = 0$	$\left[\frac{dw}{dx}\right] = 0$	$M = 0$
	$[M] = 0$	
	$[V] = P$	

(4.2.21)

Note that there is no concentrated bending moment applied $\bar{M} = 0$ so that the bending moment field is continueous across $x = a$. The concentrated force produces a jump in the distribution of the shear forces, so $\bar{V} = P$.

We leave it to the reader to apply the above condition and solve the problem. More on this problem can be found in two sections of this notes: Problem Sets and Recitations.

The method of superposition says that the deflections and slopes of the beam subjected to a system of loads are equal to the sum of those quantities due to individual loads. In other words the individual results may be superimposed to determine a combined response, hence the term method of superposition.

This is a very powerful and convenient method since solutions for many support and loading conditions are readily available in various engineering handbooks. Using the principle of superposition, we may combine these solutions to obtain a solution for more complicated loading conditions.

As an example, consider a clamped-clamped beam loaded by a uniform line load q and concentrated force at the center P. The deflection formulas for the two individual loading are

$$w|_{\text{uniform}} = \frac{q x^2}{24EI}(l - x)^2 \tag{4.2.22}$$

$$w|_{\text{point}} = \frac{P x^2}{48EI}(3l - 4x) \tag{4.2.23}$$

The solution for both loads acting together is

$$w_{\text{total}} = w|_{\text{uniform}} + w|_{\text{point}} \tag{4.2.24}$$

4.3: Statically Determined Beams

Beam for which the distribution of bending moments and shear forces can be determined from the equilibrium alone are called statically determinate beams. For such beams $M(x)$ and $V(x)$ are known and determination of beam deflection will be a much easier task. Combining Equation (4.1.9) with Equation (4.1.2) one ends up with the following second order linear differential equation

$$-EI\frac{d^2w}{dx^2} = M(x) \tag{4.3.1}$$

The bending moment, which by itself should satisfy the second order differential equation, Equation (4.1.7) should now obey two stress boundary conditions at the beam ends. The static boundary conditions are indicated in Figure **4.3.1**) for a pin-pin supported and cantilever beam.

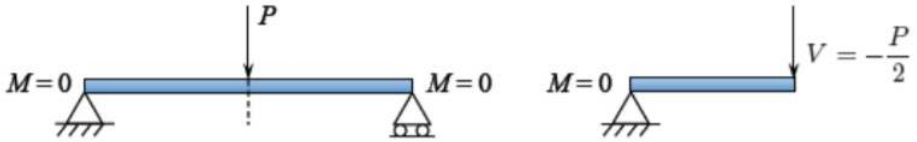

Figure **4.3.1**: The static boundary conditions for a full and half of a beam.

Determination of bending moment and shear force diagrams is the subject of elementary courses in statics, and the general procedure is not explained here. In the case of the simply supported beam with a point load at the mid-span, the bending moments

$$M(x) = \begin{cases} \frac{Px}{2}, & 0 < x < \frac{l}{2} \\ \frac{P(l-x)}{2}, & \frac{l}{2} < x < l \end{cases} \tag{4.3.2}$$

The bending moment vanishes at $x = 0$ and $x = l$.

The corresponding shear force $V = \frac{dM}{dx}$ is

$$V(x) = \begin{cases} \frac{P}{2}, & 0 < x < \frac{l}{2} \\ -\frac{P}{2}, & \frac{l}{2} < x < l \end{cases} \tag{4.3.3}$$

At the beam center

$$[V] = \frac{P}{2} - \left[-\frac{P}{2}\right] = P \tag{4.3.4}$$

Because of shear force discontinuity at the beam center, the solution will be sought for a half of the beam. Each half of the beam is carrying half of the load. We have shown that the bending moment distribution satisfy two satin boundary condition. Therefore the differential equation **4.3.2** is subjected only to two kinematic boundary conditions

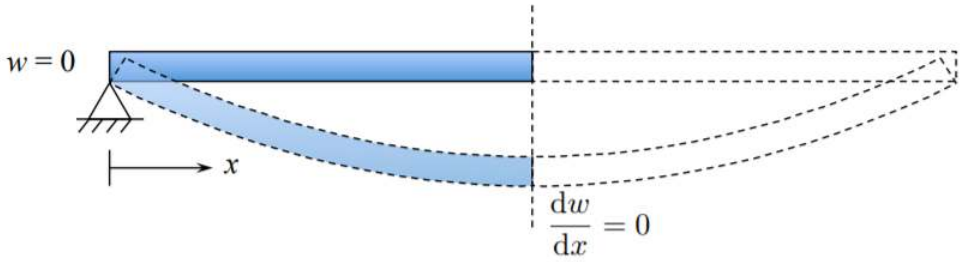

Figure **4.3.2**: Symmetry boundary condition.

Integrating Equation **4.3.1** twice one gets

$$-EIw = \frac{Px^3}{12} + C_1x + C_2 \tag{4.3.5}$$

The two integration constants, determined from the boundary conditions $w(0) = 0$, $\frac{dw}{dx}\Big|_{x=\frac{l}{h}} = 0$, are

$$C_1 = -\frac{Pl^2}{16}, \quad C_2 = 0 \tag{4.3.6}$$

and the deflection line of the beam is given by

$$w(x) = \frac{Px}{48EI}(3l^2 - 4x^2) \quad 0 < x < \frac{l}{2} \tag{4.3.7}$$

The second half of the beam is the mirror reflection, by symmetry. In particular, the central deflection $w_o = w(x = \frac{l}{2})$ is expressed by all input parameters of the beam as

$$w_o = \frac{Pl^3}{48EI} \tag{4.3.8}$$

It will be helpful to remember the above formula for the rest of your professional life.

In summary, determination of deflections of statically determinate beams is much easier than its statically indeterminate counterparts. The governing equation is of the second order, and for symmetric problems there are only two integration constants.

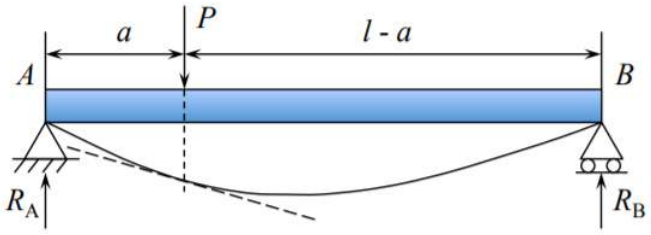

Figure **4.3.3**: Beam under off-center point load.

4.4: Continuity Conditions, an Example

In Section 4.4 the continuity requirements were formulated, but the system of eight algebraic equations was not solved. Here a complete solution will be presented for a beam loaded by a point force acting at an arbitrary location $x = a$.

The reaction forces are calculated from moment equilibrium:

$$R_A = P\frac{l-a}{l} \tag{4.4.1}$$

$$R_B = P\frac{a}{l} \tag{4.4.2}$$

The sum of the reaction forces is equal to P. The corresponding bending moments and shear forces are

$$M(x) = \begin{cases} R_A x = \frac{P(l-a)x}{l}, \\ R_B(l-x) = \frac{Pa(l-x)}{l}, \end{cases}, \quad V(x) = \begin{cases} \frac{P(l-a)}{l}, & 0 < x < a \\ -\frac{Pa}{l}, & a < x < l \end{cases} \tag{4.4.3}$$

The jump in the shear force across the discontinuity point $x = a$ is

$$[V] = V^+ - V^- = \frac{P(l-a)}{l} - (-\frac{Pa}{l}) = P \tag{4.4.4}$$

The bending moments are continuous on both sides, $[M] = 0$. Therefore the static continuity conditions are automatically satisfied at $x = a$. The kinematic continuity conditions, formulated in Equations (4.2.6-4.2.7) require displacements and slopes to be continuous. Integrating the governing equations (4.3.1) with **4.4.3** in two regions gives

$$-EIw^{\mathrm{I}} = \frac{P(l-a)x^3}{6l} + C_1 x + C_2 \quad 0 < x < a \tag{4.4.5}$$

$$-EIw^{\mathrm{II}} = \frac{Pa}{l}(\frac{lx^2}{2} - \frac{x^3}{6}) + C_3 x + C_4 \quad a < x < l \tag{4.4.6}$$

The four integration constants are found from two boundary condition and two continuity condition

$$w(0) = w(l) = 0,\ w^{\mathrm{I}}(a) = w^{\mathrm{II}}(a),\ \left.\frac{dw^{\mathrm{I}}}{dx}\right|_{x=a} = \left.\frac{dw^{\mathrm{II}}}{dx}\right|_{x=a} \tag{4.4.7}$$

This gives rise to the system of four linear inhomogeneous algebraic equations for C_1, C_2, C_3, and C_4

$$\begin{cases} C_2 = 0 \\ \frac{Pal^2}{3} + C_3 l + C_4 = 0 \\ \frac{Pba^3}{6l} + C_1 a = \frac{Pa}{l}\left(\frac{la^2}{2} - \frac{a^3}{6}\right) + C_3 a + C_4 \\ \frac{Pba^2}{2l} + C_1 = \frac{Pa}{l}\left(la - \frac{1}{2}a^2\right) + C_3 \end{cases} \tag{4.4.8}$$

A simple problem has led to a quite complex algebra. Now, you understand why the previous example with eight unknown coefficients was only formulated but not solved. The solution to the system **4.4.8** is

$$C_1 = -\frac{Pa(a^2 - 3al + 2l^2)}{6l} \tag{4.4.9}$$

$$C_2 = 0 \tag{4.4.10}$$

$$C_3 = -\frac{Pa(a^2 + 2l^2)}{6l} \tag{4.4.11}$$

$$C_4 = \frac{Pa^3}{6} \tag{4.4.12}$$

and the final solution of unsymmetrically loaded beam is

$$w^{\mathrm{I}}(x) = \frac{Px[a^3 - 3a^2 l - lx^2 + a(2l^2 + x^2)]}{6EIl} \quad 0 < x < a \tag{4.4.13}$$

$$w^{II}(x) = -\frac{Pa(l-x)[a^2 + x(-2l+x)]}{6EIl} \quad a < x < l \tag{4.4.14}$$

One can easily check that the continuity conditions are met at $x = a$. The above example teaches us that symmetry in nature and engineering not only means beauty, but also brings simplicity.

CHAPTER OVERVIEW

5: Moderately Large Deflection Theory of Beams

5.1: General Formulation

Compare to the classical theory of beams with infinitesimal deformation, the moderately large deflection theory introduces changes into the strain-displacement relation and vertical equilibrium, but leaves the constitutive equation and horizontal equilibrium unchanged. The kinematical relation, Equation (1.9.5) acquires now a new term due to finite rotations of beam element.

$$\epsilon^{\circ} = \frac{du}{dx} + \boxed{\frac{1}{2}\left(\frac{dw}{dx}\right)^2} - \text{ new term} \tag{5.1.1}$$

The definition of curvature has also a nonlinear rotation term

$$\kappa = -\frac{\frac{d^2w}{dx^2}}{\left[1+\left(\frac{dw}{dx}\right)^2\right]^{3/2}} \tag{5.1.2}$$

The square of the slope can be large, as compared with the term $\frac{du}{dx}$ and must be retained in Equation 5.1.1. At the same time the square of the slope (beam rotation) are small compared to unity. Why? This is explained in Figure (5.1.1), where the square of the slope is plotted against the slope.

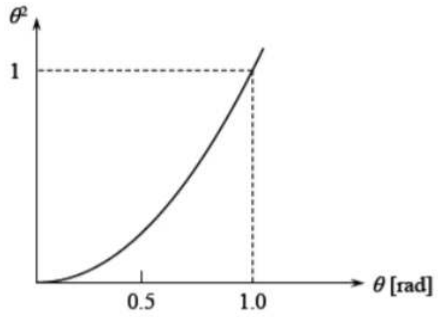

Figure 5.1.1: The significance of the square of the slope term.

At $\theta = 1$ rad $= 57$ degrees the two terms in the denominator of Equation 5.1.2 are equal. However, the theory of moderately large deflections are valid up to $\theta = 10^{\circ} \approx 0.175$ rad. The term θ^2 amounts to 0.03, which is negligible compared to unity. Therefore the curvature is defined in the same way as in the theory of small deflections

$$\kappa = -\frac{d^2w}{dx^2} \tag{5.1.3}$$

It was shown in Chapter 2 that the equation of equilibrium in the horizontal direction is not affected by the finite rotation. Therefore, we infer from Equation (2.7.4) that the axial force is either constant or zero

$$N = \text{ constant} \tag{5.1.4}$$

The vertical equilibrium, given by Equation (3.79) has a new nonlinear term

$$\frac{d^2M}{dx^2} + \overbrace{\boxed{N\frac{d^2w}{dx^2}}}^{\text{new term}} + q = 0 \tag{5.1.5}$$

Finally, the elasticity law is unaffected by finite rotation

$$N = EA\epsilon^{\circ} \tag{5.1.6}$$

$$M = EI\kappa \tag{5.1.7}$$

The solution to the coupled problem depends on the boundary conditions in the horizontal direction. Referring to Figure 4.1.1, two cases must be considered:

- Case 1, beam free to slide, $N = 0,\ u \neq 0$.
- Case 2, beam fixed, $u = 0,\ N \neq 0$.

5.2: Solution for a Beam on Roller Support

Consider first case 1. From the constitutive equation, zero axial force beams that there is no extension of the beam axis, $\epsilon^{\circ} = 0$. Then, from Equation (5.1.1)

$$\frac{du}{dx} = \frac{1}{2}\left(\frac{dw}{dx}\right)^2 \tag{5.2.1}$$

At the same time, the nonlinear term in the vertical equilibrium vanishes and the beam response is governed by the linear differential equation

$$EI\frac{d^4w}{dx^4} = q(x) \tag{5.2.2}$$

which is identical to the one derived for the infinitesimal deflections. As an example, consider the pin-pin supported beam under mid-span point load. From Equations (4.3.7) and (4.3.8), the deflection profile is

$$w(x) = w_o\left[3\frac{x}{l} - 4\left(\frac{x}{l}\right)^3\right] \tag{5.2.3}$$

and the slope is

$$\frac{dw}{dx} = \frac{w_o}{l}\left[3 - 12\left(\frac{x}{l}\right)^2\right] \tag{5.2.4}$$

where w_o is the central deflection of the beam. Now, Equation 5.2.1 can be used to calculate relative horizontal displacement Δu. Integrating Equation 5.2.1 in the limits $(0, l)$ gives

$$\int_0^l \frac{du}{dx}dx = u|_0^l = u(l) - u(0) = \Delta u = -\int_0^l \frac{1}{2}\left(\frac{dw}{dx}\right)^2 dx \tag{5.2.5}$$

The result of the integration is

$$\Delta u \approx 7\frac{w_o^2}{l} \tag{5.2.6}$$

In order to get a physical sense of the above result, the vertical and horizontal displacements are normalized by the thickness h of the beam

$$\frac{\Delta u}{h} = \frac{7}{l/h}\left(\frac{w_o}{h}\right)^2 \tag{5.2.7}$$

For a beam with $\frac{l}{h} = 21$, the result

$$\frac{\Delta u}{h} = \frac{1}{3}\left(\frac{w_o}{h}\right)^2 \tag{5.2.8}$$

is ploted in Figure (5.2.1).

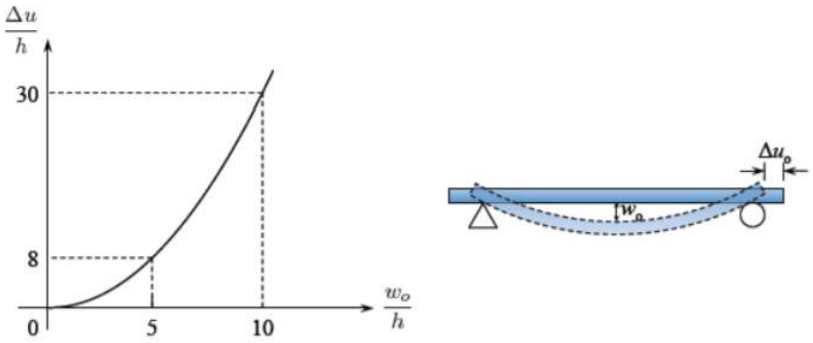

Figure **5.2.1**: Sliding of a beam from the roller support.

It is seen that the amount of sliding in the horizontal direction can be very large compared to the thickness.

To summarize the results, the roller supported beam can be treated as a classical beam even though the displacements and rotations are large (moderate). The solution of the linear differential equation can then be used a posteriori to determine the magnitude of sliding. The analysis of fully restrained beam is much more interesting and difficult. This is the subject of the next section.

5.3: Solution for a Beam with Fixed Axial Displacements

The problem is solved under the assumption of simply-supported end condition, and the line load is distributed accordingly to the cosine function. The beam is restrained in the axial direction. There is a considerable strengthening effect of the beam response due to finite rotations of beam elements. The axial force N (non-zero this time) is calculated from Equation (5.1.6-5.1.7) with Equation (5.1.1)

$$N = EA\left[\frac{du}{dx} + \frac{1}{2}\left(\frac{dw}{dx}\right)^2\right] \tag{5.3.1}$$

From Equation (5.1.4) we know that N is constant but unknown. In order to make use of the kinematic boundary conditions, let us integrate both sides of Equation 5.3.1 with respect to x

$$\frac{Nl}{EA} = u(l) - u(0) + \int_0^l \frac{1}{2}\left(\frac{dw}{dx}\right)^2 dx \tag{5.3.2}$$

Using the boundary conditions for u, the axial force is related to the square of the slope by

$$\frac{Nl}{EA} = \frac{1}{2}\int_0^l \left(\frac{dw}{dx}\right)^2 dx \tag{5.3.3}$$

In order to determine the deflected shape of the beam, consider the equilibrium in the vertical direction given by Equation (5.1.5)

$$-EI\frac{d^4w}{dx^4} + N\frac{d^2w}{dx^2} + q = 0 \tag{5.3.4}$$

Dividing both sides by $(-EI)$ one gets

$$\frac{d^4w}{dx^4} - \lambda^2\frac{d^2w}{dx^2} = \frac{q_o}{EI}\cos\frac{\pi x}{l} \tag{5.3.5}$$

where

$$\lambda^2 = \frac{N}{EI} \tag{5.3.6}$$

The roots of the characteristic equations are $0, 0, \pm\lambda$. Therefore the general solution of the homogeneous equation is

$$w_g = C_o + C_1 x + C_2\cosh\lambda x + C_3\sinh\lambda x \tag{5.3.7}$$

As the particular solution of the inhomogeneous equation we can try

$$w_p(x) = C\cos\frac{\pi x}{l} \tag{5.3.8}$$

$$\frac{d^2w_p}{dx^2} = -\frac{\pi^2}{l^2}C\cos\frac{\pi x}{l} \tag{5.3.9}$$

$$\frac{d^4w_p}{dx^4} = \frac{\pi^4}{l^4}C\cos\frac{\pi x}{l} \tag{5.3.10}$$

Substituting the above solution to the governing equation 5.3.4 one gets

$$\left[\frac{\pi^4}{l^4}C - \lambda^2\frac{\pi^2}{l^2}C - \frac{P_o}{EI}\right]\cos\frac{\pi x}{l} = 0 \tag{5.3.11}$$

The above solution satisfy the differential equation if the amplitude C is related to input parameters and the unknown tension N

$$C = \frac{\frac{q_o}{EI}}{\frac{\pi^2}{l^2}\left(\lambda^2 + \frac{\pi^2}{l^2}\right)} = \frac{q_o}{EI\left(\frac{\pi}{l}\right)^4 + N\left(\frac{\pi}{l}\right)^2} \tag{5.3.12}$$

The general solution of Equation 5.3.4 is a sum of the particular solution of the inhomogeneous equation w_p and general solution of the homogeneous equation, w_g

$$w(x) = w_g + w_p \tag{5.3.13}$$

There are five unknowns, C_o, C_1, C_2, C_3 and N and five equations. Four boundary conditions for the transverse deflections

$$w = 0, \quad \frac{d^2w}{dx^2} = 0 \quad \text{at} \quad x = \pm\frac{l}{2} \tag{5.3.14}$$

and equation 5.3.3 relating the horizontal and vertical response. The determination of the integration constants is straightforward. Note that the problem is symmetric. Therefore the solution should be an even function[1] of x. The terms C_1x and \(C_3 \sinh \lambda x are odd functions. Therefore the respective coefficients should vanish

$$C_1 = C_3 = 0 \tag{5.3.15}$$

$$w(x) = C_o + C_2 \cosh \lambda x + C \cos \frac{\pi x}{l} \tag{5.3.16}$$

The remaining two coefficients are determined only from the boundary conditions at one side of the beam

Missing argument for w column declaration

The solution of the above system is

$$C_o = C_2 = 0 \tag{5.3.17}$$

The slope of the deflection curve, calculated from Equation 5.3.16 is

$$\frac{dw}{dx} = -C\frac{\pi}{2}\sin\frac{\pi x}{2} \tag{5.3.18}$$

Expressing N in terms of x in Equation 5.3.3 gives

$$\lambda^2\left(\frac{Il}{A}\right) = \frac{1}{2}\int_0^l \left(\frac{dw}{dx}\right)^2 dx \tag{5.3.19}$$

Combining the above two equations one gets

$$\lambda^2\left(\frac{Il}{A}\right) = \frac{1}{2}\int_0^l \left(-\frac{C\pi}{l}\sin\frac{\pi x}{l}\right)^2 dx \tag{5.3.20}$$

or after integration

$$\frac{\lambda^2 Il}{A} = \frac{1}{4}C^2\left(\frac{\pi}{l}\right)^2\frac{l}{2} \tag{5.3.21}$$

Recalling the definition of λ, the membrane force N becomes a quadratic function of the deflection amplitude

$$N = \frac{EA}{4}C^2\left(\frac{\pi}{l}\right)^2 \tag{5.3.22}$$

The membrane force can be eliminated between Equations 5.3.12 and 5.3.22 to give the cubic equation for the deflection amplitude C

$$C + C^3\frac{A}{4I} = \frac{q_o}{EI}\left(\frac{l}{\pi}\right)^4 \tag{5.3.23}$$

To get a better sense of the contribution of various terms, consider a beam of the square cross-section $h \times h$, for which

$$I = \frac{h}{12}, \; A = h^2, \; \frac{A}{I} = \frac{12}{h^2} \tag{5.3.24}$$

Also, the ventral deflection is dimensionalized with respect to the beam thickness $\bar{w}_o = \frac{C}{h}$

$$\bar{w}_o + 3w_o^3 = \left(\frac{q_o}{Eh}\right)\left(\frac{l}{\pi h}\right)^4 \tag{5.3.25}$$

The present solution is exact and involves all information about the material (E), load intensity (q_o), length (l) and cross-sectional dimension. The distribution of line load and boundary conditions are reflected in the specific numerical coefficients in the

respective terms.

In order to get a physical insight about the contributions of all terms in the above solution, consider two limiting cases:

I. Pure bending solution for which $N\frac{dw}{dx} = 0$.
II. Pure membrane (string, cable) solution with zero flexural resistance (bending rigidity, $EI \to 0$).

(i) The bending solution is obtained by dropping the cubic term in Equations 5.3.23 or 5.3.25

$$C = \frac{q_o l^4}{EI}\frac{1}{\pi^4} \tag{5.3.26}$$

where the coefficient $\pi^4 = 97.4$. this result for the sinusoidal distribution of the line load should be compared with the uniform line load (coefficient 77) and point load (coefficient 48).

(ii) The membrane solution is recovered by neglecting the first linear term

$$C^3 = \frac{q_o l^4}{EI}\frac{4}{\pi^4} \tag{5.3.27}$$

The plot of the full bending/membrane solution and two limiting cases is shown in Figure (5.3.1).

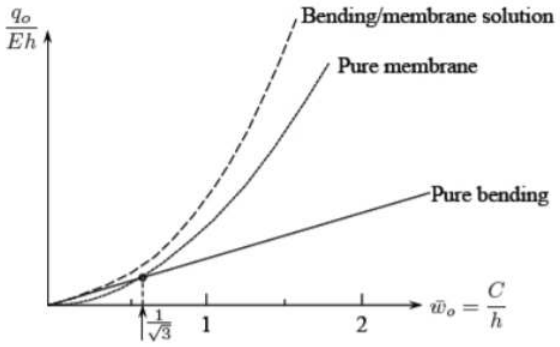

Figure 5.3.1: Comparison of a bending and membrane solution for a beam.

The question is at which magnitude of the central deflection relative to the beam thickness the non-dimensional load $\frac{q_o}{Eh}$ is the same. This is the intersection of the straight line with the third order parabola. By eliminating the load parameter between Equations 5.3.26 and 5.3.27 one gets

$$C^2 = \frac{4I}{A} = \frac{4\rho^2 A}{A} = 4\rho^2 \tag{5.3.28}$$

where ρ is the radius of gyration of the cross-section. For a square cross-section

$$C = 2\rho = 2\sqrt{\frac{I}{\rho}} = 2\sqrt{\frac{h^4}{12h^2}} = \frac{h}{\sqrt{3}} \cong 0.58h \tag{5.3.29}$$

It is concluded that the transition from bending to membrane action occurs quite early in the beam response. As a rule of thumb, the bending solution in the beam restrained from axial motion is restricted to deflections equal to half of the beam thickness. If deflections are larger, the membrane response dominate. For example, if beam deflection reaches three thicknesses, the contribution of bending and membrane action is 3:81. In the upper limit of the applicability of the theory of moderately large deflection of beams $C \cong 10h$, the contribution of bending resistance is only 0.3% of the membrane strength.

The rapid transition from bending to membrane action is only present for axially restrained beams. If the beam is free to slide in the axial direction, no membrane resistance is developed and load is always linearly related to deflections.

The above elegant closed-form solution was obtained for the particular sinusoidal distribution of line load, which coincide with the deflected shape of the beam. For an arbitrary loading, only approximate solutions could be derived. One of such solution method, applicable to the broad class of non linear problems for plates and shells is called the Galerkin method.

[1]The function is even when $f(-A) = f(A)$. The function is odd when $f(-A) = -f(A)$.

5.4: Galerkin Method of Solving Non-linear Differential Equation

Beris Galerkin, a Russian scientist, mathematician and engineer was active in the first forty ears of the 20th century. He is an example of a university professor who applied methods of structural mechanics to solve engineering problems. At that time (World War I), the unsolved problem was moderately large deflections of plates. In 1915, he developed an approximate method of solving the above problem and by doing it made an important and everlasting contribution to mechanics.

The theoretical foundation of the Galerkin method goes back to the Principle of Virtual Work. We will illustrate his idea on the example of the moderately large theory of beams. If we go back to Chapter 2 and follow the derivation of the equations of equilibrium from the variational principle, the so called "weak" form of the equilibrium is given by Equation (2.5.10). Adding the non-linear term representing the contribution of finite rotations, this equation can be re-written as

$$\int_0^l (M'' + N'' + q)\delta w dx + \int_0^l N'\delta u dx + \text{ Boundary terms} \tag{5.4.1}$$

where

$$M = -EIw'' \tag{5.4.2}$$

$$N = EA[u' + \frac{1}{2}(w')^2] \tag{5.4.3}$$

From the weak (global) equilibrium one can derive the strong (local) equilibrium by considering an infinite class of variations. But, what happens if, instead of a "class", we consider only one specific variation (shape) that satisfies kinematic boundary conditions? The equilibrium will be violated locally, but can be satisfied globally in average

$$\int_0^l \left[-EIw^{\text{IV}} + EA\left(u' + \frac{1}{2}(w')^2 w'' + q\right)\right]\delta w dx = 0 \tag{5.4.4}$$

Consider the example of a simply supported beam, restrained from axial motion. The exact solution of this problem fro the sinusoidal distribution of load was given in the previous section. Assume now that the same beam is loaded by a uniform line load $q(x) = q$. No exact solution of this problem exists.

Let's solve this problem approximately by means of the Galerkin method. As a trial approximate deflected shape, we take the same shape that was found as a particular solution of the full equation

$$w(x) = C\sin\frac{\pi x}{l} \tag{5.4.5}$$

$$\delta w(x) = \delta C\sin\frac{\pi x}{l} \tag{5.4.6}$$

With the condition of ends fixity in the axial direction, $u = u' = 0$, and Equation 5.4.4 yields

$$\delta C\int_0^l \left[-EIw^{\text{IV}} + \frac{EA}{2}(w')^2 w'' + q\right]\sin\frac{\pi x}{l}dx = 0 \tag{5.4.7}$$

Evaluating the derivatives and integrating, the following expression is obtained

$$\frac{l}{2}C + \frac{l}{8}\frac{C^3 A}{2I} - \frac{q_1}{EI(\frac{\pi}{l})^4\pi}\frac{2l}{\pi} = 0 \tag{5.4.8}$$

After re-arranging, the dimensionless deflection amplitude $\frac{C}{h} = \frac{w_o}{h}$ is related to the remaining

$$\frac{w_o}{h} + \frac{3}{2}\left(\frac{w_o}{h}\right)^3 = \left(\frac{q_1}{EI}\right)\frac{48}{\pi^5}\left(\frac{l}{h}\right)^4 \tag{5.4.9}$$

The above cubic equation has a simple solution.

Let's discuss the two limiting cases. Without the non-linear term, Equation 5.4.9 predicts the following deflection of the beam under pure bending action for the square section

$$\frac{w_o}{h} = \left(\frac{q_1}{Eh}\right)\frac{48}{\pi^5}\left(\frac{l}{h}\right)^4 \tag{5.4.10}$$

In the exact solution of the same problem, the numerical coefficient is $\frac{60}{384} = \frac{1}{6.4}$, which is only 1.5% smaller than the present approximate solution $\frac{48}{\pi^5} = \frac{1}{6.3}$. If on the other hand the flexural resistance is small, $EI \to 0$, the first term in Equation 5.4.9 vanishes giving a cubic load-deflection relation

$$\left(\frac{w_o}{h}\right)^3 = \frac{32}{\pi^5}\left(\frac{q_1}{EI}\right)\left(\frac{l}{h}\right)^4 \tag{5.4.11}$$

There is no closed-form solution for the pure membrane response of the beam under uniform pressure. However, the present prediction compares favorably with the Equation (5.3.28) for the moderately large deflection, if the total load under the uniform and sinusoidal pressure is the same

$$P = q_1 l = q_o \int_0^l \sin\frac{\pi x}{l} dx = q_o \frac{2l}{\pi} \tag{5.4.12}$$

Replacing q_1 by $\frac{2}{\pi}q_o$, the pure membrane solution takes the final form

$$\left(\frac{w_o}{h}\right)^3 = \frac{6.4}{\pi^4}\left(\frac{q_o}{Eh}\right)\left(\frac{l}{h}\right)^4 \tag{5.4.13}$$

One can see that not only the dimensionless form of the exact and approximate solutions are identical, but also the coefficient 6.4 in Equation 5.4.13 is of the same order as the coefficient 4 in Equation (5.3.29).

5.5: Generalization to Arbitrary Non-linear Problems in Plates and Shells

The previous section felt with the application of the Galerkin method to solve the non-linear ordinary differential equation for the bending/membrane response of beams. Galerkin name is forever attached to the analytical or numerical solution of partial differential equation, such as describing response of plates and shells. In the literature you will often encounter such expression as Galerkin-Bubnov method, Petrov-Galerkin method, the discontinuous Galerkin method or the weighted residual method. The essence of this method is sketched below.

Denote by $F(w,x)$ the non-linear operator (the left hand side of the partial differential equation) is defined over a certain fixed domain in the 2-D space S. Now, a distinction is made between the exact solution $w^*(x)$ and the approximate solution $w(x)$. The approximate solution is often referred to as a trial function. The exact solution makes the operator F to vanish

$$F(w^*,x)=0 \tag{5.5.1}$$

The approximate solution does not satisfy exactly the governing equation, so instead of zero, there is a residue on the right hand of the Equation 5.5.2

$$F(w,x)=R(x) \tag{5.5.2}$$

The residue can be positive over part of S and negative elsewhere. If so, we can impose a weaker condition that the residue will become zero “in average” over S, when multiplied by a weighting function $w(x)$

$$\int_S R(x)w(x)dS=0 \tag{5.5.3}$$

Mathematically we say that these two functions are orthogonal. In general, there are also boundary terms in the Galerkin formulation. For example, in the theory of moderately large deflection of plates, Equation 5.5.3 takes the form

$$\int_S (D\nabla^4 w-N_{\alpha\beta}w_{,\alpha\beta})wdS=0 \tag{5.5.4}$$

The counterpart of Equation 5.5.4 in the theory of moderately large deflection of beams is Equation (5.4.7) which was solved in the previous section of the notes. The solution of partial differential equations for both linear and non-linear problems is extensively covered in textbooks on the finite element method and therefore will not be covered here.

CHAPTER OVERVIEW

6: Bending Response of Plates and Optimum Design

6.1: Beam Deflection Equation

The three group of equations for the plate bending problem, formulated in Chapter 1, 2 and 3 are:

$$\textbf{Geometry} \quad \kappa_{\alpha\beta} = -w_{,\alpha\beta} \tag{6.1.1}$$

$$\textbf{Equilibrium} \quad M_{\alpha\beta,\alpha\beta} + p = 0 \tag{6.1.2}$$

$$\textbf{Elasticity law} \quad M_{\alpha\beta} = D[(1-\nu)\kappa_{\alpha\beta} + \nu\kappa_{\gamma\gamma}\delta_{\alpha\beta}] \tag{6.1.3}$$

Eliminating $\kappa_{\alpha\beta}$ between Equations 6.1.1 and 6.1.2

$$M_{\alpha\beta} = D[(1-\nu)w_{,\alpha\beta} + \nu w_{,\gamma\gamma}\delta_{\alpha\beta}] \tag{6.1.4}$$

and substituting the result into Equation 6.1.3 gives

$$D[(1-\nu)w_{,\alpha\beta} + \nu w_{,\gamma\gamma}\delta_{\alpha\beta}]_{,\alpha\beta} + p = 0 \tag{6.1.5}$$

The second term in the brackets is non-zero only when $\alpha = \beta$. Therefore Equation 6.1.4 transforms to

$$Dw_{,\alpha\alpha\beta\beta}[-1+\nu-\nu] + p = 0 \tag{6.1.6}$$

or finally

$$Dw_{,\alpha\alpha\beta\beta} = p \tag{6.1.7}$$

Introducing the definition of Laplacian ∇^2 and bi-Laplacian ∇^4 in the rectangular coordinate system,

$$\nabla^2 = \frac{\partial^2}{\partial x^2} + \frac{\partial^2}{\partial y^2}, \nabla^4 = \nabla^2\nabla^2 \tag{6.1.8}$$

an alternative form of Equation 6.1.6 is

$$D\nabla^4 w = p \tag{6.1.9}$$

This is a linear inhomogeneous differential equation of the fourth order. The boundary conditions in the local coordinate system were given by Equations (2.8.4 - 2.8.7).

A separate set of equations must be stetted for the in-plane response of the plate

$$\textbf{Geometry} \quad \epsilon^{\circ}_{\alpha\beta} = \frac{1}{2}(u_{\alpha,\beta} + u_{\beta,\alpha}) \tag{6.1.10}$$

$$\textbf{Equilibrium} \quad N_{\alpha\beta,\beta} = 0 \tag{6.1.11}$$

$$\textbf{Elasticity} \quad N_{\alpha\beta} = C[(1-\nu)\epsilon^{\circ}_{\alpha\beta} + \nu\epsilon^{\circ}_{\gamma\gamma}\delta_{\alpha\beta}] \tag{6.1.12}$$

Eliminating the strains $\epsilon^{\circ}_{\alpha\beta}$ and membrane force $N_{\alpha\beta}$ between the above system, one gets two coupled partial differential equations of the second order for $u_\alpha(u_1, u_2)$.

$$(1-\nu)u_{\alpha,\beta\beta} + (1+\nu)u_{\beta,\alpha\beta} = 0 \tag{6.1.13}$$

Such system is seldom solved, because in practical application constant membrane forces are considered.

In either case the in-plane and out-of-plane response of plates is uncoupled in the classical, infinitesimal bending theory of plates. These two system are coupled through the finite rotation term $N_{\alpha\beta}w_{,\alpha\beta}$. The extended governing equation in the theory of moderately large deflection is

$$D\nabla^4 w + N_{\alpha\beta}w_{,\alpha\beta} = 0 \tag{6.1.14}$$

The above equation will be re-derived and solved for few typical loading cases in Chapter 9. The analysis of the differential equation 6.1.9 in the classical bending theory of plates along with exemplary solutions can be found in the lecture notes of the course 2.081 plates and shells. In this section we will look into the bending problem of circular plates, which is governed by the linear ordinary differential equation.

6.2: Deflections of Circular Plates

The governing equation (6.1.9) still holds but the Laplace operator ∇^2 should now be defined in the polar coordinate system (r, θ)

$$\nabla^2 w = \frac{\partial^2 w}{\partial r^2} + \frac{1}{r}\frac{\partial w}{\partial r} + \frac{1}{r^2}\frac{\partial^2 w}{\partial \theta^2} \tag{6.2.1}$$

In the circular plate subjected to axi-symmetric loading $p = p(r)$, the third term in Equation 6.2.1 vanishes and the Laplace operator can be put in the form

$$\nabla^2 w = \frac{\partial^2 w}{\partial r^2} + \frac{1}{r}\frac{\partial w}{\partial r} = \frac{1}{r}\frac{d}{dr}\left(r\frac{dw}{dr}\right) \tag{6.2.2}$$

With the above definition, the plate bending equation becomes

$$\frac{1}{r}\frac{d}{dr}\left\{r\frac{d}{dr}\left[\frac{1}{r}\frac{d}{dr}\left(r\frac{dw}{dr}\right)\right]\right\} = \frac{p(r)}{D} \tag{6.2.3}$$

and the solution is obtained by four successive integration

$$w(r) = \int \frac{1}{r}\int r \int \frac{1}{r}\int \frac{rp(r)}{D} dr dr dr dr \tag{6.2.4}$$

Assuming a uniform loading of the intensity p_o, the above integration can be easily performed to give

$$w(r) = C_1 \ln r + C_2 r^2 + C_3 r^2 \ln r + C_4 + \frac{p_o r^4}{64D} \tag{6.2.5}$$

As an illustration, consider clamped boundary conditions:

$$\text{at } r = R \quad w = 0 \text{ and } \frac{dw}{dr} = 0 \tag{6.2.6}$$

$$\text{at } r = 0 \quad \frac{dw}{dr} = 0 \text{ and } \bar{V}_r = 0 \tag{6.2.7}$$

where the shear force (per unit length), acting on a plate element at a distance r is

$$V_r = -\frac{1}{2\pi r}\int_0^r p_o 2\pi r dr = -\frac{p_o r}{2} \tag{6.2.8}$$

The two terms in Equation 6.2.5 involving logarithms tend to infinity at $r \to 0$. Therefore, in order for the solution to give finite values of deflections at the center, $C_1 = C_3 = 0$. Now, the expression for the slope is

$$\frac{dw}{dr} = 2C_2 r + \frac{p_o r^3}{18D} \tag{6.2.9}$$

Now, the boundary conditions at $r = 0$ are satisfied identically. From two boundary conditions at $r = R$, one finds the integration constants

$$C_2 = -\frac{p_o R^2}{32D}, \quad C_4 = \frac{p_o R^4}{64D} \tag{6.2.10}$$

The final form of the solution for the plate deflection is

$$w(r) = \frac{p_o R^4}{64D}\left[1 - \left(\frac{r}{R}\right)^2\right]^2 \tag{6.2.11}$$

For comparison, the solution for the simply supported plate will be derived. The boundary conditions are mixed so the moment-curvature relation must be used

$$M_r = D\left[\frac{d^2 w}{dr^2} + \nu\frac{1}{r}\frac{dw}{dr}\right] \tag{6.2.12}$$

$$M_\theta = D\left[\frac{1}{r}\frac{dw}{dr} + \nu\frac{d^2w}{dr^2}\right] \tag{6.2.13}$$

where the definition of moments in the cylindrical coordinate system was used. At the plate edge

$$w = 0 \text{ and } M_r = 0 \quad \text{at } r = R \tag{6.2.14}$$

From Equations 6.2.5, 6.2.12 - 6.2.13 and 6.2.14, the system of two algebraic equations for C_2 and C_4 is obtained, where solution is

$$C_2 = -\frac{p_o R^2}{32D}\frac{3+\nu}{1+\nu}, \quad C_4 = \frac{p_o R^4}{64D}\frac{5+\nu}{1+\nu} \tag{6.2.15}$$

The formula for the plate deflection is

$$w(r) = \frac{pR^4}{64D}\left[\left(\frac{r}{R}\right)^4 - 2\left(\frac{r}{R}\right)^2\frac{3+\nu}{1+\nu} + \frac{5+\nu}{1+\nu}\right] \tag{6.2.16}$$

The ratio of the maximum deflection of the simply supported and clamped plate at $r = 0$ is

$$\frac{w_{\text{simplysupported}}}{w_{\text{clamped}}} = \frac{5+\nu}{1+\nu} \approx 4 \tag{6.2.17}$$

It is interesting that a similar ratio for beams is exactly 5.

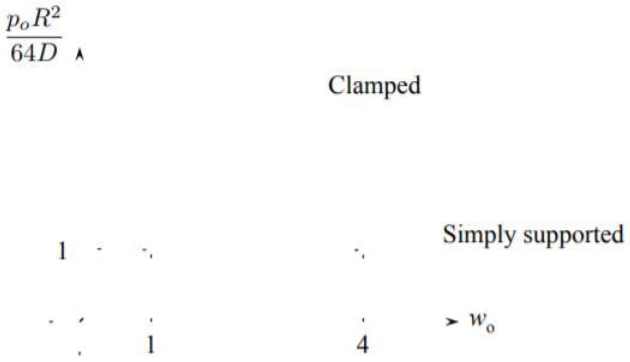

Figure 6.2.1: Clamped plate is four times stiffer than the simply supported circular plate.

The clamped circular plate can leave at a prototype of the whole family of similar plates. It is therefore of interest to explore the properties of the above solution further. From Equation 6.2.11 the radial and circumferential curvatures are:

$$\kappa_r = -\frac{d^2w}{dr^2} = \frac{p_o R^2}{16D}\left(1 - \frac{3r^2}{R^2}\right) \tag{6.2.18}$$

$$\kappa_\theta = -\frac{1}{r}\frac{dw}{dr} = \frac{p_o R^2}{16D}\left(1 - \frac{r^2}{R^2}\right) \tag{6.2.19}$$

From the constitutive equations, the radial and circumferential bending moments are

$$M_r = D[\kappa_r + \nu\kappa_\theta] + \frac{p_o R^2}{16}\left[(1+\nu) - (3+\nu)\left(\frac{r}{R}\right)^2\right] \tag{6.2.20}$$

$$M_\theta = D[\kappa_\theta + \nu\kappa_r] + \frac{p_o R^2}{16}\left[(1+\nu) - (1+3\nu)\left(\frac{r}{R}\right)^2\right] \tag{6.2.21}$$

At the plate center, by symmetry

$$M_r = M_\theta = (1+\nu)\frac{p_o R^2}{16} \tag{6.2.22}$$

Another extreme value occurs at the clamped edge

$$M_r = \frac{p_o R^2}{8}, \quad M_\theta = -\nu\frac{p_o R^2}{8} \text{ at } r = R \tag{6.2.23}$$

By comparing Equations 6.2.22 and 6.2.23, it is seen that the maximum bending moment occurs at the edge $r = R$. From the stress formula, Equation (3.7.7)

$$|\sigma_{rr}| = \left| \frac{M_r z}{h^3/12} \right|_{z=\frac{h}{2}} = p_o \frac{3}{4} \left(\frac{R}{h} \right)^2 \tag{6.2.24}$$

At the same time, the circumferential bending moment at $r = R$ is

$$|\sigma_{\theta\theta}| = \frac{M_\theta z}{h^3/12} = p_o \frac{1}{4} \left(\frac{R}{h} \right)^2 \tag{6.2.25}$$

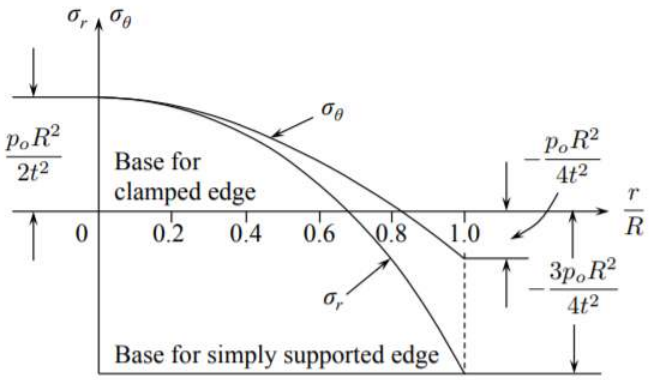

Figure 6.2.2: Variation of radial and circumferential stresses along the radius of the plate.

6.3: Equivalence of Square and Circular Plates

In the section of Chapter 6 on stiffened plates, the analogy between the response of circular and square plates was exploit to demonstrate the effectiveness of stiffeners. It was stated that stiffness of these two types of plates are similar if the arial surface was identical. We are now in the position to assess accuracy of the the earlier assertion.

Consider a clamped square plate $2a \times 2a$, uniformly loaded by the pressure p_o. The total potential energy of the system $\prod$ is

$$\prod = \frac{D}{2}\int_S [(\kappa_x^2 + \kappa_y^2) + 2(1-\nu)\kappa_G]ds - \int_S -q_o w ds \tag{6.3.1}$$

It can be shown (Shames & Dign 1985) that for the fully clamped boundary conditions, the integral of the Gaussian curvature κ_G vanishes. The expression for $\prod$ simplifies to

$$\prod = \frac{D}{2}\int_0^a \int_0^a \left[\frac{d^2w}{dx^2} + \frac{d^2w}{dy^2}\right] dxdy - a^2 q \int_0^a \int_0^a w dxdy \tag{6.3.2}$$

For simplicity only one quarter of the plate is considered with the origin at the plate center. As a trial deflection shape, we assume

$$w(x,y) = C(x^2 - a^2)^2(y^2 - a^2)^2 \tag{6.3.3}$$

$$\frac{dw}{dx} = C2(x^2 - a^2)2x(y^2 - a^2)^2 \tag{6.3.4}$$

$$\frac{dw}{dy} = C(x^2 - a^2)^2 2(y^2 - a^2)2y \tag{6.3.5}$$

It is seen that both the deflections and slopes are zero at the clamped boundary. Furthermore, the slopes at the plate center $x = y = 0$ vanishes, as they should due to symmetry. The maximum amplitude is at center and is equal to $Ca^8 = w_o$. Thus, the kinematic boundary conditions are satisfied identically for any value of the unknown constant C. Substituting the expression 6.3.3 - 6.3.5 into Equation 6.3.2 and performing integration yields

$$\prod = 9a^4 DC^2 - 0.384 q_o C \tag{6.3.6}$$

According to the Ritz method, equilibrium is maintained if

$$\delta\prod = \frac{\partial \prod}{\partial C}\delta C = 0 \tag{6.3.7}$$

This means that for a given load intensity and the assumed normalized shape function, the true deflection amplitude is chosen by the condition

$$\frac{\partial \prod}{\partial C} = 0 \quad \text{or} \quad 18a^4 DC - 0.383 q_o = 0 \tag{6.3.8}$$

Having found the amplitude C, the load-displacement relation of the square plate becomes

$$w_o = \frac{p_o a^4}{47D} \tag{6.3.9}$$

The corresponding solution for the clamped circular plate is

$$w_o = \frac{p_o R^4}{64D} \tag{6.3.10}$$

The stiffnesses of both plates are identical if $\frac{R^4}{64} = \frac{a^4}{47}$ or if $a = 0.92R$. The area equivalence $4a^2 = \pi R^2$ gives a similar result $a = 0.88R$. For simplicity in the qualitative analysis throughout the present lecture notes one can approximately assume $a = R$. The difference between the exact and approximate solution from the area and stiffness equivalence does exist, but it is small. It is interesting that the approximate solution obtained by the Ritz method is very close to the exact series solution where the coefficient 47 in Equation 6.3.9 should be replaced by 49.5.

6.4: Design Concept for Plates

The plates loaded in the transverse direction can be design for:

- Stiffness
- Strength(yielding or plastic collapse)
- fracture

Plastic collapse and fracture of ductile materials will be covered in separate lectures. Stiffness is a global property of the plate and is the ratio of force to displacement. For a uniformly loaded plate the stiffness is defined as

$$K = \frac{\pi R^2 p_o}{w_o} \tag{6.4.1}$$

For the clamped plate with $\nu = 0.3$

$$K = 18.5 \equiv \frac{h^3}{R^2}\left[\frac{N}{m}\right] \tag{6.4.2}$$

Stiffness can be controlled by choosing a suitable material (E), thickness (h) and distance between support (R). The boundary conditions enter through the numerical coefficient. The concept of optimum design includes the weight and cost of a given structure. Leaving the complex issue of cost, the wight can be easily included by calculating stiffness per unit weight. The wight of the circular plate $W = \pi R^2 \rho$, so the stiffness per unit weight is

$$\bar{K} = \frac{K}{W} = \frac{\pi R^2 p_o}{\pi R^2 \rho w_o} = \frac{p_o}{\rho w_o} \tag{6.4.3}$$

In the case of a clamped plate

$$\bar{K} = 4.8\frac{E}{\rho}\frac{h^2}{R^4}\left[\frac{N}{mKg}\right] \tag{6.4.4}$$

The dependance of K and $\bar{K}$ on h and R is different. While the stiffness favors thicker plates, the stiffness per unit weight increases faster with a large radius. The effect of the ratio E/ρ can be shown on the example of steel and aluminum plates, see Table (6.4.1).

Table 6.4.1: Basic properties of steel and aluminum

	E[GPa]	$\rho[g/cm^3]$	E/ρ
Steel	2.1	7.8	3.7
Al	0.8	2.8	3.5

Aluminum alloys seem much lighter but they lose elasticity modulus in the same proportion. It is seen that there are not much gain in the stiffness per unit weight by replacing steel by aluminum. So, what else could be done to increase plate stiffness? The answer is:

- Sandwich plates
- Stiffened plates

Each of the above concept is studied separately.

6.5: Sandwich Plates

Sandwich plates are composed of face sheets and a lightweight core, Figure (**6.5.1**).

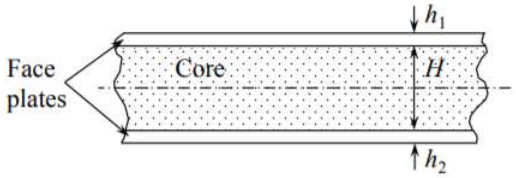

Figure **6.5.1**: There are two materials and three different thicknesses in sandwich plates.

The core is transmitting shear stresses while the face plates are working mostly in tension or compression. Typical materials for a core are polyuritine foam, Aluminum foam, aluminum or nomex honeycombs, polymeric material of various kinds etc. In many steel structures, there is a discrete core made of corrugated sheets welded stiffeners of different topologies or truss structures. Pictures of some typical core materials and sandwich sets are shown in Figure (6.6.1).

In order to determine the bending and axial stiffness of the sandwich plate, we must revisit the definition of bending moment. For cylindrical bending,

$$M_{xx} = \int \sigma z dz = \int_{-\frac{H}{2}}^{\frac{H}{2}} \sigma_c z dz + \sigma_f h H \tag{6.5.1}$$

$$N_{xx} = \int \sigma dz = \int_{-\frac{H}{2}}^{\frac{H}{2}} \sigma_c dz + 2\sigma_f h \tag{6.5.2}$$

The Young's modulus of the core material is usually two orders of magnitude smaller than that of the face plates, so $\sigma_f \gg \sigma_c$. Neglecting the first term in Equation 6.5.1 - 6.5.2 and extending the above definitions to plates, the bending moments and axial forces are

$$M_{\alpha\beta} = \sigma_{\alpha\beta} h H \tag{6.5.3}$$

$$N_{\alpha\beta} = 2\sigma_{\alpha\beta} h \tag{6.5.4}$$

where $\sigma_{\alpha\beta}$ is related to the face plate strain by the plane stress elasticity law, Equations (3.6.1- 3.6.5). The Love-Kirchhoff hypothesis is still valid so the strains in the face plates are

$$\epsilon_{\alpha\beta} = \epsilon^{\circ}_{\alpha\beta} \pm \frac{H}{2} \kappa_{\alpha\beta} \tag{6.5.5}$$

where the "$\pm$" sign apply to the tensile and compressive side of the panel. The resulting moment-curvature relations become

$$M_{\alpha\beta} = D_s[(1-\nu)\kappa_{\alpha\beta} + \nu\kappa_{\gamma\gamma}\delta_{\alpha\beta}] \tag{6.5.6}$$

$$N_{\alpha\beta} = C_s[(1-\nu)\epsilon^{\circ}_{\alpha\beta} + \nu\epsilon_{\gamma\gamma}\delta_{\alpha\beta}] \tag{6.5.7}$$

where the bending and axial rigidities of the sandwich plates are

$$D_s = \frac{EhH^2}{(1-\nu^2)}; \quad C_s = \frac{EhH}{1-\nu^2} \tag{6.5.8}$$

Now, there is more room for the optimum design, because instead of a thickness of a monolithic plate, we have two geometrical parameter to play with. Replacing the bending rigidity D of the monolithic plate by Equation 6.5.8, the bending stiffness of the circular sandwich plate become

$$K_s = 222E\frac{hH^2}{R^2} \tag{6.5.9}$$

Assuming the mass density of the core to be two orders of magnitude smaller than the face plate, the total wight of the sandwich plate is

$$W_s = \pi R^2 2h\rho \tag{6.5.10}$$

Then, the formula for the bending stiffness per unit weight is

$$\bar{K}_s = 35\frac{E}{\rho}\frac{H^2}{R^4}\left[\frac{N}{mKg}\right] \tag{6.5.11}$$

Two observations can be made. First, K_s is independent on the thickness of face-plates. Secondly, the stiffness per unit weight increases parabolically with the core thickness H. Does it mean that one can make K_s as large as desired by increasing H? This is too good to be true. With increasing H, the sandwich plate may fail in either of the three failure modes:

i. Yielding or fracture of face plate on the tensile side;
ii. Face plate buckling on the compressive side;
iii. Delamination due to excessive shear.

None of these failure modes are present in monolithic plates. It can be concluded that sandwich plates bring substantial improvements in the bending stiffness but at the same time introduces new unwanted features. Fracture, buckling and shear stresses will be the subject of subsequent lecture. But even at this point we can say that optimization of sandwich plates are possible by determining the maximum core thickness H_{opt} slightly less than that causing one of the above failure modes.

6.6: Stiffened Plates

Another way of light weighting plates is to provide a system of uni-directional or orthogonal stiffeners. As opposed to sandwich structures which are symmetric, stiffened plates are asymmetric with the neutral axis positioned usually outside the profile of the plate. A stiffened plates consists of a system of beams interacting with a uniform thickness plate. Photos of typical stiffened plates used in civil engineering, ship buildings and other segment of the economy are shown in Figure (**6.6.2**).

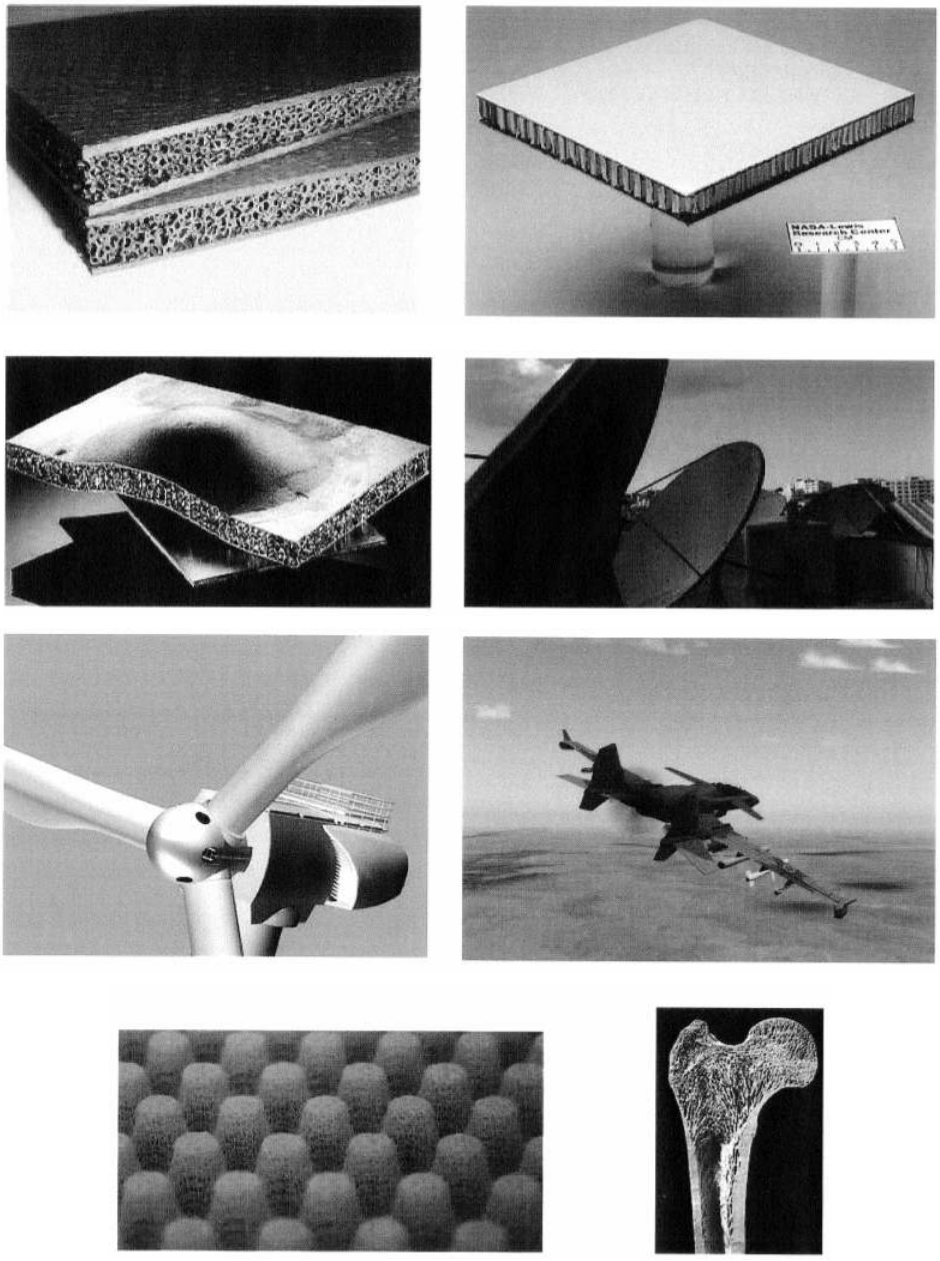

Figure **6.6.1**: Pictures of foam-filled and honeycomb core sandwich plates and panels with some applications.

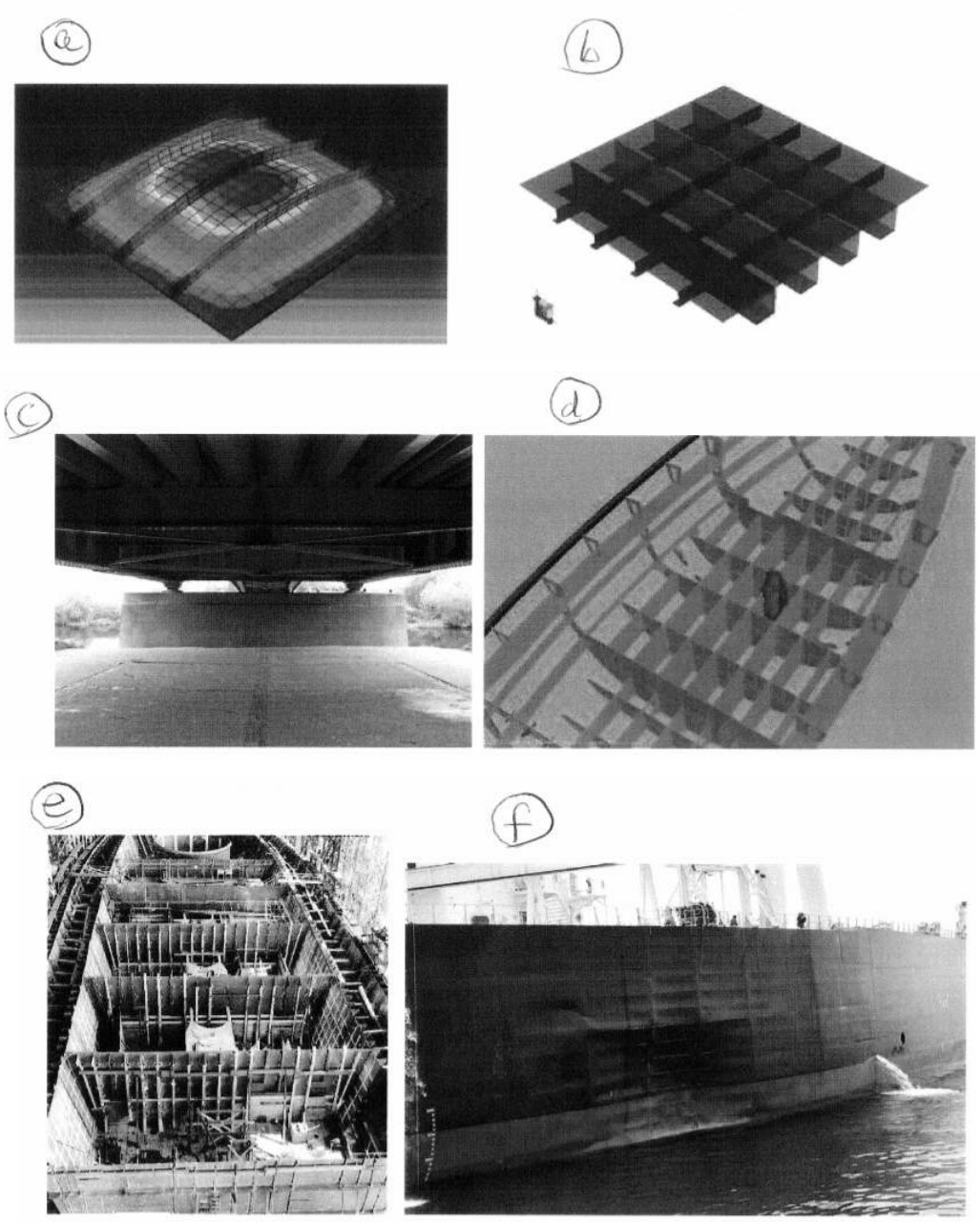

Figure **6.6.2**: Stiffened panels are fundamental building blocks of modern structures.

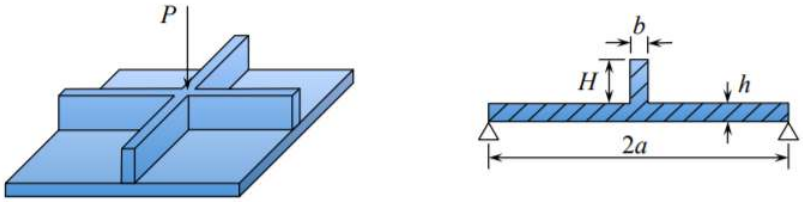

Figure **6.6.3**: Geometry of the stiffened plate.

To illustrate the response of stiffened plates to transverse loads consider an example of a simply supported plate stiffened by two cross-beams, Figure (**6.6.3**).

The structure is loaded by a point force P at the center. For simplicity, shown is the simplest flat bar stiffener but the analysis is valid for any beam defined by the moment of inertia I. Can we determine the stiffness of the system using our existing knowledge of beams and plates? Let's see.

The solution for the beam problem is

$$w(x) = w_o^b \frac{x}{l}\left[3 - 4\left(\frac{x}{l}\right)^2\right] \tag{6.6.1}$$

$$w_o^b = \frac{P^b l^3}{48EI} \tag{6.6.2}$$

where $l = 2a$ is the length of the stiffener. The solution for the circular plate under the concentrated point load is given by Equation (6.2.16)

$$\bar{w} = \frac{w(r)}{w_o^p} = \left[2\left(\frac{r}{a}\right)^2 \ln\frac{r}{a} + \frac{3+\nu}{1+\nu}\left(1 - \left(\frac{r}{a}\right)^2\right)\right] \tag{6.6.3}$$

$$w_o^p = \frac{p^p a^2}{16\pi D} \tag{6.6.4}$$

Here the analogy between the response of a circular and square plate was used with $a \approx R$.

The comparison of the deflected shapes of the beam and the plate is shown in Figure (**6.6.4**). This means that in terms of vertical deflections w the beam shape fits on the deform plate. What about the horizontal displacements? This is shown in Figure (**6.6.5**). The beam and the plate deform separately and there is an incompatibility of the displacement u. This corresponds to the situation that both components are not connected, with sliding allowed. Should sliding be prevented, for example by welding, the neutral axis of the plate-beam combination will be shifted. Therefore the actual stiffness of the welded stiffen structure will be greater than simply adding their individual contributions. The present model will give only the lower bound. Let's calculate the lower bound stiffness of the system.

The almost perfect compatibility of the vertical displacement, shown in Figure (**6.6.4**), means that we are dealing with two linear springs in parallel, Figure (**6.6.6**). The total resisting force is the sum of individual components, while the displacements are the same

$$P = P_p + P_b; \quad w_o^p = w_o^b = w_o \tag{6.6.5}$$

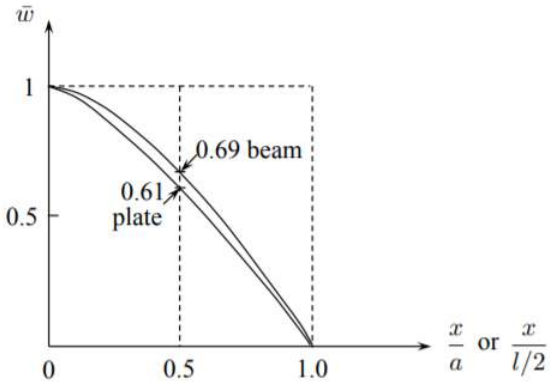

Figure **6.6.4**: Normalized deflected shapes of a beam and a plate is very similar.

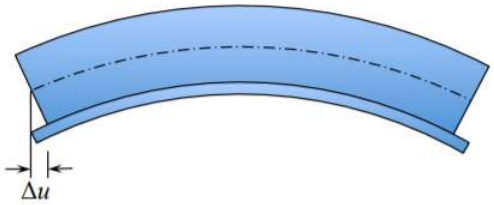

Figure **6.6.5**: The length of the bent plate is the same as the beam axes. Relative displacement at the interface is denoted by Δu.

From Equations 6.6.1 - 6.6.2 and 6.6.3 - 6.6.4 one gets

$$P = \left(\frac{16\pi D}{a^2} + \frac{6EI}{a^3}\right) w_o \tag{6.6.6}$$

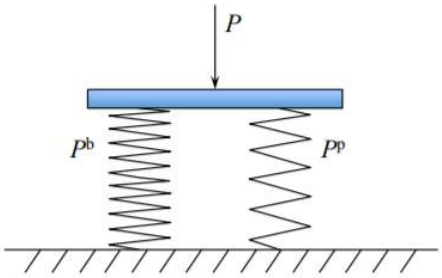

Figure **6.6.6**: Two spring in series.

If we assume for simplicity that the flat bar stiffener is of the same thickness as the plate, $b = h$, then Equation 6.6.6 simplifies to

$$P = \frac{1}{2} E h w_o \left[\frac{8\pi}{3(1-\nu^2)}\left(\frac{h}{a}\right)^2 + \left(\frac{H}{a}\right)^3\right] \tag{6.6.7}$$

To get a feel, the plate and beam will equally contribute to the stiffen of the system if

$$\left(\frac{3h}{a}\right)^2 = \left(\frac{H}{a}\right)^3 \tag{6.6.8}$$

For a typical plate with span to thickness ratio $a/h = 30$, the hight of the stiffener is $H \cong 0.2a$. How good the above lower bound solution is? This is a difficult question to which no general and simple solution can be derived.

It is helpful to distinguish three limiting cases shown in Figure (**6.6.7**). A very substantial and sparsely positioned stiffeners acts as an almost rigid clamped support to the plate, case (a). Light and densely distributed stiffeners, case (c), deform together with the plate. there is one deflection line and stiffeners contribute to the bending stiffness of the plate. The case (b) is a combination of the above two extreme cases. Cases (a) and (c) will be studied below.

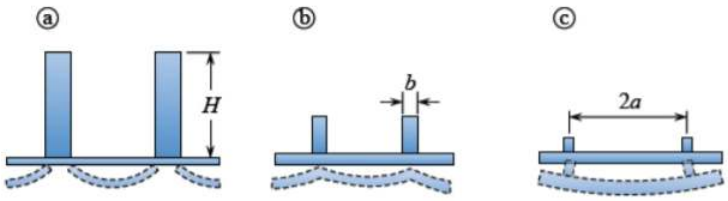

Figure **6.6.7**: Heavy, intermediate and light stiffeners.

6.7: Plates versus Grillages

Case (a). Two heavy stiffeners are subdividing the square plate shown in Figure (6.6.3) into four smaller square plates. An example of this type of design is the “hungry horse” deformation pattern of the ship hall, shown in Figure (6.6.2b).

The point load is still applied at the intersection of both beams. The solution given by Equation (6.6.6) is still valid but now the beam stiffness is much higher than the plate bending stiffness, and the first term in Equation (6.6.6) can be neglected. The solution of two intersecting beam, each carrying half of the load is exact. The stiffness of the beam system is

$$K|_{\text{two beams}} = \frac{P}{w_o} = \frac{12EI}{a^3} = \frac{EbH^3}{a^3} \tag{6.7.1}$$

while the plate stiffness from Equations (6.6.3-6.6.4) is

$$K|_{\text{plate}} = \frac{16\pi D}{a^2} = \frac{16\pi Eh^3}{12a^2(1-\nu^2)}\frac{1+\nu}{3+\nu} \tag{6.7.2}$$

Two intersecting beams form the simplest grillage

The question is which of the two types of structures, plates or grillages are more weight efficient? So, let’s keep the volume of both types of structures the same and compare their stiffnesses.

$$V_{\text{plate}} = V_{\text{beam}} \rightarrow ah = bH \tag{6.7.3}$$

The ratio of stiffnesses, keeping the volume (weight) the same is

$$\frac{K_{\text{beams}}}{K_{\text{plate}}} = 0.6\frac{b}{a}\left(\frac{H}{h}\right)^3 = 0.6\left(\frac{H}{h}\right)^3 \tag{6.7.4}$$

The stiffness of grillage is the same as that of the plate if $H = 1.25h$. Stiffeners alone or their assemblages into a grillage can thus transmit considerable concentrated loads. They cannot resist distributed pressure. For that purpose plates or stiffened plates must be used.

6.8: The Concept of Equivalent Thickness

Densely spaced and weak stiffeners follow the deflection line of the plate to which they are attached. The main load-resisting mechanism is plate bending with an additional contribution of stiffeners. The solution for the plate is still valid but the plate thickness must be increased to form an equivalent thickness h_{eq}. In plate bending problem the equivalence should be based on equal moment of inertia of two structures, Figure (6.8.1).

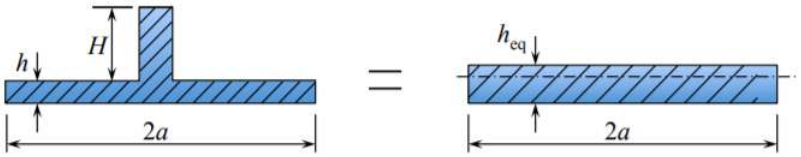

Figure 6.8.1: Geometry of plate/beam combination and the equivalent thickness plate.

The integrated beam/stiffener system is bending about the common bending axis. The equivalent plate is bending about the middle plane axis. The bending axis of any beam is defined by vanishing the first moment of inertia of the cross-section

$$Q = \int_A z dA = 0 \tag{6.8.1}$$

For simplicity, the flat bar stiffener is considered. The position of the neutral axis, normalized with respect to the plate thickness, is related to the remaining parameters of the problem by

$$\frac{\eta}{h} = \frac{1}{2}\frac{1 - \frac{b}{a}\left(\frac{H}{h}\right)^2}{1 + \frac{b}{a}\left(\frac{H}{h}\right)} \tag{6.8.2}$$

The plot of the function η/h versus the normalized hight of the stiffener H/h for several values of the plate-to-stiffener aspect ratio a/b is shown in Figure (6.8.2). In the limiting case of no stiffener, $H = 0$ and the position of the neutral axis is at the middle axis of the plate.

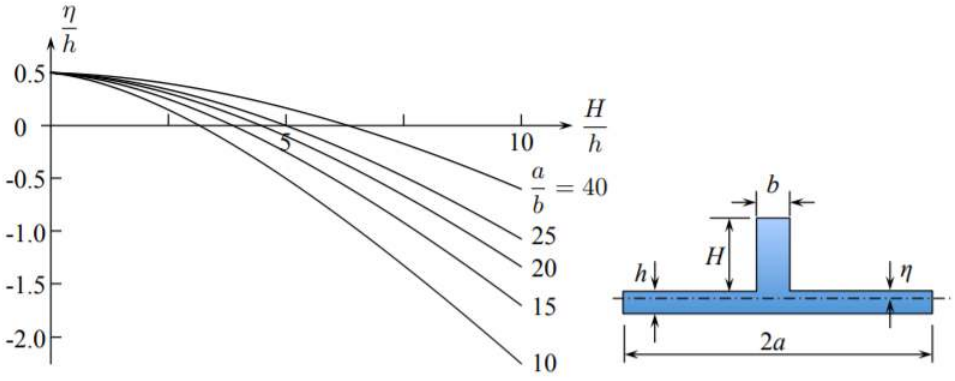

Figure 6.8.2: Neutral axis of the plate/beam combination moves from the plate center towards the original axis of the beam.

The moment of inertia of the plate/beam combination and the equivalent plate are, respectively

$$I = \frac{2a}{3}\left[(h^3 - 3h^2\eta + 3h\eta^2) + \frac{b}{2a}(H^3 + 3H^2\eta + 3H\eta^2)\right] \tag{6.8.3}$$

$$I_{eq} = \frac{2a}{12}h_{eq}^3 \tag{6.8.4}$$

By equating the respective moments of inertia, the equivalent plate thickness, normalized by the thickness of the un-stiffened plate is

$$\left(\frac{h_{eq}}{h}\right)^3 = 4\left\{\left[1 - 3\eta + 3\left(\frac{\eta}{h}\right)^2\right] + \frac{b}{2a}\left[\left(\frac{H}{h}\right)^2 + 3\left(\frac{H}{h}\right)^2\frac{\eta}{h} + 3\frac{H}{h}\left(\frac{\eta}{h}\right)^2\right]\right\} \tag{6.8.5}$$

The plot of h_{eq}/h versus H/h for several values of the a/b ratios is given in Figure (6.8.3).

The growth of plate stiffness, according to Equation 6.8.5, is parabolic with respect to $\frac{H}{h}$. At the same time the increase in weight (volume) of the orthogonally stiffened plate is linear

$$\frac{V_{eq}}{V} = 1 + \frac{b}{a}\frac{H}{h} \tag{6.8.6}$$

Therefore the stiffness per unit weight will still be an increasing function of the height of the stiffeners.

The next question is what should be the height H and spacing of stiffeners to fall under the category (c) of light stiffeners. This question can be answered by explaining the concept of the shear lag.

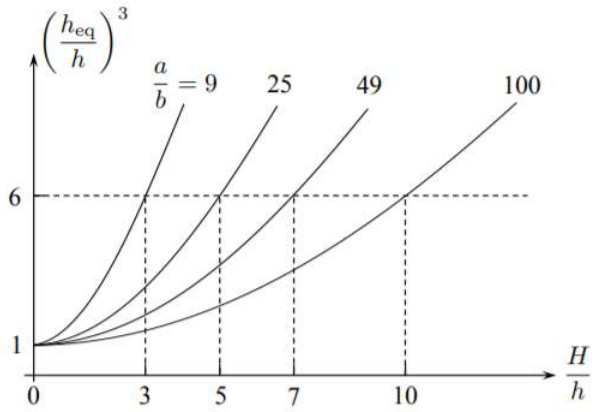

Figure 6.8.3: The equivalent thickness growth rapidly with the height of the stiffener.

6.9: Shear Lag

The question is how to remove the incompatibility of in-plane displacements between the beam and plate, shown in Figure (6.6.5). Let's magnify this figure to see what is happening at the edge.

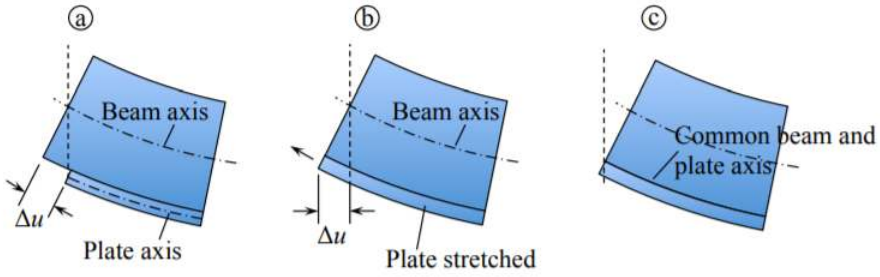

Figure **6.9.1**: Incompatible and compatible interface between beam (stiffener) and plate.

In Figure (**6.9.1***a*), the beam and the plate are bent separately about their respective bending axes. One way of making the incompatible edge displacement to vanish, $\Delta u = 0$, would be to stretch the plate to match the tensile side of the beam. This will entail considerable in-plane sheer stresses and strain on both sides of the foot of stiffener.

The finite region of the plate subjected to large in-plane shear is called the "effective breath". Most of literature dealing with bending of stiffened plates took the approach called the shear lag. This approach is based on the continuity of shear forces and stresses at the beam/plate interface. The determination of the effective breadth falls behind the scope of the present lecture notes.

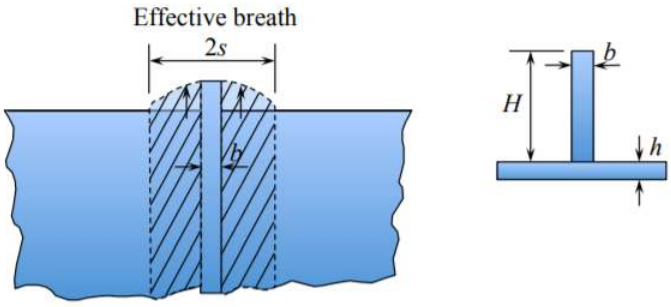

Figure **6.9.2**: In-plane shear induced by the stiffener is restricted to an immediate vicinity of the stiffener.

CHAPTER OVERVIEW

7: Energy Methods in Elasticity

The energy methods provide a powerful tool for deriving exact and approximate solutions to many structural problems.

7.1: The Concept of Potential Energy

From high school physics you must recall two equations

$$E = \frac{1}{2}Mv^2 \quad \text{kinematic energy} \tag{7.1.1}$$

$$W = mgH \quad \text{potential energy} \tag{7.1.2}$$

where H is the hight of a mass m from a certain reference level H_o, and g stands for the earth acceleration. The reference level could be the center of the earth, the sea level or any surface from which H is measured.

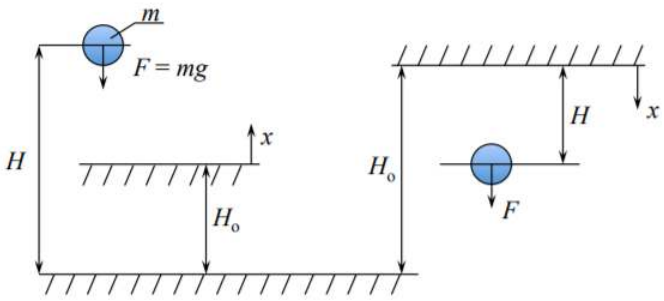

Figure 7.1.1: Gravitational potential energy.

We seldom measure H from the center of earth. Therefore what we can easily measure is the change of the potential energy

$$\Delta W = (mg)(H - H_o) \tag{7.1.3}$$

The energy is always positive. It can e zero but it cannot be negative. The gravity force $F = mg$ is directed towards the center of earth. Therefore there is a need for the negative sign in Equation 7.1.3). In the coordinate system of Figure (7.1.1), the gravity force is negative (opposite to the sense of coordinate x). The force F is acting in the sense of x but the difference $H - H_o$ is negative.

Extending the concept of the potential energy to the beam, the force is $F = qdx$ and the $w = H - H_o$ is the beam deflection.

$$W \equiv + \int_0^l qwdx \tag{7.1.4}$$

An analogous expression for plates is

$$W \equiv + \int_S pwds \tag{7.1.5}$$

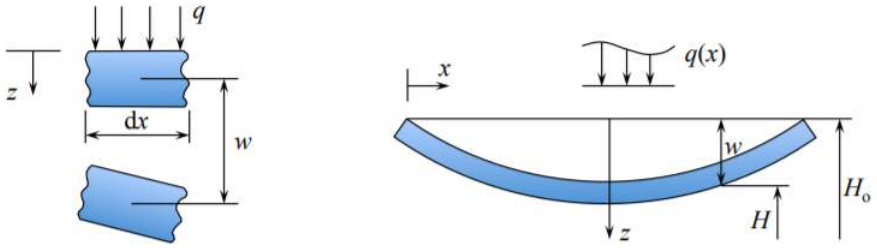

Figure 7.1.2: Potential energy of a beam element and the entire beam.

In the above definition W is negative.

The concept of the energy stored elastically U has been introduced earlier. For a 3-D body

$$U = \int_V \frac{1}{2}\sigma_{ij}\epsilon_{ij}dv \tag{7.1.6}$$

and for a beam

$$U = \int_0^l \frac{1}{2} MK dx + \int_0^l \frac{1}{2} N\epsilon^\circ dx \tag{7.1.7}$$

For plates, the bending and membrane energies are given by Equations (3.6.25), (3.6.26) and (3.6.41), (3.6.42).

The total potential energy $\prod$ is a new concept, and it is defined as the sum of the drain energy and potential energy

$$\prod = U + (-W) = U - W \tag{7.1.8}$$

Consider for a while that the material is rigid, for which $U \equiv 0$. Imagine a rigid ball being displaced by an infinitesimal amount on a flat $(\theta = 0)$ and inclined $(\theta \neq 0)$ surface, Figure (7.1.3).

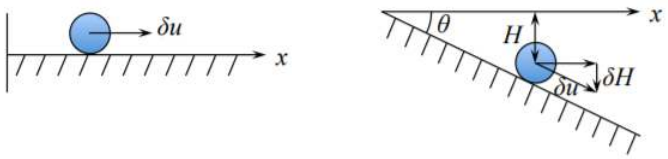

Figure 7.1.3: Test if an infinitesimal displacement δu causes the potential energy to change.

We have $H = u \sin\theta$ and $\delta H = \delta u \sin\theta$. The total potential energy and its change is

$$\prod = -W = -Fu \sin\theta \tag{7.1.9}$$

$$\delta \prod = -\delta W = -(F \sin\theta)\delta u \tag{7.1.10}$$

On the flat surface, $\theta = 0$ and $\delta \prod = 0$, and the ball is in static (neutral) equilibrium. If $\theta > 0$, $\delta \prod \neq 0$ and the ball is not in static equilibrium. Note that if the d'Alambert inertia force in the direction of motion is added, the ball will still be in dynamic equilibrium. In this lecture, only static equilibrium is considered. We can now extend the above test for equilibrium and introduce the following principle:

The system is said to be in equilibrium, if an infinitesimal change of the argument a of the total potential energy $\prod = \prod(a)$ does not change the total potential energy

$$\delta \prod(a) = \frac{\partial \prod}{\partial a} \delta a = 0 \tag{7.1.11}$$

Because $\delta a \neq 0$ ($\delta a = 0$ is a trivial case in which no test for equilibrium is performed), the necessary and sufficient condition for stability is

$$\frac{\partial \prod}{\partial a} = 0 \tag{7.1.12}$$

In case when the functional $\prod$ is a function of many (say N) variables $\prod = \prod(a_i)$, the increment

$$\delta \prod = \frac{\partial \prod}{\partial a_i} \delta a_i, \quad i = 1, \ldots, N \tag{7.1.13}$$

The system is in equilibrium if the derivative of $\prod$ with respect to each variable at a time vanishes

$$\frac{\partial \prod(a_i)}{\partial a_i} = 0, \quad i = 1, \ldots, N \tag{7.1.14}$$

The meaning of the argument(s) a_i, or independent variables will be explained next.

7.2: Equivalence of the Minimum Potential Energy and Principle of Virtual Work

The concept of virtual displacement δu_i is the backbone of the energy methods in mechanics. The virtual displacement is a small hypothetical displacement which satisfy the kinematic boundary condition. The virtual strains $\delta\epsilon_{ij}$ are obtained from the virtual displacement by

$$\delta\epsilon_{ij} = \frac{1}{2}(\delta u_{i,j} + \delta u_{j,i}) \tag{7.2.1}$$

The increment of stress $\delta\sigma_{ij}$ corresponding to the increment of strain is obtained from the elasticity law

$$\sigma_{ij} = C_{ijkl}\epsilon_{kl} \tag{7.2.2}$$

$$\delta\sigma_{ij} = C_{ijkl}\delta\epsilon_{kl} \tag{7.2.3}$$

Therefore, by eliminating C_{ijkl}

$$\sigma_{ij}\delta\epsilon_{ij} = \epsilon_{ij}\delta\sigma_{ij} \tag{7.2.4}$$

The total strain energy of the elastic system $\prod$ is the sum of the elastic strain energy stored and the work of external forces

$$\prod = \int_V \frac{1}{2}\sigma_{ij}\epsilon_{ij}dv - \int_S T_i u_i ds \tag{7.2.5}$$

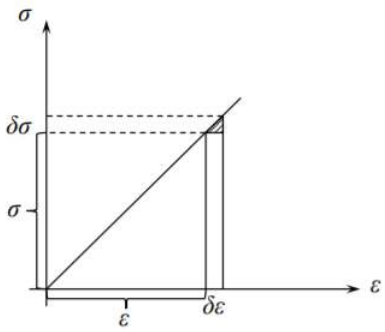

Figure 8.4: Equivalence of the strain energy and complementary strain energy.

In the above equation the surface traction are given and considered to be constant. The stresses σ_{ij} are not considered to be constant because they are related to the variable strains. For equilibrium the potential energy must be stationary, $\delta\prod = 0$ or

$$\begin{aligned} &\delta\int_V \frac{1}{2}\sigma_{ij}\epsilon_{ij}dv - \delta\int_S T_i u_i ds \\ &= \frac{1}{2}\int_V \delta(\sigma_{ij}\epsilon_{ij})dv - \int_S T_i\delta u_i ds \\ &= \frac{1}{2}\int_V (\delta\sigma_{ij}\epsilon_{ij} + \sigma_{ij}\delta\epsilon_{ij})dv - \int_S T_i\delta u_i ds = 0 \end{aligned} \tag{7.2.6}$$

The two terms in the integrand of the volume integral are equal in view of Equation 7.2.4. Therefore, Equation 7.2.6 can be written in the equivalent form

$$\int_V \sigma_{ij}\delta\epsilon_{ij}dv = \int_S T_i\delta u_i ds \tag{7.2.7}$$

which is precisely the principle of virtual work. The above proof goes also in the opposite direction. Assuming the principle of virtual work one can show that the stationarity of the total potential energy holds.

7.3: Two Formulations for Beams

In the bending theory of beams, the total potential energy is

$$\prod = \int_0^l \frac{1}{2} M\kappa dx - \int_0^l q(x) w dx \tag{7.3.1}$$

Using the moment curvature relation $M = EI\kappa$, either M or κ can be eliminated from Equation (7.2.7), leading to

$$U = \int_0^l \frac{1}{2} M\kappa dx = \begin{cases} \int_0^l \frac{EI}{2} \kappa^2 dx & \text{displacement formulation} \\ \int_0^l \frac{1}{2EI} M^2 dx & \text{stress formulation} \end{cases} \tag{7.3.2}$$

In statically determined problems the bending moments can be expressed in terms of the prescribed line load or point load. In the latter case the $M = M(P)$ and the total potential energy takes the form

$$\prod = U(P) - Pw \tag{7.3.3}$$

The above representation will lead to the **Castigliano theorem** which will be covered later in this lecture.

The more general displacement formulation will be covered next. The curvature is proportional to the second derivative of the displacement. The expression of the total potential energy becomes

$$\prod = \int_0^l \frac{EI}{2} (w'')^2 dx - \int_0^l q(x) w dx \tag{7.3.4}$$

The problem is reduced to express the displacement field in terms of a finite number of free parameters $w(x, a_i)$ and then use the stationary condition, Equation (7.1.14) to determine these unknown parameters. This could be done in three different ways:

i. Polinomial representation or Taylor series expansion
ii. Fourier series expansion
iii. Finite element or finite difference method

Each of the above procedure will be explained separately.

7.4: Fourier Series Expansion and the Ritz Method

Consider a symetrically loaded simply supported plate by the point force at the center. The total potential energy of the system is

$$\prod = \int_0^l \frac{EI}{2}(w'')^2 dx - Pw \tag{7.4.1}$$

The objective is to find the amplitude and shape of the deflection function that is in equilibrium with the prescribed load P. In other words we will be looking the deflection and shape that will make the total potential energy stationary.

Assume the solution as a Fourier expansion function

$$w(x) = \sum_{n=1}^{N} a_n \phi_n(x) \tag{7.4.2}$$

where $\phi_n(x)$ is a complete system of coordinate function satisfying kinematic boundary conditions. In the rectangular coordinate system this system consists of hormonic functions, in the polar coordinate system these are Bessel function, and in the spherical coordinate system this role is taken by the Legender functions. In our case

$$\phi_n(x) = \sin \frac{n\pi x}{l} \tag{7.4.3}$$

The kinematic boundary conditions $\phi_n(x = 0) = \phi_n(x = l)$ are identically satisfied. Furthermore, because of the symmetry of the problem, only the symmetric function will contribute to the solution.

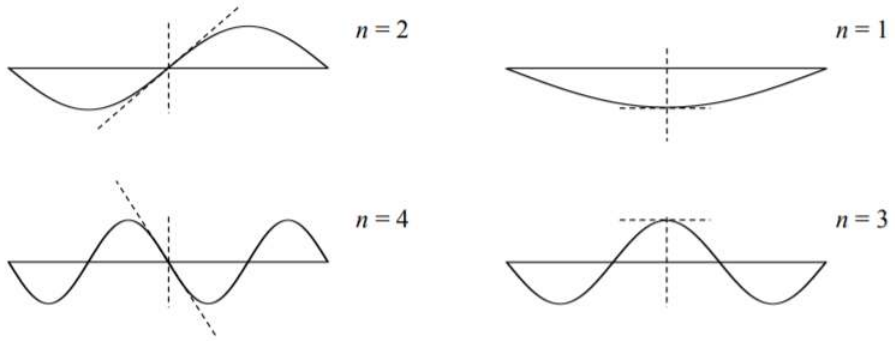

Figure 7.4.1: Asymmetric modes do not satisfy boundary condition $w'(x = \frac{l}{2}) = 0$ at the center of the beam.

The solution is then represented as

$$w(x) = a_1 \sin \frac{\pi x}{l} + a_3 \sin \frac{3\pi x}{l} + ... \tag{7.4.4}$$

Consider first one-term approximation

$$w(x) = a_1 \sin \frac{\pi x}{l} \tag{7.4.5}$$

$$w'(x) = a_1 \left(\frac{\pi}{l}\right) \cos \frac{\pi x}{l} \tag{7.4.6}$$

$$w''(x) = -a_1 \left(\frac{\pi}{l}\right)^2 \sin \frac{\pi x}{l} \tag{7.4.7}$$

The expression for the total potential energy is

$$\prod = \frac{1}{2} EI \left(\frac{\pi}{l}\right)^4 a_1^2 \int_0^l \sin \frac{\pi x}{l} - Pa_1 \tag{7.4.8}$$

where the integral is simply $l/2$. Equation 7.4.4 reduces then to

$$\prod = \frac{1}{4} EI \frac{\pi^4}{l^3} a_1^2 - Pa_1 \tag{7.4.9}$$

For equilibrium $\frac{d\prod}{da_1} = 0$, which yields

$$\frac{1}{2} EI \frac{\pi^4}{l^3} a_1 - P = 0 \tag{7.4.10}$$

The load-displacement relation is finally given by

$$(a_1)_{\text{opt}} = \frac{Pl^3}{\frac{\pi^4}{2} EI} = \frac{Pl^3}{48.7EI} \tag{7.4.11}$$

The numerical coefficient in the exact solution of this problem is 48. The error of the approximate solution is 1.4%. Such a good accuracy of just one-term approximation can be explained by making the Taylor series expansion of the sign function

$$\sin \frac{\pi x}{l} = \frac{\pi x}{l} - \frac{1}{6}\left(\frac{\pi x}{l}\right)^3 + \ldots \tag{7.4.12}$$

The two term expansion has a linear and cubic terms in x, the same as the exact solution.

Let's examine next the stationary property of the functional $\prod$. Defining the normalized total potential energy as $\bar{\prod} = \frac{\prod}{Pw_o}$, one gets

$$\bar{\prod} = \frac{1}{2} \frac{a_1}{w_o} \left(\frac{a_1}{w_o} - 2\right) \tag{7.4.13}$$

where a_1 is the amplitude of the trial function Equation 7.4.3 and w_o is the exact amplitude. The plot of the function $\bar{\prod}(a_1)$ is shown in Figure (7.4.2).

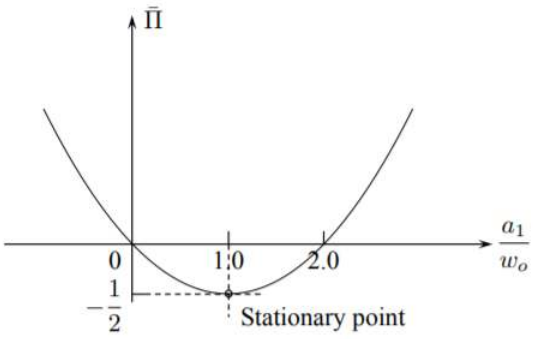

Figure 7.4.2: By varying the amplitude around $\frac{a_1}{w_o} = 1$, $\bar{\prod}$ does not change.

The function $\bar{\prod}(a_1)$ is a parabola with a stationary point at $a_1 = w_o$. The stationary point is at the same time the minimum. The negative value of the minimum (actual) value of the total potential energy comes from the choice of the reference level of the potential energy. In mechanics, the reference level is the position of the undeformed axis of the beam. Upon loading, the beam is loosing the potential energy and the second term in Equation (7.3.3) is negative and larger than the first term of the stored elastic energy.

Even though the accuracy of one term approximation in the Fourier series expansion, Equation (7.3.4) gave a very good approximation (1.4% error), the solution can be further improved by considering the next term in the expansion, according to Equation 7.4.2. In this case the total potential energy is the function of two unknown amplitudes, $\prod = \prod(a_1, a_3)$ and the solution is obtained from two algebraic equations

$$\frac{\partial \prod}{\partial a_1} = 0, \quad \frac{\partial \prod}{\partial a_3} = 0 \tag{7.4.14}$$

7.5: Solution by Taylor expansion

Consider the same sample problem of the cantilever beam under the tip point force. Assume the solution as a power series

$$w(x) = \sum_{n=1}^{N} a_n x^n \tag{7.5.1}$$

For illustration, truncate the series by taking the four first terms

$$w(x) = a_0 + a_1 x + a_2 x^2 + a_3 x^3 \tag{7.5.2}$$

The kinematic boundary conditions are

$$w(x=0) = 0; \quad w'(x=0) = 0 \tag{7.5.3}$$

It is easy to see that displacement boundary conditions are met if $a_o = a_1 = 0$. The displacements, slopes and curvature become

$$w(x) = a_2 x^2 + a_3 x^3 \tag{7.5.4}$$

$$w'(x) = 2a_2 x + 3a_3 x^2 \tag{7.5.5}$$

$$w''(x) = 2a_2 + 6a_3 x \tag{7.5.6}$$

The tip displacement is

$$w(x=l) = w_o = a_2 l^2 + a_3 l^3 \tag{7.5.7}$$

The expression for the total potential energy is

$$\prod = \frac{EI}{2} \int_0^l (2a + 6a_3 x)^2 dx - P(a_2 l^2 + a_3 l^3) \tag{7.5.8}$$

or after integration

$$\prod = \frac{EI}{2}(4a_2^2 l + 12 a_2 a_3 l^2 + 12 a_3^2 l^3) - P(a_2 l^2 + a_3 l^3) \tag{7.5.9}$$

The stationary of $\prod(a_2, a_3)$ implies that

$$\frac{\partial \prod}{\partial a_2} = 0, \quad \frac{\partial \prod}{\partial a_3} = 0 \tag{7.5.10}$$

which leads to two linear algebraic equations for a_2, a_3

$$4a_2 + 6a_3 l = \frac{Pl}{EI} \tag{7.5.11}$$

$$6a_2 + 12a_3 l = \frac{Pl}{EI} \tag{7.5.12}$$

where solution is

$$a_2 = \frac{Pl}{2EI}, a_3 = -\frac{P}{6EI} \tag{7.5.13}$$

The deflection of the beam is then

$$w(x) = \frac{P}{EI}\left(\frac{lx^2}{2} - \frac{x^3}{6}\right) \tag{7.5.14}$$

The tip deflection is obtained

$$w_o = w(x=l) = \frac{Pl^3}{3EI} \tag{7.5.15}$$

This is the exact solution of the problem. The exact solution was obtained in this case because the first four terms of the Taylor expansion contained the actual deflected shape. Note that the exact solution was obtained by the Ritz method without imposing the static boundary conditions at the tip $V = -P$ and $M = 0$. The graphical interpretation of the stationary condition with two degrees of freedom is obtained by plotting Equation 7.5.1 in the space $(\prod, a_2, a_3)$, Figure (7.5.1).

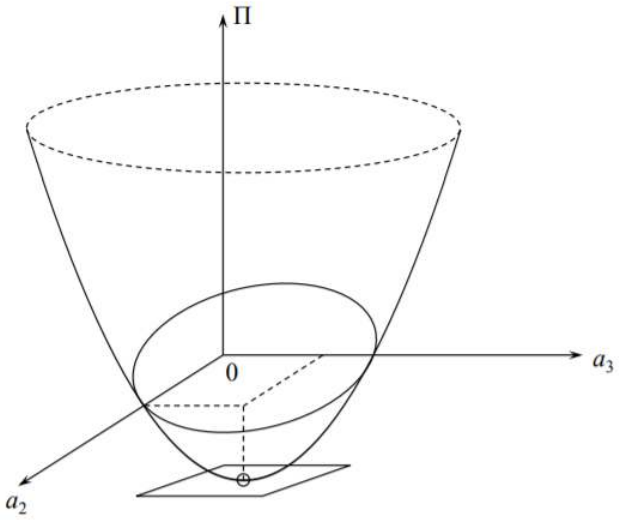

Figure 7.5.1: The potential energy as a paraboloid.

7.6: Castigliano Theorem

This theorem applies to statically determined structures and system subjected to concentrated forces or moments. The distribution of bending moments can be uniquely determined from global equilibrium as function of the forces, $U = U(P)$. The total potential energy is

$$\prod = U(P) - Pw_o \tag{7.6.1}$$

For a given deflection amplitude w_o, the magnitude of the load adjust itself so as to make the total potential energy stationary. Mathematically

$$\delta[\prod(P)] = \delta[U(P) - Pw_o] = \frac{dU}{dP}\delta P - w_o\delta P = \left[\frac{dU(P)}{dP} - w_o\right]\delta P = 0 \tag{7.6.2}$$

We have proved that the displacement under the force in the direction of the force is equal to the derivative of the elastic energy stored with respect to the force.

In order to interpret the stationary property of $\prod$, consider a cantilever beam with the force P at its tip. The bending moment distribution is $M(x) = P(l - x)$. Let's choose the force formulation of the total potential energy, Equation (??). The total potential energy is

$$[\prod = \frac{P^2}{2EI}\int_0^l (l-x)^2 dx - Pw_o \tag{7.6.3}$$

After integration

$$\prod(P) = P\left(\frac{Pl^3}{6EI} - w_o\right) \tag{7.6.4}$$

The plot of this function is shown in Fig (7.6.1).

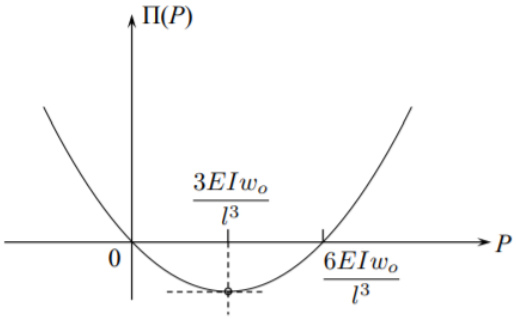

Figure 7.6.1: Parabolic variation of the total potential energy with the force P for a given central deflection.

The parabola has two roots at $P_1 = 0$ and at $P_2 = \frac{6EIw_o}{l^3}$. The stationary point is at

$$P = \frac{3EIw_o}{l^3} \tag{7.6.5}$$

which is the exact solution of the problem.

As an illustration, consider two simple structural systems. The first system of two beams is shown in Figure (7.6.2).

This problem was solved earlier using displacements and slope continuity. A much simple solution follows. The bending moment distributions are

$$\begin{aligned} &\text{Beam (A)} \quad M(x) = -Px \; 0 < x < l \\ &\text{Beam (B)} \quad M(x) = \frac{1}{2}Px \; 0 < x < l \\ &\text{Beam (C)} \quad M(x) = -\frac{1}{2}Px \; 0 < x < l \end{aligned} \tag{7.6.6}$$

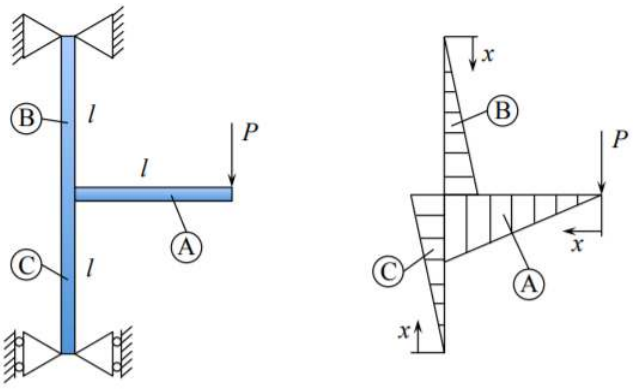

Figure **7.6.2**: Statically determined system and bending moment distribution.

The bending strain energy is

$$U(P) = \int_0^l \frac{1}{2EI}\left[P^2 + \left(\frac{P}{2}\right)^2 + \left(\frac{P}{2}\right)^2\right] x^2 dx = \frac{3}{2}P^2\frac{l^3}{3} = \frac{1}{2}P^2 l^3 \tag{7.6.7}$$

From the relative contributions of the three beams in Equation (7.5.13), it is seen that the horizontal cantilever contributes twice to the tip deflection compared to the vertical beam.

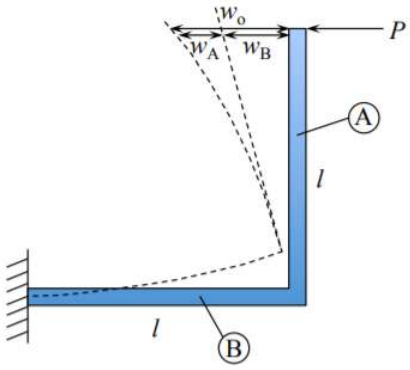

Figure **7.6.3**: two welded beams forming an elbow.

The second system consists of an elbow. From Figure (**7.6.3**), the bending moment distribution is

$$\begin{aligned} &\text{Beam (A)} \quad M(x) = Px \\ &\text{Beam (B)} \quad M(x) = Pl \end{aligned} \tag{7.6.8}$$

The elastic bending energy of the system is

$$U(P) = \frac{1}{2EI}\int_0^l (Px)^2 dx + \frac{1}{2EI}\int_0^l (Pl)^2 dx = \frac{P^2}{2EI}\frac{4l^3}{3} \tag{7.6.9}$$

The total deflection in the direction of the force is

$$w_o = \frac{dU}{dP} = \frac{4}{3}\frac{Pl^3}{EI} \tag{7.6.10}$$

Proof of the Castigliano Theorem for a system of point loads, P_i

The corresponding displacements are denoted by w_i, see Figure (**7.6.4**).

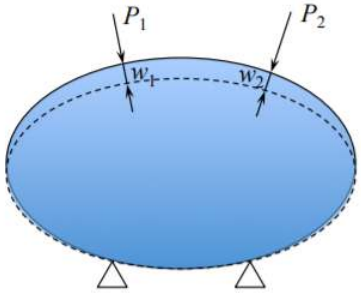

Figure 7.6.4: An elastic body (structure) loaded by a system of concentrated forces.

The work of external forces is

$$W = \sum_i P_i w_i = P_i w_i \tag{7.6.11}$$

It is assumed that the energy stored can be expressed in terms of all the point forces, $U = U(P_i)$. Let's keep all point forces at fixed values and vary only one, say P_k. For equilibrium, the total potential energy of the system should be stationary with respect to this change. Thus,

$$\begin{aligned} \delta \prod = \delta(U - W) &= \frac{dU}{dP_k}\delta P_k - w_k \delta P_k \\ &= \left(\frac{dU}{dP_k} - w_k\right)\delta P_k = 0 \end{aligned} \tag{7.6.12}$$

The extended Castigliano theorem is

$$w_k = \frac{\partial U(P_i)}{\partial P_k} \tag{7.6.13}$$

For example, if there are two point loads applied,

$$w_2 = \frac{\partial U(P_1, P_2)}{\partial P_2} \tag{7.6.14}$$

Usually the Castigliano theorem gives only deflection at a given point but not the deflected shape. The extended theorem ca be used to predict the deflected shape.

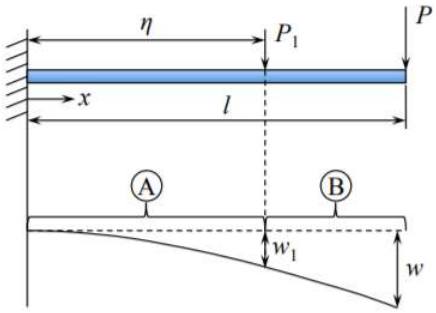

Figure 7.6.5: Cantilever beam loaded b two point forces.

Illustration

Consider a cantilever beam loaded by two point forces. One force P is applied at the tip and the other force P_1 acts at a distance η from the support.

The bending moment distribution is

$$\begin{aligned} M_A(x) &= P(l - x) + P_1(\eta - x) \quad \text{for} \quad 0 < x < \eta \\ M_B(x) &= P(l - x) \quad \text{for} \quad \eta < x < l \end{aligned} \tag{7.6.15}$$

The bending strain energy is

$$U(P,P_1)=\frac{1}{2EI}\int_0^{\eta}M_A^2dx+\frac{1}{2EI}\int_{\eta}^{l}M_B^2dx \tag{7.6.16}$$

According to Equation 7.6.3, the deflection under the point load P_1 is

$$w_1=\frac{\partial U(P,P_1)}{\partial P_1}=\frac{1}{EI}\int_0^{\eta}M_A\frac{\partial M_A}{\partial P_1}dx+\frac{1}{EI}\int_{\eta}^{l}M_B\frac{\partial M_B}{\partial P_1}dx \tag{7.6.17}$$

The derivatives of the bending moments are

$$\frac{\partial M_A}{\partial P_1}=\eta-x \tag{7.6.18}$$

$$\frac{\partial M_B}{\partial P_1}=0 \tag{7.6.19}$$

Substituting Equations 7.6.5 and (??) into (??), one gets

$$w_1=\frac{1}{EI}\int_0^{\eta}[P(l-x)+P_1(\eta-x)](\eta-x)dx \tag{7.6.20}$$

This equation is valid for any combination of P and P_1. We can therefore assume that P_1 is a "dummy" force and can be set equal to zero. Then, Equation (??) reduces to

$$w_1=\frac{1}{EI}\int_0^{\eta}[P(l-x)(\eta-x)dx \tag{7.6.21}$$

which gives, after integration,

$$w_1(\eta)=\frac{Pl^3}{3EI}\left[\frac{3}{2}\left(\frac{\eta}{l}\right)^2-\frac{1}{2}\left(\frac{\eta}{l}\right)^3\right] \tag{7.6.22}$$

In the above solution η is an arbitrary position along the beam and $w_1(\eta)$ is the corresponding deflection. By changing the variables

$$\begin{gathered}\eta\to x\\ w_1(\eta)=w(x)\end{gathered} \tag{7.6.23}$$

we can recover the exact deflected shape of the cantilever beam

$$w_1(\eta)=\frac{Pl^3}{3EI}\left[\frac{3}{2}\left(\frac{x}{l}\right)^2-\frac{1}{2}\left(\frac{x}{l}\right)^3\right] \tag{7.6.24}$$

The above example illustrated a great flexibility of the Castigliano method in solving statically determined problems.

CHAPTER OVERVIEW

8: Stability of Elastic Structures

8.1: Prelude to Stability of Elastic Structures

In Chapter 7 we have formulated the condition of static equilibrium of bodies and structures by studying a small change (variation) of the total potential energy. The system was said to be in equilibrium if the first variation of the total potential energy vanishes. The analysis did not say anything about the stability of equilibrium. The present lecture will give an answer to that question by looking more carefully what is happening in the vicinity of the equilibrium state.

To illustrate the concept, consider a rigid body (a ball) siting in an axisymmetric paraboloid. shown in Figure (**8.1.1**).

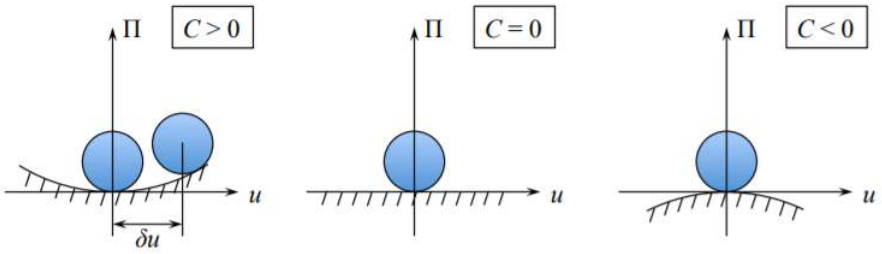

Figure **8.1.1**: Illustration of stable, neutral and unstable equilibrium.

In the case of a rigid body the total potential energy is just the potential energy

$$\prod = mgh = Cu^2 \tag{8.1.1}$$

where u is the horizontal displacement of the ball from the resting position. Let's calculate the first and second variation of the function $\prod(u)$

$$\delta \prod = \frac{\partial \prod}{\partial u}\delta u = 2Cu\delta u \tag{8.1.2}$$

$$\delta^2 \prod = \delta(\delta \prod) = 2C\delta u\delta u \tag{8.1.3}$$

At the origin of the coordinate system $u = 0$, so the first variation of $\prod$ is zero no matter what the sign of the coefficient C is. In the expression for the second variation, the product $\delta u\delta u = (\delta u)^2$ is always non-negative. Therefore, the sign of the second variation depends on the sign of the coefficient C. From Figure **8.1.1** we infer that $C > 0$ corresponds to a stable configuration. The ball displaced by a small amount δu will return to the original position. By contrast, for $C < 0$, the ball, when displaced by a tiny amount δu, will roll down and disappear. We call this an unstable behavior. The case $C = 0$ corresponds to the neutral equilibrium.

One can formalize the above consideration to the elastic body (structure), where the total potential energy is a function of a scalar parameter, such as a displacement amplitude u. The function $\prod(u)$ can be expanded in Taylor series around the reference point u_o

$$\prod(u) = \prod(u_o) + \left.\frac{d\prod}{du}\right|_{u=u_o}(u-u_o) + \frac{1}{2}\left.\frac{d^2\prod}{du^2}\right|_{u=u_o}(u-u_o)^2 + \ldots \tag{8.1.4}$$

The incremental change of the potential energy $\Delta\prod = \prod(u) - \prod(u_o)$ upon small variation of the argument $\delta u = u - u_o$ is

$$\Delta\prod = \frac{d\prod}{du}\delta u + \frac{1}{2}\frac{d^2u}{du^2}(\delta u)^2 = \delta\prod + \delta^2\prod + \ldots \tag{8.1.5}$$

For the system in equilibrium the first variation must be zero. Therefore, to the second term expansion, the sign of the increment of $\prod$ depends on the sign of the second variation of the potential energy. We can now distinguish three cases

$$\delta^2\prod \begin{cases} > 0, & \text{Positive (stable equilibrium)} \\ = 0, & \text{Zero (neutral equilibrium)} \\ < 0, & \text{Negative (unstable equilibrium)} \end{cases}$$

8.2: Trefftz Condition for Stability

In 1933 the German scientist Erich Trefftz proposed the energy criterion for the determination of the stability of elastic structures. We shall explain this criterion on a simple example of a one-degree-of-freedom structure. Consider a rigid column free at one end and hinged at the other. There is a torsional spring mounted at the hinge. Upon rotation by an angle θ, a bending moment develops at the hinge, resisting the motion

$$M = K\theta \tag{8.2.1}$$

where K is the constant of the rotational spring. The column is initially in the vertical position and is loaded by a compressive load P, Figure (8.2.1). In the deformed configuration, the force P exerts a work on the displacement u

$$u = l(1 - \cos\theta) \cong l\frac{\theta^2}{2} \tag{8.2.2}$$

The total potential energy of the system is

$$\prod = \frac{1}{2}M\theta - Pu = \frac{1}{2}K\theta^2 - \frac{1}{2}Pl\theta^2 \tag{8.2.3}$$

Upon load application the column is of course rigid and remains straight up to the critical point $P = P_c$. The path $\theta = 0$ is called the primary equilibrium path. If the column were elastic rather than rigid, there would be only axial compression along that path. This stage is often referred to as a pre-buckling configuration. At the critical load P_c the structure has two choices. It can continue resisting the force $P > P_c$ and remain straight. Or it can bifurcate to the neighboring configuration and continue to rotate at a constant force. The bifurcation point is the buckling point. The structure is said to buckle from the purely compressive stage to the stage of a combined compression and bending.

The above analysis have shown that consideration of the equilibrium with nonlinear geometrical terms, Equation 8.2.2 predicts two distinct equilibrium paths and a bifurcation (buckling) point. Let's now explore a bit further the notion of stability and calculate the second variation of the total potential energy

$$\delta^2 \prod = (K - Pl)\delta\theta\delta\theta \tag{8.2.4}$$

The plot of the normalized second variation $\delta^2 \prod / \delta\theta\delta\theta$ is shown in Figure (8.2.1).

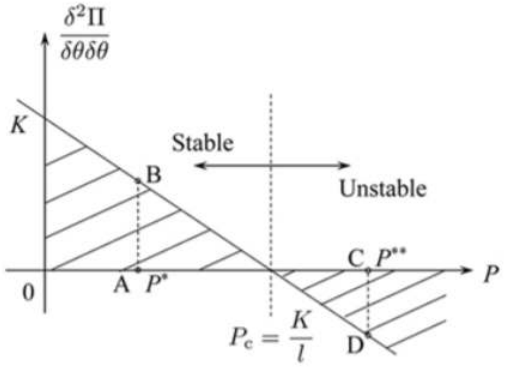

Figure 8.2.1: Stable and unstable range in column buckling.

It is seen that in the range $0 < P < P_c$, the second variation of the total potential energy is positive. In the range $P > P_c$, that function is negative. A transition from the stable to unstable behavior occurs at $\delta^2 \prod = 0$. Therefore, vanishing of the second variation of the total potential energy identifies the point of structural instability or buckling.

Physically, the test for stability looks like this. We bring the compressive force to the value P^*, still below the critical load. We then apply a small rotation $\pm\delta\theta$ in either direction of the buckling plane. The product $\delta\theta\delta\theta$ is always non-negative.

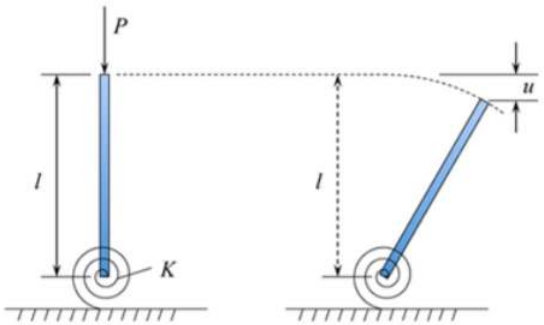

Figure 8.2.2: A discrete Euler column in the undeformed and deformed configuration.

For equilibrium the first variation of the total potential energy should banish, $\delta\theta = 0$, which gives

$$(K - Pl)\theta\delta\theta = 0 \tag{8.2.5}$$

There are two solutions of the above equation, which corresponds to two distinct equilibrium paths:

- $\theta = 0 -$ **primary equilibrium path**
- $P = P_c = \frac{K}{l} -$ **secondary equilibrium path**

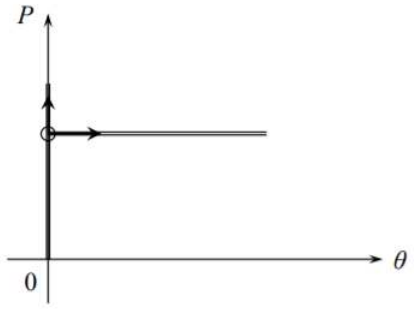

Figure 8.2.3: Two equilibrium paths intersects at the bifurcation point.

And so is the second variation of the total potential energy (length AB in Figure (8.2.1)). When the lateral load needed to displace the column by $\delta\theta$ is released, the spring system will return to the undeformed, straight position.

We repeat the same test under the compressive force $p^{**} > P_c$. The application of the infinitesimal rotation $\delta\theta$ will make the function $\delta^2/\delta\theta\delta\theta$ negative. This is a range of unstable behavior. Upon releasing of the transverse force, the column will not returned to the vertical position, but it will stay in the deformed configuration. It should be pointed up that the foregoing analysis pertains to the problem of stability of the primary equilibrium path. The secondary equilibrium path is stable, as will be shown below.

To expression for total potential, it can be constructed with the exact equation for the displacement u rather than the first two-term expansion, Equation 8.2.2

$$\prod = \frac{1}{2}K\theta^2 - lP(1 - \cos\theta) \tag{8.2.6}$$

The secondary equilibrium path obtained from $\delta\prod = 0$ is

$$\frac{P}{P_c} = \frac{\theta}{\sin\theta} \tag{8.2.7}$$

The plot of the above function is shown is Figure (8.2.4).

For small values of the column rotation, the force P is almost constant, as predicted by the two-term expansion of the cosine function. For larger rotations, the column resistance increases with the angle θ. Such a behavior is inherently stable. The force is monotonically increasing and reach infinity at $\theta \to \pi$.

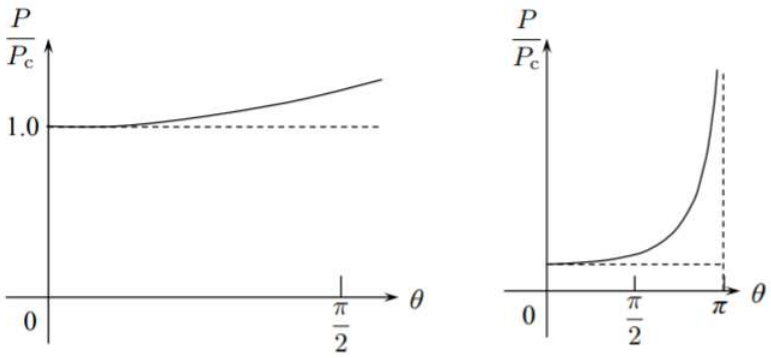

Figure **8.2.4**: Plot of the secondary equilibrium path.

8.3: Stability of Elastic Column Using the Energy Method

The Trefftz condition for stability can now be extended to the elastic column subjected to combined bending and compression. The elastic strain energy stored in the column is a sum of the bending and axial force contribution

$$U = \int_0^l \left(\frac{1}{2}M\kappa + \frac{1}{2}N\epsilon_o\right) dx \tag{8.3.1}$$

It is assumed that the column is fixed at one end against axial motion and allow to move in the direction of the axial force.

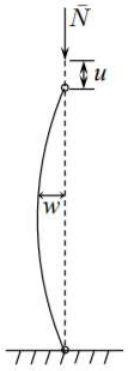

Figure **8.3.1**: Initial and deformed elastic column.

To maintain generality, no static or kinematic boundary conditions are introduced in the present derivation. The work of external forces is

$$W = \bar{N}u_o \tag{8.3.2}$$

The first variation of the total potential energy is

$$\delta\prod = \delta(U - W) = \frac{1}{2}\int_0^l (\delta M\kappa + M\delta\kappa + \delta N\epsilon + N\delta\epsilon)dx - N\delta u_o \tag{8.3.3}$$

For linear elastic material

$$M = EI\kappa, \quad \delta M = EI\delta\kappa \tag{8.3.4}$$

$$N = EA\epsilon, \quad \delta N = EA\delta\epsilon \tag{8.3.5}$$

By eliminating the bending and axial rigidity between the above equation, the following identities hold

$$M\delta\kappa = \delta M\kappa \tag{8.3.6}$$

$$N\delta\epsilon = \delta N\epsilon \tag{8.3.7}$$

Therefore, the expression 8.3.3 is reduced to

$$\delta\prod = \int_0^l (M\delta\kappa + N\delta\epsilon)dx - \bar{N}\delta u_o \tag{8.3.8}$$

Now, recall the strain-displacement relations in the theory of moderately large deflection of beams

$$\kappa = -w'', \quad \delta\kappa = -(\delta w)'' \tag{8.3.9}$$

$$\epsilon = u' + \frac{1}{2}(w')^2, \quad \delta\epsilon = (\delta u)' - w'\delta w' \tag{8.3.10}$$

Substituting the increments $\delta\kappa$ and $\delta\epsilon$ into Equation 8.3.8 yields

$$\delta\prod = -\int_0^l M\delta w''dx + N\int_0^l w'\delta w'dx + N\int_0^l \delta u'dx - N\delta u_o \tag{8.3.11}$$

In the above expression the axial load is unknown but constant over the length of the column. Therefore the load N could be brought outside the integrals. Consider now the last two terms in Equation 8.3.11

$$N\int_0^l \delta u' dx - N\delta u_o = N\delta u|_{x=0}^{x=l} - N\delta u = N\delta u_o - N\delta u_o = 0 \tag{8.3.12}$$

With the above simplification we calculate now the second variation of the total potential energy

$$\delta^2 \prod = \delta(\delta \prod) = -\int_0^l \delta M \delta w'' dx + N\int_0^l \delta w' \delta w' dx \tag{8.3.13}$$

According to the Trefftz stability criterion $\delta^2 \prod = 0$,

$$-\int_0^l EI\delta w'' \delta w'' dx + N\int_0^l \delta w' \delta w' dx = 0 \tag{8.3.14}$$

The buckling load $N = N_c$ is then

$$N = EI\frac{-\int_0^l \delta w'' \delta w'' dx}{\int_0^l \delta w' \delta w' dx} \tag{8.3.15}$$

Let's express the out-of-plane deflection of the column as a product of the amplitude A and the normalized shape function $\phi(x)$. The shape function should satisfy kinematic boundary condition of a problem

$$w(x) = A\phi(x) \tag{8.3.16}$$

We can calculate now the first and second derivatives of the function $w(x)$ and their variations

$$w' = A\phi', \quad \delta w' = \delta A\phi' \tag{8.3.17}$$

$$w'' = A\phi'', \quad \delta w'' = \delta A\phi'' \tag{8.3.18}$$

Substituting the above expression into Equation 8.3.15, we get

$$N_c = EI\frac{\int_0^l \delta A\phi'' \delta A\phi'' dx}{\int_0^l \delta A\phi' \delta A\phi' dx} = EI\frac{\int_0^l \phi'' \phi'' dx}{\int_0^l \phi' \phi' dx} \tag{8.3.19}$$

where $N_c = -N$ is he compressive buckling load.

The above equation for the critical buckling load of a column is called the Raleigh-Ritz quotient. The Trefftz criterion does not provide the shape function but for a given shape calculates the approximate value of the buckling load. This is always an upper bound. Should the shape function coincide with the exact buckling shape, the Raleigh-Ritz quotient will give the absolute minimum value.

As an illustration, consider the pin-pin supported column and assume the following buckling shape

$$\phi(x) = x(l - x) \tag{8.3.20}$$

which satisfies identically kinematic boundary conditions $\phi(x = 0) = \phi(x = l) = 0$. The first and second derivatives of the shape function are

$$\phi'(x) = 2x - l \tag{8.3.21}$$

$$\phi''(x) = 2 \tag{8.3.22}$$

After straightforward integration, the calculated buckling load is

$$N_c = \frac{12EI}{l^2} \tag{8.3.23}$$

Can the accuracy of the above solution be improved? Let's try and assume as a shape function the solution for the pin-pin beam under the uniform line load

$$\phi(x) = x^4 - 2lx^3 + l^3 x \tag{8.3.24}$$

The above function satisfies the simple support boundary condition at both ends. The slope and the curvature of the deflected shape are

$$\phi'(x) = 4x^3 - 6lx^2 + l^3 \tag{8.3.25}$$

$$\phi''(x) = 12x^2 - 12lx \tag{8.3.26}$$

Because the curvature at both ends vanish, so does the bending moment. Also the slope at mid-span is zero. This means that the static (zero bending moments) boundary conditions are also satisfied. The previously considered shape function, Equation 8.3.20 led to the constraint curvature, meaning that the static boundary conditions were violated. After straightforward calculation, the numerical coefficient become $\frac{1680}{170} = 9.88$. There was over 20% improvements in the accuracy of the solution

$$N_c = 9.88\frac{EI}{l^2} \tag{8.3.27}$$

Can the solution be further improved (lowered)? yes, but not by much. Assume a sinusoidal shape of the buckling shape

$$\phi = \sin\frac{\pi x}{l} \tag{8.3.28}$$

$$\phi' = \frac{\pi}{l}\cos\frac{\pi x}{l} \tag{8.3.29}$$

$$\phi'' = -\left(\frac{\pi}{l}\right)^2 \sin\frac{\pi x}{l} \tag{8.3.30}$$

The expression for the critical buckling load becomes

$$N_c = \frac{EI(\frac{\pi}{l})^4}{(\frac{\pi}{l})^2}\frac{\int_0^l \sin^2\frac{\pi x}{l}dx}{\int_0^l \cos^2\frac{\pi x}{l}dx} \tag{8.3.31}$$

Both integrals are identical and the solution becomes

$$N_c = \frac{\pi^2 EI}{l^2} \tag{8.3.32}$$

Because $\pi^2 = 9.86$, the sinusoidal solution is slightly lower than the previous polynomial solution. This is the lowest possible coefficient meaning that it must be an exact solution to the buckling problem. To prove it, it is sufficient to check if the local equilibrium equation is satisfied

$$EIw^{\mathrm{IV}} + Nw'' = 0 \tag{8.3.33}$$

Indeed, substituting Equations 8.3.28 - 8.3.30 and 8.3.32 into the equilibrium equation brings the left hand side of this equation identically to zero.

8.4: Effect of Structural Imperfections

Consider the same discrete strutter as in Section 8.2. This time the rigid rod is not straight but is rotated by the angle θ_o before the vertical load is applied. Upon load application the column is subjected to additional rotation θ, measured from the theoretical vertical direction, Figure (8.4.1).

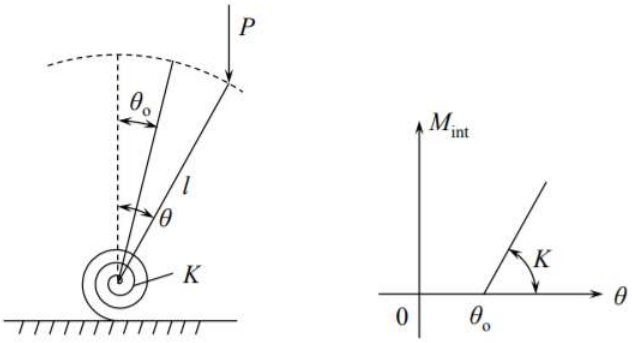

Figure 8.4.1: The initial inclination angle θ_o is a measure of structural imperfection.

The problem will be solved by means of local equilibrium. The external bending moment at the base is

$$M_{ext} = Pl\sin\theta, \text{ for } \theta \geqslant \theta_o \tag{8.4.1}$$

where $l\sin\theta$ is the arm of the force P. In the case of small angle approximation $M_{ext} = Pl\theta$. The internal resisting bending moment is

$$M_{int} = K(\theta - \theta_o) \tag{8.4.2}$$

Equating the external and internal bending moments

$$Pl\theta = K(\theta - \theta_o) \tag{8.4.3}$$

For a geometrically perfect column $\theta_o = 0$ and from Equation 8.4.3

$$P = P_c = \frac{K}{l} \tag{8.4.4}$$

Equation 8.4.3 can be re-written in terms of the normalized compressive force P/P_c

$$\frac{P}{P_c}\theta = \theta - \theta_o \tag{8.4.5}$$

Solving this equation for θ yields

$$\theta = \theta_o \frac{1}{1 - \frac{P}{P_c}} \tag{8.4.6}$$

The plot of the above function is shown in Figure (8.4.2). The term $1/(1 - \frac{P}{P_c})$ is called the magnification factor. It predicts how much the initial imperfections are magnified for a given magnitude of load. When structural imperfections are present, there are no primary and secondary equilibrium paths. There is only one smooth load-deflection curve called the equilibrium path.

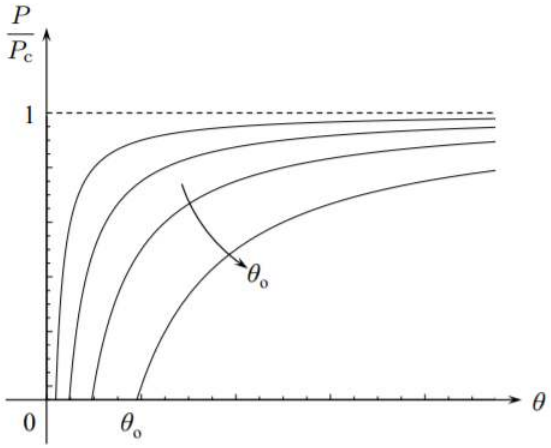

Figure 8.4.2: A family of equilibrium paths for different values of imperfections.

It is interesting to note that with smaller and smaller initial imperfections, the equilibrium paths are approaching the bifurcation point but never reach it. This type of behavior is common to all imperfect structures.

As another example of an imperfect structure consider a pin-pin elastic column. The following notation is introduced:

- $\bar{w}(x)$ – shape of initial imperfection
- $\bar{w}_o$ – amplitude of initial imperfection
- $w(x)$ – actual buckled shape measured from the vertical (perfect) position
- w_o – central amplitude of the actual deflection

The internal bending moment is

$$M_{\text{int}} = EI\Delta\kappa = -EI(w'' - \bar{w}'') \tag{8.4.7}$$

where $\Delta\kappa$ is the change of curvature from the initial curved (imperfect) column. For a simply supported column, the end (reaction) moments are zero so the external bending moment is

$$M_{\text{ext}} = Pw \tag{8.4.8}$$

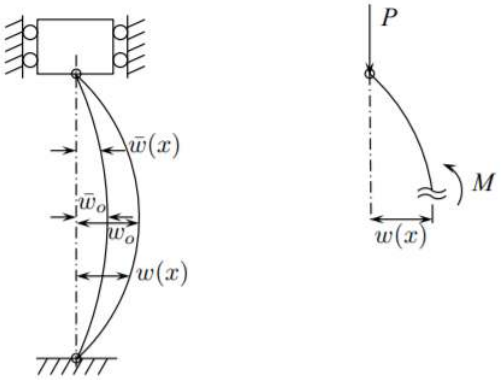

Figure \(\PageIndex{3}\): A continuous imperfect column and the free body diagram.

Equating the internal and external bending moments one gets

$$EIw'' + Pw = EI\bar{w}(x) \tag{8.4.9}$$

This is a second order, linear inhomogeneous differential equation, where the right hand side is a known shape of initial imperfection. The solution to this equation exists in terms of quadratures, but the integrals are difficult to evaluate for complex shapes of imperfections.

Let's consider the simplest case of a sinusoidal shape of imperfections. It can be shown that the solution $w(x)$ is also of the sinusoidal shape

$$w(x) = w_o \sin \lambda x \tag{8.4.10}$$

$$\bar{w}(x) = \bar{w}_o \sin \lambda x \tag{8.4.11}$$

The kinematic boundary conditions are

$$w(0) = w(l) = 0$$

which implies that

$$\sin \lambda l = 0 \quad \rightarrow \quad \lambda l = n\pi \tag{8.4.12}$$

Substituting Equations 8.4.10 - 8.4.11 into the governing equation 8.4.9

$$-EI\lambda^2(w_o - \bar{w}_o) \sin \lambda x - P w_o \sin \lambda x = 0 \tag{8.4.13}$$

which is satisfied if

$$P w_o = EI(w_o - \bar{w}_o)\lambda^2 \tag{8.4.14}$$

For a perfect column $\bar{w}_o = 0$, and Equation 8.4.14 yields

$$(P_c - EI\lambda^2)w_o = 0 \tag{8.4.15}$$

$$\text{or } P_c = EI\lambda^2 = \frac{n^2\pi^2 EI}{l^2}$$

For an imperfect column

$$P w_o = P_c(w_o - \bar{w}_o) \tag{8.4.16}$$

or solving for w_o

$$w_o = \bar{w}_o \frac{1}{1 - \frac{P}{P_c}} \tag{8.4.17}$$

The form of the magnification factor is identical to the one derived for the district column. The only difference is that a continuous column has infinity buckling mode where $n = 1$ corresponds to the lowest buckling load. The buckling load corresponding to the second buckling mode is four times larger and so on.

8.5: Stability in Tension

For some materials instability in tension manifest itself by a development of a local neck, Figure (8.5.1).

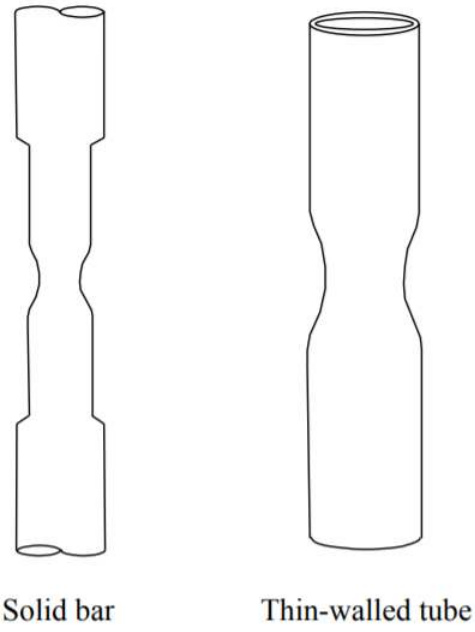

Figure 8.5.1: Necking in a solid section bar and thin-walled tube under tension.

Consider a round bar of the initial cross-sectional area A_o subjected to a tensile force P. The bar becomes longer and because the Poisson effect its cross-section shrinks to a current value A. The present analysis is valid for materials that are incompressible, that is do not change volume but only shape. Certain polymers, rubber and metals (in the plastic range) are incompressible.

The volume of an infinitesimal length l is

$$V = lA \tag{8.5.1}$$

The increment of volume for the incompressible material must be equal to zero

$$\delta V = \delta(lA) = \delta l A + l\delta A = 0 \tag{8.5.2}$$

Take the logarithmic definition of the axial strain

$$\epsilon = \ln \frac{l}{l_o}; \quad \delta\epsilon = \frac{\delta l}{l} \tag{8.5.3}$$

From the above two equations

$$\delta\epsilon = \frac{\delta l}{l} = -\frac{\delta A}{A} \tag{8.5.4}$$

Integrating both sides

$$\epsilon = -\ln A + C$$

At $A = A_o$, $\epsilon = 0$ so $C = \ln A_o$.

Therefore, the expression for the axial strain becomes

$$\epsilon = \ln \frac{A_o}{A} = \ln \frac{l}{l_o} \tag{8.5.5}$$

We conclude that axial strain can be determined by either measuring the change in length or the change in cross-sectional area. The true (Cauchy) stress is defined as the load divided by the current cross-section A

$$\sigma = \frac{P}{A} \tag{8.5.6}$$

Let's construct the total potential energy and its first variation

$$\delta \prod = \int_V \sigma \delta \epsilon dv - P \delta u \tag{8.5.7}$$

Before instability occurs, the deformation and stress (uniaxial tension) is uniform across the section of the bar of the length l

$$u = l\epsilon = l \ln \frac{A_o}{A} \tag{8.5.8}$$

$$\delta u = -l \frac{\delta A}{A} \tag{8.5.9}$$

Thus, from Equations 8.5.7 and 8.5.8 - 8.5.9

$$\delta \prod = \int_V \sigma \delta \epsilon dv + Pl \frac{\delta A}{A} \tag{8.5.10}$$

The second variation of the total potential energy is

$$\delta^2 \prod = \int_V \delta\sigma \delta \epsilon dv - Pl \frac{\delta A \delta A}{A^2} \tag{8.5.11}$$

Applying the Trefftz stability condition $\delta^2 \prod = 0$ one gets

$$lA\delta\sigma\delta\epsilon = Pl\delta\epsilon\delta\epsilon \tag{8.5.12}$$

or

$$\delta\sigma = \frac{P}{A}\delta\epsilon = \sigma\delta\epsilon \tag{8.5.13}$$

and finally

$$\frac{\delta\sigma}{\delta\epsilon} = \sigma \tag{8.5.14}$$

The incompressible bar is losing stability in tension when the local tangent to the stress-strain curve becomes equal to the value of stress at that point. A graphical interpretation is shown in Figure (8.5.2).

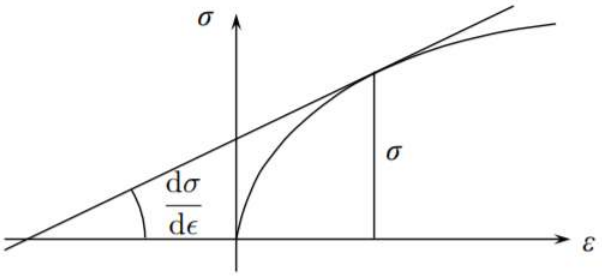

Figure 8.5.2: The construction of Considere' who was the first to derive Equation 8.5.14.

At what strain an instability develops for an elastic material? In uni-axial stress

$$\sigma = E\epsilon \tag{8.5.15}$$

$$\frac{d\sigma}{d\epsilon} = E \tag{8.5.16}$$

Equation 8.5.14 is satisfied if $\epsilon = 1$. For metals such strain is not attainable in the elastic range because yield will be reached at the strain $\epsilon_y = \frac{\sigma_y}{E} \cong 10^{-3}$. However, for rubber and similar polymeric materials the Young's modulus is four orders of magnitude smaller, so necking is of common occurrence. The derivation of the instability condition 8.5.14 was done without any assumption on the stress-strain relation of the material. Therefore this condition is valid for an elastic as well as plastic material. This brings us to the next topic which is plastic buckling of columns.

8.6: Plastic Buckling of Columns

Let's consider the pin-pin column for which the critical buckling load is

$$P_c = \frac{\pi^2 EI}{l^2} \tag{8.6.1}$$

The corresponding critical buckling stress σ_c is

$$\sigma_c = \frac{P_c}{A} = \frac{\pi^2 E}{l^2}\frac{I}{A} \tag{8.6.2}$$

where A is the cross-sectional area. Note that the stress is calculated over the pre-buckling, primary equilibrium path, for which there is no bending. Denoting by ρ the radius of gyration, $A\rho^2 \equiv I$, Equation 8.6.2 can be re-written in terms of the slenderness ratio $\beta = l/\rho$

$$\sigma_c = \pi^2 E \frac{1}{\beta^2} \tag{8.6.3}$$

The buckling stress is small for long, slender column and is rapidly increasing for short columns. At some critical column length, the yield stress of the material σ_y will be reached, Figure (8.6.1).

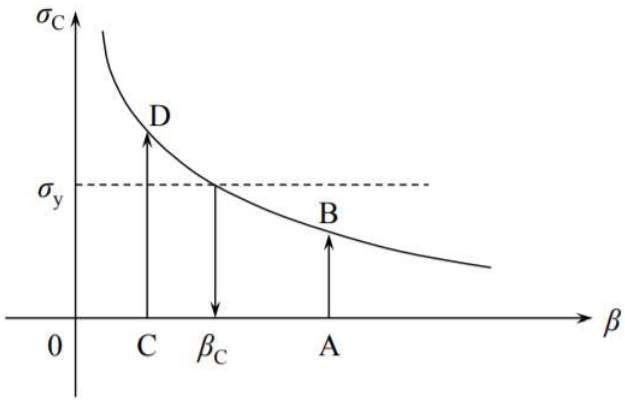

Figure 8.6.1: A hyperbolic dependence of the buckling stress on the slenderness ratio.

The critical slenderness ratio at which the buckling stress reaches the yield stress of the material is obtained from Equation 8.6.3 by setting $\sigma_c = \sigma_y$

$$\beta_c = \frac{l_c}{\rho} = \pi\sqrt{\frac{E}{\sigma_y}} \tag{8.6.4}$$

To give you the feel of the critical slenderness, consider a mild steel column with $E = 210$ GPa, $\sigma_y = 250$ MPa and square cross-section $A = h^2$, for which the radius of gyration is $\rho^2 = h^2/12$

$$\left(\frac{l}{h}\right)_c = \pi\sqrt{\frac{E}{\sigma_y}} \cdot \frac{1}{2\sqrt{3}} \approx 30 \tag{8.6.5}$$

Columns more slender than the critical will buckle elastically before yielding (path AB). Shorter column or stocky column will yield before buckling. What will happen with such columns? They will deform plastically in axial compression and eventually buckle in the plastic range.

Gerrard (1948) extended the predictive capability of Equation 8.6.3 into the plastic range by replacing the elastic modulus by the tangent modulus $E_t = \frac{d\sigma}{d\epsilon}$

$$(\sigma_c)_{\text{plastic}} = \pi^2 E_t \frac{1}{\beta^2}, \text{ for } \beta < \beta_c \tag{8.6.6}$$

For example, for a plastic material obeying the power hardening rule,

$$\sigma = B \cdot \epsilon^n \tag{8.6.7}$$

$$\frac{d\sigma}{d\epsilon} = nB\epsilon^{n-1} \tag{8.6.8}$$

Substituting Equation 8.6.7 - 8.6.8 into Equation 8.6.6, the critical buckling strain ϵ_c is

$$\epsilon_c = \frac{\pi^2 n}{\beta^2} \tag{8.6.9}$$

Using the hardening rule, the buckling stress is

$$\sigma_c = B\left[\frac{\pi^2 n}{\beta^2}\right]^n \tag{8.6.10}$$

In the above equation B is the amplitude of the hardening law and n is the hardening exponent. For most structural steels $n \approx 0.1 - 0.2$.

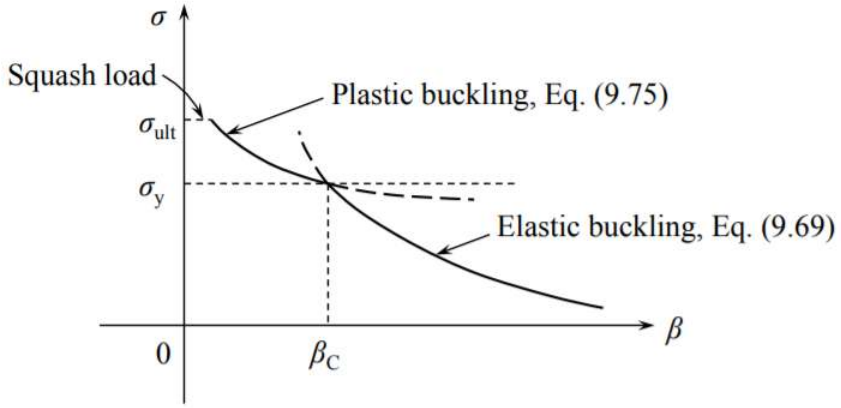

Figure 8.6.2: Range of elastic and plastic buckling.

Very short columns are beyond the scope of the elementary theory of thin and slender beams. They will never buckle but flatten as a pancake.

8.7: Mode Transition (Advanced)

Moment Equilibrium Equation

For a pin-pin supported column, the shape of the imperfection $\bar{w}(x)$ and the deformation $w(x)$ satisfy the moment equilibrium equation

$$EIw'' + Pw = EI\bar{w}'' \tag{8.7.1}$$

The solutions should satisfy the boundary conditions

$$\begin{aligned} w(0) &= 0 \\ w''(0) &= 0 \\ w(l) &= 0 \\ w''(l) &= 0 \end{aligned}$$

Of course, the solutions should also satisfy the continuous conditions: $w(x)$ and $w'(x)$ are continuous along the entire length of the column, namely, no step or kink occurs in the solutions.

We can expand the imperfection $\bar{w}(x)$ in Fourier series as

$$\bar{w}(x) = \sum_{n=1}^{\infty} A_n \sin\frac{n\pi x}{l} \tag{8.7.2}$$

The coefficients A_n can be determined by Fourier transformation of $\bar{w}$:

$$A_n = \frac{2}{l}\int_0^l \bar{w}(x)\sin\frac{n\pi x}{l}dx \tag{8.7.3}$$

The deformation $w(x)$ under a load P can be written as a summation of a complete set of Fourier series

$$w(x) = \sum_{n=1}^{\infty} B_n \sin\frac{n\pi x}{l} \tag{8.7.4}$$

where B_n can be determined by Equation 8.7.1.

Equation 8.7.1 now becomes

$$-\sum_{n=1}^{\infty} B_n \left(\frac{n\pi}{l}\right)^2 \sin\frac{n\pi x}{l} + \frac{P}{EI}\sum_{n=1}^{\infty} B_n \sin\frac{n\pi x}{l} = -\sum_{n=1}^{\infty} A_n \left(\frac{n\pi}{l}\right)^2 \sin\frac{n\pi x}{l} \tag{8.7.5}$$

To make the equation hold, the coefficients should satisfy

$$-B_n\frac{n^2\pi^2}{l^2} + \frac{P}{EI}B_n = -A_n\frac{n^2\pi^2}{l^2} \tag{8.7.6}$$

Solve for B_n, we get

$$B_n = A_n\frac{1}{1-\bar{P}/n^2} \tag{8.7.7}$$

here, we defined $\bar{P} = P/P_c$ and $P_c = \frac{\pi^2 EI}{l^2}$. So, the deformation $w(x)$ is

$$w(x) = \sum_{n=1}^{\infty} A_n\frac{1}{1-\bar{P}/n^2}\sin\frac{n\pi x}{l} \tag{8.7.8}$$

The solution tells us what is the shape of the deformation, but it does not tell us any thing about the stability of the equilibrium shape. If we want to study the stability, we have to use potential energy method.

Potential Energy Method

Under a load P, the total potential energy of the column system is (due to Equation (9.2.1) in Chapter 9):

$$\prod = \frac{EI}{2}\int_0^l (w'' - \bar{w}'')^2 dx - \frac{P}{2}\int_0^l (w'^2 - \bar{w}'^2) dx \tag{8.7.9}$$

Substitute Equations 8.7.2 and 8.7.4 into it, we have

$$\begin{aligned}
\prod &= \frac{EI}{2}\int_0^l (w'' - \bar{w}'')^2 dx - \frac{P}{2}\int_0^l (w'^2 - \bar{w}'^2) dx \\
&= \frac{EI}{2}\int_0^l \left[-\sum_{n=1}^{\infty} B_n \left(\frac{n\pi}{l}\right)^2 \sin\frac{n\pi x}{l} + \sum_{n=1}^{\infty} A_n \left(\frac{n\pi}{l}\right)^2 \sin\frac{n\pi x}{l}\right]^2 dx \\
&\quad - \frac{P}{2}\int_0^l \left\{\left[\sum_{n=1}^{\infty} B_n \left(\frac{n\pi}{l}\right)\cos\frac{n\pi x}{l}\right]^2 - \left[\sum_{n=1}^{\infty} A_n \left(\frac{n\pi}{l}\right)\cos\frac{n\pi x}{l}\right]^2\right\} dx \\
&= \frac{\pi^4 EI}{4l^3}\sum_{n=1}^{\infty}(B_n - A_n)^2 n^4 - \frac{\pi^2 P}{4l}\sum_{n=1}^{\infty} B_n^2 n^2 + \frac{\pi^2 P}{4l}\sum_{n=1}^{\infty} A_n^2 n^2 \\
&= \frac{\pi^2 P_c}{4l}\left\{\sum_{n=1}^{\infty}[(B_n - A_n)^2 n^4 - \bar{P}(b_n^2 - a_n^2) n^2]\right\}
\end{aligned}$$

The orthogonality of Fourier series is used to simplify the integration.

In order to obtain the equilibrium solution, we need the first derivative of potential energy

$$\frac{\partial \prod}{\partial B_n} = 0 \quad \rightarrow \quad B_n = A_n \frac{1}{1 - \bar{P}/n^2} \tag{8.7.10}$$

which is exactly the same as the solution given by solving the equilibrium equation.

To see the stability of the solution, we need the second derivative of potential energy

$$\frac{\partial \Pi}{\partial B_n^2} > 0 \quad \rightarrow \quad \bar{P} < n^2 \tag{8.7.11}$$

We can see the following points directly from Equations 8.7.10 and 8.7.11:

- The critical buckling load for the n^{th} mode is $P_c = \frac{n^2\pi^2 EI}{l^2}$.
- The modes that satisfy $n^2 > \bar{P}$ are in stable equilibrium.
- For the modes that satisfy $n^2 < \bar{P}$, we can still solve for a value of B_n, but those modes are unstable and will snap into either plus or minus infinity.

Example 8.7.1

The imperfection $\bar{w}(x)$ consists of only the first two modes, namely

$$\bar{w}(x) = A_1 \sin\frac{\pi x}{l} + \sin\frac{2\pi x}{l} \tag{8.7.12}$$

If $A_1 = 0$, the zero point is at the center of the column. If $A_1 \neq 0$, the zero point is displaced by a distance u. u is given by

$$u = \frac{\sin^{-1}\frac{A_1}{2}}{\pi} l, \quad 0 \leq A_1 \leq 2 \tag{8.7.13}$$

The deformation amplitudes vs. load curves are plotted in Figure (8.7.1) for the case $A_1 = 0.5$, Figure (8.7.2) for $A_1 = 1$, and Figure (8.7.3) for $A_1 = 1.5$.

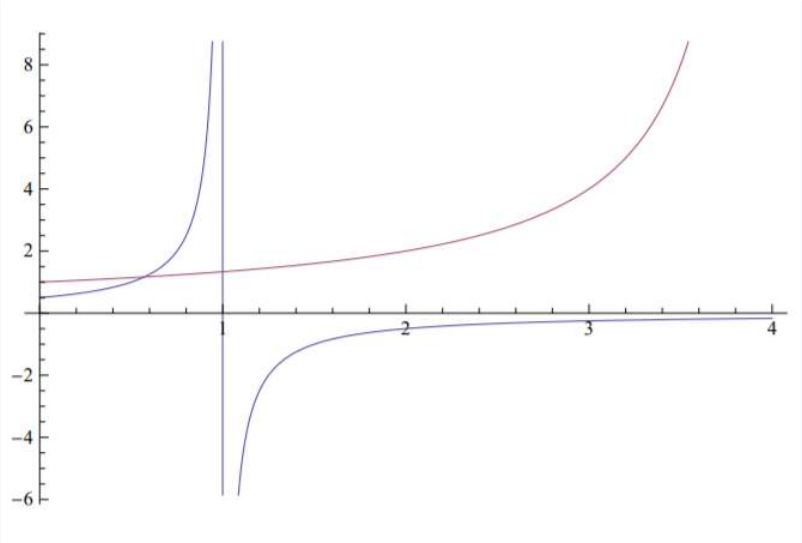

Figure 8.7.1: The deformation amplitudes B_1, B_2 vs. load $\bar{P}$ curves, for the case $A_1 = 0.5$.

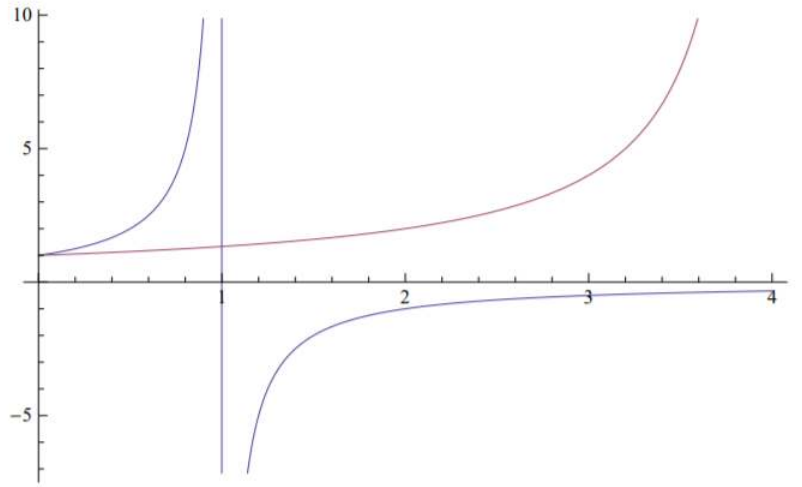

Figure 8.7.2: The deformation amplitudes B_1, B_2 vs. load $\bar{P}$ curves, for the case $A_1 = 1$.

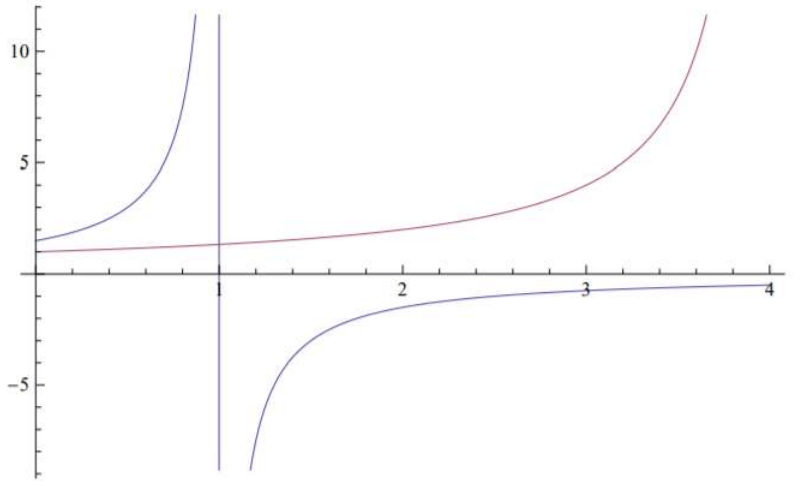

Figure 8.7.3: The deformation amplitudes B_1, B_2 vs. load $\bar{P}$ curves, for the case $A_1 = 1.5$.

Example 8.7.2

The imperfection is in such a shape that the zero point is displaced while both sections are self-symmetric. Such a shape can be described as

$$\bar{w}(x) = \begin{cases} \sin\frac{\pi x}{\eta l} & 0 < x < \eta l \\ -\frac{1-\eta}{\eta}\sin\frac{\pi(x-\eta l)}{(1-\eta)l} & \eta l < x < l \end{cases} \tag{8.7.14}$$

where $0.5 \le \eta \le 1$. When $\eta = 0.7$, $\bar{w}(x)$ can be expanded in Fourier series as:

$$\bar{w}(x) = 0.634\sin\frac{\pi x}{l} + 0.563\sin\frac{2\pi x}{l} - 0.174\sin\frac{3\pi x}{l} + 0.071\sin\frac{4\pi x}{l} + \ldots \tag{8.7.15}$$

As expected, in this case, the first two modes dominate, but there are still higher modes in the expansion.

We plot the mode amplitudes vs. load in Figure (8.7.4). If the load $\bar{P} > 4$, for example, $\bar{P} = 7.5$, the amplitude of mode III becomes largest. So, the solved deformation shape looks more like mode III, although the initial imperfection seems having nothing to do with mode III. Nevertheless, this shape is very unstable; since $\bar{P} > 2^2$, both mode I and mode II are in unstable equilibrium. Under such a load, mode I and mode II will amplify exponentially.

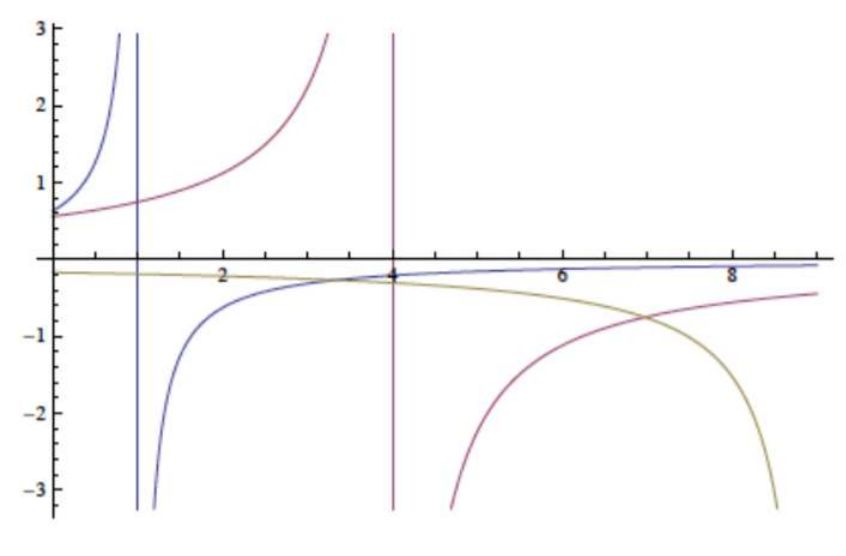

Figure 8.7.4: The deformation amplitudes of the first three modes vs. load $\bar{P}$ curves, for the imperfection shape described by Eqn. 8.7.14.

CHAPTER OVERVIEW

9: Advanced Topic in Column Buckling

9.1: The Tallest Column

In 1757 the Swiss mathematician Leonard Euler presented the famous solution for buckling of a pin-pin column under compressive loading at its end. He also formulated and solved the much more difficult problem of a clamped-free column loaded by its own weight. The practical question was how tall the prismatic column could be before it buckles under its own weight. In order to formulate this problem, the equation of equilibrium of a beam/column in the axial direction must be re-visited. Instead the equation $N' = 0$ or $N =$const, we must assume that there is a body force q per unit length $q = A\rho$, where A is the cross-sectional area of the column and ρ is its mass density. Then, the equilibrium in the axial direction requires that

$$N' = q \quad \text{or} \quad N = qx + C \tag{9.1.1}$$

In the coordinate system shown in Figure (**9.1.1**), the axial force must be zero at $x = l$.

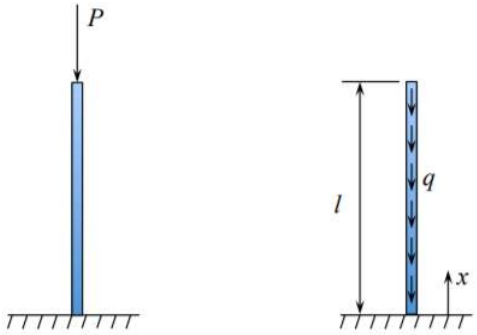

Figure **9.1.1**: Column loaded at its tip (left) and loaded by its own weight (right).

The distribution of axial force along the length of the column is

$$N(x) = -q(l - x) \tag{9.1.2}$$

where the minus sign indicates that N is the compressive force. As before, the input parameters of the problem are E, I and q and the unknown is the critical length l_c.

The derivation of the buckling problem for a classical column presented in Chapter 8 is still valid but the axial force in Equation (8.3.11) is no longer constant and thus should be kept inside the integral.

For the present problem the first variation of the total potential energy is

$$\delta \prod = -\int_0^l M\delta w''\,dx + \int_0^l q(l - x)w'\delta w'\,dx \tag{9.1.3}$$

Integrating the right hand side of Equation 9.1.3 by part, one gets

$$\int_0^l M'' + q(l - x)w'\delta w dx + \text{ Boundary terms } = 0 \tag{9.1.4}$$

where

$$\text{Boundary terms } = -M\delta w'|_0^l + M'\delta w|_0^l + q(l - x)w'\delta w \tag{9.1.5}$$

at $x = 0$, $\delta w = \delta w' = 0$; and at $x = l$, $M = 0$, $V = M' = 0$ and $l - x = 0$. Therefore the boundary terms vanish (see the dedication in Section 2.5). Using the elasticity law, $M = -EIw''$, the local equilibrium equation for the column self buckling becomes

$$EI\frac{d^4w}{dx^4} + \frac{d}{dx}\left[q(l - x)\frac{dw}{dx}\right] = 0 \tag{9.1.6}$$

Integrating once, we get

$$EI\frac{d^3w}{dx^3} + q(l - x)dw = 0 \tag{9.1.7}$$

The integration constant is zero because the shear force vanishes at the free end $x = l$. The governing equation is the third order linear differential equation with a variable coefficient. The solution is no longer represented by the harmonic function. The way to solve the problem is to introduce two new variables

$$\xi = \frac{2}{3}\sqrt{\frac{q(l-x)^3}{EI}}, \quad u = \frac{dw}{d\xi} \tag{9.1.8}$$

Then, Equation 9.1.7 transforms to the Bessel equation

$$\frac{d^2u}{d\xi^2} + \frac{1}{\xi}\frac{du}{d\xi} + (1 - \frac{1}{9\xi^2})u = 0 \tag{9.1.9}$$

Omitting the details of the calculation, the critical length of the column is found to be

$$l_c^3 = \frac{9EI}{4q} j_{\frac{1}{3}}^2 \tag{9.1.10}$$

where $j_{\frac{1}{3}} = 1.866$ is the root of the Bessel function of the third kind. Finally

$$l_c^3 = 7.837\frac{EI}{q} \tag{9.1.11}$$

The total weight of the column material is $N_c = l_c q$. In terms of the total weight, the critical length is

$$l_c^2 = 7.84\frac{EI}{N_c} \tag{9.1.12}$$

For comparison, the length of the free-clamped column at buckling loaded by the same weight is

$$l_c^2 = \frac{\pi^2}{4}\frac{EI}{N_c} = 2.47\frac{EI}{N_c} \tag{9.1.13}$$

The bottom of both column sees the same weight, but the critical length of the column undergoing self-buckling is $\sqrt{\frac{7.84}{2.47}} = 1.78$ times taller than a similar cross-section column loaded at its tip.

Example 9.1.1

A steel tubular mast solidly built-in the foundation and is free on its top. The cylinder is $t = 3$ mm thick and has a radius of $R = 50$ mm. What is the critical length of the mast to buckle under its own weight?

The total weight of the mast is

$$N_c = Al\rho \tag{9.1.14}$$

where A is the cross-sectional area, $A = 2\pi Rt$. The second moment of inertia of the thinwalled tube is $I = \pi R^3 t$. From Equation 9.1.12

$$l_c^2 = 7.84\frac{E\pi R^3 t}{2\pi R t l_c \rho} \tag{9.1.15}$$

from which one gets

$$l_c = \sqrt[3]{\frac{3.92ER^2}{\rho}} = 65m \tag{9.1.16}$$

The above solution applies to a prismatic column of a constant cross-section.

Approximate solution can be derived from the Trefftz condition $\delta^2 \prod = 0$. Starting from Equation 9.1.3 and performing the second variation one gets

$$EI\int_0^l \delta w'' \delta w' dx + \int_0^l q(l-x)\delta w' \delta w dx \tag{9.1.17}$$

The critical compressive body force is then

$$q = EI\frac{\int_0^l \phi''\phi'' dx}{\int_0^l (l-x)\phi'\phi' dx} \tag{9.1.18}$$

As compared with the standard Trefftz formula for tip loaded column, there is the term $(l-x)$ in the denominator. As an example consider the simplest parabolic deflection shape

$$\phi = x^2 \tag{9.1.19}$$

$$\phi' = 2x \tag{9.1.20}$$

$$\phi'' = 2 \tag{9.1.21}$$

Introducing the above expression into Equation 9.1.18, the critical buckling weight per unit length is

$$q = \frac{12EI}{l^3} \tag{9.1.22}$$

The error in this approximation is $\frac{12-7.837}{7.837} = 53\%$ which is not good. As a second trial consider a power shape function with a fractional exponent α

$$\phi = x^\alpha \tag{9.1.23}$$

$$\phi' = \alpha x^{\alpha-1} \tag{9.1.24}$$

$$\phi'' = \alpha(\alpha-1)x^{\alpha-2} \tag{9.1.25}$$

The resulting solution is

$$q = \frac{2EI}{l^3}\frac{\alpha(\alpha-1)(2\alpha-1)}{2\alpha-3} \tag{9.1.26}$$

The critical buckling parameter attains a minimums at $\alpha = 1.75$. The minimum buckling load is

$$q_{\min} = 9.8\frac{EI}{l^3} \tag{9.1.27}$$

The error is slashed by half but it is still large at 25%. In the third attempt, let's consider the trigonometric function

$$\phi = 1 - \cos\frac{\pi x}{2l} \tag{9.1.28}$$

$$\phi' = \left(\frac{\pi}{2l}\right)\sin\frac{\pi x}{2l} \tag{9.1.29}$$

$$\phi'' = \left(\frac{\pi}{2l}\right)^2\cos\frac{\pi x}{2l} \tag{9.1.30}$$

In addition to satisfying clamped kinematic condition at $x = 0$, the cosine shape gives the zero bending moment at the top. Substituting Equations 9.1.28 - 9.1.30 into the Trefftz condition, Equation (10.18), the following closed-form solution is obtained

$$q = \frac{EI}{l^3}\frac{\pi^4}{2(\pi^2-4)} = 8.29\frac{EI}{l^3} \tag{9.1.31}$$

which differs by only 6% from the exact solution. The true shape of the column which buckles by its own weight is the Bessel function but the trigonometric function provides a very good approximation.

For over 200 years the Euler solution of buckling of a column under its own weight remains unchallenged. In 1960 Keller and Niordson asked the question by how much can the height of the column be increased. If the same volume of material is distributed as a constant cross-section prismatic structure of the radius $r = 0.1$ m, the length of the column would be

$$l = \frac{V}{\pi r^2} = \frac{1}{\pi 0.1^2} = 32m$$

and the weight per unit length of a still column will be

$$q = \frac{V}{l} = \frac{7.8 \times 10^4}{32} = 24N/m$$

Using Equation 9.1.12 we can check if such a column will stay or buckle under its own weight

$$l_c^2 = 7.84\frac{EI}{N}$$

where $I = \frac{\pi r^4}{4}$, $N = V\rho$ and $E = 2.1 \times 10^{11} N/m^2$. Substituting the above values, the critical length becomes $l_c = 26$ m. This means that the 32 m prismatic column will buckle and cannot be erected. By shaping the column according to Figure (9.1.2) its length can be increase by a factor of $86/26 = 3.3$.

If the cross-section is variable, this question has led to a very complex mathematical problem. Some aspects of this solution are still studied up to now. The problem is well-posed if the optimal solution is sought under a constant, given volume of the material. There is no simple closed-form solution to the problem so the answer is obtained through numerical optimization, see Figure (9.1.2).

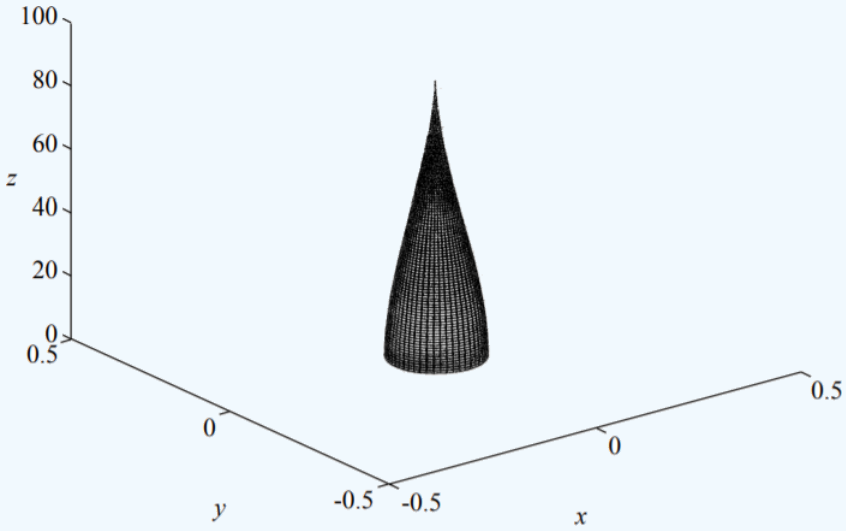

Figure 9.1.2: The shape of the tallest column.

Note that the height of the column was scaled down to fit on the page. To give you an idea, the steel column of the total volume of 1.0 m^3 and the bare radius of 10 cm could be as high as $l = 86$ m.

9.2: Deflection Behavior for Beam with Compressive Axial Loads and Transverse Loads

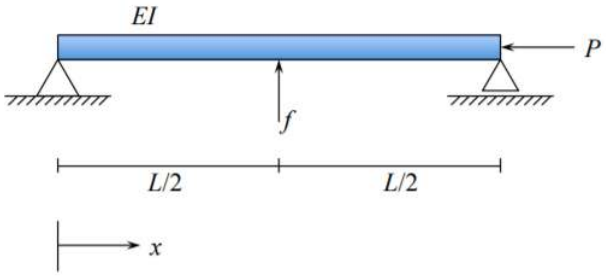

Figure **9.2.1**: Simply supported beam with intermediate transverse load.

Consider a simply supported beam with a fixed load f applied at the middle as shown in Figure (**9.2.1**). Additionally, the beam is subjected to a compressive axial load P. The total potential energy for this mechanical system is

$$\prod_{\text{total}} = \int_0^L \frac{1}{2} EI(v'')^2 dx - \int_0^L \frac{1}{2}(v')^2 dx - fv\left(\frac{L}{2}\right) \tag{9.2.1}$$

If $f = 0$, we are looking at a classical buckling problem; viz., the beam remains straight until a critical load is reached after which the beam bends suddenly. The critical load for the configuration shown is $P_{cr} = \pi^2 EI/L^2$. Let's investigate the behavior for $f \neq 0$.

The stationary points of the potential energy still give the solutions $v(x)$ which satisfy equilibrium. Let's compute an approximate solution using the form

$$v(x) \approx C \sin\left(\pi \frac{x}{L}\right) \tag{9.2.2}$$

The derivatives of this function are

$$v'(x) = C\frac{\pi}{L}\cos\left(\pi\frac{x}{L}\right)$$

$$v''(x) = -C\left(\frac{\pi}{L}\right)^2 \sin\left(\pi\frac{x}{L}\right)$$

Inserting these into the potential energy yields

$$\begin{aligned}
\prod_{\text{total}} &= \int_0^L \frac{1}{2} EI\left(\frac{\pi}{L}\right)^4 C^2 \sin^2\left(\pi\frac{x}{L}\right) dx \\
&- P\int_0^L \frac{1}{2}\left(\frac{\pi}{L}\right)^2 C^2 \cos^2\left(\pi\frac{x}{L}\right) dx - fC\sin\left(\pi\frac{L/2}{L}\right) \\
&= \int_0^L \frac{1}{2} EI\left(\frac{\pi}{L}\right)^4 C^2 \left[\frac{1}{2} - \frac{1}{2}\cos\left(\frac{2\pi x}{L}\right)\right] dx \\
&- P\int_0^L \frac{1}{2}\left(\frac{\pi}{L}\right)^2 C^2 \left[\frac{1}{2} + \frac{1}{2}\cos\left(\frac{2\pi x}{L}\right)\right] dx - fC \\
&= \frac{1}{4} EI\left(\frac{\pi}{L}\right)^4 C^2 L - P\frac{1}{4}\left(\frac{\pi}{L}\right)^2 C^2 L - fC
\end{aligned}$$

The stationary condition yields

$$\begin{aligned}
0 = \frac{d\prod_{\text{total}}}{dC} &= \frac{1}{2} EI\left(\frac{\pi}{L}\right)^4 CL - P\frac{1}{2}\left(\frac{\pi}{L}\right)^2 CL - f \\
&= C\left[\frac{1}{2} EI\left(\frac{\pi}{L}\right)^4 L - P\frac{1}{2}\left(\frac{\pi}{L}\right)^2 L\right] - f = 0
\end{aligned} \tag{9.2.3}$$

and thus

$$C = \frac{f}{\frac{EI\pi^4}{2L^3} - P\frac{\pi^2}{2L}} = \frac{f2L/\pi^2}{\frac{EI\pi^2}{L^2} - P} = \frac{2L}{\pi^2}\frac{f}{P_{cr} - P} \tag{9.2.4}$$

The approximate solution has the form

$$v(x) \approx \frac{2L}{\pi^2}\frac{f}{P_{cr} - P}\sin\left(\pi\frac{x}{L}\right) \tag{9.2.5}$$

The central deflection $w_o = v(x = \frac{l}{2})$ is

$$w_o = \frac{fl^3}{48.7EI}\frac{1}{1 - \frac{P}{P_c}} \tag{9.2.6}$$

For zero axial load, Equation 9.2.6 predicts a linear relation between the lateral point load and deflection w_o. The approximate coefficient $\frac{\pi^4}{2} \cong 48.7$ is very close to the exact value 48 for the pin-pin column loaded by the point force f. The linear relation holds also for any constant value of P/P_c. A much more interesting picture is obtained by fixing the lateral load and changing the axial load. Equation 9.2.6 can be written as

$$w_o = \frac{\eta}{1 - \frac{P}{P_c}}, \text{ where } \eta = \frac{fl^3}{48.7EI} \tag{9.2.7}$$

which is plotted in Figure (9.3.1). Note that the positive force is in compression while the negative in tension. Application of the lateral force deflects the beam by the amount η. Then, on application of the in-plane compressive load, the beam-column behaves as an imperfect column. By reversing the sign of the in-plane load from compression into tension, the central deflection becomes smaller and vanishes with $P/P_c \to \infty$. This is fully consistent with our everyday experience that by tightening the rope/cable, its deflection is reduced.

9.3: Snap-through of a Two Bar System

This is a very interesting problem, because it summaries and even extends our knowledge.

There are three hinges so that each rod is a pin-pin column. The rods are elastic characterized by the bending rigidity EI, axial rigidity EA. The initial stress-free configuration is defined by the height $\bar{w}_o$, which was previously called the amplitude of initial imperfection.

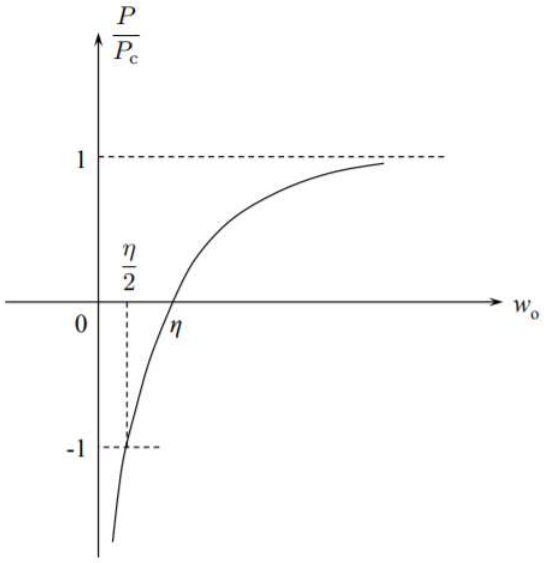

Figure **9.3.1**: Relationship between the axial load and lateral deflections.

Here, $\bar{w}_o$ should be regarded as the initial shape of the structure. Upon application of the load, a compressive axial force develops in the rod, their length shortens allowing for a straight (flat) configuration. The system snaps into a new configuration where tensile force develops in the rods. Depending on the slenderness ratio, they may buckle sometime during the loading process.

Pre-buckling solution

Due to the unmovable hinges, the in-plane components of the displacement is zero, $u = 0$. The strain in the bars develops by the presence of finite rotations

$$\epsilon = \frac{1}{2}(w')^2 - \frac{1}{2}(\bar{w}')^2 \tag{9.3.1}$$

In the pre buckling configuration the rods are straight, so

$$w' = \frac{w_o}{l}, \quad \bar{w}' = \frac{\bar{w}_o}{l} \tag{9.3.2}$$

and Equation 9.3.1 reduces to

$$\epsilon = \frac{1}{2}\left(\frac{w_o}{l}\right)^2 - \frac{1}{2}\left(\frac{\bar{w}_o}{l}\right)^2 \tag{9.3.3}$$

The plot of the dimensionless strain versus the ratio $w_o/\bar{w}_o$ is shown in Figure (**9.3.3**). From the elasticity law, the axial force in the rod is

$$N = EA\epsilon = \frac{EA}{2}\left[\left(\frac{w_o}{l}\right)^2 - \left(\frac{\bar{w}_o}{l}\right)^2\right] = \begin{cases}\text{compressive for } -w_0 \leqslant w_o \leqslant \bar{w}_o \\ \text{tensile for } w_o < -\bar{w}_o\end{cases} \tag{9.3.4}$$

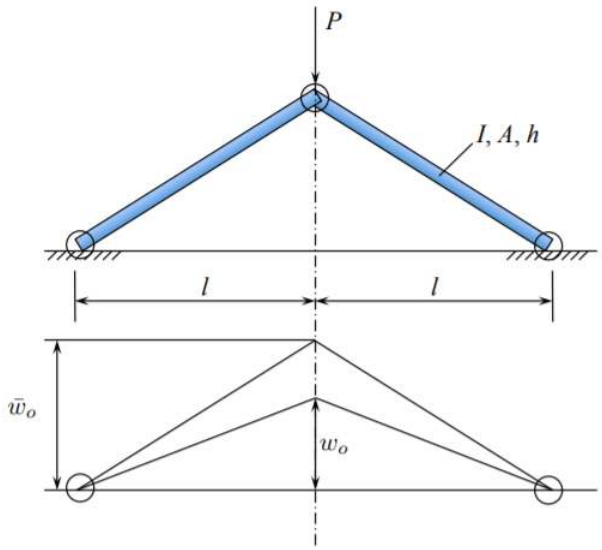

Figure **9.3.2**: Initial and current shape of the two bar system.

Equilibrium between the external load P and the membrane force N requires that

$$P = -2N\frac{w_o}{l} \tag{9.3.5}$$

Eliminating the force N between Equations 9.3.4 and 9.3.5 yields

$$-\frac{P}{2}\frac{l}{w_o} = EA\left[\frac{1}{2}\left(\frac{w_o}{l}\right)^2 - \frac{1}{2}\left(\frac{\bar{w}_o}{l}\right)^2\right] \tag{9.3.6}$$

or in a dimensionless form

$$\bar{P} = \delta(\bar{\delta}^2 - \delta^2) \tag{9.3.7}$$

where

$$\bar{P} = \frac{P}{EA}, \quad \delta = \frac{w_o}{l}, \quad \bar{\delta} = \frac{\bar{w}_o}{l} \tag{9.3.8}$$

The equilibrium path given by Equation 9.3.7 is the third order parabola with three roots at $\delta = 0, \delta = \pm\bar{\delta}$, see Figure (**9.3.4**).

The loading process starts at A and the portion of the trajectory AB is stable. The point B is the instability point. In the process is force controlled, there is a jump to the next equilibrium configuration which is point E. So the system “snaps” into a tensile configuration and this transition is in reality a dynamic problem. The process can be displacement control and then the force $\bar{P}$ is the reaction force which is positive on the segments ABC and EF but negative on the segment CDE of the trajectory. This means that an opposite force $\bar{P}$ is required on CDE to keep the system in static equilibrium. By contrast, in the force controlled process the inertia force is equilibrating the system at any time. The maximum force occurs when

$$\frac{dP}{d\delta} = \bar{\delta}^2 - 3\delta^2 = 0 \tag{9.3.9}$$

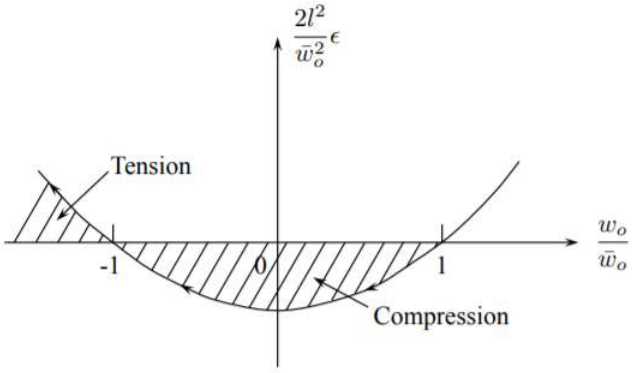

Figure **9.3.3**: Transition from compressive into tensile strain.

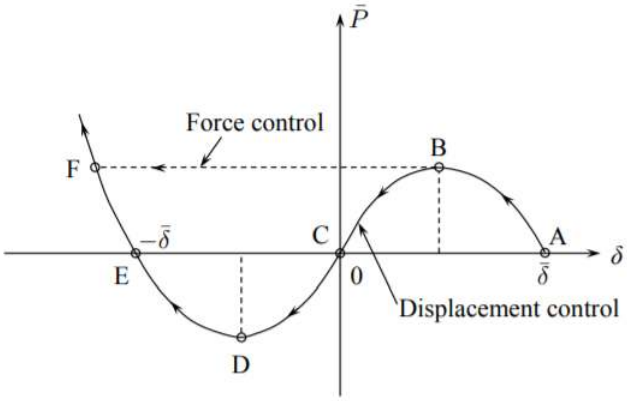

Figure **9.3.4**: Equilibrium path in the snap-through problem.

The maximum occurs at $\delta = \bar{\delta}/\sqrt{3}$ and the maximum force is $\bar{P}_{\max} = \frac{2}{3\sqrt{3}}\bar{\delta}^3$.

Any time during the loading phase AB there is a possibility for the rods to buckle. The instant of buckling is detected by equating the axial force from Equation (10.37) to the critical buckling force of the pin-pin column

$$N = \frac{P_{cr}}{2}\frac{l}{w_o} = \frac{\pi^2 EI}{l^2} \tag{9.3.10}$$

The dimensionless version of this equation is

$$\bar{P}_{cr} = \frac{P_{cr}}{EA} = 2\pi^2\frac{\delta}{\beta^2} \tag{9.3.11}$$

where $\beta = \frac{l}{r}$ is the slenderness ratio, and $r^2 = \frac{I}{A}$ is the radius of gyration of the crosssection. In the coordinate system $(\bar{P}, \delta)$, the buckling point is determined by the intersection of the straight line, Equation 9.3.10, and the third order parabola

$$\frac{2\pi^2}{\beta^2}\delta = \delta(\bar{\delta}^2 - \delta_c^2) \tag{9.3.12}$$

The displacement to buckle is

$$\delta_c = \sqrt{\bar{\delta}^2 - \frac{2\pi^2}{\beta^2}} \tag{9.3.13}$$

and the corresponding buckling force $\bar{P}_c$ is

$$\bar{P}_c = \frac{2\pi^2}{\beta^2}\sqrt{\bar{\delta}^2 - \frac{2\pi^2}{\beta^2}} \tag{9.3.14}$$

The graphical interpretation of the above analysis is shown in Figure (**9.3.5**).

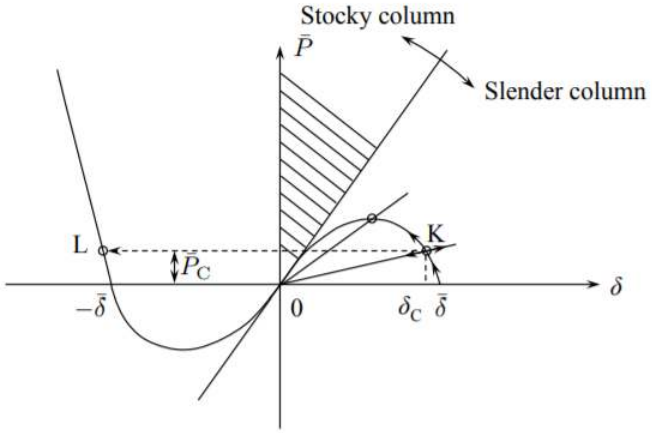

Figure **9.3.5**: Non-linear pre-buckling path intersects with a linear post-buckling path.

There is a family of straight lines with the slenderness ratio as a parameter. The critical slenderness ratio for which buckling will never occur is

$$\beta_{cr}^2 = \frac{2\pi}{\bar{\delta}} \tag{9.3.15}$$

This situation corresponds to the straight line tangent to the third order parabola. Of practical interest is the situation in which the bifurcation point occurs before the maximum force is reached at $\delta_{\max} = \bar{\delta}/\sqrt{3}$ and $\bar{P}_{\max} = \frac{2}{3\sqrt{3}}\bar{\delta}^3$. The corresponding minimum slenderness ratio, calculated from Equation 9.3.10 is

$$\beta_{\min}^2 = \frac{\sqrt{3}\pi}{\bar{\delta}} \tag{9.3.16}$$

To sum up, there are three ranges of the slenderness ratio:

Table **9.3.1**: Ranges of buckling response

	$\beta_{\min} < \beta < \infty$	$\beta = \beta_{\min}$	$\beta = \beta_{\min}$
$\bar{P}_{\max}$		$\frac{2}{3\sqrt{3}}\bar{\delta}^3$	No buckling static or dynamic equilibrium path
$\delta_{\max}$		$\frac{\bar{\delta}}{\sqrt{3}}$	No buckling static or dynamic equilibrium path

For the square cross-section $h \times h$, the critical combination of the geometrical parameters

$$\frac{\bar{w}_o}{h} = 36\pi\frac{h}{l} \tag{9.3.17}$$

From the above solution, we conclude that snap-through of the bar system without buckling will occur only for very shallow systems.

9.4: Dynamic Snap-Through

The present lecture notes are restricted to static and quasi-static problems. However, the nature of the snap-through problem calls for the consideration of the full dynamic analysis. Assume that the loading of the two-bar system is load controlled. There is a stable equilibrium path on the portion AB. When $\bar{P}_{\max} = \frac{2}{3\sqrt{3}}\bar{\delta}^3$ is reached, the system jumps instantaneously to the next equilibrium point F in the static solution. The magnitude of the force is the same, but the corresponding displacement is determined from the solution of the cubic equation

$$\frac{2}{3\sqrt{3}}\bar{\delta}^3 = \delta\bar{\delta}^2 - \delta^3 \tag{9.4.1}$$

This equation has three real roots

$$\delta_1 = \frac{\bar{\delta}}{\sqrt{3}}, \delta_2 = \delta_3 = -\frac{2\bar{\delta}}{\sqrt{3}} \tag{9.4.2}$$

By adding inertia forces into the equation of equilibrium, the snap-through process occurs in time. The bar system is first accelerated on the portion BCD of the descending force and then decelerated on the rising portion DEF.

The dynamic solution is straight forward if the distributed mass of the rod is lumped into two discrete point masses $m = lA\rho$, as shown in Figure (9.4.1).

By adding d'Alambert inertia forces into static equilibrium, Equation (9.3.5), one gets

$$-P - 2m\frac{\ddot{w}_o}{2} = 2N\frac{w_o}{l} \tag{9.4.3}$$

where now P is positive in tension.

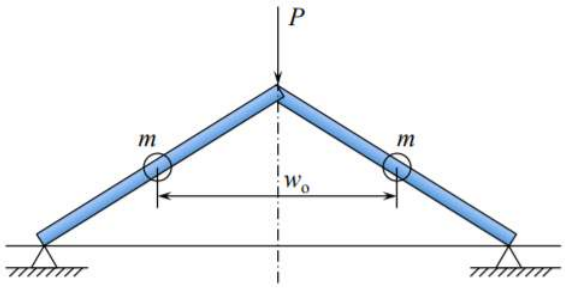

Figure 9.4.1: The equivalent two massless bars and two lumped masses.

Eliminating the axial force N in the bars between Equations (9.3.4) and 9.4.3, one gets the following differential equation

$$-\bar{P} - \frac{l^2\rho}{E}\ddot{\delta} = \delta[\delta^2 - \bar{\delta}^2] \tag{9.4.4}$$

where the dot denotes differentiation with respect to time. It is convenient to introduce the dimensionless time $\bar{t} = \frac{t}{t_1}$, where $t_1 = \frac{l}{c}$ is the reference time, and $c^2 = \frac{E}{\rho}$ is the speed of the longitudinal stress wave in a bar. In the force controlled system, the exciting term is constant $\bar{P} = \frac{2}{3\sqrt{3}}\bar{\delta}^3$. In the new dimensionless coordinate, Equation 9.4.4 takes the form

$$-\bar{P} - \ddot{\delta} = \delta^3 - \bar{\delta}^2\delta \tag{9.4.5}$$

where the dot denotes differentiation with respect to the dimensionless time $\bar{t}$. Using the chain rule of differentiation,

$$\ddot{\delta} = \frac{d\dot{\delta}}{d\bar{t}} = \frac{d\dot{\delta}}{d\delta}\frac{d\delta}{d\bar{t}} = \frac{d\dot{\delta}}{d\delta}\dot{\delta} \tag{9.4.6}$$

one can get a solution on the phase plane $(\delta, \dot{\delta})$ rather tan in the time domain. Substituting Equation 9.4.6 into Equation 9.4.5, the following equation is obtained

$$-\bar{P}d\delta - \dot{\delta}d\dot{\delta} = (\delta^3 - \bar{\delta}^2\delta)d\delta \tag{9.4.7}$$

which can be readily integrated to give

$$-\bar{P}\delta - \frac{1}{2}\dot{\delta}^2 = \frac{\delta^4}{4} - \frac{\bar{\delta}^2\delta^2}{2} + C \tag{9.4.8}$$

The integration constant C is determined from the initial condition that the velocity $\dot{\delta}$ is zero when the deflection reaches $\delta = \frac{1}{\sqrt{3}}$ (point B). The solution for the velocity $\dot{\delta}$ is

$$\dot{\delta} = 2\bar{\delta}^2\sqrt{-P\left(\frac{\delta}{\bar{\delta}}\right) + \frac{1}{2}\left(\frac{\delta}{\bar{\delta}}\right)^2 - \frac{1}{4}\left(\frac{\delta}{\bar{\delta}}\right)^4 + \frac{1}{12}} \tag{9.4.9}$$

In terms of the normalized velocity $\frac{\dot{\delta}}{2\bar{\delta}^2} = \bar{v}$ and the normalized deflection $\eta = \frac{\delta}{\bar{\delta}}$, Equation 9.4.9 reads

$$\bar{v} = \sqrt{-\frac{2}{3\sqrt{3}}\eta + \frac{1}{2}\eta^2 - \frac{1}{4}\eta^4 + \frac{1}{12}} \tag{9.4.10}$$

The plot of $\bar{v}$ versus η is shown in Figure (9.4.2).

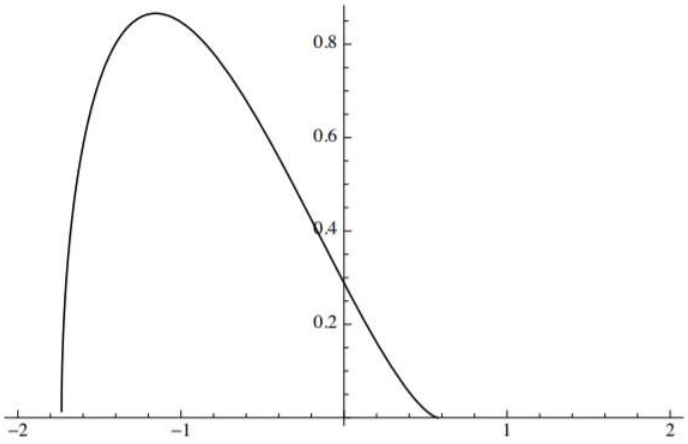

Figure 9.4.2: The plot of $\bar{v}$ versus η in dynamic snap through.

The polynomial in η under the square root in Equation 9.4.10 has two real roots, at $\eta = \frac{1}{\sqrt{3}}$ and $\eta = -\sqrt{3}$. The dynamic motion starts at B, increases slowly, reaches a maximum in F and falls rapidly to zero at the point G with the coordinate $\eta_f = \sqrt{3}$. Note that the dynamic deflection overshoots considerably the deflection reached in the static problem $\eta_{stat} = \frac{2}{\sqrt{3}} = 1.15$.

At the final stage when the motion of the system stops, there is enough tensile energy stored in the bar to initial free vibration with the forcing term $\bar{P}$ removed. The solution to this phase is given by Equation 9.4.8 with $\bar{P} = 0$, and the new integration constant $C_1 = \frac{3}{4}$ so that continuity of velocity is achieved. The plot of the free vibration of the system, governed by

$$\bar{v} = \sqrt{\frac{1}{2}\eta^2 - \frac{1}{4}\eta^4 + \frac{3}{4}} \tag{9.4.11}$$

is shown in Figure (9.4.3), in comparison with the dynamic snap-through plot.

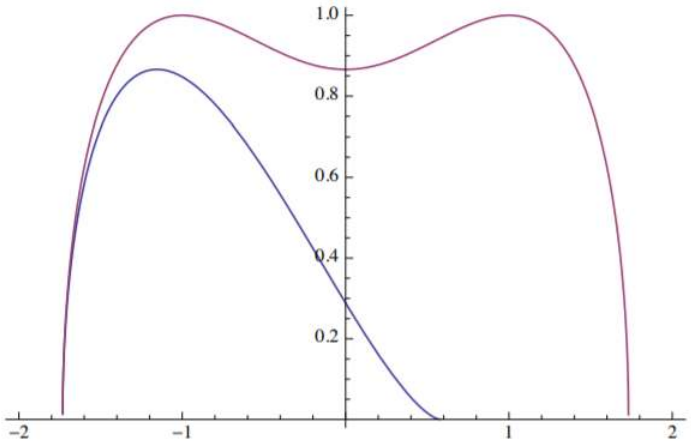

Figure **9.4.3**: The plot of $\bar{v}$ versus η in free vibration, in comparison with the dynamic-through plot.

CHAPTER OVERVIEW

10: Buckling of Plates and Sections

Most of steel or aluminum structures are made of tubes or welded plates. Airplanes, ships and cars are assembled from metal plates pined by welling riveting or spot welding. Plated structures may fail by yielding fracture or buckling. This chapter deals with a brief introduction to the analysis of plate buckling. A more complete treatment of this subject is presented in the 2.081 course of Plates and Shells, which is available on the Open Course. For additional reading, the following monographs are recommended:

1. Stephen P. Timoshenko and James M. Gere, Theory of Elastic Stability.
2. Don. O. Brush and Bo. O. Almroth, Buckling of Bars, Plates and Shells.

10.1: Governing Equations and Boundary Conditions

In the present notes the column buckling was extensively studied in Chapter 8. The governing equation for a geometrically perfect column is

$$EIw^{\mathrm{IV}} + Nw'' = 0 \tag{10.1.1}$$

A step-by-step derivation of the plate buckling equation was presented in Chapter 6

$$D\nabla^4 w + \bar{N}_{\alpha\beta} w_{,\alpha\beta} = 0 \tag{10.1.2}$$

where $N_{\alpha\beta}$ is a set of constant, known parameters that must satisfy the governing equation of the pre-buckling state, given by Equations (6.1.10-6.1.12). The classical buckling analysis of plates is best explained on an example of a rectangular plate subjected to compressive loading in one direction, Figure (10.1.1).

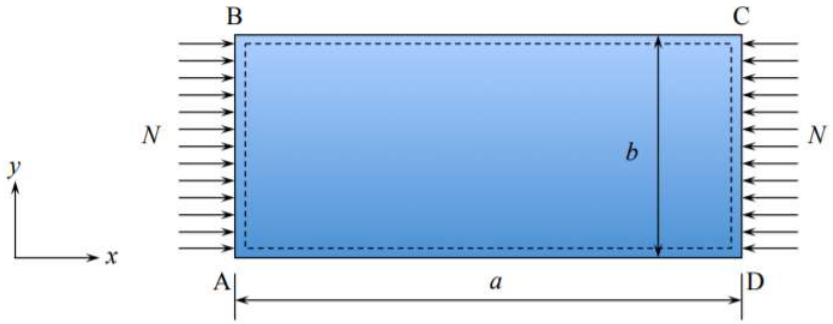

Figure 10.1.1: Geometry and loading of the classical plate buckling problem.

The plate is simply supported along all four edges. The edges AB and CD are called the loaded edges because in-plane loading $N\left[\frac{N}{M}\right]$ is applied to these edges. The other two edges AD and BC are called the unloaded edges. The simply supported boundary conditions apply to vanishing of transverse deflections and the normal bending moments

$$w = 0 \quad \text{on ABCD} \tag{10.1.3}$$

$$M_n = 0 \quad \text{on ABCD} \tag{10.1.4}$$

Separate boundary condition must be formulated in the in-plane direction in the normal and tangential direction

$$(N_n - \bar{N}_n)\delta u_n = 0 \tag{10.1.5}$$

$$(N_t - \bar{N}_t)\delta u_t = 0 \tag{10.1.6}$$

In the case of the present rectangular plate Equations 10.1.3 - 10.1.4 reduce to

$$\left.\begin{aligned} \left(N_{xx} - \bar{N}_{xx}\right)\delta u_x = 0 \\ \left(N_{xy} - \bar{N}_{xy}\right)\delta u_y = 0 \end{aligned}\right\} \text{ on AB and CD}$$
$$\left.\begin{aligned} \left(N_{yy} - \bar{N}_{yy}\right)\delta u_y = 0 \\ \left(N_{xy} - \bar{N}_{xy}\right)\delta u_x = 0 \end{aligned}\right\} \text{ on AD and BC} \tag{10.1.7}$$

In the present problem the stress boundary conditions are applied and the tensor of external loading is

$$\bar{N}_{\alpha\beta} = \begin{vmatrix} \bar{N} & 0 \\ 0 & 0 \end{vmatrix}, \quad N_{\alpha\beta} = \begin{vmatrix} N & 0 \\ 0 & 0 \end{vmatrix} \tag{10.1.8}$$

With the above field of membrane forces the equilibrium equations are satisfied identically. From the constitutive equations

$$N_{xx} = C(\epsilon^{\circ}_{xx} + \nu\epsilon^{\circ}_{yy}) \tag{10.1.9}$$

$$0 = C(\epsilon^{\circ}_{yy} + \nu\epsilon^{\circ}_{xx}) \tag{10.1.10}$$

Therefore $\epsilon^{\circ}_{yy} = -\nu\epsilon^{\circ}_{xx}$ and so $N_{xx} = Eh\epsilon^{\circ}_{xx}$. The displacement is calculated by solving two equations

$$\epsilon^{\circ}_{xx} = \frac{du_x}{dx} \tag{10.1.11}$$

$$\epsilon^{\circ}_{yy} = \frac{du_y}{dy} \tag{10.1.12}$$

With the origin of the coordinate system placed at the point A in Figure (10.1.1), The solution is

$$u_x = u_o\left(1 - \frac{x}{a}\right), \quad u_y = \nu u_o \frac{y}{a}, \quad N = \frac{Eh}{a}u_o \tag{10.1.13}$$

Note that $\tilde{N}$ has been defined as positive in compression. Therefore the plate will be compressed in the x-direction and will expand laterally in the y-direction because of the effect of the Poison ratio. In setting up the experiment or developing the FE model, the plate should be left free in the in-plane direction.

10.2: Buckling of a Simply Supported Plate

The expanded form of the governing equation corresponding to the assumed type of loading is

$$D\left[\frac{\partial^4 w}{\partial x^4}+2\frac{\partial^4 w}{\partial x^2 \partial y^2}+\frac{\partial^4}{\partial y^4}\right]+\bar{N}\frac{d^2 w}{dx^2}=0 \tag{10.2.1}$$

The solution of the above linear partial differential equation with constant coefficient is sought as a product of two harmonic functions

$$w(x,y)=\sin\frac{m\pi x}{a}\sin\frac{n\pi y}{b} \tag{10.2.2}$$

where m and n are number of half waves in the longitudinal and transverse directions, respectively. The function $w(x,y)$ satisfies the boundary condition for displacement. The bending moment M_n

$$M_n=M_{xx}=D[\kappa_{xx}+\nu\kappa_{yy}]=-D\left[\left(\frac{m\pi}{a}\right)^2+\nu\left(\frac{n\pi}{b}\right)^2\right]\sin\frac{m\pi x}{a}\sin\frac{n\pi y}{b} \tag{10.2.3}$$

vanishes at $x=0$ and $x=a$ edges. Also at $y=0$ and $y=b$, $M_n=M_{yy}$ is zero. Therefore the proposed function satisfy the simply supported boundary condition at all four edges. Substituting the function $w(x,y)$ into the governing equation, one gets

$$\left\{D\left[\left(\frac{m\pi}{a}\right)^4+2\left(\frac{m\pi}{a}\right)^2\left(\frac{n\pi}{b}\right)^2+\left(\frac{n\pi}{b}\right)^4\right]-\bar{N}\left(\frac{m\pi}{a}\right)^2\right\}\sin\frac{m\pi x}{a}\sin\frac{n\pi y}{b}=0 \tag{10.2.4}$$

The differential equation is satisfied for all values of (x,y) if the coefficients satisfy

$$\bar{N}=D\left(\frac{\pi a}{m}\right)^2\left[\left(\frac{m}{a}\right)^2+\left(\frac{n}{b}\right)^2\right]^2 \tag{10.2.5}$$

It is seen that the smallest value of $\bar{N}$ for all values of a, b and m is obtained if $n=1$. This means that only one half wave will be formed in the direction perpendicular to the load application. Then, Equation 10.2.3 can be put into a simple form

$$\bar{N}_c=k_c\frac{\pi^2 D}{b^2} \tag{10.2.6}$$

where the buckling coefficient k_c is a function of both the plate aspect ratio a/b and the wavelength parameter

$$k_c=\left(\frac{mb}{a}+\frac{a}{mb}\right)^2 \tag{10.2.7}$$

The parameter m is an integer and determines how many half waves will fit into the length of the plate. The aspect ratio a/b is known, but the wavelength parameter is still unknown. Its value must be found by inspection, i.e., by plotting the buckling coefficient as a function of a/b for subsequent values of the parameter m. This is shown in Figure (10.2.1).

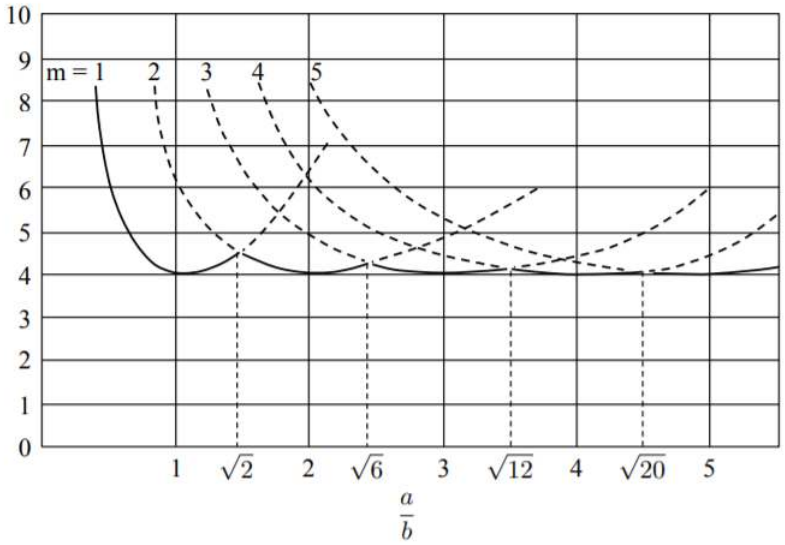

Figure **10.2.1**: Plot of the buckling coefficient for a simply supported plate as a function of the plate aspect ratio a/b and different wave numbers.

For example, the buckling coefficient corresponding to the first five buckling modes corresponding to $\frac{a}{b} = 2$ are

Table **10.2.1**

m	1	2	3	4	5
k_c	6.2	4	4.7	6.2	8.4

The lowest buckling load $k_c = 4$ occurs when there are two half waves along the length of the plate, $m = 2$. The line separating the safe, shaded area in Figure (**10.2.2**) and the unsafe while area defines uniquely the buckling coefficient for all combination of a/b and m.

Consider now a long plate, $a \gg b$ for which the parameter m can be treated as a continuous variable. In this case there is an analytical minimum of the buckling coefficient

$$\frac{dk_c}{dm} = 0 \quad \rightarrow \quad a = mb \tag{10.2.8}$$

The above result means that the plate divides itself into an integer number of squares with alternating convex and concave dimples.

What happens when the rectangular plate shown in Figure (10.1.1) is restricted from lateral expansion

$$u_y(y = 0) = u_y(y = b) = 0 \tag{10.2.9}$$

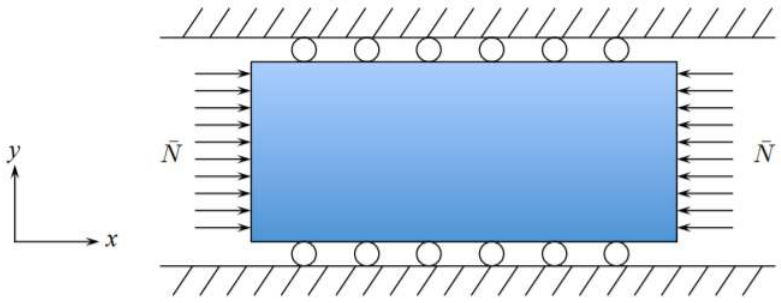

Figure **10.2.2**: Constrained compression of the plate.

With no strain in the y-direction, $\epsilon_{yy} = 0$, the constitutive equations (11.6) reduces to

$$N_{xx} = C\epsilon^{\circ}_{xx} \tag{10.2.10}$$

$$N_{yy} = C\nu\epsilon^{\circ}_{xx} \tag{10.2.11}$$

This means that a reaction force $N_{yy} = \nu N_{xx}$ develops in the transverse direction. The buckled shape of the plate is the same and the solution, Equation (**??**) still holds but the new expression for the buckling coefficient is

$$k_c = \frac{\left[\left(\frac{mb}{a}\right)^2 + n^2\right]^2}{\left(\frac{mb}{a}\right)^2 + \nu n^2} \tag{10.2.12}$$

The least value of the buckling coefficient can be found by inspection. Taking again as an example $a/b = 2$, the values of the buckling coefficient corresponding to the nine first buckling modes are

Table **10.2.2**

$n \setminus m$	1	2	3
1	10/7	3	4.09
2	3.8	10.7	10.9
3	26	25	24.1

The lowest value of the buckling coefficient $k_c = 3$ corresponds to two half-waves in the loading direction and one half wave in the transverse direction. It is seen that restricting the in-plane deformation does not change the buckling mode but reduces the buckling load by a factor of $3/4$. The reaction compressive force makes the plate to buckle more easily. This example underscores the importance of properly defining the boundary conditions not only in the out-of-plane direction but also in the in-plane directions.

10.3: Effect of Boundary Conditions

The unloaded edges of rectangular plates can be either simply supported (ss), clamped (c) or free. (The sliding boundary conditions will convert the eigenvalue problem into the equilibrium problem and therefore are not considered in the buckling analysis of plates). The loaded edges could be either simply supported or clamped. This gives rise to ten different combination. The buckling coefficient is plotted against the plate aspect ratio a/b for all these combinations in Figure (10.4.1). It is seen that the lowest buckling coefficient with $m = 1$ corresponds to a simply supported plate on three edges and free on the fourth edge.

An approximate analytical solution for the case "E" was derived by Timoshenko and Gere in the form

$$k_c = 0.456 + \left(\frac{b}{a}\right)^2 \tag{10.3.1}$$

For example $k_c = 0.706$ for $a/b = 2$, which is very close to the value that could be read off from Figure (10.4.1). An angle element, shown in Figure (10.4.2) is composed of two plates that are simply supported along the common edge and free on the either edges. Both plates rotate by the same amount at the common edges so that no edge restraining moment is developed. This corresponds to a simply supported boundary conditions.

In a similar way it can be proved that the prismatic square column consists of four simply supported long rectangular plates. Upon compression, the buckling pattern has a form shown in Figure (10.4.3). Again, there are no relative rotations at the intersection line of any of the neighboring plates ensuring the simply supported boundary condition along four edges.

Another very practical case is shear loading. For example "I" beams with a relatively high web or girders may fail by shear buckling, Figure (10.4.4), in the compressive side when subjected to bending.

The solution to the shear buckling is much more complicated than in the previous cases of compressive buckling. The general form of the solution is still given by Equation (**??**) but there is no simple closed form solution for the buckling coefficient. An approximate solution for k_c, derived by Timoshenko and Gere has the form

$$k_c = 5.35 + 4\left(\frac{b}{a}\right)^2 \tag{10.3.2}$$

For a square plate the buckling coefficient is 9.35 while for an infinitely long plate, $a \ll b$ it reduces to 5.35. Loading the plate in the double shear experiment for beyond the elastic buckling load produces a set of regular skewed dimples seen in Figure (10.4.5).

10.4: Buckling of Sections

Cold-form or welded profiles are encountered in almost every aspect of the engineering practice. Typical cross-sectional geometries of prismatic members are shown in Figure (**10.4.6**).

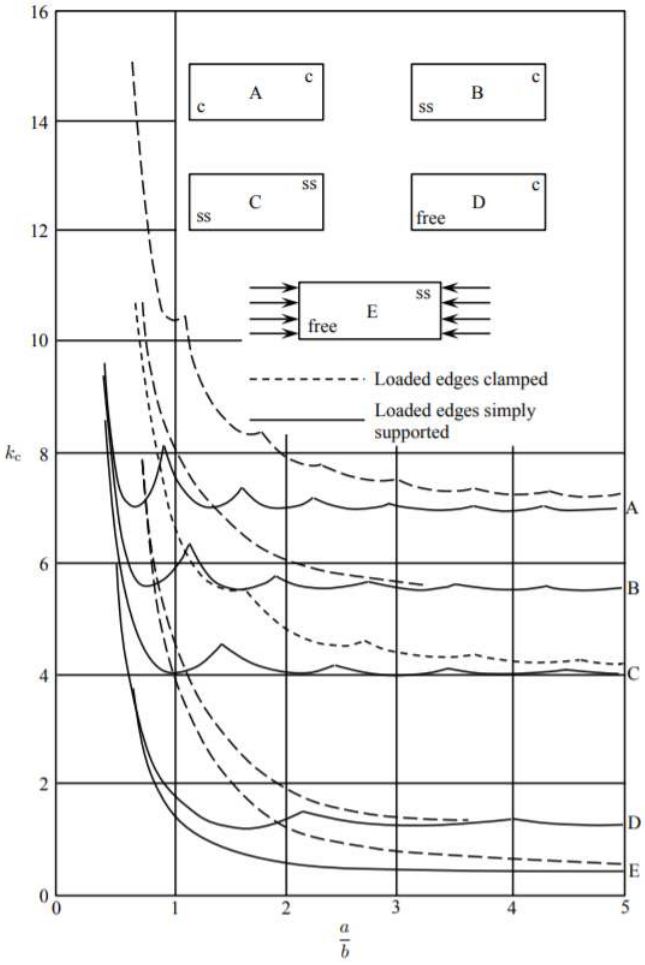

Figure **10.4.1**: Effect of boundary conditions on the buckling coefficient of rectangular plates subjected to in-plane boundary conditions.

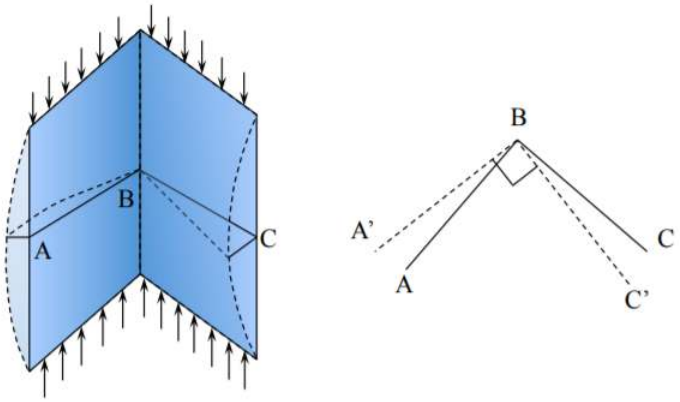

Figure **10.4.2**: Buckling mode of an angle element.

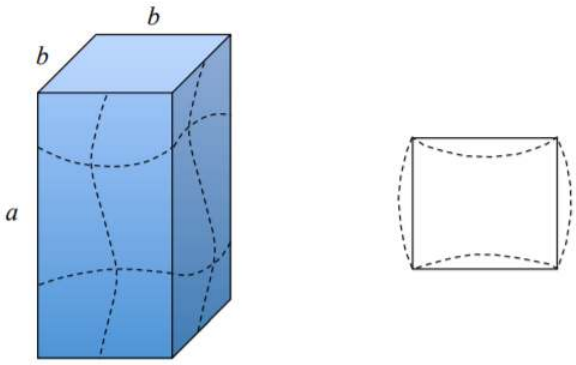

Figure **10.4.3**: The buckling mode of a prismatic square column.

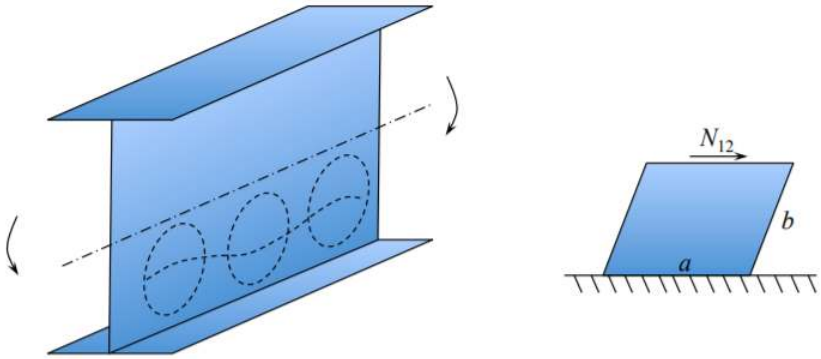

Figure **10.4.4**: Buckling due to shear or bending.

Figure **10.4.5**: A photograph of shear buckling of a plate representing the damage pattern on the ship's hull inflicted upon grounding.

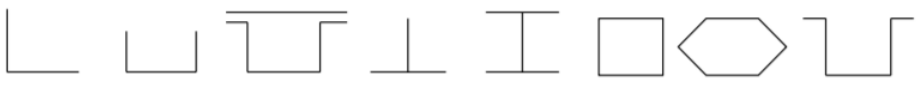

Figure **10.4.6**: Some typical open and closed cross-sectional shape of prismatic members.

Except of symmetric angle, "T", cruciform and square box profile where buckling strength of the entire section is a sum of buckling loads of contributing plates, the analysis of other shape requires consideration of restraining bending moments and

continuity conditions along the common edges. The easiest way to illustrate the problem is to consider a rectangular section prismatic column, Figure (10.4.7). According to Equation (??) the buckling load is inversely proportional to the width of the plate. The two opposite wider plates would like to buckle first, but the shorter sides are not ready to buckle with $k = 4$. They provide clamped boundary condition for the wider flanges for which $k \cong 7$. There must be a transfer of information between the adjacent plates so that they will buckle "in sympathy" to one another with a different k_c.

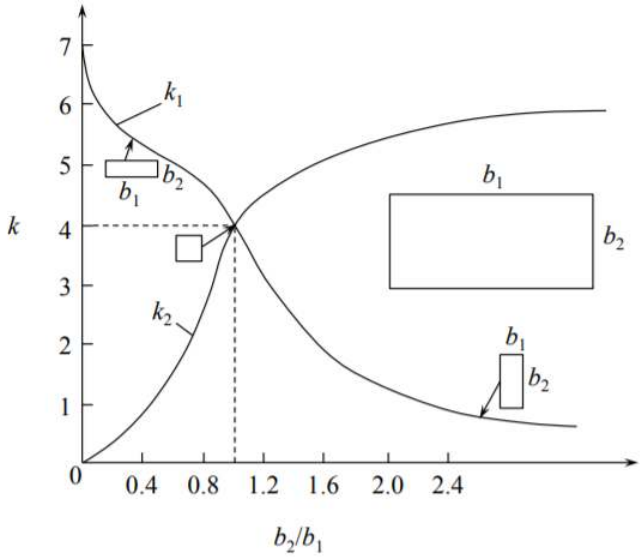

Figure 10.4.7: Buckling coefficients of a rectangular plate as a function of b_2/b_1.

The numerically obtained function $k_1(b_2/b_1)$ is shown in Figure (10.4.7) by a solid line. The buckling coefficient is uniquely related to k_1 through the pre-buckling analysis. Before buckling the strains and compressive stresses in the adjacent plates are the same

$$\sigma_1 = \frac{N_1}{h_1} = \sigma_2 \frac{N_2}{h_2} \tag{10.4.1}$$

where

$$N_1 = k_1 \frac{\pi^2 D_1}{b_1^2}, \quad N_2 = k_2 \frac{\pi^2 D_2}{b_2^2} \tag{10.4.2}$$

From the above equation it follows that

$$k_2 = k_1 \left(\frac{b_2}{b_1}\right)^2 \tag{10.4.3}$$

k_1 is shown in Figure (10.4.7) (solid line). The buckling coefficient k_2 calculated from Equation (??) is shown on the same figure by the dashed line. With the above result one can prove that for a given weight (cross-section area) the square column will have the largest buckling resistance for all rectangular shapes.

For more complex cross-sectional shape the buckling coefficient can be presented in a graphical form, as shown in Figure (10.4.8). Knowing the buckling coefficient k_1 for a flange with the width b_1 and thickness h_1, the buckling coefficients of all other flanges is then calculated from:

$$k_i = k_1 \left(\frac{h_i b_1}{h_1 b_i}\right) \tag{10.4.4}$$

In most cases nothing dramatic happens at the point of buckling. The purely compressive state switches into a combined bending/compression but the plate continues to carry additional load with a reduced stiffness. The post-buckling and ultimate load response is discussed in the next section of this chapter.

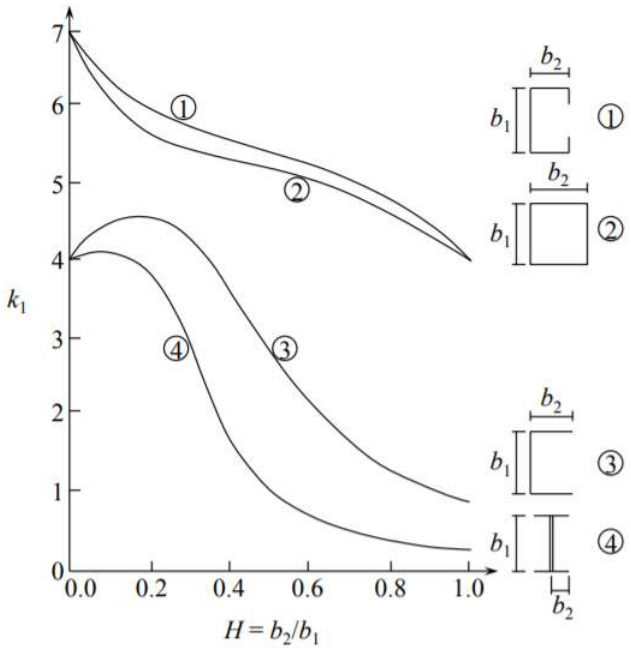

Figure **10.4.8**: Buckling coefficients for four types of sections.

10.5: Post-buckling Response of Plates (Advanced)

Let's assumed that the plate is subjected to a monotonically increasing axial compression u_o, Figure (10.5.1).

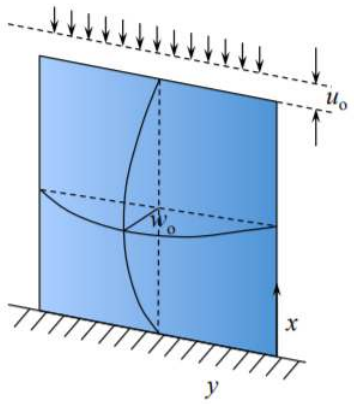

Figure 10.5.1: Two degree-of-freedom model of the buckled plate.

Initially the plate is straight and in the pre-buckling state there is uniaxial compression and bi-axial deformation. This stage was analyzed in Section 6.1. there was no out-of-plane displacement w_o. The bifurcation point was tested by imposing an arbitrary small field of out-of-plane displacement. Now, some of the compression energy is relieved, but the bending energy appears so that the total potential energy of the system remains the same.

The corresponding value of the load (buckling load) under which this happens was derived in Section 6.2. What happens to the plate after buckling has occurred is the subject of the present section. The deformation of the plate is assumed to be a superposition of the in-plane compression. The form of the in-plane displacement is similar as in the prebuckling solution, Equation (??), but now one more term should be added to the expression for u_y in order to satisfy zero traction at the unloaded edges.

$$u_x = u_o\left(1-\frac{x}{a}\right) \tag{10.5.1}$$

$$u_y = \nu u_o\frac{y}{a} + f(x) \tag{10.5.2}$$

The field of out-of-plane deformation is taken identical as in the buckling solution

$$w = w_o \sin\frac{\pi x}{a}\sin\frac{\pi y}{b} \tag{10.5.3}$$

which satisfies the simply supported boundary conditions at all four edges. Here it is assumed that the plate is either infinitely long or is square so that $a = b$.

The total potential energy of the system is

$$\prod = U_b + U_m - PU_o \tag{10.5.4}$$

where $P = bN$ and expression for the bending and membrane energies are given by Equations (3.6.25) and (3.6.41), respectively. The curvature tensor is defined by

$$\kappa_{\alpha\beta} = -w_{,\alpha\beta} \tag{10.5.5}$$

and for the assumed shape $w(x,y)$ has three components

$$\kappa_{\alpha\beta} = w_o\left(\frac{\pi}{a}\right)^2\begin{vmatrix} \sin\frac{\pi x}{a}\sin\frac{\pi y}{a} & -\cos\frac{\pi x}{a}\cos\frac{\pi y}{a} \\ -\cos\frac{\pi x}{a}\sin\frac{\pi y}{a} & \sin\frac{\pi x}{a}\sin\frac{\pi y}{a}\end{vmatrix} \tag{10.5.6}$$

The membrane strain results from the gradient of in-plane displacement vector and the moderately large rotation of plate elements

$$\epsilon_{\alpha\beta} = \frac{1}{2}(u_{\alpha,\beta}+u_{\beta,\alpha}) + \frac{1}{2}w_{,\alpha}w_{,\beta} \tag{10.5.7}$$

The components of the in-plane strain tensors are

$$\left.\begin{aligned}\epsilon_{xx} &= -\tfrac{u_o}{a} + \tfrac{w_o^2}{2}\left(\tfrac{\pi}{a}\right)^2 \cos^2\tfrac{\pi x}{a}\sin^2\tfrac{\pi y}{a} \\ \epsilon_{yy} &= \nu\tfrac{u_o}{a} + f'(x) + \tfrac{w_o^2}{2}\left(\tfrac{\pi}{a}\right)^2 \sin^2\tfrac{\pi x}{a}\cos^2\tfrac{\pi y}{a}\end{aligned}\right\} \tag{10.5.8}$$

$$\epsilon_{xy} = \frac{w_o^2}{2}\left(\frac{\pi}{a}\right)^2 \cos^2\frac{\pi x}{a}\cos^2\frac{\pi y}{a} \tag{10.5.9}$$

It is seen that the form of the axial strain ϵ_{xx} provides coupling between the in-plane amplitude u_o and the out-of-plane amplitude w_o.

The general expression for the bending energy of the plate, Equation (3.6.25) is

$$U_b = \frac{D}{2}\int_0^a \int_0^a \{(\kappa_{xx} + \kappa_{yy})^2 - 2(1-\nu)\kappa_G\}dxdy \tag{10.5.10}$$

where $\kappa_G = \kappa_{xx}\kappa_{yy} - \kappa_{xy}^2$ is the Gaussian curvature. It can be easily shown that the Gaussian curvature integrated over the surface of the plate is zero. Therefore, the second term in the integrand of Equation (10.3.1) vanishes. Finally, the total bending energy of the plate is calculated to be

$$U_b = \frac{1}{2}Dw_o^2\frac{\pi^4}{a^2} \tag{10.5.11}$$

Before proceeding to calculate the membrane strain energy, the unknown function $f(x)$ in Equation (??) should be determined from the boundary condition $N_{yy}(y = a \text{ and } y = 0) = 0$. The plane stress elasticity law is

$$N_{xx} = C(\epsilon_{xx} + \nu\epsilon_{yy}) \tag{10.5.12}$$

$$N_{yy} = C(\epsilon_{yy} + \nu\epsilon_{xx}) \tag{10.5.13}$$

$$N_{xy} = (1-\nu)C\epsilon_{xy} \tag{10.5.14}$$

From Equation (10.2.10-10.2.11), the in-plane membrane force in the y-direction is

$$\begin{aligned}N_{yy} = C\Bigg[&\nu\frac{u_o}{a} + \frac{1}{2}w_o^2\left(\frac{\pi}{a}\right)^2 \sin^2\frac{\pi x}{a}\cos^2\frac{\pi y}{a} + f' \\ &-\nu\frac{u_o}{a} + \frac{\nu}{2}w_o^2\left(\frac{\pi}{a}\right)^2 \cos^2\frac{\pi x}{a}\sin^2\frac{\pi y}{a}\Bigg]\end{aligned} \tag{10.5.15}$$

The membrane force changes from point to point and at the unloaded edges $y = 0$ and $y = a$ is

$$N_{yy}(0,a) = C\left[\frac{1}{2}w_o^2\left(\frac{\pi}{a}\right)^2 \ sin^2\frac{\pi x}{a} + f'\right] \tag{10.5.16}$$

Now, the total membrane energy of the plate can be calculated. After lengthy algebra, the final expression is

$$U_m = \frac{C}{2}\left[(1-\nu^2)u_o^2 - 2(1-\nu^2)\frac{\pi^2}{8}\frac{u_o}{a}w_o^2 + (3-2\nu)\frac{\pi^4}{64}\frac{w_o^4}{a^2}\right] \tag{10.5.17}$$

The total potential energy of the system is

$$\prod(u_o, w_o) = U_b + U_m - Pu_o \tag{10.5.18}$$

The equilibrium of the system requires that the first variation of the total potential energy vanishes $\delta\prod(u_o, w_o) = 0$. This leads to two equations

$$\frac{\partial\prod}{\partial u_o} = 0 \rightarrow P = (1-\nu^2)C\left[u_o - \frac{\pi^2}{8}\frac{w_o^2}{a}\right] \tag{10.5.19}$$

$$\frac{\partial\prod}{\partial w_o} = 0 \rightarrow 64\left(\frac{\pi}{a}\right)^2 w_o\left[\frac{4\pi^2 D}{C} - (1-\nu^2)au_o + (3-2\nu)\frac{\pi^2}{8}w_o^2\right] = 0 \tag{10.5.20}$$

There are two solutions of the above system. The pre-buckling solution is recovered by setting $w_o = 0$. Then from Equation (??)

$$P = (1-\nu^2)Cu_o = (1-\nu^2)\frac{Eh}{1-\nu^2}u_o = Ehu_o \tag{10.5.21}$$

and Equation (??) is satisfied identically. The solution (??) is exact and is equal to the one derived in Section 10.1 of Chapter 10. In the post-buckling range $w_o > 0$ and Equation (??) provides a unique relation between the in-plane and out-of-plane amplitude of the assumed displacement field

$$\frac{\pi^2}{8}\left(\frac{w_o}{a}\right)^2 = \frac{1-\nu^2}{3-2\nu}\frac{u_o}{a} - \frac{4D\pi^2}{C(3-2\nu)a^2} \tag{10.5.22}$$

The plot of the function $w_o = w_o(u_o)$ is shown in Figure (10.5.2).

The critical displacement $(u_o)_c$ to buckle, corresponding to the point of buckling, is obtained from Equation (??) by setting $w_o = 0$

$$(u_o)_c = \frac{4\pi^2 D}{a}\frac{1}{C(1-\nu^2)} \tag{10.5.23}$$

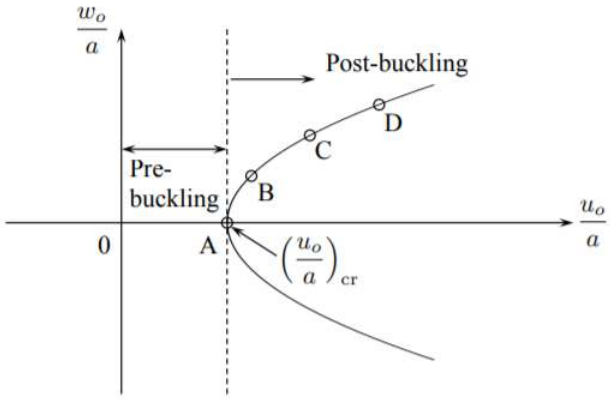

Figure 10.5.2: The out-of-plane displacement amplitude.

Eliminating w_o between Equations (??) and (??) gives a linear post-buckling solution

$$P = \frac{13}{25}(1-\nu^2)Cu_o + \frac{1-\nu^2}{3-2\nu}\frac{4\pi^2 D}{a} \tag{10.5.24}$$

The post-buckling stiffness $K_{\text{post}} = \frac{dD}{du_o}$ is

$$K_{\text{post}} = \frac{13}{25}(1-\nu^2)C = 0.52K_{\text{pre}} \tag{10.5.25}$$

where K_{pre} is the pre-buckling stiffness. For all practical purposes it can be assumed that the plate is loosing half of its stiffness after buckling but is able to carry additional loads. Based on the above analysis, the load-displacement relation of an elastic plate is depicted in Figure (10.5.3).

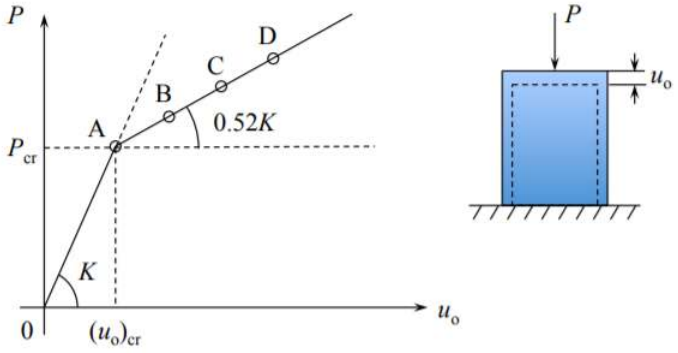

Figure 10.5.3: Pre and post-buckling response of a plate.

Substituting the expression for $(u_o)_c$ into Equation 10.5.21, the predicted buckling load is

$$P_c = \frac{4\pi^2 D}{a} \tag{10.5.26}$$

which is the exact solution of the problem.

10.6: Ultimate Strength of Plates

In the previous section we have shown that after buckling the plate continues to take additional load but with half of its pre-buckling stiffness. In order to understand what happens next, let's examine the distribution of in-plane compressive stresses σ_{xx} at $x = a$. From Equations (10.2.10-10.2.11) and (??) the components σ_{xx} is

$$\sigma_{xx}(y) = \frac{N_{xx}}{h} = \frac{E}{1-\nu^2}\left[-(1-\nu^2)\frac{u_o}{a} + \frac{\pi^2}{2}\left(\frac{w_o}{a}\right)^2 \sin^2\frac{\pi y}{a}\right] \tag{10.6.1}$$

The first term represents negative, compressive stress, uniform along the width of the plate. The second term describes the relieving tensile stress produced by finite rotation. The relation between w_o and u_o is given by Equation (??) and is depicted in Figure (10.5.2). A plot of the function $\sigma_{xx}(y)$ for several values of the time-like parameter u_o is shown in Figure (10.6.1). Note that the curves labeled A, B, C and D corresponds to the respective points in Figs. (10.5.2) and (10.5.3).

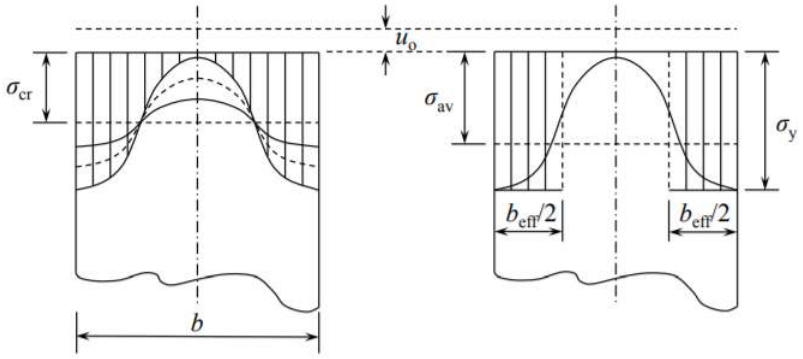

Figure 10.6.1: Re-distribution of compressive stresses along the loaded edge and simple approximation by von Karman.

With increasing plate compression there is a re-distribution of stresses along the loaded edge $x = 0$ and $x = a$. The stress at the unloaded edge $y = 0$ and $y = a$ keeps increasing while the stress at the plate symmetry plane $y = \frac{a}{2}$ diminishes to zero.

It was the German scientist and engineer, Theodore von Karman who in 1932 made use of the observation presented in Figure (10.6.1). He assumed that the central, unloaded portion of the plate carries zero stress while the edge zone, each of the width $b_{eff}/2$ reaches the yield stress at the point of ultimate load. As a starting point, von Karman used the expression for the critical buckling load N_c and looked at the relation between the stress at the loaded edge σ_e and the plate width b

$$\sigma_e = \frac{N_e}{h} = \frac{N_c}{h} = \frac{4\pi^2 D}{hb^2} = \frac{4\pi^2 E h^2}{12(1-\nu^2)b^2} = 1.9^2 E\left(\frac{h}{b}\right)^2 \tag{10.6.2}$$

Normally b is the input parameter and the stress σ_e is an unknown quantity. The ingenuity of von Karman was that he inverted what is known and unknown in Equation (??). He asked what should be the width of the plate b_{eff} so that the edge stress reaches the yield stress. Thus

$$\sigma_y = 1.9^2 E\left(\frac{h}{b_{eff}}\right)^2 \tag{10.6.3}$$

Solving the above equation for b_{eff}

$$b_{eff} = 1.9h\sqrt{\frac{E}{\sigma_y}} \tag{10.6.4}$$

Taking for example $E = 200000$ MPa, $b_{eff}\sigma_y = 320$ MPa, the effective width becomes

$$b_{eff} = 1.9h\sqrt{625} = 47.5h \tag{10.6.5}$$

The effective width depends on the Young's modulus and yield stress is proportional to the plate thickness. Approximately 40-50 thicknesses of the plate near the edges carries the load, the remaining central part is not effective. The total load on the plate can be expressed in two ways

$$P_{\text{ult}} = b_{\text{eff}} \cdot \sigma_y = b \cdot \sigma_{\text{av}} \tag{10.6.6}$$

where $\sigma_{\text{av}} = \sigma_{\text{ult}}$ is the average stress on the loaded edge at the point of ultimate strength,

$$\frac{\sigma_{\text{av}}}{\sigma_{\text{ult}}} = \frac{b_{\text{eff}}}{b} = 1.9\frac{h}{b}\sqrt{\frac{E}{\sigma_y}} \tag{10.6.7}$$

The group of parameters

$$\beta = \frac{b}{h}\sqrt{\frac{\sigma_y}{E}} \tag{10.6.8}$$

is referred to as the slenderness ratio of the plate. Note that this is a different concept than the slenderness ratio of the column l/ρ. Using the parameter β, the ultimate strength of the plate normalized by the yield stress is

$$\frac{\sigma_{\text{ult}}}{\sigma_y} = \frac{1.9}{\beta} \tag{10.6.9}$$

Recall that the normalized buckling stress of the elastic plate is

$$\frac{\sigma_{\text{cr}}}{\sigma_y} = \left(\frac{1.9}{\beta}\right)^2 \tag{10.6.10}$$

Plots of both functions are shown in Figure (10.6.2).

From this figure one can identify the critical slenderness ratio

$$\beta_{\text{cr}} = 1.9 \tag{10.6.11}$$

when both the ultimate load and the critical buckling load reach yield. From Equation (??) one can see that at $\beta = \beta_{\text{cr}}$, the effective width is equal to the plate width, $b_{\text{eff}} = b$.

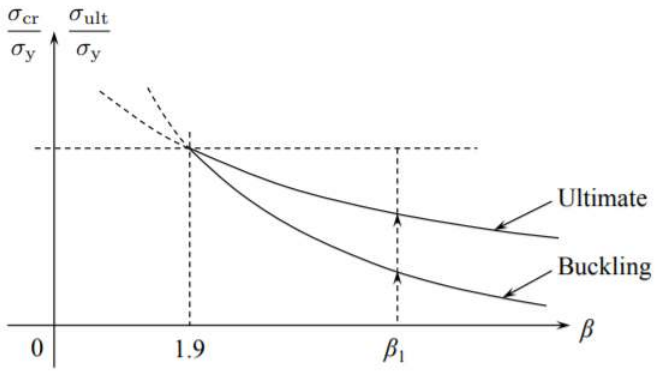

Figure 10.6.2: Dependence of the buckling stress and ultimate stress on the slenderness ratio.

Eliminating the parameter β between Equations (??) and (??), the ultimate stress is seen to be the geometrical average between the yield stress and critical buckling stress

$$\sigma_{\text{ult}} = \sqrt{\sigma_{\text{cr}} \cdot \sigma_y} \tag{10.6.12}$$

For example, continuous loading of a plate with the slenderness ratio β_1 will first encounter the buckling curve and then the ultimate strength curve, as illustrated in Figure (10.6.2). The foregoing analysis was valid for plates simply supported along all four edges, for which the buckling coefficient is $k_c = 4$. For other type of support Equation (??) is still valid with the coefficient 1.9 replaced by $1.9\ \frac{k_c}{4}$.

Much effort has been devoted in the past to validate experimentally the prediction of the von Karman effective width theory. It was found that a small correction to Equation (??) provides good fit of most of the test data

$$\frac{\sigma_{\text{ult}}}{\sigma_y} = \frac{b_{\text{eff}}}{b} = \frac{1.9}{\beta} - \frac{0.9}{\beta^2} \tag{10.6.13}$$

For example, for a relatively short (stocky plate) $\beta = 2\beta_{cr} = 3.8$, the original formula over predicts by 15% than the more exact empirical equation (**??**). For slender plates, the difference is small. The latter has been the basis for the design of thin-walled compressive elements in most domestic and international standards such as AISI, Aluminum Association and AISC.

10.7: Effect of Initial Imperfection

Plates may be geometrically imperfect due to the manufacturing process, welding distortion or mishandling during transportation. The shape of the imperfect plate can be measured as is defined by the function $\bar{w}(x,y)$. In general the initial out-of-plane shape can be expanded in a Fourier series. The first fundamental mode grows more rapidly. Therefore it is sufficient to consider that imperfections are distributed in the first mode

$$\bar{w}(x,y) = \bar{w}_o \sin\frac{\pi x}{a}\sin\frac{\pi y}{a} \tag{10.7.1}$$

With the initial imperfection the definition of the curvatures and membrane strains must be modified

$$\kappa_{\alpha\beta} = -(w-\bar{w})_{,\alpha\beta} \tag{10.7.2}$$

$$\epsilon_{\alpha\beta} = \frac{1}{2}(u_{\alpha,\beta}+u_{\beta,\alpha}) + \frac{1}{2}w_{,\alpha}w_{\beta} - \frac{1}{2}\bar{w}_{,\alpha}\bar{w}_{,\beta} \tag{10.7.3}$$

which reduce to Equations (10.2.7) and (10.1.7), respectively, when $\bar{w}(x,y) = 0$. The derivation presented in Section 10.5 is still valid and the expression for the total potential energy is the same, except all terms involving wo should now be replaced by $(w_o - \bar{w}_o)$. The structural imperfections are usually small and comparable to the thickness of the plate. A plot of the load-displacement curve for the geometrically perfect plate and the plate with two magnitudes of initial imperfections is shown in Figure (10.7.1). The load has been normalized with the critical buckling load and displacements by the critical buckling displacement.

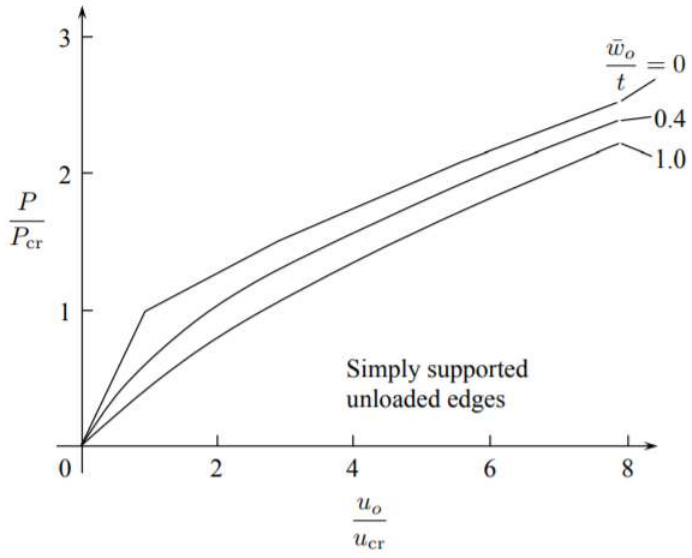

Figure 10.7.1: Load-displacement curves for imperfect simply supported plates.

CHAPTER OVERVIEW

11: Fundamental Concepts in Structural Plasticity

Plastic properties of the material were already introduced briefly earlier in the present notes. The critical slenderness ratio of column is controlled by the yield stress of the material. The subsequent buckling of column in the plastic range requires the knowledge of the hardening curve. These two topics were described in Chapter 8. In Chapter 9 the concept of the ultimate strength of plates was introduced and it was shown that the yield stress is reached first along the supported or clamped edges and the plastic zones spread towards the plate center, leading to the loss of stiffness and strength. In the present lecture the above simple concepts will be extended and formalized to prepare around for the structural applications in terms of the limit analysis. There are five basic concepts in the theory of plasticity:

- Yield condition
- Hardening curve
- Incompressibility
- Flow rule
- Loading/unloading criterion

All of the above concept will first be explained in the 1-D case and then extended to the general 3-D case.

11.1: Hardening Curve and Yield Curve

If we go to the lab and perform a standard tensile test on a round specimen or a flat dogbone specimen made of steel or aluminum, most probably the engineering stress-strain curve will look like the one shown in Figure (**11.1.1***a*). The following features can be distinguished:

Point A - proportionality limit

Point B - 0.02% yield

Point C - arbitrary point on the hardening curve showing different trajectories on loading/unloading

Point D - fully unloaded specimen

For most of material the initial portion of the stress-strain curve is straight up to the proportionality limit, point A. From this stage on the stress-strain curve becomes slightly curved but there is no distinct yield point with a sudden change of slope. There is in international standard the yield stress is mapped by taking elastic slope with 0.02% strain ($\epsilon = 0.0002$) offset strain.

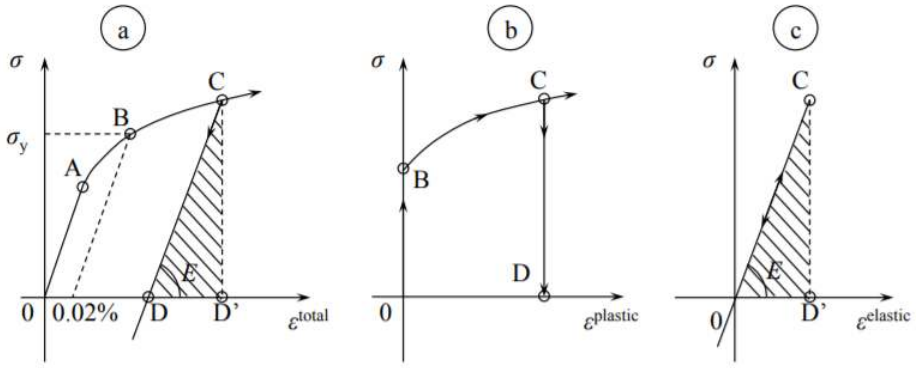

Figure **11.1.1**: Elastic, plastic and total stress-strain curve.

Upon loading, the material hardens and the stress is increasing with diminishing slop until the testing machine (either force or displacement controlled) is stopped. There are two possibilities. On unloading, meaning reversing the load or displacement of the cross-load of the testing machine, the unloading trajectory is straight. This is the elastic unloading where the slop of the stress-strain curve is equal to the initial slope, given by the Young's modulus. At point D the stress is zero but there is a residual plastic strain of the magnitude OD. The experiment on loading/unloading tell us that the total strain ϵ^{total} can be considered as the sum of the plastic strain $\epsilon^{\text{plastic}}$ and elastic strain $\epsilon^{\text{elastic}}$. Thus

$$\epsilon^{\text{total}} = \epsilon^{\text{plastic}} + \epsilon^{\text{elastic}} \tag{11.1.1}$$

The elastic component is not constant but depends on the current stress

$$\epsilon^{\text{elastic}} = \frac{\sigma}{E} \tag{11.1.2}$$

The plastic strain depends on how far a given specimen is loaded, and thus there is a difference between the total (measured) strain and known elastic strain. Various empirical formulas were suggested in the literature to fit the measured relation between the stress and the plastic strain. The most common is the swift hardening law

$$\sigma = A(\epsilon^{\text{plastic}} + \epsilon_o)^n \tag{11.1.3}$$

where A is the stress amplitude, n is the hardening exponent and ϵ_o is the strain shift parameter.

In many practical problems the magnitude of plastic strain is mud larger than the parameter ϵ_o, giving rise to a simpler power hardening law, extensively used in the literature.

$$\sigma = A\epsilon^n \tag{11.1.4}$$

For most metals the exponent n is the range of $n = 0.1 - 0.3$, and the amplitude can vary a lot, depending on the grade of steel. A description of the reverse loading and cycling plastic loading is beyond the scope of the present lecture notes.

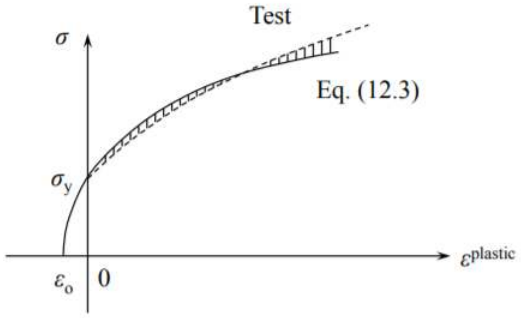

Figure **11.1.2**: The experimentally measured stress-strain curve and the fit by the swift law.

Various other approximation of the actual stress-strain curve of the material are in common use and some of then are shown in Figure (**11.1.3**).

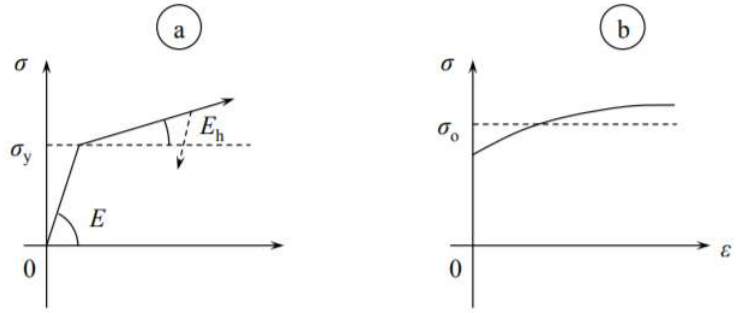

Figure **11.1.3**: Elastic-linear hardening material (a) and rigid-plastic hardening material (b).

A further simplification is obtained by considering the average value σ_o of the stress-strain curve, illustrated in Figure (**11.1.3*b***). This concept gave rise to the concept of the rigid-perfectly plastic material characteristic time, depicted in Figure (11.2.1).

The material model shown in Figure (11.2.1) is adopted in the development of the limit analysis of structures. The extension of the concept of the hardening curve to the 3-D case will be presented later, after deriving the expression for the yield condition.

11.2: Loading/Unloading Condition

In the 1-D case the plastic flow rule is reduced to the following statement:

$$\dot{\epsilon}^p > 0 \quad \sigma = \sigma_o \tag{11.2.1}$$

$$\dot{\epsilon}^p < 0 \quad \sigma = -\sigma_o \tag{11.2.2}$$

$$\dot{\epsilon}^p = 0 \quad \sigma_o < \sigma < -\sigma_o \tag{11.2.3}$$

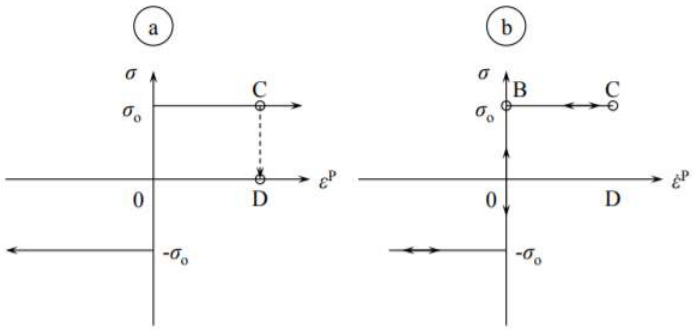

Figure 11.2.1: The flow stress $|\sigma_o|$ is assumed to be identical in tension and compression in the rigid-perfectly plastic material model.

In the case of unloading, the stress follow the path CD on the $\sigma - \epsilon^p$ graph. If the strain rate is an independent variable, the path of all unloading cases is the same CBO, as shown in Figure (11.2.1)

11.3: Incompressibility

Numerous experiments performed over the past 100% have shown that metals are practically incompressible in the plastic range. Let's explore the consequences of this physical fact in the case of one-dimensional case. Denote the gauge length of the prismatic bar by l and its cross-sectional area by A. The current volume of the gauge section is $V = Al$. Incompressibility means that the volume must be unchanged or $dV = 0$.

$$dV = d(Al) = dAl + Adl = 0 \tag{11.3.1}$$

From Equation 11.3.1 we infer that the strain increment $d\epsilon$ can be calculated either by tracking down the gauge length or the cross-sectional area

$$d\epsilon = \frac{dl}{l} = -\frac{dA}{A} \tag{11.3.2}$$

Integrating the first part of Equation 11.3.2

$$\epsilon = \ln l + C_1 \tag{11.3.3}$$

The integration constant is obtained by requiring that the strain vanishes when the length l is equal to the gauge initial, reference length l_o, which gives $C = -\ln l_o$. Thus

$$\epsilon = \ln \frac{l}{l_o} \tag{11.3.4}$$

which is the logarithmic definition of strain, introduced in Chapter 1. Similarly, integrating the second part of Equation 11.3.2 with the initial condition at $A = A_o$, $\epsilon = 0$, one gets

$$\epsilon = \ln \frac{A_o}{A} \tag{11.3.5}$$

In tension $l > l_o$ or $A < A_o$, so both Equations 11.3.4 and 11.3.5 gives the positive strain. In compression the strain is negative. The same is true for strain increments $d\epsilon$ or strain rates

$$\dot{\epsilon} = \frac{\dot{l}}{l} \quad \text{or} \quad \dot{\epsilon} = -\frac{\dot{A}}{A} \tag{11.3.6}$$

From the above analysis follows a simple extension of the plastic incompressibility condition into the 3-D case. Consider an infinitesimal volume element $V = x_1 x_2 x_3$, Figure (11.3.1)

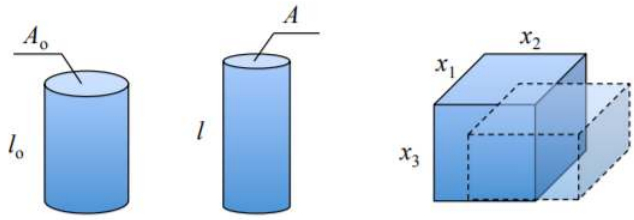

Figure 11.3.1: Undeformed and deformed 1-D and 3-D volume elements.

The plastic incompressibility requires that

$$\begin{aligned} dV = d(x_1x_2x_3) &= dx_1(x_2x_3) + x_1 d(x_2x_3) \\ &= dx_1x_2x_3 + x_1dx_2x_3 + x_1x_2dx_3 \end{aligned} \tag{11.3.7}$$

Dividing both sides of the above equation by the volume, one gets

$$\frac{dx_1}{x_1} + \frac{dx_2}{x_2} + \frac{dx_3}{x_3} = 0 \tag{11.3.8}$$

or

$$d\epsilon_{11} + d\epsilon_{22} + d\epsilon_{33} = 0, \quad d\epsilon_{kk} = 0$$

Noting that $d\epsilon_{11} = \frac{\partial \epsilon_{11}}{\partial t} dt = \dot{\epsilon}_{11} dt$, an alternative form of the incompressibility condition is

$$\dot{\epsilon}_{11} + \dot{\epsilon}_{22} + \dot{\epsilon}_{33} = 0, \quad \dot{\epsilon}_{kk} = 0 \tag{11.3.9}$$

The sum of the diagonal components of the strain rate tensor must vanish to ensure incompressibility. It follows from the flow rule (to be formulated later) that in uniaxial tension in x_1 direction the components $\dot{\epsilon}_{22} = \dot{\epsilon}_{33}$. Therefore $\dot{\epsilon}_{11} + 2\dot{\epsilon}_{22} = 0$ or $\dot{\epsilon}_{11} + 2\dot{\epsilon}_{33} = 0$. Finally we obtain

$$\dot{\epsilon}_{22} = -0.5\dot{\epsilon}_{11}, \quad \dot{\epsilon}_{33} = -0.5\dot{\epsilon}_{11} \tag{11.3.10}$$

The coefficient 0.5 can be interpreted as the Poisson ratio

$$\nu = -\frac{\dot{\epsilon}_{22}}{\dot{\epsilon}_{11}} = -\frac{\dot{\epsilon}_{33}}{\dot{\epsilon}_{11}} = 0.5 \tag{11.3.11}$$

We can conclude that plastic incompressibility requires that the Poisson ratio be equal to $1/2$, which is different from the elastic Poisson ratio, equal $\tilde{0.3}$ for metals. Many other materials such as rubber, polymers and water are incompressible.

11.4: Yield Condition

From the previous section, the uniaxial yield condition under tension/compression in the x-direction is

$$\sigma_{11} = \pm\sigma_y \tag{11.4.1}$$

In the general 3-D, all six components of the stress tensor contribute to yielding of the material. The von Mises yield condition takes the form

$$\frac{1}{2}[(\sigma_{11}-\sigma_{22})^2+(\sigma_{22}-\sigma_{33})^2+(\sigma_{33}-\sigma_{11})^2]+3(\sigma_{12}^2+\sigma_{23}^2+\sigma_{31}^2)] = \sigma_y^2 \tag{11.4.2}$$

or in a short-hand notation

$$F(\sigma_{ij}) = \sigma_y$$

The step-by-step derivation of the above equation is given in the next section. Here, several special cases are considered.

Principle coordinate system

All non-diagonal components of the stress tensor vanish, $\sigma_{12} = \sigma_{23} = \sigma_{31} = 0$. Then, Equation (11.3.8) reduces to

$$(\sigma_1-\sigma_2)^2+(\sigma_2-\sigma_3)^2+(\sigma_3-\sigma_1)^2 = 2\sigma_y^2 \tag{11.4.3}$$

where σ_1, σ_2 σ_3 are principal stresses. The graphical representation of Equation (??) is the open ended cylinder normal to the octahedral plane, Figure (11.4.1).

The equation of the straight line normal to the octahedral plane and passing through the origin is

$$\sigma_1+\sigma_2+\sigma_3 = 3p \tag{11.4.4}$$

where p is the hydrostatic pressure. Since the hydrostatic pressure does not have any effect on yielding, the yield surface is an open cylinder.

Plane stress

Substituting $\sigma_{13} = \sigma_{23} = \sigma_{33} = 0$ in Equation (11.3.8), the plane stress yield condition becomes

$$\sigma_{11}^2-\sigma_{11}\sigma_{22}+\sigma_{22}^2+3\sigma_{12}^2 = \sigma_y^2 \tag{11.4.5}$$

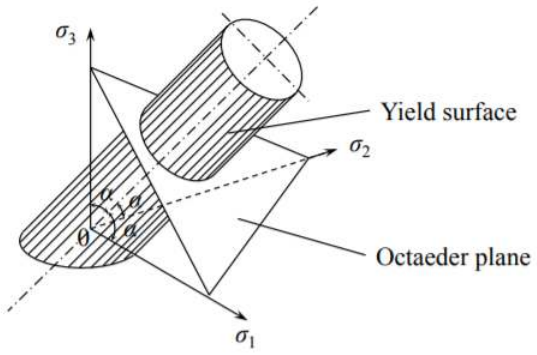

Figure 11.4.1: Representation of the von Mises yield condition in the space of principal stresses.

In particular, in pure shear $\sigma_{11} = \sigma_{22} = 0$ and $\sigma_{12} = \sigma_y/\sqrt{3}$. In the literature $\sigma_y/\sqrt{3} = k$ is called the yield stress in shear corresponding to the von Mises yield condition. In the principal coordinate system $\sigma_{12} = 0$ and the yield condition takes a simple form

$$\sigma_1^2-\sigma_1\sigma_2+\sigma_2^2 = \sigma_y^2 \tag{11.4.6}$$

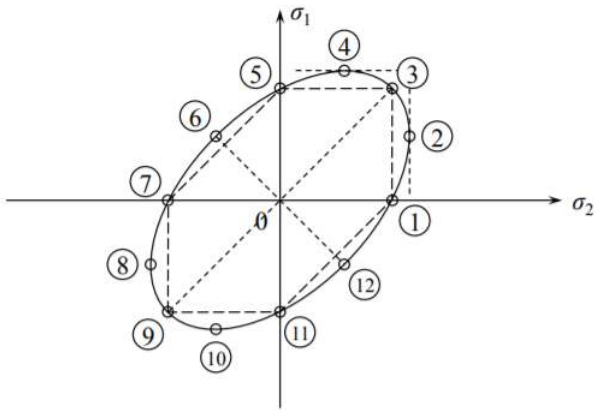

Figure **11.4.2**: The von Mises ellipse in the principal coordinate system.

The graphical representation of Equation (**??**) is the ellipse shown in Figure (**11.4.2**). Several important stress states can be identified in Figure (**11.4.2**).

- Point 1 and 2: Uniaxial tension, $\sigma_1 = \sigma_2 = \sigma_y$
- Point 7 and 11: Uniaxial compression, $\sigma_1 = \sigma_2 = -\sigma_y$
- Point 3: Equi-biaxial tension, $\sigma_1 = \sigma_2$
- Point 9: Equi-biaxial compression, $-\sigma_1 = -\sigma_2$
- Points 2, 4, 8 and 10: Plain strain, $\sigma_1 = \frac{2}{\sqrt{3}}\sigma_y$
- Points 6 and 12: Pure shear, $\sigma_1 = -\sigma_2$

The concept of the plane strain will be explained in the section dealing with the flow rule.

Equivalent stress and equivalent strain rate

In the finite element analysis the concept of the equivalent stress $\bar{\sigma}$ or the von Mises stress is used. It is defined by in terms of principal stresses

$$\bar{\sigma} = \frac{1}{2}[(\sigma_{11} - \sigma_{22})^2 + (\sigma_{22} - \sigma_{33})^2 + (\sigma_{33} - \sigma_{11})^2] \tag{11.4.7}$$

The equivalent stress $\bar{\sigma}(\sigma_{ij})$ is the square root of the left hand side of Equation (11.3.8). Having defined the equivalent stress, the energy conjugate equivalent strain rate can be evaluated from

$$\bar{\sigma}\dot{\bar{\epsilon}} = \sigma_{ij}\dot{\epsilon_{ij}} \tag{11.4.8}$$

and is given by

$$\dot{\bar{\epsilon}} = \left\{\frac{2}{9}[(\dot{\epsilon}_{11}-\dot{\epsilon}_{22})^2+(\dot{\epsilon}_{22}-\dot{\epsilon}_{33})^2+(\dot{\epsilon}_{33}-\dot{\epsilon}_{11})^2]\right\}^{1/2} \tag{11.4.9}$$

The equivalent strain is obtained from integrating in time the equivalent strain rate

$$\bar{\epsilon} = \int \dot{\bar{\epsilon}} dt \tag{11.4.10}$$

11.5: Isotropic and Kinematic Hardening

It should be noted that in the case of uniaxial stress, $\sigma_2 = \sigma_3 = 0$ and Equation (11.3.10) reduces to $\bar{\sigma} = \sigma_1$. Likewise, for uniaxial stress $\dot{\epsilon}_2 = -0.5\epsilon_1$ and $\dot{\epsilon}_3 = -0.5\epsilon_1$ and the equivalent strain rate becomes equal to $\bar{\dot{\epsilon}} = \dot{\epsilon}_1$. Then, according to Equation (??), $\bar{\epsilon}_1 = \epsilon_1$. The hypothesis of the isotropic hardening is that the size of the instantaneous yield condition, represented by the radius of the cylinder (Figure (11.4.1)) is a function of the intensity of the plastic strain defined by the equivalent plastic strain $\bar{\epsilon}$. Thus

$$\bar{\sigma} = \sigma_y(\bar{\epsilon}) \tag{11.5.1}$$

The hardening function $\sigma_y(\bar{\epsilon})$ is determined from a single test, such as a uniaxial tension. In this case

$$\bar{\sigma} = \sigma_1 = \sigma_y(\bar{\epsilon}) = \sigma_y(\epsilon_1) \tag{11.5.2}$$

Thus the form of the function $\sigma_y(\bar{\epsilon})$ is identical to the hardening curve obtained from the tensile experiment. If the tensile test is fit by the power hardening law, the equivalent stress is a power function of the equivalent strain

$$\bar{\sigma} = A\bar{\epsilon}^n \tag{11.5.3}$$

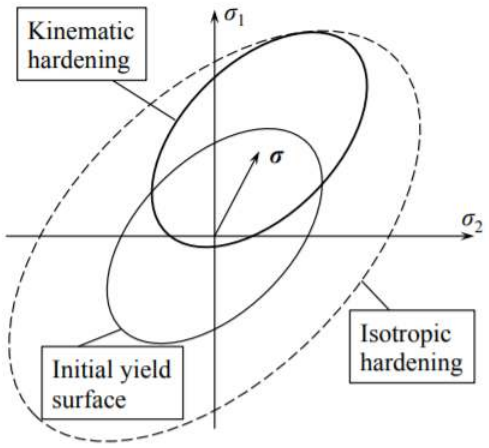

Figure 11.5.1: Comparison of the isotropic and kinematic hardening under plane stress.

The above function often serves as an input to many general purpose finite element codes. A graphical representation of the 3-D hardening rule is a uniform growth of the initial yield ellipse with equivalent strain $\bar{\epsilon}$, Figure (11.5.1).

In the case of kinematic hardening the size of the initial yield surface remains the same, but the center of the ellipse is shifted, see Figure (11.5.1). The coordinates of the center of the ellipse is called the back stress. The concept of the kinematic hardening is important for reverse and cyclic loading. It will not be further pursued in the present lecture notes.

11.6: Flow Rule

The simplest form of the associated flow rule for a rigid perfectly plastic material is given by

$$\dot{\epsilon}_{ij} = \dot{\lambda}\frac{\partial F(\sigma_{ij})}{\partial \sigma_{ij}} \tag{11.6.1}$$

where the function $F(\sigma_{ij})$ is defined by Equation (11.3.8), and $\dot{\lambda}$ is the scalar multiplication factor. Equation (11.3.11) determines uniquely the direction of the strain rate vector, which is always directed normal to the yield surface at a given stress point. In the case of plane stress, the two components of the strain rate vector are

$$\dot{\epsilon}_1 = \dot{\lambda}(2\sigma_1 - \sigma_2) \tag{11.6.2}$$

$$\dot{\epsilon}_2 = \dot{\lambda}(2\sigma_2 - \sigma_1) \tag{11.6.3}$$

The magnitudes of the components $\dot{\epsilon}_1$ and $\dot{\epsilon}_2$ are undetermined, but the ratio, which defines the direction $\dot{\epsilon}/\epsilon_2$, is uniquely determined.

In particular, under the transverse plain strain $\dot{\epsilon}_2 = 0$, so $\sigma_1 = 2\sigma_2$ and $\sigma_1 = \frac{2}{\sqrt{3}}\sigma_y$.

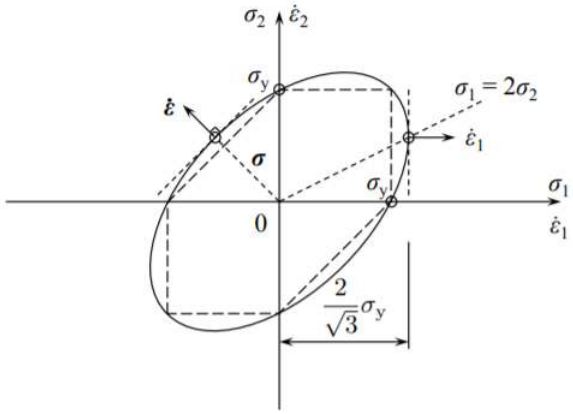

Figure **11.6.1**: The strain rate vector is always normal to the yield surface.

11.7: Derivation of the Yield Condition from First Principles (Advanced)

The analysis starts from stating the stress-strain relations for the elastic material, covered in Chapter 3. The general Hook's law for the isotropic material is

$$\epsilon_{ij} = \frac{1}{E}[(1+\nu)\sigma_{ij} - \nu\sigma_{kk}\delta_{ij}] \tag{11.7.1}$$

The elastic constitutive equation can also be written in an alternative form, separately for the distortional and dilatational part

$$e_{ij} = \frac{1+\nu}{E}s_{ij} \quad - \quad \text{distorsion} \tag{11.7.2}$$

$$\epsilon_{kk} = \frac{1-2\nu}{E}\sigma_{kk} \quad - \quad \text{dilatation} \tag{11.7.3}$$

The next step is to invoke the basic property of the elastic material that the strain energy density $\bar{U}$, defined by

$$\bar{U} = \oint \sigma_{ij} d\epsilon_{ij} \tag{11.7.4}$$

does not depend on the loading path of the above line integral but only on the final state. Thus, evaluating the strain energy on the proportional (straight) loading path, one gets

$$\bar{U} = \frac{1}{2}\sigma_{ij}\epsilon_{ij} \tag{11.7.5}$$

The next step is to prove that the strain energy density can be decomposed into the distortional and dilatational part. This is done by recalling the definition of the stress deviator s_{ij} and strain deviator e_{ij}

$$\sigma_{ij} = s_{ij} + \frac{1}{3}\sigma_{kk}\delta_{ij} \tag{11.7.6}$$

$$\epsilon_{ij} = e_{ij} + \frac{1}{3}\epsilon_{kk}\delta_{ij} \tag{11.7.7}$$

Introducing Equation (11.4.5) into Equation (11.4.4), there will be four terms in the expression for $\bar{U}$

$$2\bar{U} = s_{ij}e_{ij} + s_{ij}\frac{1}{3}\epsilon_{kk}\delta_{ij} + \frac{1}{3}\sigma_{kk}\delta_{ij}e_{ij} + \frac{1}{3}\sigma_{kk}\delta_{ij}\frac{1}{3}\epsilon_{kk}\delta_{ij} \tag{11.7.8}$$

Note that $s_{ij}\delta_{ij} = s_{ii} = 0$ from the definition, Equation (11.4.5). Likewise $e_{ij}\delta_{ij} = e_{jj} = 0$, also from the definition. Therefore the second and third term of Equation (??) vanish and the energy density becomes

$$\bar{U} = \frac{1}{2}s_{ij}e_{ij} + \frac{1}{6}\sigma_{kk}\epsilon_{ll} = \bar{U}_{dist} + \bar{U}_{dil} \tag{11.7.9}$$

Attention is focused on the distortional energy, which with the help of the elasticity law Equation (11.4.2) can be put into the form

$$\bar{U}_{dist} = \frac{1+\nu}{2E}s_{ij}s_{ij} \tag{11.7.10}$$

The product $s_{ij}s_{ij}$ can be expressed in terms of the components of the stress tensor

$$\begin{aligned} s_{ij}s_{ij} &= (\sigma_{ij} - \frac{1}{3}\sigma_{kk}\delta_{ij})(\sigma_{ij} - \frac{1}{3}\sigma_{kk}\delta_{ij}) \\ &= \sigma_{ij}\sigma_{ij} - \frac{1}{3}\sigma_{ij}\sigma_{kk}\delta_{ij} - \frac{1}{3}\sigma_{kk}\delta_{ij}\sigma_{ij} + \frac{1}{9}\sigma_{kk}\sigma_{kk}\delta_{ij}\delta_{ij} \\ &= \sigma_{ij}\sigma_{ij} - \frac{2}{3}\sigma_{kk}\sigma_{kk} + \frac{1}{3}\sigma_{kk}\sigma_{kk} \end{aligned}$$

The final result is

$$\bar{U} = \frac{1+\nu}{2E}(\sigma_{ij}\sigma_{ij} - \frac{1}{3}\sigma_{kk}\sigma_{kk}) \tag{11.7.11}$$

In 1904 the Polish professor Maximilian Tytus Huber proposed a hypothesis that yielding of the material occurs when the distortional energy density reaches a critical value

$$\sigma_{ij}\sigma_{ij} - \frac{1}{3}\sigma_{kk}\sigma_{kk} = C \tag{11.7.12}$$

where C is the material constant that must be determined from tests. The calibration is performed using the uni-axial tension test for which the components of the stress tensor are

$$\sigma_{ij} = \begin{vmatrix} \sigma_{11} & 0 & 0 \\ 0 & 0 & 0 \\ 0 & 0 & 0 \end{vmatrix} \tag{11.7.13}$$

From Equation (11.4.6) we get

$$\sigma_{11}\sigma_{11} - \frac{1}{3}\sigma_{11}\sigma_{11} = \frac{2}{3}\sigma_{11}\sigma_{11} = C \tag{11.7.14}$$

Yielding occurs when $\sigma_{11} = \sigma_y$ so $C = \frac{2}{3}\sigma_y^2$. The most general form of the Huber yield condition is

$$(\sigma_{11} - \sigma_{22})^2 + (\sigma_{22} - \sigma_{33})^2 + (\sigma_{33} - \sigma_{11})^2 + 6(\sigma_{12}^2 + \sigma_{23}^2 + \sigma_{31}^2) = 2\sigma_y^2 \tag{11.7.15}$$

which was the starting point of the analysis of various special cases in Section 11.4. A similar form of the yield condition for plane stress was derived by von Mises in 1913, based on plastic slip consideration and was later extended to the 3-D case by Hencky. The present form is reformed to in the literature as the Huber-Mises-Hencky yield criterion, called von Mises for short.

11.8: Tresca Yield Condition

The stress state in uni-axial tension of a bar depends on the orientation of the plane on which the stresses are resolved. In Chapter 2 it was shown that the shear stress τ on the plane inclined to the horizontal plane by the angle α is

$$\tau = \frac{1}{2}\sigma_{11}\sin 2\alpha \tag{11.8.1}$$

where σ_{11} is the uniaxial tensile stress, see Figure (11.8.1).

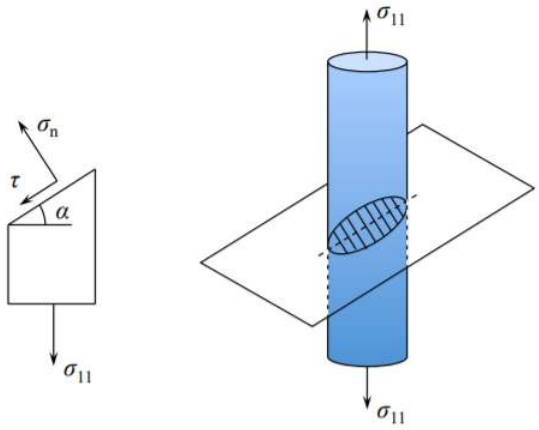

Figure 11.8.1: Shear and normal stresses at an arbitrary cut.

The maximum shear occurs when $\sin 2\alpha = 1$ or $\alpha = \frac{\pi}{4}$. Thus in uniaxial tension

$$\tau_{\max} = \frac{\sigma_{11}}{2} \tag{11.8.2}$$

Extending the analysis to the 3-D case (see for example Fung) the maximum shear stresses on three shear planes are

$$\tau_1 = \frac{|\sigma_1 - \sigma_2|}{2}, \quad \tau_2 = \frac{|\sigma_2 - \sigma_1|}{2}, \quad \tau_3 = \frac{|\sigma_3 - \sigma_1|}{2} \tag{11.8.3}$$

where σ_1, σ_2, σ_3 are principal stresses. In 1860 the French scientist and engineer Henri Tresca put up a hypothesis that yielding of the material occurs when the maximum shear stress reaches a critical value

$$\tau_o = \max\left\{\frac{|\sigma_1 - \sigma_2|}{2}, \frac{|\sigma_2 - \sigma_3|}{2}, \frac{|\sigma_3 - \sigma_1|}{2}\right\} \tag{11.8.4}$$

The unknown constant can be calibrated from the uniaxial test for which Equation (11.4.9) holds. Therefore at yield $\tau_o = \sigma_y/2$ and the Tresca yield condition takes the form

$$\max\left\{|\sigma_1 - \sigma_2|, |\sigma_2 - \sigma_3|, |\sigma_3 - \sigma_1|\right\} = \sigma_y \tag{11.8.5}$$

In the space of principal stresses the Tresca yield condition is represented by a prismatic open-ended tube, whose intersection with the octahedral plane is a regular hexagon, see Figure (11.8.2).

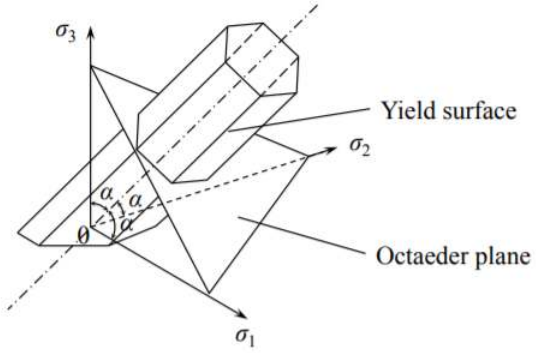

Figure 11.8.2: Representation of the Tresca yield condition in the space of principal stresses.

For plane stress, the intersection of the prismatic tube with the plane $\sigma_3 = 0$ forms a familiar Tresca hexagon, shown in Figure (11.8.3).

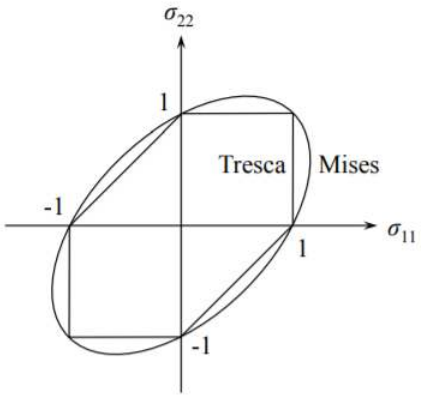

Figure 11.8.3: Tresca hexagon inscribed into the von Mises ellipse.

The effect of the hydrostatic pressure on yielding can be easily assessed by considering $\sigma_1 = \sigma_2 = \sigma_3 = p$. Then

$$\sigma_1 - \sigma_2 = 0 \tag{11.8.6}$$

$$\sigma_2 - \sigma_3 = 0 \tag{11.8.7}$$

$$\sigma_3 - \sigma_1 = 0 \tag{11.8.8}$$

Under this stress state both von Mises yield criterion (Equation (??)) and the Tresca criterion (Equation (??)) predict that there will be no yielding.

11.9: Experimental Validation

The validity of the von Mises and Tresca yield criteria and their comparison has been the subject of extensive research over the past century. The easiest way to generate the complex state of stress is to perform tension/compression/torsion tests of thin-walled tubes, sometimes with added internal pressure. The results from the literature are collected in Figure (**11.9.1**) where the experimental points represent a combination of the measured two principal stresses causing yielding. There is a fair amount of spread of the data so that there is no clear winner between the two competing theories. After all, the physics behind both approaches is similar: shear stresses (Tresca) produces shape distortion, and shape distortion (von Mises) can only be achieved through the action of shear stresses (in a rotated coordinate system). The maximum difference between the von Mises and Tresca yield curve occurs at the transverse plane strain and is equal to $(2/r_3 - 1) = 0.15$.

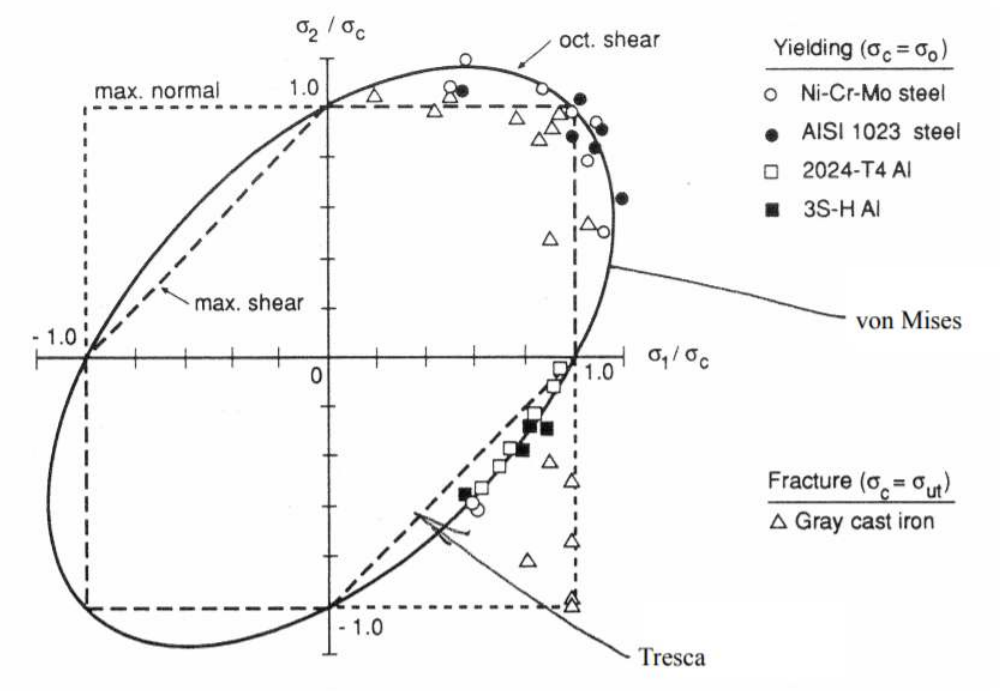

Figure **11.9.1**: Plane stress failure loci for three criteria. These are compared with biaxial yield data for ductile steels and aluminum alloys, and also with biaxial fracture data for gray cast iron.

Quasi-brittle materials, such as cast iron behave differently in tension and compression. They can be modeled by the pressure dependent or normal stress dependent (CoulombMohr) failure criterion. The comparison of theory with experimental data is shown in Figure (**11.9.2**).

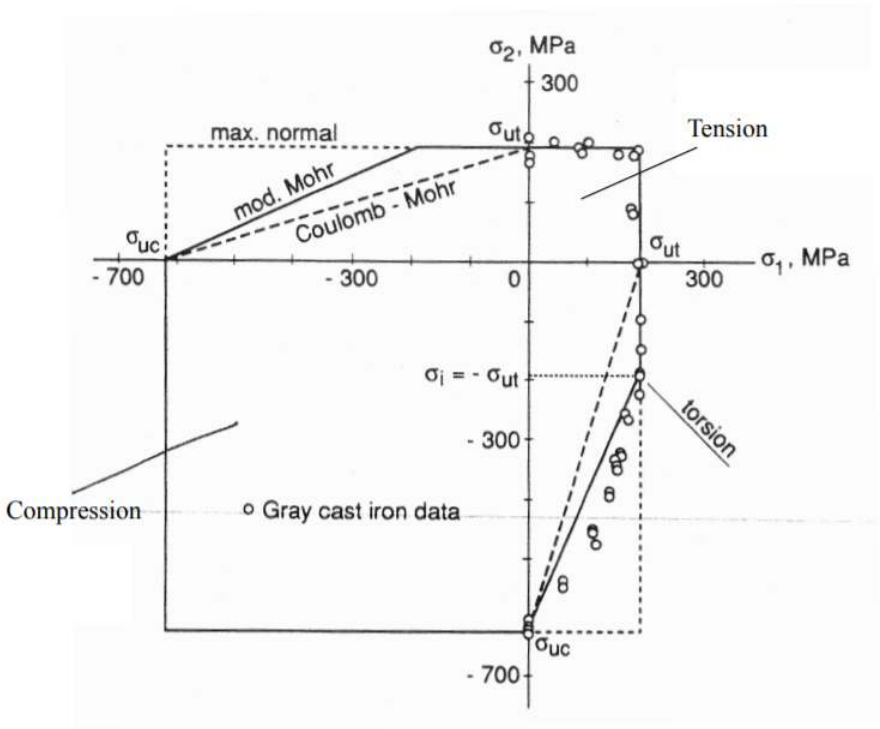

Figure **11.9.2**: Biaxial fracture data of gray cast iron compared to various fracture criteria.

11.10: Example of the Design against First Yield

Safety of pressure vessels and piping systems is critical in design of offshore, chemical and nuclear installation. The simplest problem in this class of structures is a thick pipe loaded by an internal pressure p. The tube is assumed to be infinitely long and the internal and external radii are denoted respectively by a and b. In the cylindrical coordinate system $(r, \theta, z), \sigma_{zz} = 0$ for the open-ended short tube and $\sigma_{rr} = \sigma_r$ and $\sigma_{\theta\theta} = \sigma_\theta$ are the principal radial and circumferential stresses. The material is elastic up to the point of the first yield. The objective is to determine the location where the first yield occurs and the corresponding critical pressure p_y.

The governing equation is derived by writing down three groups of equations:

Geometrical relation:

$$\epsilon_r = \frac{d}{dr}u, \quad \epsilon_\theta = \frac{u}{r} \tag{11.10.1}$$

where u is the radial component of the displacement vector, $u = u_r$. The hoop component is zero because of axial symmetry.

Equilibrium:

$$\frac{d}{dr}\sigma_r + \frac{\sigma_r - \sigma_\theta}{r} = 0 \tag{11.10.2}$$

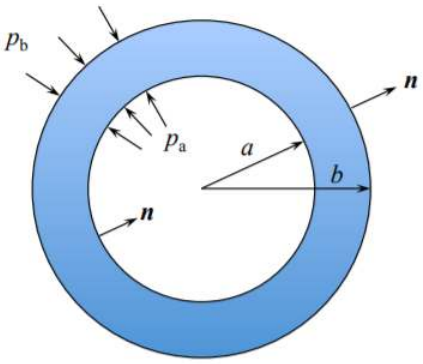

Figure **11.10.1**: Expansion of a thick cylinder by an internal pressure.

Elasticity law:

$$\sigma_r = \frac{E}{1-\nu^2}(\epsilon_r + \nu\epsilon_\theta) \tag{11.10.3}$$

$$\sigma_\theta = \frac{E}{1-\nu^2}(\epsilon_\theta + \nu\epsilon_r) \tag{11.10.4}$$

There are five equations for five unknowns, σ_r, σ_θ, ϵ_r, ϵ_θ and u. Solving the above system for u, one gets

$$r^2\frac{d^2}{dr^2}u + r\frac{d}{dr}u - u = 0 \tag{11.10.5}$$

The solution of this equation is

$$u(r) = C_1 r + \frac{C_2}{r} \tag{11.10.6}$$

where C_1 and C_2 are integration constants to be determined from the boundary conditions. The stress and displacement boundary condition for this problem are

$$(T - \sigma_r) = 0 \quad \text{or} \quad \delta u = 0 \tag{11.10.7}$$

In the case of pressure loading, the stress boundary condition applies:

$$\text{at } r = a \quad \sigma_r = -p_a \tag{11.10.8}$$

$$\text{at } r = b \quad \sigma_r = -p_b \tag{11.10.9}$$

The minus sign appears because the surface traction T, which in our case is pressure loading, acts in the opposite direction to the unit normal vectors n, see Figure (12.15). In the present case of internal pressure, $\sigma_r(r = a) = -p$ and $\sigma_r(r = b) = 0$. The radial stress is calculated from Equations (11.5.3) and (11.6.2-11.6.3)

$$\sigma_r = \frac{E}{1-\nu^2}\left[(1+\nu)C_1 - (1-\nu)\frac{C_2}{r^2}\right] \tag{11.10.10}$$

The integration constants can be easily calculated from two boundary conditions, and the final solution for the stresses is

$$\sigma_r(r) = \frac{a^2 p}{b^2 - a^2}\left(1 - \frac{b^2}{r^2}\right) \tag{11.10.11}$$

$$\sigma_\theta(r) = \frac{a^2 p}{b^2 - a^2}\left(1 + \frac{b^2}{r^2}\right) \tag{11.10.12}$$

Eliminating the term $(b/r)^2$ between the above two equations gives the straight line profile of the stresses, shown in Figure (11.10.2).

$$\sigma_r + \sigma_\theta = 2p\frac{1}{\left(\frac{b}{a}\right)^2 - 1} \tag{11.10.13}$$

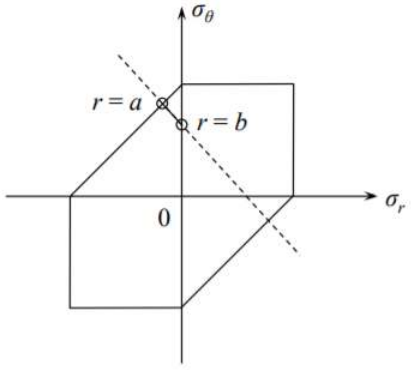

Figure 11.10.2: The stress profile across the thickness of the cylinder.

It is seen that the stress profile is entirely in the second quadrant and the tube reaches yield at $r = a$, for which the stresses are

$$\sigma_r = -p \tag{11.10.14}$$

$$\sigma_\theta = p\frac{b^2 + a^2}{b^2 - a^2} \tag{11.10.15}$$

In the case of the Tresca yield condition

$$|\sigma_\theta - \sigma_r| = \sigma_y \tag{11.10.16}$$

The dimensionless yield pressure is

$$\frac{p}{\sigma_y} = \frac{1}{2}\left[1 - \left(\frac{a}{b}\right)^2\right] \tag{11.10.17}$$

The von Mises yield condition predicts

$$\frac{p}{\sigma_y} = \frac{1 - (a/b)^2}{\sqrt{3 + (a/b)^4}} \tag{11.10.18}$$

For example, if $\frac{a}{b} = \frac{1}{2}$, the first yield pressure according to the von Mises yield condition is $\frac{p_y}{\sigma_y} = \frac{3}{7}$ while the Tresca yield criterion predicts $\frac{p_y}{\sigma_y} = \frac{3}{8}$. The difference between the above two cases is 14%.

Index

D

E

F

T

U

V

W

Y

Glossary

Sample Word 1 | Sample Definition 1

Detailed Licensing

Overview

Title: Structural Mechanics (Wierzbicki)

Webpages: 99

Applicable Restrictions: Noncommercial

All licenses found:

- CC BY-NC-SA 4.0: 93.9% (93 pages)
- Undeclared: 6.1% (6 pages)

By Page